Institute of Anatomy and Special Embryology

University of Fribourg (Switzerland)

Electrophysiological Characterisation of Spectral Response Properties in the Visual System of the Tree Shrew (Tupaia belangeri)

DOCTORAL DISSERTATION

in order to obtain the title of ***Doctor rerum naturalium***

granted by the Faculty of Mathematics and Natural Science of the

University of Fribourg in Switzerland

presented by

Luis Fernando Murillo Othon

Mexico City

Thesis No. 1273

Imprimerie St. Paul, Fribourg

2000

Accepted by the Faculty of Mathematics and Natural Science of the

University of Fribourg, Switzerland on the proposal of:

Prof. Dr. Marco Celio, University of Fribourg
President of the Jury

Prof. Dr. Robert Kretz, University of Fribourg

Prof. Dr. Heywood Petry, University of Louisville, U.S.A.

Prof. Dr. Eric-Michel Rouiller, University of Fribourg

Fribourg, 13th December 2000

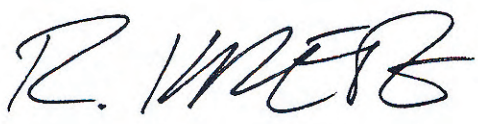

Prof. Dr. Robert Kretz
Thesis Supervisor

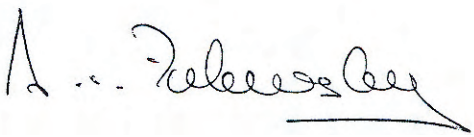

Prof. Dr. A. von Zelewsky
Dean of the Faculty

á mon amie Özlem

á M. et Mme. Hernandez

á la mémoire de Pierre

Acknowledgements

The burden of keeping me in relative sanity has, for the last few years, befallen on my dear Özlem Duvarci. I wish to thank her for her patient and loving companionship.

M. and Mme. Hernandez have drawn deep into their abundant reserves of humor and good-heartedness, dissolving the distance between my home, and these inhospitable latitudes.

The German word for ”doctoral supervisor” is Doktorvater, which suggests the remote possibility that the individual vested with such lofty honor might actually, although this is not very orthodox, show some interest for his intellectual ”offspring”. In this respect, Prof. Kretz has been quite beyond reproach. For his helpfulness and solicitude, I thank him most warmly, and for initiating me to the refinements of Jodel music at 4 o’clock in the morning.

For supporting a philosopher in his bid to experience the human brain “first hand”, with its rich formaldehyde bouquet, I wish to thank the Institute’s director, Prof. Rager.

I wish to thank Dr. Ulrich Drenhaus, whose erudition and rigor have been a source of inspiration.

Amongst the tasks of sumptuously ungrateful monotony, fate has devised laboratory work as supreme punishment to mortals. This is all the more reason to acknowledge my recognition of Mme. Marguerite Kaczarowski’s exquisite work.

Of equal merit and courage are the labors of programmers competing with capricious computers for the upper hand. I therefore extend my gratitude to Patrick Faeh.

Monsieur Marcel Donzallaz, our Institute's animal keeper, must be thanked for the lavish solicitude he has bestowed on our animals, which at times, would almost make us a little jealous. His intuitive knowledge of this species competes with any expert's.

It is a pleasure to acknowledge my debt of gratitude to Prof. Eric Rouiller for scrutinizing the first version of this thesis, and for his patient and supportive advice in preparing the final version.

I also thank Prof. Heywood Petry, whose work has been a source of inspiration and who has agreed to act as an external expert on the thesis committee.

I am very grateful also to Corinne Moussavian and Dr. Michel Pfulg, who have provided me with much needed support during the last stage of the preparation of this manuscript.

Naturally, I wish to thank my parents, for without their collaboration in bringing me to the world, it would have been utterly strenuous to for me to lay any convincing claims on the authorship of this work.

But foremost in my appreciation is my now departed friend, Pierre Cuennet, who teased me by calling me “Dr. Plattfuss”, well before this thesis was finished. It is to him that I wish especially to dedicate this work, for whatever it is worth.

Table of Contents

Page

2 Materials and Methods

3 Results

4 Discussion

General Abbreviations

A17	Area 17, primary visual area
A18	Area 18, secondary visual area
CFF	Critical Flicker Fusion
CIE	Commission Internationale d'Eclairage
Contra	contralateral
CS	Colliculus superior
SGS	Stratum griseum superficiale (in Colliculus superior)
SO	Stratum opticum (in Colliculus superior)
Deg	degree
Ipsi	ipsilateral
LGN	dorsal lateral geniculate nucleus
mW	milliwatt
LWC	long-wavelength sensitive cone
"PSTH" or "PS"	refers to file names containing spike data
RF	receptive field
RLR	red light reared
SWC	short-wavelength sensitive cone
T.AD. X	Tupaia adult experiment number X

Summary

An electrophysiological study was conducted in the visual system of the tree shrew (*Tupaia belangeri*) in order to explore the response properties to chromatic stimuli (chromatic filtered light of different intensities). A limited number (15 %) of narrow-band cells were found illustrating various modes of chromatic tuning.

These cells were found not only in the cortex, but also in the Colliculus superior, confirming previous psychophysical findings that the animal's color discrimination capabilities are not undermined by removal of visual cortex, and confirming postulated mesencephalic color detecting circuitry.

Of the two narrow band cells found in primary visual cortex (A17), one was localized in sublayer IVb; the other was at the border of sublayers IIIa and IIIb. The latter is consistent with the finding that sublayer IIIb is the target of cells in lamina 3 of the dLGN, where color-selective units have been found (Kretz 1989, Conley et al. 1984).

A subset of the narrow band cells showed preference for moving stimuli, confirming the suggestion that color discrimination channels are not motion blind. The converse proposition that motion channels are not color blind has been proven in other species, particularly in the macaque (Gegenfurtner, et al. 1994).

One of the cells in our study showed higher responses to short-wavelengths only when faster moving stimuli were used, challenging the notion that the blue-channel has lower temporal resolution (Zrenner 1983).

One of the cells in our study had narrow band characteristics in the ON-channel, responding only to long-wavelength stimulation, but acted as a broadband cell in the OFF-channel. There was a clear OFF response (phasic) to short-wavelength stimulation, which is in disagreement with the idea that the short-wavelength system is lacking an OFF-response (Zrenner 1983, pp. 26, 82).

Cortical cells showing preference to short-wavelength stimulation occurred, as expected, more frequently in those areas representing the upper visual field (i.e. ventral retina), where histochemical studies have revealed the greatest density of short-wavelength sensitive cones in the retina (Müller and Peichl 1989).

In one broadband cell, the similarity of the response/intensity (R/I) curves allowed us to determine the relative cone weights.

Although the narrow band cells in primary visual cortex showed a definite chromatic preference, their wavelength tuning was not as crisp as that evidenced in some dLGN cells (Kretz, 1989). This is in agreement with findings in *Macaca fascicularis* (Lennie et al. 1990). Double opponent cells were not found.

It has been proposed that in the tree shrew, the cell sparse-cleft between sublayers IVa and IVb in primary visual cortex may be the locus of color processing cells. One of the cells in our study is located precisely in this sublayer. It displayed poor orientation tuning and center-surround color opponency. The cell gave higher responses in all wavelengths to contrast invariant stimuli. This confirms the suggestion that this sublayer contains cells which are not primarily luminance driven (Petry 1993).

From this we conclude that besides the Colliculus superior, the most likely places for color-opponent or color-biased cells to be found are lamina 3 of the dLGN and its principal projection in the primary visual cortex, which is the cell-sparse cleft and sublayer IIIb.

Zusammenfassung

Eine elektrophysiologische Untersuchung des visuellen Systems des Spitzhörnchens (*Tupaia belangeri)* wurde durchgeführt, um die Antwortcharakteristika einzelner Zellen auf chromatische Stimuli verschiedener Intensitäten zu erforschen. Es wurde eine Anzahl schmalbandiger Zellen (15 %) mit verschiedenen farbspezifischen Typen gefunden.

Diese Zellen wurden nicht nur im Kortex, sondern auch im Colliculus superior lokalisiert. Somit wird, in Übereinstimmung mit vorherigen psychophysischen Befunden bestätigt, dass die Fähigkeit zur Farbdiskriminierung dieses Tieres sogar bei Entfernung des visuellen Kortex weiterbesteht. Damit wird die Existenz von mesencephalischen Farbverarbeitungsschaltkreisen elektrophysiologisch bestätigt.

Von den zwei schmalbandigen Zellen im primären visuellen Kortex wurde die eine in Schicht IVb, die andere in Schicht IIIa/b gefunden. Letzteres stimmt mit der schon bekannten Projektion aus der Lamina 3 des dLGN überein, wo eine farbspezifische Zelle beschrieben worden ist. (Kretz 1989, Conley et al. 1984).

Eine Anzahl schmalbandiger Zellen antwortete stark auf bewegte Stimuli, was die Auffassung bestätigt, dass farbdiskriminierende Kanäle nicht „bewegungsblind“ sind. Es wurde schon bei Makaken nachgewiesen, dass bewegungsempfindliche Kanäle nicht farbenblind sind (Gegenfurtner et al., 1994).

Eine der Zellen in unserer Untersuchung zeigte bessere Antworten auf kurzwellige Stimuli, aber ausschliesslich wenn diese schnell bewegt wurden. Dieses scheint der Idee, dass die sog. Blaukanäle eine tiefere zeitliche Auflösung haben, zu widersprechen (Zrenner, 1983).

Eine andere Zelle wies schmalbandige Eigenschaften bei Licht "ON" auf, indem sie bloss auf kurzwellige Stimulation antwortete. Sie reagierte aber als breitbandige Zelle bei Licht "OFF". Somit gab die Zelle eine klare "OFF"-Antwort auf kurzwellige Stimuli. Dieses ist im Widerspruch mit der Auffassung, dass das kurzwellige System zu keiner OFF-Antwort fähig sei (Zrenner, 1983, S. 26, 82).

Zellen, die im kurzwelligen Berreich empfindlicher sind, liessen sich häufiger in jenen Regionen des visuellen Kortex finden, in denen das obere Gesichtsfeld repräsentiert ist. Gemäss histochemischer Untersuchungen hat die ventrale Netzhaut die höchste Dichte von kurzwelligen Zapfen (Müller und Peichl, 1989).

Von einer der breitbandigen Zellen konnten, dank der Ähnlichkeit der R/I-Kurven, die relativen Einflüsse der verschiedenen Zapfentypen bestimmt werden.

Obwohl die kurzbandigen Zellen im primären visuellen Kortex eine chromatische Preferenz aufzeigten, war ihre Farbabstimmung nicht so eindeutig wie diejenige der dLGN Zellen. Letzteres ist in Übereinstimmung mit aus *Macaca fascicularis* gewonnenen Daten (Lennie, et al. 1990). Doppelt-Gegenfarbenneurone wurden nicht gefunden.

Petry (1993) hat den sogenannten „zellarmen Spalt“ zwischen den Schichten IVa und IVb als möglichen Locus für Farbverarbeitungszellen im visuellen Kortex vorgeschlagen. Eine der Zellen in unserer Untersuchung wurde an dieser Stelle abgeleitet. Ihre Eigenschaften waren: schlechte Orientierungsabstimmung mit Zentrum/Umfeld-Gegenfarbigkeit. Zusätzlich gab die Zelle stärkere Antworten auf kontrast-invariante Stimuli. Dies stimmt mit der Auffassung überein, dass diese Zwischenschicht Zellen beinhaltet, welche vorwiegend nicht durch die Leuchtdichte („luminance“) aktiviert werden.

Zusammenfassend können wir folgern, dass ausser dem Colliculus superior auch Zellen der Lamina 3 des dLGN und dessen Hauptprojektionsgebiet im primären visuellen Kortex, d.h. Zellen im sogenannten "zellarmen Spalt" und der Schicht IIIb gute Kandidaten sind, um Gegenfarbenneurone oder farbspezifische Neurone zu finden.

Introduction

1 Introduction

1.1 The Classification of the Tree Shrew

The tree shrew (*Tupaia belangeri)* is a member of the mammalian family of **Tupaiidae**. Within this family there are two subfamilies – Ptilocercinae and Tupaiinae. Aside from the single nocturnal species *Ptilocercus lowii,* belonging to the former subfamily, all other species are diurnal.

The Tupaia belangeri's habitat is the rain forests of South East Asia (Martin 1990). Like European squirrels, which they resemble in their habits and external appearance, they lead a semiarboreal lifestyle and move very rapidly. Indeed the word "tupai" from which the generic name is derived, means squirrel in the Malay language. The animals are –as already mentioned- diurnal, and posses high visual acuity. They are small, have a body weight of about 200-250g and feed principally on arthropods and small fruits, although they are omnivorous. Tree shrews were originally considered unspecialized placental mammals and were classified as Insectivora (Haeckel 1866, Weber 1928).

The brain of the tree shrew is lissencephalic, and there is a reduction in the areas related to the sense of olfaction, and a corresponding elaboration of the visual apparatus, indicating an advancement from the conditions found in Insectivora. The relative size of the Corpus callosum is too big to suggest a classification with insectivora.

The visual cortex of Tupaiae is well developed and contains a duplication of the inner granular layer. This and the presence of the white line of Gennari, have suggested to some that the animal should be classified with primates (Le Gros Clark, 1924).

But tree shrews differ from primates in having smaller, laterally oriented eyes. As a result of the latter feature, the projection of retinofugal fibers is overwhelmingly

contralateral. The projection to the lateral geniculate nucleus differs from that of primates (Kaas, et al. 1978). The Sylvian and Calcarine sulcus, found in all primate brains, is lacking. (Martin, 1990).

Most authors now agree that tree shrews are either insectivores or primates that lie close to the “insectivore-primate boundary”. Butler (1972) has proposed to place the tree shrews in the separate order Scandentia. Possibly, the similarities between tree shrews and primates are a result of coevolution.

For legal purposes, Tupaiae are considered as primates in Switzerland and there use for experimental purposes is regulated by the specific rules issued by the Federal Veterinarian Office concerning primate species.

1.2 Peculiarities of the Tupaia visual system

1.2.1 Retina

Müller and Peichl have performed immunohistochemical studies of the retina of the tree shrew and report that it is cone dominated. Only four to five percent of the photoreceptors are rods (Müller and Peichl, 1989). The cone population is predominantly represented by long- wavelength cones (LWCs) and only four to nine percent SWCs (short-wavelength cones). The absorption maxima as revealed by microspectrophotometrical studies are at 555 and 428 nm, respectively (Petry and Harosi 1990).

Furthermore, the highest percentage of SWCs is localized in the ventral retina (Müller and Peichl 1989, see also Petry et al. 1993, Petry and Murphy 1995). **Figure 1** illustrates the distribution of SWCs over the entire cone population for two retinae.

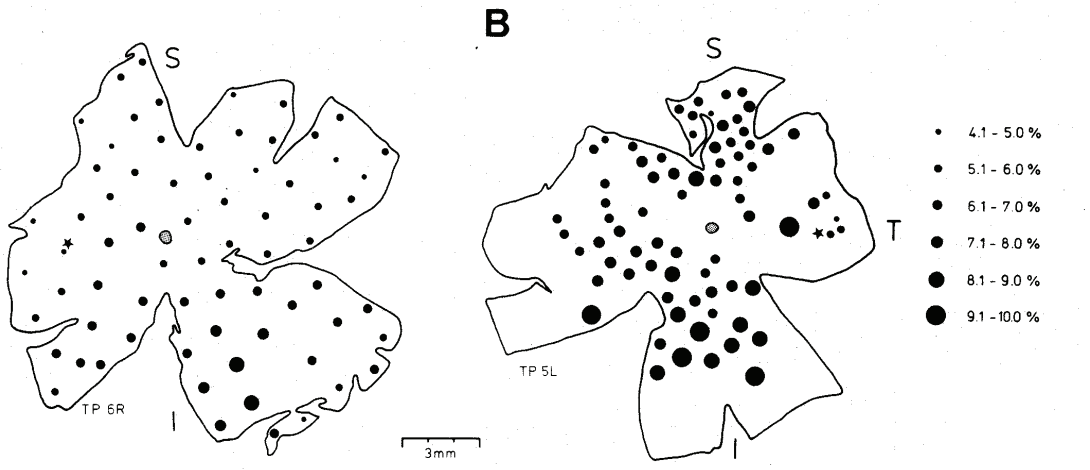

Fig. 1 Proportion of blue-sensitive cones in the entire cone population of two retinae. Each dot represents a sample field. Dot size represents the local blue cone percentage. Notice that ventral retina contains the highest SWC densities (From Müller and Peichl 1989). S=superior I=inferior T=temporal. Star indicates central area.

The blue-sensitive cones or SWCs represent 4 to 10 % of all cones. According to Müller and Peichl (1989), in the dorsal retina this subpopulation makes out 4 to 6.5%, whereas in ventral retina the value exceeds 7 % with maxima of 10% in inferior and inferonasal midperiphery. These maps are based on the darker toluidine-blue staining of the blue-sensitive cones and were confirmed with immunohistochemistry using the S-antigen antibody. For many mammalian species, cone-specific monoclonal antibodies have been developed. OS-2 is a specific monoclonal marker for blue-sensitive cones. Using the OS-2 monoclonal antibody, Petry et al. (1993) confirmed Müller and Peichl's findings.

More recently, Petry and Murphy (1995) used NADPH diaphorase histochemistry as a means for investigating the architecture of tree shrew retina. Neuronal NADPH diaphorase has been shown to be a nitric oxide synthase. NO plays a role in photoreceptor function and NADPH can be used reliably as a marker of nitric oxide synthase activity. Their findings reveal that, while all cones show intense labeling of inner segment ellipsoids, short-wavelength-sensitive cones and rods displayed intense staining of the myoid inner segment subcompartments as well. Only SWCs and rods had surface labeling of their nuclei, suggesting biochemical differences within cone subpopulations.

Petry (1995) postulates that some of the unusual functional properties reported in the short-wavelength sensitive cone system may arise from differences in photoreceptor biochemistry. The short-wavelength sensitive cones are reported to possess the following specific characteristics: a) poorer spatial acuity, b) low temporal resolution, c) response saturation at low light levels, d) longer response latencies, e) lack of an OFF-response (for review see Zrenner 1983).

Tree shrews are comparable with ground squirrels (Citellus), which also have a cone-dominated retina and a negligibly small rod population of 5-10 % (Green et al. 1975, Long et al. 1983). Under dark-adapted conditions during ERG (electroretinogram), two thirds of the ground squirrels showed a Purkinje shift and a spectral sensitivity function resembling that predicted by the rhodopsin nomogram. In the tree shrew, however, no ERG or behavioral evidence for rod-mediated scotopic vision has been found (Tigges et al. 1967, Schäfer 1969). Müller and Peichl suggest that the sparse rod population of about 5 % in the tree shrew retina is probably below the limits detectable by these methods.

1.2.2 Dorsal Lateral Geniculate Nucleus (dLGN)

Only 20% of the retinal ganglion cell axons project into the dLGN. The rest project to the tectum opticum (Colliculi superiores). This fact is significant for our studies, as it constitutes an important difference with primates (Tigges 1966). Sherman et al. (1975) identified two populations of ganglion cells differing in receptive field size, response latency and duration, and conduction velocity. This cluster of features resembled the X- and Y-cell classes in the cat. Although it is unclear whether these two classes are segregated, the dLGN is highly organized, with six cell laminae, ON and OFF segregation as well as laminar organization of ocularity (Conway and Schiller 1983, Holdefer and Norton 1995). Laminae 1 and 5 receive ipsilateral inputs; 2, 3, 4 and 6 contralateral inputs. Laminae 1 and 2 have ON characteristics, 4, 5 have OFF characteristics. Laminae 3 shows ON and OFF characteristics, and 6 shows ON and OFF but mostly ON-OFF characteristics. The projections to the cortex are shown in **Figure 2**. As Lund (1985) points out lamina three is the target of separate retinal inputs. Cells in this lamina are pale in a Nissl stain, and are considerably smaller than the neurons in other LGN layers. The cells receive input from fine-caliber axon terminals from the retina (Casagrande 1974, Conley et al. 1984). These features are characteristic of the parvocellular C laminae in the cat LGN, which receive input from slowly conducting "W" retinal ganglion cells.

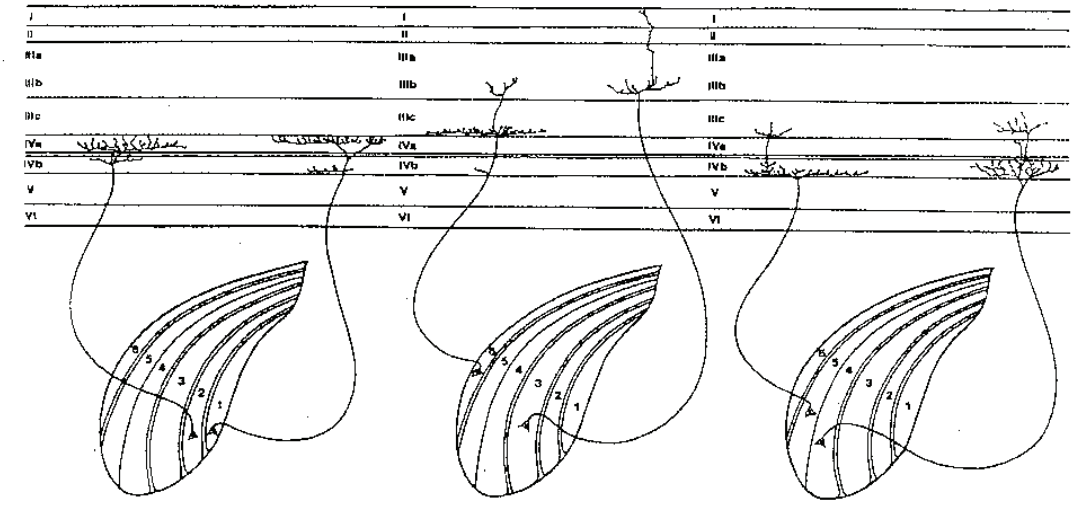

Fig. 2 – Projections of the dLGN to the striate cortex. Observe that ON and OFF laminae of the dLGN project predominantly to ON and OFF sublayers in the cortex: see text (Conley et al. 1984).

1.2.3 Striate Cortex, comparison with other species

Figure 3 depicts a comparison of cortical structure of the tree shrew with other mammals. While Tupaiae have the typical six layered isocortex homologous with other taxa, they also possess a relatively high degree of cortical sublayering. This specific tangential specialization is a derived condition, which is absent in the postulated ancestor and which in Tupaia has important functional consequences.

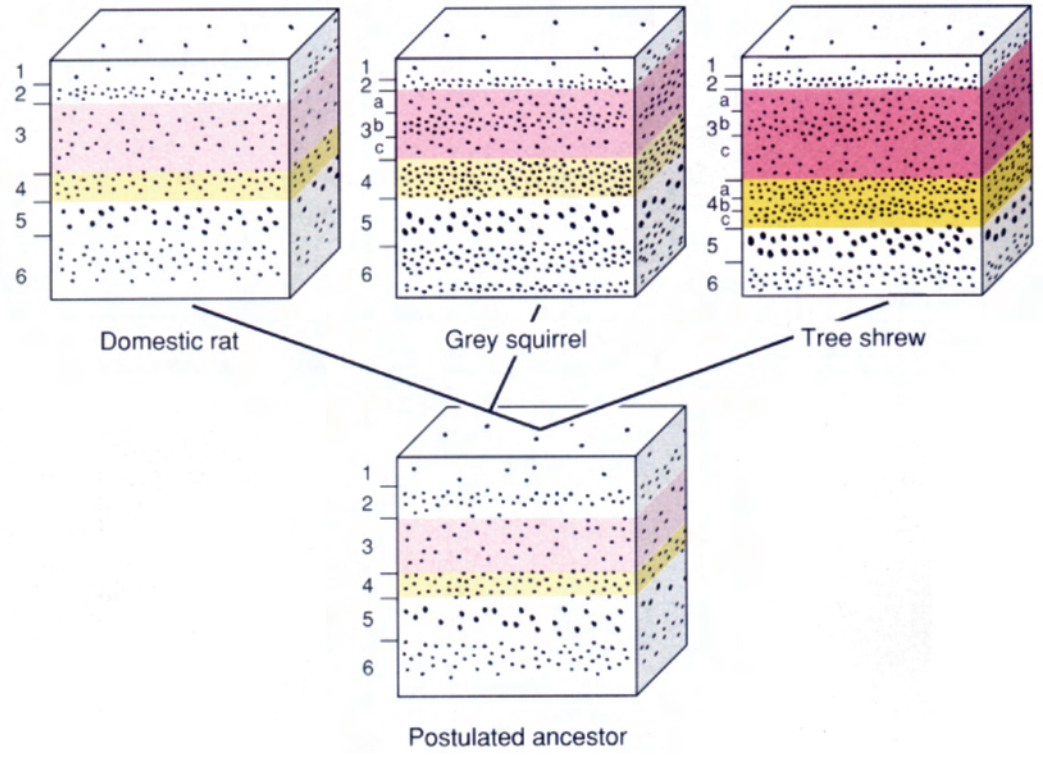

Fig. 3 – Phylogenetic comparison of tree shrew visual cortex. In each of the shown taxa, cortex is divided into six layers (homology), underscoring the phylogenetic continuity of tree shrews with other species. Out-group analysis of visual cortex lamination in **rodents** and **lagomorphs** and **edentates** (not shown) suggest that absence of division of layers III and IV is the primitive condition for mammalian visual cortices. In grey squirrels and tree shrews lamina 3 is divided into three sublayers which is a derived specialization (parallel homoplasy). A further degree of tangential specialization is witnessed in tree shrews, with their subdivision of layer IV. (Figure taken from Northcutt and Kaas, 1995).

Ocular dominance columns are absent, and transport of radioactive aminoacids show a projection of the contralateral eye to sublayer IIIb and all of layer IV, whereas the ipsilateral eye projects to the outer segment of both sublayers IVa and IVb while leaving the cell sparse cleft free (Hubel 1975, Rager and Nowakowski 1983). The geniculate afferences, therefore, overlap partially (IVa and IVb), and are segregated partially (IIIb and cell-sparse cleft) with domination of the contralateral eye. **Thus, ocularity is organized tangentially, rather than the predominantly "vertical", i.e. perpendicular, columnar organization witnessed in cats and primates.**

Moreover, this pattern of tangential rather than perpendicular organization affects not only ocularity but other aspects as well. In other species, there exists a segregation of ON and OFF channels in the different layers of the dLGN. This segregation is lost in A17. However Tupaia is the first mammal in which a persistent laminar segregation of ON and OFF responses is observed in primary visual cortex. Indeed, Tupaiae manifest a highly structured tangential organization of A17 with a cell-sparse cleft dividing layer IV into ON and OFF sublayers (Kretz 1986,1990; Rager 1983, 1991). This segregation is confirmed by cytochrome oxidase studies in combination with APB (DL-2-amino-4-phosphonobutyrat). This substance blocks the ON-channels in the retina. Following its administration, layer IVa showed much weaker cytochrome oxidase staining (Kretz and Rager 1990). Furthermore, when electrophysiologicaly identified ON and OFF axons in the optic radiation were filled with HRP and reconstructed, it was shown that the former terminate in layer IVa while the latter in IVb (Fitzpatrick and Raczkowski 1990). **Thus, in contrast to other species, one finds in Tupaia A17 a tangential segregation of ON and OFF channels** (Rager 1991)**.**

The development of retino-geniculo-cortical projections in Tupaia is different from other species. **In cats and primates the geniculate afferences project initially into layer IV and segregate subsequently into the ocular dominance columns. In Tupaia, the afferences grow from the very beginning in the same sublayers in which they are found in adult animals** (Rager 1991).

The ON-laminae of the dLGN (lamina 1 and 2) project to sublayer IVa. The ipsilateral fibers from dLGN lamina 1 project predominantly in the upper half of sublayer IVa, while the contralateral fibers from dLGN lamina 2 project additionally in the cell–sparse cleft. The OFF-laminae of the dLGN project symmetrically: the ipsilateral lamina 5 projects into the lower half of sublayer IVb, whereas the contralateral lamina 4 projects into sublayer IVb and the cell-sparse cleft. Furthermore, contralateral dLGN lamina 3 projects into sublayer IIIb and dLGN lamina 6 projects into sblayer IIIc/IVa. **Whereas in other species during development there is an exuberance of synapses which is subsequently curtailed, no such overproduction of synapses is observed in Tupaiae** (Rager 1991).

The aforementioned differences between Tupaiae and other species are summarized in **Table I**.

	Primates and Cats	**Tupaiae**
Ocularity	Organized in vertical columns	Organized tangentially within sublayers. Outer layers of IVa and IVb receive ipsilateral input. Layer IV, cell-sparse cleft and layer IIIb receive contralateral input.
Segregation of ON and OFF responses	Segregation into different laminae of the dLGN but not in cortex.	Segregation in **both** dLGN laminae and cortical layers. Cortical segregation is tangential IVa=ON, IVb=OFF.
Development of retino-geniculo-cortical projections	Genicular afferences project initially into layer IV and segregate subsequently into ocular dominance columns.	Afferences grow from the beginning in the same sublayers in which they are found in adult animals.

Table I – Summary of differences in cortical organization between Tupaia and primates and cats. Refer to text above. (Summarized from G. Rager 1991).

1.2.3.1 Topology of visual field representation in the cortex

Area 17 can be divided into binocular and monocular regions. The former are located dorsally and medially, the latter are ventral. The vertical meridian is represented along the area 17/18 border. The horizontal meridian is a line more or less perpendicular to the vertical meridian. Consequently, the upper hemifield (ventral retina) is represented caudally, and the lower hemifield is represented rostrally (see **Figure 4**). The smallest receptive fields lie at the intersection between horizontal and vertical meridians. The cortex of area 18 has a second representation of the visual field. Kaufmann and Somjen (1979a) reported the presence of both simple and complex receptive fields in area 17 and 18. Receptive fields tended to be large. Few cells were found with receptive fields narrower than one degree of arc, although these are common in the cat. Cells in area 17 preferred dark over light stimuli.

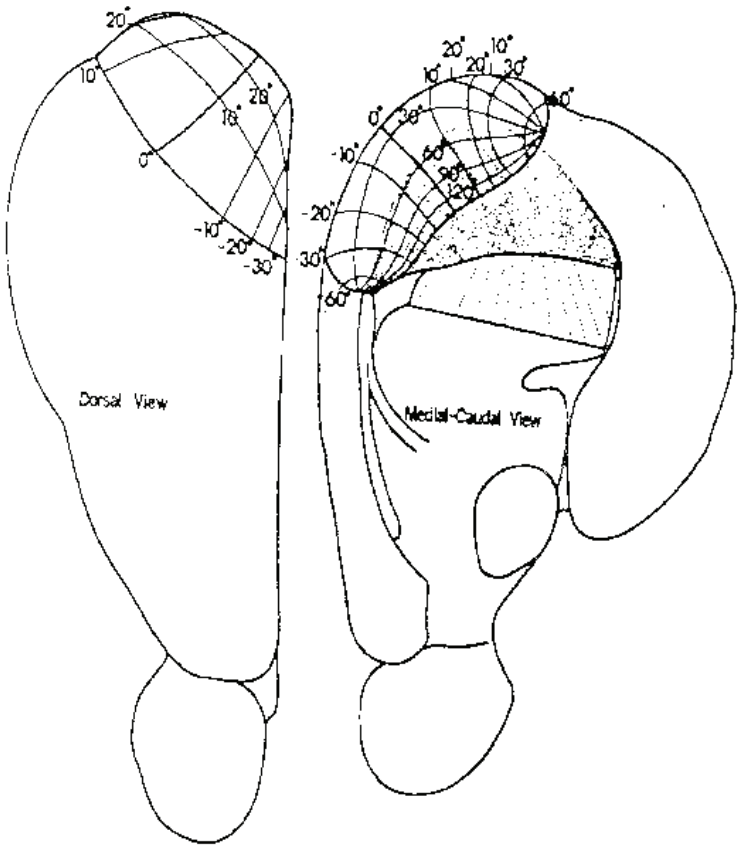

Fig 4 – Visuotopic organization of the striate cortex in the tree shrew. figure taken from Kaas 1980, see also Lund 1985). The binocular regions are represented dorsally and medially; the monocular periphery is represented in ventral cortex. There is a representation of the vertical meridian on the border with A 18. The upper visual field (ventral retina) is represented caudally.

1.2.3.2 Cytochrome oxidase reactivity

Layer IV, which receives the majority of geniculo-cortical afferents, shows high cytochrome oxidase reactivity (Wong-Riley & Norton, 1988). There are highly reactive bands in sublayers IVa and IVb, with a paler zone in between (sublayer IVm). This middle zone is wider than the cell-sparse cleft seen in Nissl staining. Supragranular layers (in particular sublayer IIIb) show a characteristic patchiness that is reminiscent of that found in primates although it is neither as well defined nor as regular (See **Figure 5**).

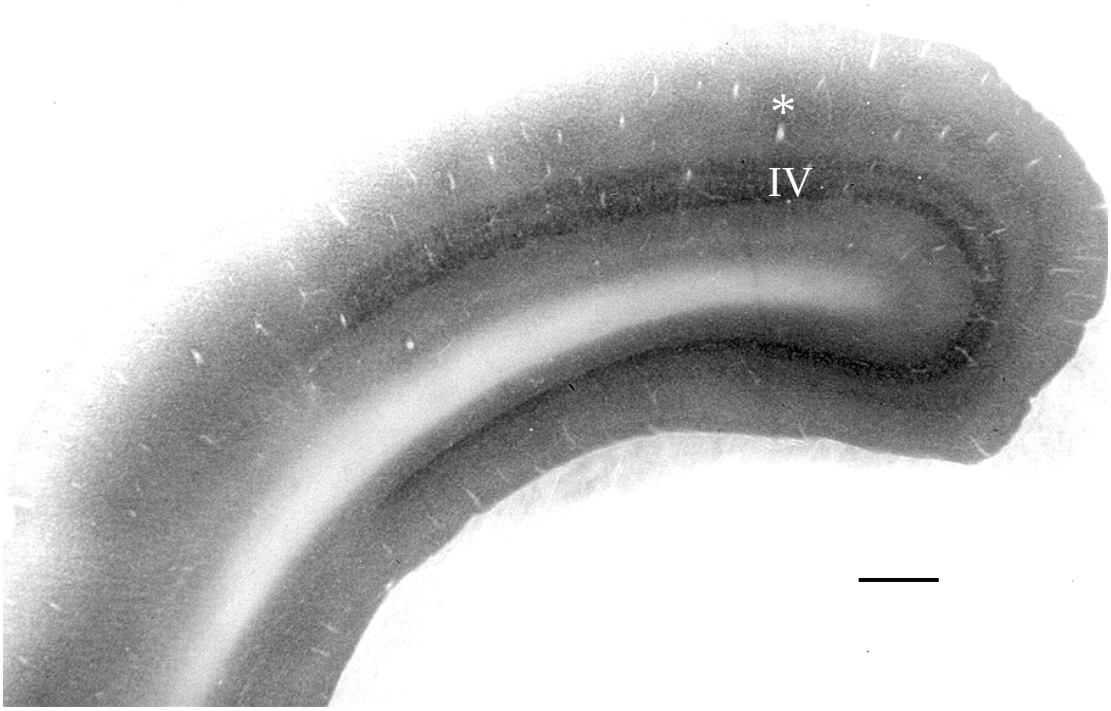

Fig. 5- Cytochrome oxidase staining of visual cortex in the tree shrew. Notice the strong labeling in the two sublayers IVa and IVb separated by lightly labeled IVm. In supragranular sublayer IIIb (indicated by asterisk) a slight degree of patchiness can be observed. Scale bar: 500 μm.

1.2.4 The question of encephalization

An important issue addressed by Kaufmann and Somjen (1979b) is the ease with which tree shrews retain high visual acuity after cortical lesions of striate and extrastriate visual cortex leading to degeneration of the entire lateral geniculate nucleus. The tree shrew, with its highly developed visual cortex, also has a highly developed extrageniculate visual system. Snyder et al. (1968) showed that tree shrews were capable of hue discrimination after cortical ablation. These results suggest that encephalization of function i.e. the transfer of information processing from subcortical to cortical regions in the course of evolution remains in the tree shrew at some intermediate stage, with redundant circuitry (Ward et al. 1970, Ware et al. 1972, Casagrande et al. 1974).

1.3 Present state of research on color vision in tree shrews

1.3.1 Early work by Tigges on Color Vision in the Tupaia

Little was known about color vision in the tree shrew previous to the work of Tigges (1963). His was primarily a primatological study seeking to come to grips with the evolution of color vision in prosimians, of whom he considered the tree shrew to be a member.

The method used in his study was behavioral and consisted mainly of two- and four-choice discriminations between chromatic and achromatic stimuli, using graded series of color and gray papers. The color series was the so-called Ostwald pigment papers and the achromatic was the Baumann series comprising 62 levels of gray. A 200 Watt light bulb was used for illuminating the stimuli.

The animals were initially trained to associate the colored, as opposed to gray paper stimuli, with a reward. Once the animals preferred the former consistently (72 % correct) they were tested for different levels of gray. In this way red, green, blue, and yellow were tested successively.

The animals preferred red to white, black, and all the gray levels in between. This was also the case for blue, green, and yellow. In tests of paired colors, all of the colors were discriminated from each other in a statistically significant way.

The above mentioned tests were repeated while varying the illumination of the experiment cage. When the latter was lower than 1 to 2 Lux, the percentage of correct choices decreased to chance levels for the four tested colors.

1.3.2 The work of Shriver and Noback on Color Vision in the Tree Shrew

Together with the article by Tigges (1963), Shriver and Noback's 1967 article on color vision in this animal represents some of the earliest attempts to investigate spectral sensitivity in this species. The authors discuss the animal's color discrimination capabilities in the context of its phylogenetic status.

At the time, color vision was generally agreed to be a capacity specific to primates (including man) and the tree shrews ability to discriminate color was one of the primary arguments adduced by those wishing to classify Tupaia as the most primitive primates.

The authors tested the animal's color vision behaviorally. Tests consisted of a random series of two-choice discriminations. Panels were illuminated using a slide projector with two lights of different wavelengths. Kodak Wratten color filters were utilized to vary the spectral composition of the stimuli. The color specification numbers of the filters used were 25A (red), 15G (yellow), 61 (green), and 47 (blue) with transmission maxima at 615, 586, 536, and 470 nm respectively. Neutral density filters in the paths of the stimulus beams were used to modulate the intensity.

Four tree shrews were trained to press a stimulus lever with a given light. One subject was conditioned to choose red, another subject blue, another green, and another yellow. The animal's task consisted basically in discriminating the "positive" color from a "negative" color; the colors were presented in a random series of two-choice trials. Each of the four "positive" colors was paired with the other three "negative" colors.

The evidence presented suggests the capacity to discriminate among different hues. Once a subject was conditioned to one of these colors, this positive-color stimulus was selected with a high degree of accuracy except in the case of red and yellow combinations. The fact that the animals chose the positive color in a statistically significant manner irrespective of the position or illumination of either color in the pair, supports the notion that hue was the criterion of the discrimination.

The authors make the following conclusions regarding color vision and taxonomic status. If the Tupaia is a representative of a primitive primate or a “missing link” group between insectivores and primates, then the following alternatives are suggested (a) These descendants of primitive primates possess good color vision systems. (b) If the original progenitors of these primates could not discriminate color, then this ability evolved independently in the tupaiid group of primates. (c) The similarities in color vision of the tupaiids and certain New World monkeys may be examples of convergent evolution.

If, however, the Tupaia is an insectivore, then, the authors say, the Tupaia would be the sole example of color vision in insectivores. This feature would be an exception since good color vision in the long wavelength end of the spectrum is not a characteristic of non-primate mammals with color vision.

1.3.2.1 Shortcomings of Tigges’ and Shriver and Noback’s work

Both of these studies constitute a first contribution to the understanding of color vision in this species. Thanks to this work, the tree shrew’s capacity for color discrimination was established, and initial behavioral data was obtained.

Nonetheless, both Tigges and Shriver and Noback relied on vary large variations in brightness to control for brightness cues. Subsequent and more precise control of stimulus intensity, as witnessed in Polson’s work, was needed in order to determine spectral sensitivity (Polson 1968).

1.3.3 Polson's Doctoral Dissertation on Color Vision in Tupaia

Polson's investigation of the properties of color vision of Tupaia glis, submitted in 1968 to the University of Indiana as a doctoral thesis but not published otherwise, in the form of an article, constitutes the most thorough examination of the properties of color vision in the tree shrew. Her investigation seeks to establish the spectral sensitivity function of Tupaia and determine whether color vision in these animals is based on a trichromatic or dichromatic mechanism. Furthermore it compares the Tupaia visual system with that of humans.

The work involved no electrophysiology but examined the psychophysics of color discrimination in this species using different behavioral forced-choice tests in which the animal had to choose between different alternatives. In every experiment, all the alternatives were the same, except one, which was different in some relevant dimension to be tested. The following tests were conducted: Purkinje shift test and luminosity function using critical flicker fusion, neutral point test, saturation function, wavelength discrimination function, and determination of isochromatic lines. The following is a summary of each test.

1.3.3.1 Purkinje shift test and luminosity function

Tupaia has a cone-dominated retina. Polson set out to confirm the presence of a single photopic visual mechanism. In that way she tried to determine, if Tupaia indeed has a morphologically *and functionally* all cone retina ruling out the possibility that the animal has both photopic and scotopic visual functions with a corresponding shift in spectral sensitivity or Purkinje shift.

The method used to test sensitivity is the critical flicker fusion (CFF) test. This test is based on the observation that as flickering light is dimmed, there is a point at which it no longer appears to flicker. This point depends on the subject's sensitivity to a given light. The more sensitive a subject is to a given wavelength, the dimmer it can be made before fusion occurs. For lights of equal luminance, the fusion intensity is the same regardless of

wavelength. The flicker rate-fusion intensity function shows that the light intensity required to detect flicker increases as the flicker rate increases.

Critical flicker fusion should not be confused with flicker photometry. The latter is another means of determining spectral sensitivities using flicker. It is based on the fact that if two lights of different wavelengths are alternated at a given flicker rate, the impression of flicker will be minimized when the lights are of equal luminance.

Polson's first test used the critical flicker fusion (CFF) principle to measure the sensitivity of the tree shrew to different wavelengths, and, by examining this data, decided whether stimuli of low intensity gave evidence that there was a Purkinje shift. The Purkinje shift is an increased sensitivity to shorter wavelengths under scotopic conditions (such as is found in humans).

Animals were trained to select a flickering panel in an experimental cage containing other panels illuminated with non-flickering (continuous) light of the same wavelength. At first only two widely separated wavelengths were tested (480, 633 nm), in order to determine whether there was a Purkinje Shift. Then different wavelengths were tested: 452, 494, 506, 538, 576, 605, 633, 646 nm to determine the spectral sensitivity. The light beams used as stimuli came from tungsten filament lamps, they were filtered using Kodak Wratten filters.

It was necessary to correct for the change in luminance of the positive window produced by the episcotistor, used to generate flicker, which cut out half the light. Without any correction, the positive stimulus would be lower in luminance than the other three windows. Because it would be difficult to exactly match the windows in brightness and because a light below the fusion intensity appears brighter than would be expected on the basis of average luminance, the other windows were not darkened exactly 0.3 log units, which would be the correction based on average luminance. Instead, they were randomly darkened on each trial by 0.1 to 0.4 log units so that the positive window varied in brightness relative to the darkest, eliminating any systematic brightness cues.

The procedure was repeated until 20 trials were collected at each intensity level on all combinations of flicker rate and wavelength. The criterion for flicker fusion intensity was

arbitrarily defined as the intensity at which the animal chose flickering light correctly 60% of the time.

Dual visual systems (those incorporating both photopic and scotopic mechanisms) sample visual data in two ways. The photopic (cone) system analyzes visual data with great detail and provides chromatic information. However it requires a sufficiently intense stimulation and thus has lower sensitivity. Furthermore, its temporal resolution is lower. The scotopic visual system is more sensitive and has higher temporal resolution (flicker fusion occurs at lower frequencies), but lower acuity.

This means that when we plot the flicker rate-fusion intensity curve of a dual visual system for any given wavelength, there is a photopic branch (higher frequencies and intensities) and a scotopic branch (lower frequencies and intensities). When the photopic branches for different wavelengths have been aligned, the variation with wavelength of the slope and position of the lower frequency and intensity branches of the flicker rate-fusion intensity curve reflect a difference in relative sensitivity of scotopic and photopic vision. This is the Purkinje shift.

Polson's results showed that there is no clear rod-cone break in the Tupaia curve such as is found in the human curve between 20 and 25 cps (cycles per second). The difference in sensitivity to the two wavelengths (487,633 nm) does not change appreciably as the flicker rate varies, indicating that there is no Purkinje shift.

Tupaiae are .56 log units more sensitive to the No 29 filter (633 nm) than to the No 45 filter (487 nm). Normal humans are .73 log units more sensitive to filter No.29 in the photopic branch, but 0.9 log units more sensitive to the No 45 filter in the scotopic branch. This shift towards higher sensitivity in the short-wavelength under scotopic conditions is the Purkinje shift. Polson's data indicates no such shift in Tupaia: the animal has only one spectral sensitivity function and it is photopic in nature.

The same CFF method with different wavelengths was used to measure spectral sensitivity. The results of Polson's measurements are given in **Figure 6.**

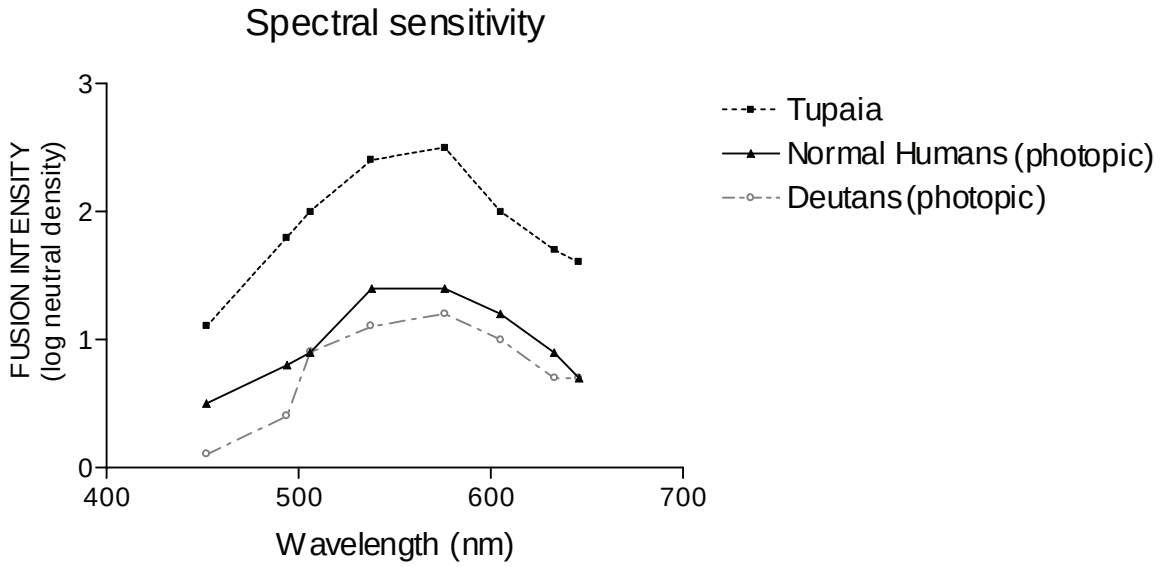

Fig. 6 – Mean photopic spectral sensitivity function of five Tupaia glis, five normal observers and four deutanopic observers plotted in terms of log neutral density filters in beams at point of 60% correct flicker fusion discrimination. (Figure generated from Polson's data p.185).

1.3.3.2 Color discrimination tests

1.3.3.2.1 Neutral point test

We can learn a great deal about a visual system by observing if and when a subject confuses monochromatic light with filtered light. According to the Young-Helmholz theory, subjects with trichromatic vision can distinguish any wavelength of light from white light, whereas subjects with monochromatic vision (a single photopigment) will confuse all wavelengths of light with white light given the proper brightness match. If color vision is dichromatic there must be one region of the spectrum in which both photopigments are stimulated in the same proportion as they are by white light. Such monochromatic light will be indistinguishable from white light.

The same animals as in the previous experiments were trained to choose monochromatic light from the three white light standards (negative stimuli). The colored light came from a grating monochromator with slit width of 12 nm. White light came from tungsten filament light bulbs. Intensity modulation was done using neutral density filters for both the standard and comparison beams. To avoid brightness clues, all beams were randomly varied in brightness by 0.0 to 0.3 log units. The task for the animal was to choose the colored stimulus from the white light. Five trials were collected at each spectral point from 440 nm to 640 nm in 5 nm steps.

For all animals, performance was near 100% at wavelengths below 490 and above 525 nm. Performance drops to 60 % by 497 nm and 516 nm. It is at chance level or below by 504 nm and stays so until 507 nm. This value is close to that obtained in human deuteranopes. However protanopia cannot be ruled out, since the neutral point of a human dichromat shows a great deal of variability depending on the degree of ocular pigmentation as well as the color temperature of the standard white light used. A further possibility is that Tupaiae are anomalous trichromats, hence, additional color discrimination experiments are required to confirm the dichromacy hypothesis. These experiments are the saturation discrimination, wavelength discrimination, and color confusion tests, which will be summarized in the following sections.

1.3.3.2.2 Saturation test

Saturation is defined as the degree of difference between a given hue and gray of the same intensity. It is calculated by determining the least intensity of spectral color that must be added to a white light in order for the mixture to be discriminated from white light of the same luminance as the mixture. If a pure spectral light can just be discriminated from white light, then the saturation index is zero. The saturation index increases for wavelengths both longer and shorter than the neutral point. The threshold for saturation discrimination is greater for color defective subjects than for subjects with normal color vision.

The saturation discrimination test is a corollary of sorts of the neutral point experiment. While the latter determines what pure spectral colors can be distinguished from white, the former specifies what is the least amount of pure light that needs to be added to white in order for the subject to distinguish it from white. Hence, the saturation index can be seen as a quantificational epilogue of the neutral point test.

Polson's method was the following: on any given trial three of the four stimulation windows were illuminated with white light of luminance L_{WS}. The fourth window contained a mixture of white light at a given luminance L_{WV} and monochromatic light of some wavelength at a stated luminance L_{λ}. The task for the animal was to pick out the mixture.

The intensity of the mixture $L_{WV} + L_{\lambda}$ was kept constant by adding or subtracting half of the neutral density value necessary for the proper brightness correction in the monochromatic beam and the other half in the white beam.

At each wavelength, the animal was first presented the most saturated light possible in the first series. If it could discriminate this mixture, the amount of monochromatic light was decreased until the mixture could still be discriminated 100 % of the time. At this point data collection began. The amount of monochromatic light was decreased in 0.1 log unit steps until performance decreased to chance level.

The saturation function of Tupaia shows the clear break in the region of the neutral point, which is expected from dichromats. The curve also has the same general shape as other investigators have found for dichromats of the protanopic and deutanopic type.

1.3.3.2.3 Wavelength discrimination

The wavelength discrimination function is a plot of the smallest wavelength difference $\Delta\lambda$ that can be detected for various wavelengths (given that the two wavelengths are matched for brightness).

For humans, the curve reaches one minimum at 480 nm, where differences as small as 1 nm are detected, then rises to a maximum near 540 nm. There is another minimum at 600 nm. The functions are U-shaped for protanopes and deuteranopes with minima at or near the neutral point.

Polson's procedure and apparatus were the same as in the neutral point experiment, except various wavelengths of light other than white were used. For a given standard wavelength λ_S the three standard windows were set at that wavelength, and the variable window was set at the wavelength λ_V that should be discriminated from the standard. The difference between λ_S and λ_V was then decreased in small steps until performance broke down. The difference was then gradually increased until performance was 100 % again. This was repeated with λ_S set at various wavelengths across the spectrum.

All standard wavelengths were equated for luminance on the basis of the Tupaia luminosity function. The function was also used to equate the brightness of the variable beam at each point to that of the standard. In addition, to avoid brightness cues, all four beams were varied in luminance by 0.0 to 0.3 log units.

Both longer and shorter wavelengths could be discriminated from λ_S=506 nm and λ_S=490 nm. A 15 nm wavelength difference in either direction was discriminated almost 100% of the time in the case of either of these standard wavelengths.

For λ_S=470 nm discrimination was near 100% when λ_V was 530 nm, dropped to chance as λ_V approached 510 nm, was below chance from 510 nm to 470 nm and only slightly above chance from 470 to 435 nm. Thus, in the case of a standard wavelength considerably shorter than the neutral point wavelength, wavelengths longer than the neutral point could be discriminated from it while those shorter than the neutral point could not.

A similar situation was true for the standard longer that the neutral point: λ_S=539 nm. Wavelengths shorter than the neutral point were discriminated, while those longer were not. In each case, wavelength on opposite sides of the neutral point could be discriminated from each other, whereas those on the same side could not.

This is accord with the hypothesis that Tupaiae are dichromats. The wavelength discrimination function has the same general U-shape with minima near the neutral point as found by other investigators for dichromats of the protanopic and deuteranopic type.

The fact that Tupaia cannot discriminate among wavelengths that are on the same side of the neutral point gives conclusive proof that they are dichromats and not anomalous trichromats.

1.3.3.2.4 Isochromatic lines

In addition to confusing certain colors with each other, as discussed in the wavelength discrimination experiment, dichromats confuse some spectral colors with certain extraspectral colors. When the colors, which are confused with each other by dichromats, are plotted in the xyz coordinates of the CIE system, they fall approximately on a straight line, called the isochromatic line for that individual. For a given type of trichromat, these lines converge at a certain point on the chromaticity diagram called the copunctal point. The CIE coordinates are conceived for trichromats, and the chromaticity value of the copunctal point represents the chromaticity which would theoretically have been given, had the dichromat been a trichromat.

The apparatus and procedure used by Polson were the same as in her neutral point tests, except that instead of using white light in the standard beam, she used Wratten filters No. 31, No. 34A, and No. 34 whose chromaticity coordinates are (x=0.6095 y=0.2623), (x=0.3917, y=0.1286), and (x=0.2764 and y=0.0692) respectively. These chromaticity coordinates are all close to the lower extraspectral boundary.

Tupaia confused the extraspectral colors with the blues, greens, and yellows (wavelengths 465-560 nm). Tupaia isochromatic matches do not converge to a point, so a copunctal point could not be calculated. The confusion range (497-516 nm) for white light includes the predicted matches for deuteranopes (497, 498, 501 nm) but not those for protanopes (493 and 494 nm).

Therefore, Polson concluded from the isochromatic matches on the three extraspectral colors and white light that Tupaiae are definitely dichromats of the deuteranopic rather than the protanopic or tritanopic type.

1.3.3.3 Conclusions drawn from Polson's study

In the Purkinje shift test, Tupaia exhibits only a photopic CFF function when tested with widely separated wavelengths of 487 and 633 nm. Subsequent testing with different wavelengths gives spectral sensitivity functions, which confirm this finding. The slope of the flicker rate-fusion intensity curves was approximately the same as in the photopic branch of the normal human function.

In the neutral point experiment, Tupaia shows a definite neutral point around 505 nm. This location agrees with the point of maximum error for human deutans and is longer than that of protans tested on similar apparatus (494 nm). Tupaiae can discriminate wavelengths in the yellows and blues from white light, indicating that they are not tritans.

The Tupaia wavelength discrimination function is U-shaped with the minimum near the neutral point of 505 nm. Tupaiae are unable to discriminate among wavelengths on the same side of the neutral point. This confirms that Tupaia are not anomalous trichromats. Furthermore, tritanopes cannot discriminate among nearby wavelengths in the region of 490 nm where the discrimination of Tupaia is relatively good.

The results of the isochromatic lines experiment definitely show that Tupaiae are dichromats of the deuteranopic type. The three extraspectral purples tested by Polson were confused with blues, greens, and yellows (470 to 537 nm). Matches in this region are predicted for deuteranopes from copunctal points. Nonetheless, their isochromatic matches are located at somewhat longer wavelengths than those of human deuteranopes.

However one cannot conclude from the results that Tupaiae have color vision identical with that of human deuteranopes. The Tupaia relative photopic luminosity function has a slight loss in the long wavelength relative to the CIE photopic, which humans do not exhibit. Furthermore, their photopic sensitivity is nearly a log unit higher than that of either humans deutans or normals. Neutral point and saturation discrimination functions, nonetheless, resemble closely that of human deutans.

1.3.3.3.1 Polson's evolutionary considerations

If Tupaiae are considered primates and ancestors of higher primates, then their dichromatic color vision indicates that trichromatic vision in higher primates evolved from dichromatic vision. If Tupaiae are not ancestors of primates, but rather belong to insectivores or some other separate classification, then Tupaiae and higher primates could have inherited color vision from some common ancestor or parallel evolution took place with both developing color vision at some later date.

1.3.3.3.2 Interest of the study of Tupaia according to Polson

According to Polson, the interest of studying Tupaia is grounded on the following two reasons:

a) no other mammal at the time was known to possess dichromatic color vision,

b) the nearly total isolation of a photopic visual system from scotopic mechanisms offers a unique opportunity for understanding the neural coding of color vision.

1.3.4 The work of Jacobs and Neitz on Color Vision in Tupaia

Jacobs and Neitz, working at the Department of Psychology of the University of California in Santa Barbara, published an important article concerning the spectral mechanisms of the tree shrew visual system (Jacobs and Neitz 1985). They confirmed the postulated dichromacy of these animals as proposed by Polson in her 1968 doctoral dissertation.

In their view the animals cone dominated retina (according to their figures rods comprise only 3-4 % of the total receptor complement) is an extreme adaptation to diurnal life only comparable, among mammals, to the ground-dwelling sciurids. Their study consists of behavioral and ERG measurements of the tree shrews spectral sensitivity.

For the behavioral testing a three-alternative, forced-choice discrimination task was used. Three panels (2.5 cm diameter) were mounted in a row. Of these two were illuminated identically to one another with achromatic light. One of the panels, selected randomly, was illuminated with monochromatic light from an Instruments SA, Model H-10 monochromator (half energy passband = 16nm).

The animals were trained to select the uniquely illuminated stimulus panel among the three panels. Over trials, animals were required to discriminate the monochromatic from the achromatic lights as the wavelength of the former was varied from 475 to 514 nm in steps of 3 nm. The intensity of the monochromatic light was varied in steps of 0.1 log unit over a range of intensities.

Once the animals were consistently discriminating the 475 and 514 nm lights at all of the intensity values, the test was expanded to include all of the intermediate wavelengths. An increment threshold procedure was used to measure sensitivity. At each tested wavelength, the intensity of the light was varied in steps of 0.3 log unit until performance reached a level of 90 % correct.

The result of these psychometric functions is that the animals learned successfully to discriminate 475 and 514 nm lights from achromatic light. However as the test light approached the postulated neutral point of 505 nm, performance deteriorated dramatically.

The dichromatic vision of tree shrew's postulated in Polson's dissertation was thus confirmed. The location of the neutral point suggests a striking similarity with human deuteranopes.

These results are confirmed by flicker photometry tests (ERG) during conditions of long and short-wavelength adaptation. In this study, the behavioral and physiological results indicate two sensitivity peaks at approximately 440 nm and 550-560nm with an intermediate region of lowered sensitivity centered at about 500 nm.

In summary, this study confirms the psychophysical findings of Polson's dissertation. The authors suggest that the animal's straightforward dichromacy uncomplicated by a great heterogeneity of retinal architecture or by a large population of rods makes it an attractive model for the analysis of dichromatic color vision.

1.3.5 The work of Van Dongen et al. on the functional classification of cells in the optic tract

This article, published in 1976, reports the results of recordings made from single optic tract fibers by means of tungsten microelectrodes. In total, 93 units were investigated and they were classified in the following groups:

tonic	29
phasic	29
on-off	7
OFF	2
direction-selective	16
orientation-selective	6
opponent-color	1
edge-inhibitory-off-centre	1
not classified	2
Total	93

According to this study only one out of 93 cells was color-opponent. The cell gave a sustained on-response to blue light and sustained off-response to red light. The maximum sensitivity for short wavelengths was at about 440 nm and for long wavelengths at about 560 nm. The reversal point for on- and off-responses was at about 500 nm. This is in accordance with Polson's behavioral measurements. (Polson 1968). The receptive field centers of both mechanisms (measured with area-response curves) were equally large (1.2 deg.). The red mechanism had an on-surround, as was demonstrated with a monochromatic far red (656 nm) annulus (2.4-9.6 degs.) and a small (0.6 deg.) steady central red spot. The blue mechanism did not reveal an off-surround.

1.3.6 Kretz' Study of Color Opponent Units in the Tupaia dLGN and A 17

Kretz et al. (1989) carried out single-unit recordings in the dorsal lateral geniculate nucleus and in the primary visual cortex (A17). The goal of this study was to investigate the spectral interactions involved of the two types of cone (short-wavelength sensitive and long-wavelength sensitive) of the cone-dominated visual system of tree shrews.

The authors concluded that most cells in the dLGN and visual cortex were broad-band, responding to stimulus onset and offset throughout the spectrum. Color-opponent units could also be found, but far less frequently. Color opponency was shown to be based on the two different cone receptor types (see **Figure 7**).

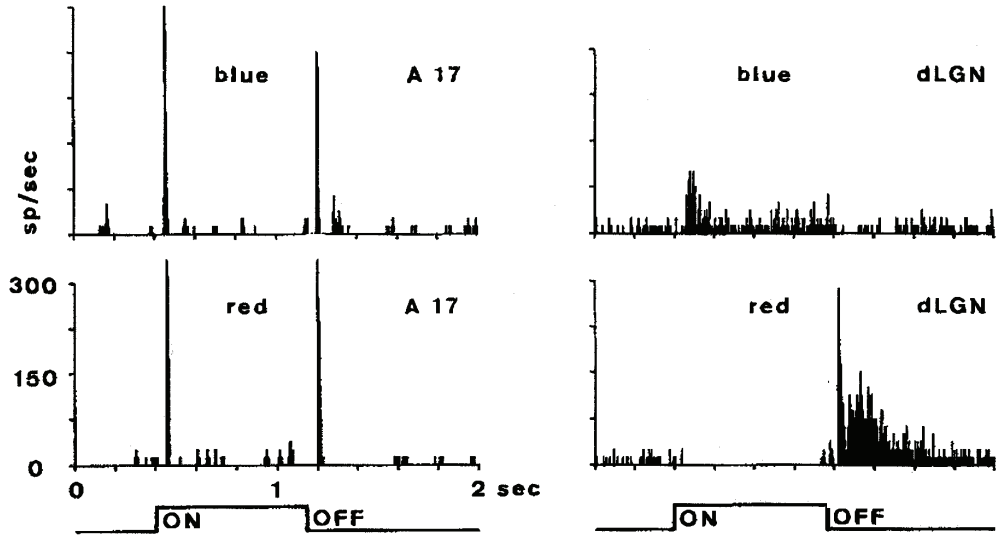

Fig. 7 – Histograms showing the response characteristics of a broad-band cell in area 17 and a color opponent unit in the dLGN (lamina 3). The cell activity measured in response to the spectral stimuli (blue and red refers to Wratten filters No 47B and No 29, respectively) is given in spikes per second. Twenty stimulus repetitions were used to produce each histogram (Kretz et al. 1989). Histograms above and below are plotted using the same units. Binwidth = 4 ms.

1.3.7 The work of Snyder et al. dealing with the role of the Colliculus superior in color-vision

In the evolutionary history of color vision, two mechanisms are involved, those found in the retina, and those found beyond, in the central nervous system. While a restricted set of genes determine the last chemical steps required for the expression of the complete set of pigments required for color vision, much less is known about the steps leading up to color processing circuitry in the brain.

In lower vertebrates, the optic tectum is the target of the optic nerves and the locus of color coding circuits. Primates however cannot perform color discrimination tasks after ablation of visual cortex (Kluver, 1941).

In their article on color discrimination in the Tupaia after occipital lobectomy, Snyder et al. (1969) showed that the test animals performed color discrimination tasks with ease, concluding that the Colliculus superior mediates color vision in this species. In this section we wish to discuss this article in some detail.

Lesioned animals were trained to choose a chromatic stimulus of 610 nm (orange light) rather than achromatic (neutral-density filtered) light in order to get food. The task was mastered with astonishing ease in view of the severe deficits in relearning habits based on simple pattern recognition (presumably a consequence of the lesions).

The intensities of both the chromatic and achromatic stimuli were varied over a range of 5 log units, and the training continued. Subsequently, alternative hues were substituted for the orange light on every third trial with the hope that the animals would transfer hue preference to colors other than orange. The transfer was successful, meaning the animals were basing their choice on wavelength cues and not on luminance since the intensities of both chromatic and achromatic stimuli continued to be varied systematically.

The animals carried out the color discrimination tasks with near perfect performance levels. The lesions in both hemispheres went well beyond A17 and included extrastriate cortex up to the auditory areas (in one hemisphere). Retrograde degeneration covered all of the dLGN and most of the pulvinar.

1.3.7.1 Comparisons of tree shrews and monkeys with regard to color vision mechanisms

Kluver (1941) has shown that occipital lobectomy abolished color-vision in monkeys. Normal monkeys trained to prefer violet and reject yellow, continued to reject yellow in later tests, when this color was presented with either black or white, and persisted in accepting violet in preference to either black or white. “This shows that hue and not intensity or brightness was the basis for the original discrimination.” (Snyder et al. 1969).

However, monkeys having undergone a bilateral occipital cortex ablation and “responding to one of two colors or to a color instead of white light, will immediately respond to the other color or to white light, if the proper intensity changes are made” (Kluver, op.cit.)

Unlike these monkeys, the tree shrew reported in the paper by Snyder et al. (1969), correctly discriminated colors from gray light after cortical lesions. Excluding the unlikely explanation that the residual capacity is mediated by the severely damaged pathway connecting the secondary visual area to temporal cortex via the pulvinar (practically all of it showed retrograde degeneration), one is led to the conclusion that the tree shrew’s superior colliculus can mediate color in the absence of all of the visual cortical areas.

This leaves us with the thought-provoking prospect that the tectal mechanisms for color in Tupaia are homologous with those present in reptiles and birds. As the telencephalon evolved in mammals, there were transition stages in which either the

forebrain or the midbrain played the leading part and the tree shrew may, as Snyder suggests, represent an intermediate stage of evolution. (For discussion of this and other theories of brain evolution see Butler and Hodos 1996.) The extent of the cortical lesions in their experiment is shown in **Figure 8**.

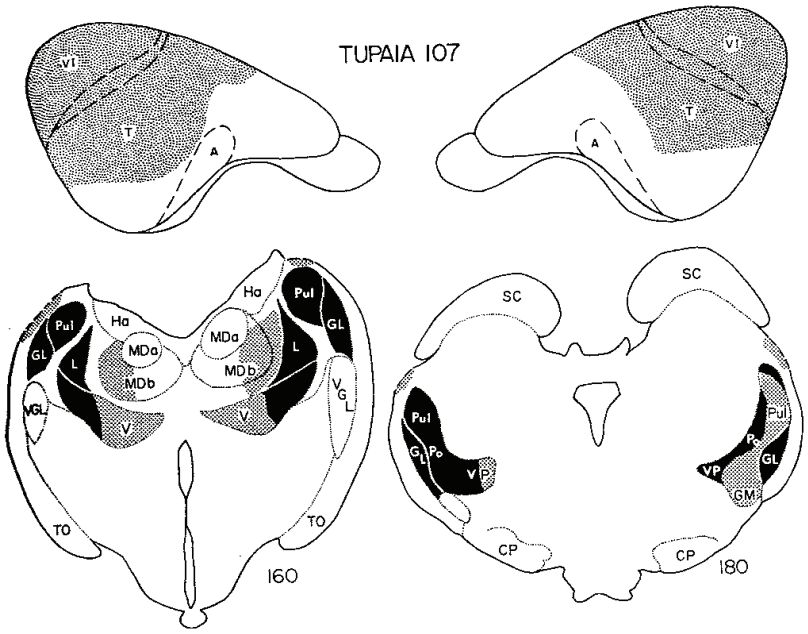

Fig. 8– Cortical lesions and degeneration in the thalamus in Tupaia 107 (from Snyder et al. 1969). Stippling shows ablated area. Extent of thalamic degeneration: Severe degeneration in black, moderate or slight degeneration shown by stippling. Abbreviations: A, auditory area; CP, cerebral peduncle; GL, dorsal lateral geniculate body; GM, medial geniculate body; Ha, habenular complex; L, lateral nuclei,; MD mediodorsal nucleus; Po, posterior nuclei; Pul, pulvinar; SC, superior colliculus; T, temporal area; TO, optic tract; V, ventral nuclei; VGL, ventral lateral geniculate body; VP, ventroposterior nucleus; V1, primary visual area .

1.3.8 Petry's study of differential stimulation of color and luminance channels during development

Cells in the luminance channel receive additive inputs from the different classes of cones. Cells in the color-opponent channel, on the other hand, antagonize signals from two or more cone types. In the tree shrew, only two types of cone receptors exist: long-wavelength sensitive cones (LWCs) and short-wavelength sensitive cones (SWCs); the latter constitute a marginal 5% of the total cone population. The proportion of rods is also minimal, and represents only about 5 % of the total photoreceptor population. Hence, it can be plausibly hypothesized that the respective cone contributions to the luminance and color-opponent channels are as described in **Fig. 9**.

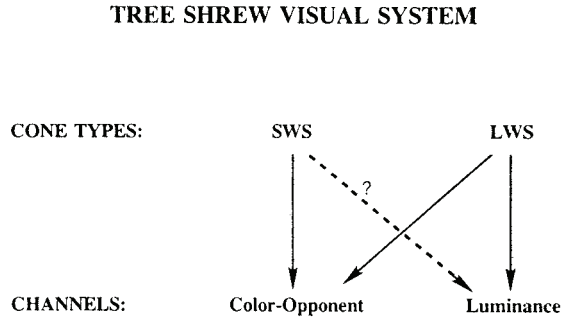

Fig. 9 Cone inputs to the color-opponent and luminance channels in the tree shrew. The dashed line indicates the -- possibility of a small (inhibitory) contribution of the SWCs cones to the luminance channels. (Figure taken from Petry 1993)

It is known that early visual experience is necessary for the development of synaptic connections in the visual system. It has been shown that suture or enucleation of one eye, causes an expansion of the ocular dominance columns of the other (functional) eye, suggesting a mechanism of binocular competition (for summary see Hubel 1978).

The peculiarities of the Tupaia visual system allow us to test if this principle applies also to functional visual channels (i.e. the color opponent vs. luminance channel). In other species the differential stimulation of one of these channels is a difficult condition to achieve experimentally. In the tree shrew this is easier. The tree shrew's deutan-type cone-dominated retina with the respective absorption spectra of the two cone types widely separated along the wavelength axis makes it possible to selectively deprive one set of cones of photic stimulation, without affecting the others. By rearing the animals in light of wavelengths greater than 600 nm, one can ensure no stimulation of the short-wavelength sensitive cones or of the minimal (5%) rod sub-population as illustrated in **Figure 10**.

This is a specific advantage of dichromats. In trichromats, red light would stimulate both long- and middle-wavelength sensitive cones, activating both the luminance and the color-opponent channels. This experimental paradigm in Tupaia was used by Petry to examine the developmental consequences of such a deprivation (Petry 1993). It can help to determine if, like ocular dominance column expansion, there is an encroachment of luminance channel circuits upon understimulated color-opponent ones.

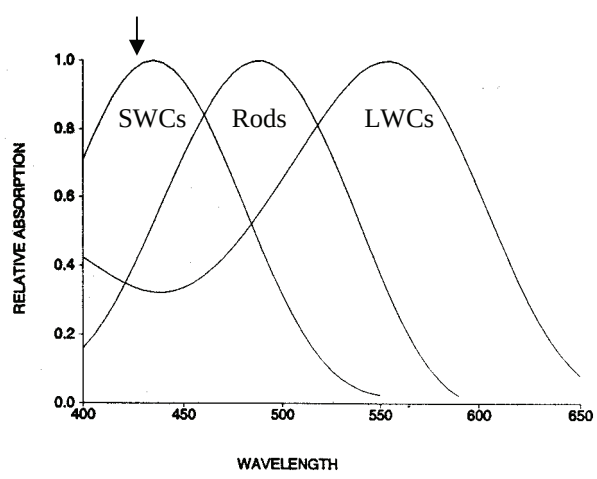

Fig. 10 Relative absorption of tree shrew visual pigments. Petry used Kodak safelight 1A filters for red light rearing. They do not transmit wave-lengths shorter than 600 nm. Thus only the LWCs could have been stimulated. (Figure taken from Petry 1993).

Red-light-reared animals performed above chance level for at least some regions of the spectrum, indicating that these animals preserved color vision. However, the performance of the red-light-reared tree shrews was overall poorer than that of control animals. Further examination revealed that this loss in performance, was due neither to loss of SWCs or altered retinal spectral sensitivity in red-light-reared (RLR) and control animals.

It was the level of cytochrome oxidase reactivity in the primary visual cortex that gave the most conspicuous difference RLR and control animals. In all of the tree shrews reared from birth in the red light, C.O. reactivity in layer IV was more uniform**.** Measurement of optical density in layer IV showed all sublayers including IVm to be more darkly stained in RLR animals than in controls.

The relative deprivation of the color-opponent channel following red light rearing explains the differences in C.O. reactivity of RLR animals and their poor performance on tasks involving chromatic/achromatic discrimination. In a manner analogous to the relative expansion of non-deprived into deprived ocular dominance columns, the apparently luminance driven, and cytochrome rich cells in sublayers IVa and IVb progressively invade IVm. Petry (1993) concluded that cells in this sublayer probably belong to the color-opponent channel.

1.4 Interest of the Tupaia as an alternative experimental model for the study of color vision

Given that the Tupaia retina is cone-dominated it provides a unique model for studying color vision in isolation from other (scotopic) mechanisms. This nearly total isolation of a photopic visual system from scotopic mechanisms offers a unique opportunity for understanding the neural coding of color vision. Regardless of whether the Tupaiae be considered as closer to primates, with whom they share many characteristics (Le Gros Clark 1960), or more akin to insectivores, the study of this animal may, aside from its intrinsic interest, provide some insight into the evolution of color vision.

Furthermore, as Petry (1993) has eloquently pointed out, the peculiarities of the Tupaia visual system make it an ideal model for testing the effects of differential stimulation of the luminance and color-opponent channels. With its deutan-type retina characterized by widely separated absorption spectra of the two cone types, it is possible to deprive one set of cones of photic stimulation, an experimental condition difficult to achieve in other species.

It is interesting to inquire into the respective roles played by neocortical and subcortical (i.e. mesenchephalic) circuits in color vision in this animal, since it has been shown by Snyder and collaborators (1969) that the animals discriminate color correctly after ablation of the visual cortex. In this respect, the Tupaia continues to be a subject of intense discussion. That the animals represent an intermediate degree of function transfer from tectum-like to neocortical regions is not only thought provoking but continues to be cited in textbooks on Comparative Neuroanatomy (Butler, Hodos 1996) as an example to back one of the influential theories of brain evolution.

Besides this, there are other aspects of this animal's cortical architecture which make it a unique and valuable model, most significantly of which is perhaps the fact that the animal has a tangentially organized visual cortex with clear segregation of ON- and OFF-units and no ocular dominance columns (Hubel 1975, Kretz 1986, Rager 1991).

1.5 Objectives of Our Study

From the aforesaid, it is clear that the retina of the Tupaia possesses three types of photoreceptors: rods (λ_{max}= 490 nm), SWC (λ_{max}=425 nm), and LWC (λ_{max}= 555 nm) (Petry and Harosi 1987, 1990). In this thesis, we seek to examine the nature of spectral processing interactions in the visual system of tree shrew. We wish to characterize the electrophysiological responses to different wavelengths and intensities, and in this way to come to grips with the neural coding of color in this animal. Specifically, we are seeking to determine the relative contribution of the two cone types to the spectral sensitivity of A17 neurons and thus to determine what is the nature of color processing mechanisms in a dichromatic color system. Furthermore, we wish to determine what is the proportion of broadband to color-opponent units and whether there is a specific lamination of color specific units.

In this way we wish to fill a gap in the literature: practically no electrophysiological studies of color vision in tree shrew cortex exists.

We also wish to characterize the electrophysiological responses to spectral stimulation in the extragenicular system, i.e. in the Colliculus superior and thus determine what role this structure may play in color vision. It has been shown that removal of cortex does not suppress color vision in tree shrews, but no investigation color in the mesencephalon are available for this species.

Finally, since there is a higher density of short-wavelength sensitive cones in certain parts of the retina (e.g. ventral retina), we wish to determine if in the cortical areas representing this part of the retina there is some preferential tuning for this part of the spectrum.

Materials and Methods

2 Materials and Methods

2.1 Surgical Preparation of the animals

Adult tree shrews were drawn from the colony at the Institute of Anatomy in Fribourg. Preoperative anesthesia was initiated with Ketamine (Ketalar, 100mg/kg i.m. Parke-Davis). Supplemental doses of Ketalar (50 mg/kg i.m.), were given as required checking reflex state. Atropine sulfate (0.02mg/kg i.m. Gattiker) was administered to reduce mucus secretion about five minutes after the initial dose of Ketalar. Any incisions with the scalpel were preceded by application of the local anaesthetic Scandicain (0.5%, Globopharm AG). The femoral vein was then cannulated with a heparinized (Liquemin, Roche) polyethylene tubing (PE-10, Clay Adams) for administration of paralytic agents. The bladder was catheterized to facilitate drainage in the paralyzed animals (Kaufmann and Somjen, 1979).

The craniotomy was initiated by an incision along the midline on the animal's head, and followed by removal of the left temporal muscle. A bolt attached to the stereotaxic frame was cemented to the skull (Paladur, Kulzer) allowing removal of cumbersome ear, mouth, and eye bars. Following craniotomy, the dura was protected with a layer of 2% agar in 0.9% saline. The agar acted also as a mechanical stabilization of the cortex caused by the animal's respiration. The position of the midline was traced on the tangential screen and the optic discs were projected into the Faraday cage within which the experiment took place. This was done in order to determine the position of the eyes and the receptive fields. This operation was repeated several times during the experiment.

The tree shrews were paralyzed with a continuous infusion of a solution containing Alloferin (1 mg/kg/h, Roche), Nembutal (3 mg/kg/h, Abbot) and a 2:1 mixture of 5% glucose and 0.9% saline, respectively. The animals were artificially respirated with a 70:30% mixture of N_2O and O_2 containing 5% CO_2 at 100 strokes per minute and a stroke volume of 1.5-2.0 ml. The electrocardiogram was monitored. Body temperature was maintained at 37.5 % by a heating pad with a feedback circuit. Carbon dioxide expiration was monitored using an HP 47210 A capnometer. Following application of ophthalmic atropine sulfate (0.5 %, Dispersa) to dilate the pupils, plastic (PMMA) contact lenses (3.7 mm radius) were used to focus the eyes on a tangent screen which was located at either 57 or 114 cm in front of the animal.

2.1.1 Animals Studied

In **Table II**, we list the animals examined and sacrificed in our experiments. The following data are indicated: number of the experiment (preceded by the letters « T.AD. » meaning Tupaia adult), identification number, sex, weight, and age. The animal's weight varied between 161 and 260 g. In total, nine males and ten females were studied. The heart rate during the experiments was between 360-500 pulses/min. Body temperature was kept at 37.5° C ± 0.5° C. The respiration was monitored and the end-tidal CO_2 fluctuated between 17-26 mmHg i.e. 3.2-4.8 %. (See also F. Mooser, 1998). All experiments were carried out in accordance with the guidelines published by the Swiss Academy of Medical Sciences (SAMW) and the Swiss Academy of Natural Sciences (SANW) regarding the care and use of animals for experimental procedures.

Tree shrews (Tupaia belangeri)

Number of experiment	Identification number	Sex	Weight [g]	Age [days]
T.AD. 162	R372E	FEMALE	218	286
T.AD. 170	R355E	MALE	194	476
T.AD. 172	R361E	MALE	175	412
T.AD. 175	R367E	MALE	236	626
T.AD. 180	R384E	FEMALE	177	428
T.AD. 182	R379E	MALE	193	448
T.AD. 185	R303D	MALE	220	1457
T.AD. 186	R306D	FEMALE	200	1464
T.AD. 187	R352D	FEMALE	192	834
T.AD. 189	R366E	FEMALE	181	823
T.AD. 191	R226A	FEMALE	232	2705
T.AD. 199	R412E	FEMALE	175	332
T.AD. 200	R426E	FEMALE	161	183
T.AD. 209	R380A	FEMALE	205	854
T.AD. 210	R369A	MALE	260	946
T.AD. 211	R371A	MALE	236	930
T.AD. 212	R377A	MALE	212	930
T.AD. 213	R430C	FEMALE	209	358
T.AD. 214	R401A	MALE	227	731

Table II – Summary of the animals used in this study. Of the 19 animals used, 10 were females and 9 were males. The first column indicates the number of the experiment, preceded by T.AD. (T=Tupaia and AD=adult).

2.2 Electrophysiological procedure

2.2.1 Glass-coated platinum-plated tungsten microelectrodes

The microelectrodes used are called “Merrill and Ainsworth electrodes”. Their name is drawn from their original manufacturers, who provide instructions for their production (Merrill and Ainsworth, 1972). Following these instructions, these were hand-made at the Institute of Anatomy, Fribourg. These microelectrodes have the advantage of recording selectively from cells practically excluding signals from the white matter (Kretz et al., 1986).

The electrodes were covered with glass using a DKI vertical pipette puller (David Kopf Instruments, Tujunga, California). The glass insulation on the tip was removed under microscopic control using a low melting glass (Corning, No. 7570, solder glass). After the plating procedure, the electrical characteristics of the electrode in a calibrating solution of 0.85 % NaCl were measured by visualizing the impedance with the aid of a dual beam oscilloscope (Tektronix, 5112) coupled with a preamplifier (Grass P15) and a differential amplifier (Tektronix, AM502) with 1 kHz pulses.

The microelectrodes had a tip of 7-22.5 µm in length and 3-7 µm in diameter. The resistance measured after platinum plating was in the order of 0.1 megaohms at 1 kHz AC. The electrodes were advanced into striate cortex, dLGN, and superior colliculus using stereotaxic coordinates. The coordinates of the cortical penetrations were selected to be in the binocular region by using a Tupaia brain atlas (Tigges and Shantha, 1969) and a receptive-field map (Kaas, et al., 1972). The microelectrodes were introduced perpendicularly to the structure studied (in most cases) using a hydraulic micro-drive (David Kopf Instruments).

Extracellular, single-unit neural activity was amplified and recorded and a level discriminator (Schmitt-Trigger) was used in order to convert the pre-amplified responses to transistor-transistor-logic (TTL) pulses. These, in turn, were stored on a PDP 11/73 computer running data acquisition software created by Michael Stephan at the Max-Planck Institute für Hirnforschung in Frankfurt. The raw data were subsequently transferred to a Unix station (Silicon Graphics) for further analysis using custom built software developed by Patrick Faeh using PV-Wave at the Institute for Anatomy, Fribourg. This program generated peri-stimulus time histograms (PSTHs) of the single-unit activity.

During the experiment, signals were monitored using an oscilloscope as well as an audio monitor. The electrode was advanced gradually until single units were found. At this point, light stimuli consisting of slits or spots were projected on the tangent screen using a hand-held ophthalmoscope (Keeler). By paying close attention to the cell's response on the audio monitor while moving the light stimuli across the visual field, it was possible to determine the approximate receptive field perimeter. This was plotted and measured on the tangent screen.

Ocularity was tested by covering one eye at a time. For cells responding to moving stimuli, the approximate RF position was determined by sweeping the light stimulus over the entire screen at different directions until a response was clearly heard.

Once an RF was found, a computer controlled slide projector (PRADO UNIVERSAL, lamp XENOPHOT HLX 64655, 24V, 250 W) was used to generate a stimulus covering the presumptive RF, which had been plotted during ophthalmoscope stimulation. The computer triggered the opening and closing of the projector shutter at predetermined moments of the acquisition interval and plotted the Schmitt-Trigger discriminated responses in point raster form on a video screen.

2.2.2 Focusing of Receptive Fields

Using the video monitor, and the DAP (Data Acquistion Program) software mentioned above, it was possible to visualize spikes in dot raster format and to synchronize the shutter sequences with specific moments in the data acquisition interval. The servomotors controlling the mirrors projecting the image onto the screen were also computer driven. They were adjusted so that the stimulus fell on the spot where the RF had been located with the help of the ophthalmoscope. The size of the RF could be varied, while maintaining the center in the same position. Thus, different stimulation trials were tested using white light and monitoring the response with the audio and video monitors. Usually the response peaked at a certain stimulus size, smaller or larger stimuli giving a lesser response. And thus, optimal stimulus sizes were determined and measured (in cm.) on the tangent screen. The size in degrees was then computed trigonometrically for every RF.

2.2.3 Duration and synchronization of stimuli

The duration of the stimuli could be controlled using the computer. For most stationary stimuli, stimulus duration was 750 ms. For cells responding to moving stimuli, the effective duration of the stimulus depended on the speed at which the stimulus (usually light bars) passed over the receptive field.

The opening and closing of the projector shutter as well as the movement of any given stimulus (including control of angle and speed), was programmed into the PDP-11 computer running DAP (Data Acquisition Program) software. By computer control it was possible to synchronize stimuli and acquisition of response profiles.

2.2.4 Constant contrast stimuli

These were obtained by stimulation not only of a receptive field center, but also a surround. The contrast between center and surround was kept constant by ensuring that every increase or decrease in the intensity of one was matched by the same increase or decrease in the other. In this way the ratio of stimulus and surround intensity remained constant. This is carried out under the assumption that the RF-size remains static.

2.2.5 Moving stimuli

Moving stimuli (4-215 deg/s) passed over the receptive field in one direction (forward), stopped for an interval of 4-1400 ms., and moved back with the same angular velocity in the opposite direction (backwards). The moments of the data acquisition intervals at which movement was initiated, stopped, and returned were controlled with the help of the computer (see **Fig. 11).**

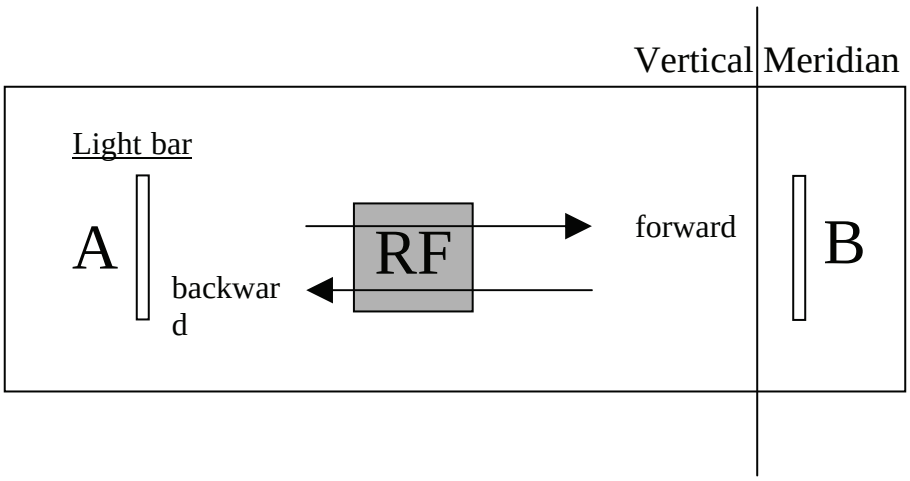

Fig. 11 – This figure illustrates the type of stimulation used with cells responsive to movement. A and B indicate the initial and final position of the light bar, which is moved at a constant, predetermined speed across the receptive field, approaching it from one side or the other. Movement could also vertical or diagonal.

In order to test for orientation selectivity, we measured response to light bars with different inclinations. These inclined light bars of a length corresponding approximately to the optimal stimulus size and width varying from 2 to 4 degrees. In cells responding optimally to moving stimuli, different directions of stimulus movement were tested and the responses were measured to determine direction selectivity.

2.2.6 Determination of spectral properties

The spectral properties of cells were tested by plotting their activity in response to filtered light corresponding to short, medium, and long wavelengths. Kodak Wratten filters numbers 47B, 99, and 29 with transmission maxima at 430, 548, and 625 nm corresponding to our perception of blue, green, and red, respectively were used. The transmission curves of these filters are given in **Appendix III.** For each wavelength, neutral (1%, 10%, 25%, 50%, 75%) filters and the projector diaphragm were employed to modulate the intensity of the stimuli. Additionally, the projector had two power settings (hence referred to as “Stufe I” and “Stufe II”) of which the latter was approximately 10 % more powerful.

The intensity of each stimulus was measured using a Tektronix J16 digital photometer by illuminating a 2 deg x 2 deg area in the center of the tangent screen. Each of the Wratten chromatic filters was tested with different filter and diaphragm settings as well as the two projector power settings (Stufe I and Stufe II). The values of these measurements are given in the tables in **Appendix III.**

For the generation of response to intensity curves, the intensity values as given in Appendix III are plotted on the abscissa and the value of the ordinate is given by the evoked responses of each cell. Evoked response was defined as total spikes during an interval minus spontaneous activity measured during an equivalent reference interval. In this way, different wavelengths were tested, namely white light (no filter), red, green, and blue. These values were used to plot response to intensity curves (from here on referred to as R/I curves). An example of one such set of curves is presented in **Figure 12.**

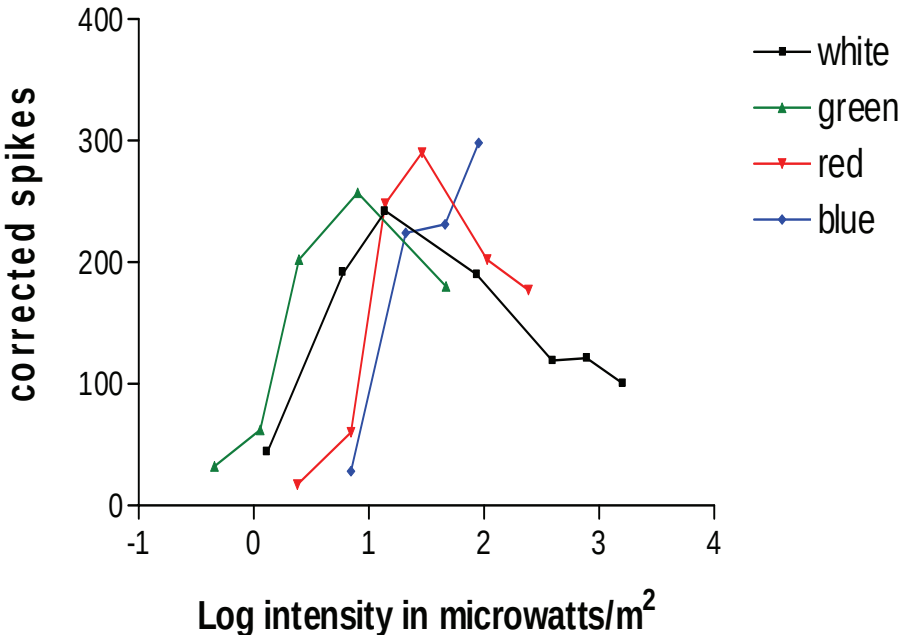

Fig. 12 – Response/Intensity curves of a cell stimulated with different wavelengths. Observe the shape of the curves, as well as the dynamic and post-saturated ranges. (Cell 21, dLGN lamina 6). Cell numbers correspond to list in **Appendix I** q.v.

2.2.7 Determination of evoked response – the term “Corrected spikes”

In all the figures showing R/I (response to intensity) curves, the term “corrected spikes” is used to refer to the evoked response of cells in response to stimuli of different wavelength and intensity. The value for the corrected spikes is calculated by subtracting the baseline (spontaneous) activity from the number of spikes within a stimulus presentation interval. In each test trial, stimuli were presented 20 times (i.e. 20 sweeps) and a PSTH (peri-stimulus time histogram) was generated with the sum of the spikes per bin generated during this period of 20 sweeps. The standard binwidth was 4 ms. From the number of spikes per bin, it is possible to calculate the mean firing frequency in spikes per second. In all the given histograms we have used the former form of presentation. Using the custom made SHOWDAP program, developed by Patrick Faeh, at the Institute of Anatomy, Fribourg, the number of spikes within a given interval could be calculated, ASC files generated, and these then exported to EXCEL for further analysis.

For example, in the data series shown in **Table III**, the first field indicates the filename. The next two fields (A1, A2) labeled “start” and “end” indicate the interval (in bins) during which the response was measured. One bin equals 4 ms. Thus the interval is from 287*4 to 475*4, i.e. from 1148 to 1900 ms. The next column, A4, indicates the total number of spikes counted within this interval i.e. the sum of the spikes in the given interval during the 20 sweeps. Columns A5 and A6 refer to the interval for measuring baseline activity. Column A7 gives us the total number of spikes within this interval.

In order to obtain the “corrected spikes” we first take the response within the reference interval, which was 25 spikes. We divide this number by the duration of the reference interval 25/(999-500) and obtain 0.05. We then take this number and multiply it by the duration of the « stimulation » interval: 0.05*(475-287)= 9.42. This number is then subtracted from the spikes in the stimulation interval (column A4) in order to obtain the corrected spikes. The result is rounded off.

A1	A2	A3	A4	A5	A6	A7	A8
filename	start	end	spikes	refstart	refend	spikesinref	Corrected
PS0000	287	475	112	500	999	25	103

Table III – Example to show computation of corrected spikes

Evoked spikes were thus defined as the difference between the number of spikes in a specific interval and the background calculated to the corresponding intervals, in accordance with the formula: **Corrected spikes = A4- [A7/(A6-A5)]*(A3-A2)**. In the cells studied, the signal-to-noise ratio was extremely high, as can be seen in the example in **Fig. 13**.

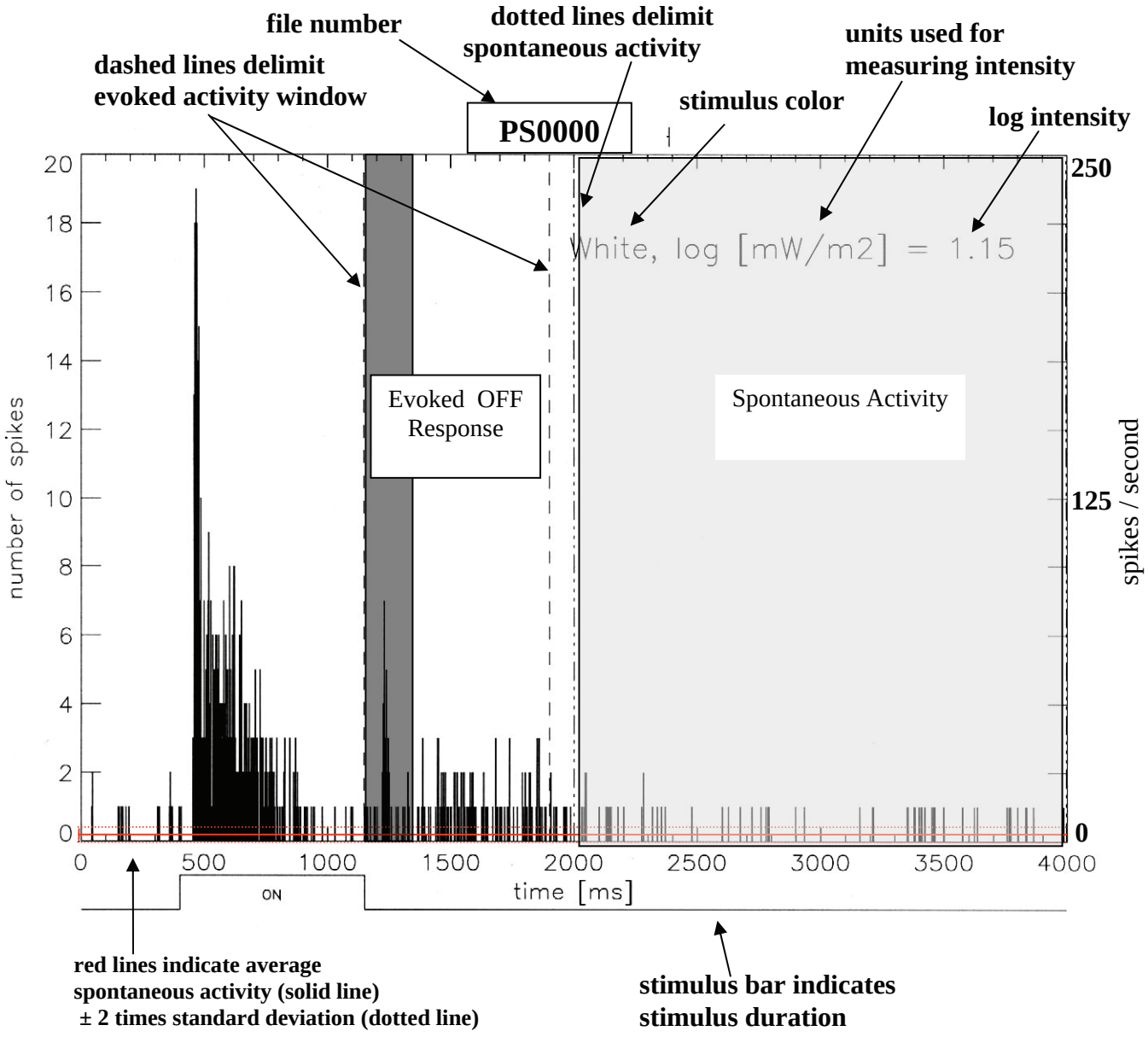

Fig. 13 – Peristimulus time histogram. Ordinate scale on the right indicates mean firing frequency in spikes/second calculated from the number of spikes per bin indicated on the ordinate scale on the left (binwidth: 4ms). Solid red line indicates the average spontaneous activity. Dashed red lines indicate avg. spontaneous activity ± the standard deviation multiplied by two. The signal to noise ratio was typically extremely high.

2.2.8 Analysis of R/I Curves

As can be seen from **Figure 12** above, cell responses to stimuli of increasing intensity are non-monotonic. Once the saturation level is reached, the response will decrease or fluctuate, as is here the case with green and white. This is probably due to lateral-inhibition mechanisms triggered by the relative increase of surround luminosity.

Within the dynamic range of a cell's response there can be slight discontinuities. Small segments of the curve may contain negative slopes, although the dynamic range should, in principle, have a positive slope through out. Fluctuations of this nature are probably imputable to the modulatory influence of the *formatio reticularis*, although temporally limited photoreceptor bleaching may also play a role.

2.3 Histological procedure

At the end of each electrode penetration, two or three small electrolytic lesions (3μA for 3 sec) were made to aid in the histological reconstruction of the recording sites. The appearance of such lesions can be seen on the histological sections shown in **Fig. 14** (following page).

After a lethal intravenous injection of Nembutal, the animals were transcardially rinsed with a 0.9% saline solution and perfused with 2.5% glutaraldehyde and 1% paraformaldehyde in 0.1M phosphate buffer. The brains were postwashed in 10% and 20% cold sucrose buffer and cut in 52 μm coronal sections with a cryotome. The sections were stained with cresyl violet, and in order to detect the presence of high metabolic blobs, cytochrome oxidase staining was carried out on alternate sections.

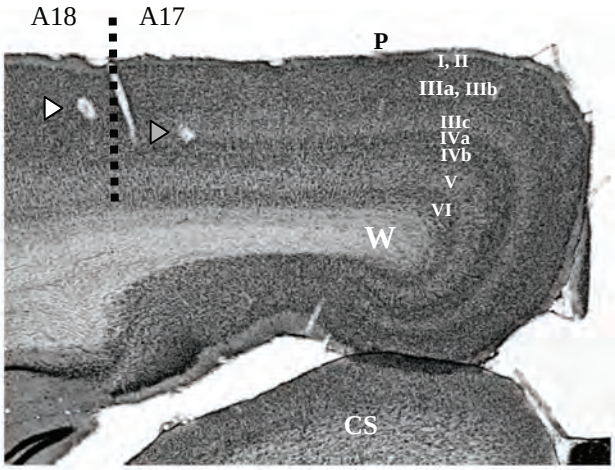

A Visual Cortex

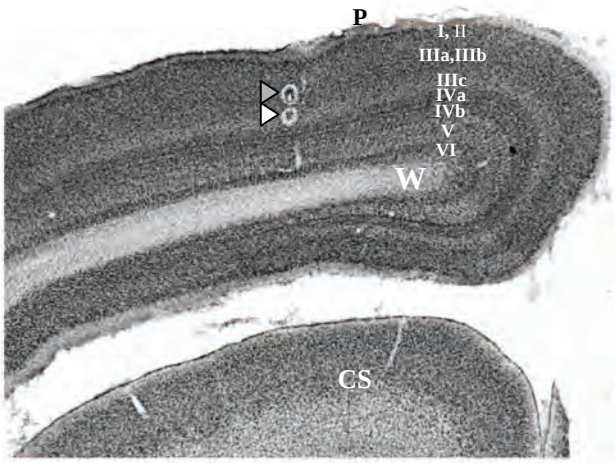

B Visual Cortex

Fig. 14 Nissl-stained coronal sections of the tree shrew brain showing electrolytic lesions (arrowheads) and cytoarchitectonic layers.

A. T.AD. 180 The stippled line marks the boundary between areas 17 and 18. The white arrowhead corresponds to **cell 8** in area 18. The gray arrowhead (lesion in area 17) in layer IIIc corresponds to a position where no recordings were made.

B. T.AD. 185 The gray arrowhead points to a lesion in layer III a/b where no recordings were made. The white arrowhead points to a lesion in layer IIIc corresponding to **cell 14**.

C. T.AD. 191 Example of a lesion (shown by arrowhead) in the dLGN, lamina 2 (ON, contra) corresponding to **cell 28**.

D. T.AD. 185 Example of a lesion in the Colliculus superior. The arrowhead indicates the position of the lesion in the Stratum opticum, corresponding to **cell 13**.

Abbreviations: A17 area 17, A18 area 18, Am Aqueductus mesencephali, CS Colliculus superior, dLGN dorsal lateral geniculate nucleus, Hip Hippocampus, P pial surface, PAG Peri-aqueductal gray, SGS Stratum griseum superficiale, SO Stratum opticum, SGI Stratum griseum intermedium,VL ventriculus lateralis, W white matter.

Scale bar: 1000 μm.

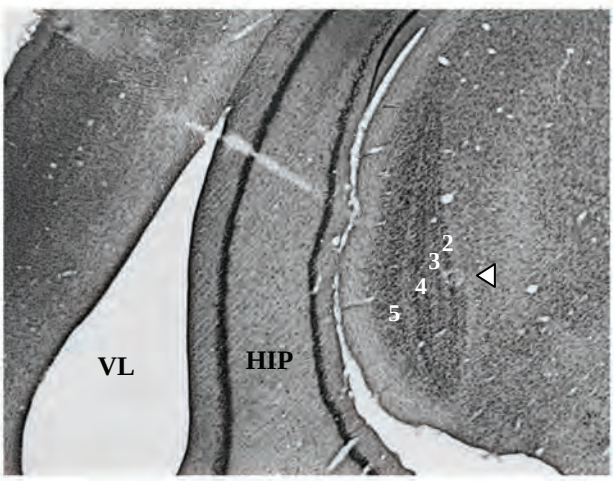

C dLGN

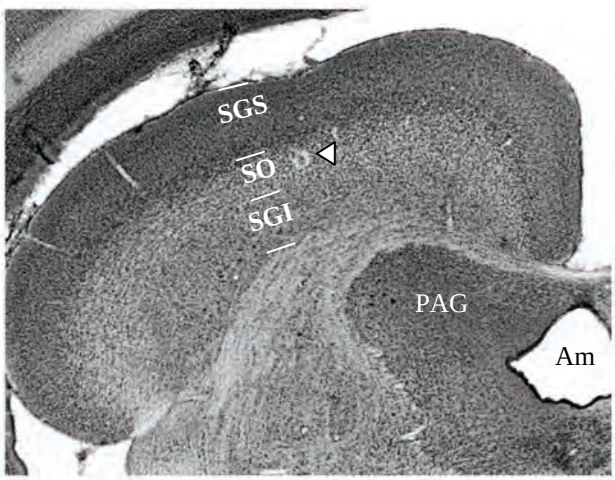

D Colliculus superior

Results

3 RESULTS

3.1 Generalities

In total, 53 cells were studied. An exhaustive inventory of these cells, with their respective locations and response properties can be found in **Appendix I**. Of the cells studied, 7 were recorded from the dLGN, 13 from the Colliculus superior, 29 from Area 17, 2 from the border between Areas 17 and 18, and 2 from Area 18. A diagram showing the different visual system locations and the cells found therein is shown in **Figure 15**. As can be seen from the chart the majority of cells we have recorded from were located in the primary visual cortex, or in the extragenicular system (i.e. Colliculus superior).

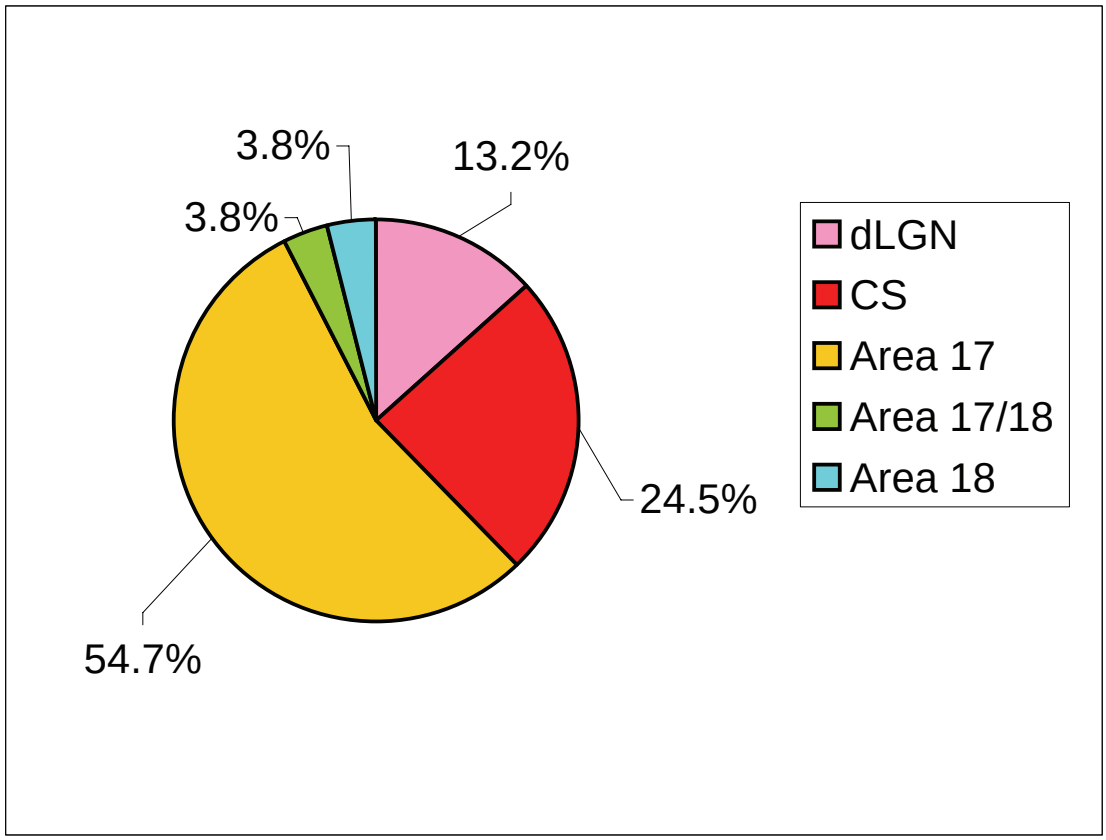

Fig. 15 - This diagram shows the proportion of cells recorded from each region of the visual system

In **Table 4**, we provide a detailed listing of the regions of the visual system where we carried out recordings. The corresponding cell identification numbers are given for reference.

Location		Cell Numbers	Total
dLGN - laminae			
	l		
	2	27	1
	3	26	1
	4	25	1
	5	23,24	2
	6	21,22	2
		Total	**7**
Coll. Sup.			
	SGS	2,4,11,12,15,16,17,18,19,20	10
	SO	10,13	2
	SGI	33	1
		Total	**13**
Area 17 - layers			
	I		
	II		
	III a	30	1
	III a/b	3	1
	III b	1,5,6,31,36,41,51	7
	III b/c	52	1
	III c	14,34,38,39,53	5
	III c/IV a	32,46	2
	IV a	42,47	2
	IV b	9	1
	IV b/V	37	1
	V	7,40,48,49,50	5
	VI	45	1
	unknown	28,29	2
		Total	**29**
Area 17/18			
	III c/IV a	43	1
	V/VI	44	1
		Total	**2**
Area 18		8,35	2
		Total	**2**
		TOTAL NUMBER OF CELLS	**53**

Table 4 – Regions of the visual system were recordings were conducted.

3.1.1 General Response Characteristics of Cells

Of the cells recorded, 23 (43.4%) responded exclusively to stationary stimuli, 24 (45.3%) responded exclusively to moving stimuli, and 6 (11.3%) cells responded to both stationary and moving stimuli. Of all the cells recorded, 9 (17 %) were ON cells, 10 (18.9%) were OFF cells, and 15 (28.3%) were ON-OFF cells, for 19 cells (35.8%) reacting only to movement, it was impossible to determine whether they were ON or OFF. The majority of cells had a phasic and a tonic component in their response. These comprised 30 cells (56.6 %). However, 16 (30.2%) cells had a phasic component only. Of the latter, one third consisted of cells from the Colliculus superior (although in this region one can also find cells having a tonic response). In lamina 2 of the dLGN, we also found two cells (27,28) having a distinct caesura between the phasic and tonic components. For 7 (13.2%) we could not determine whether their response was phasic or tonic (e.g. no histograms were made).

A considerable number of cells fired vigorously in response to black circles moved across the screen. Otherwise, the preferred stimuli consisted of spots of light of varying sizes (see listing in **Appendix I** for exact dimensions). Stationary and moving light bars elicited good responses in many cells. In some cases two stimuli of different color or intensity were superposed in order to test contrast sensitivity. In most cases, a cell's response was progressively inhibited by stimuli having sizes beyond optimal dimensions (surround-inhibition).

3.1.1.1 Criterion for judging that a cell is narrow-band or color-opponent

Given the dichromat nature of the tree shrew visual system (see Introduction), there are arguments to define narrow-band cells very broadly as cells exhibiting different types of response properties to short- and long-wavelength stimulation. According to this criterion, a cell will be termed narrow-band if it gives, for example, a response to red, but not to blue, or vice versa, or if it gives a response to both colors in one eye, but not in the other, or for that matter, if there is an ON response to both, but only an OFF response to one of the two wavelengths. Color-opponent, however, are only those cells which show center surround antagonism for different wavelengths.

3.1.2 General proportions and locations of narrow-band and color-opponent cells

In our study, a total of 8 out of 53 cells gave distinct responses for long and short wavelengths. Of these 8 narrow-band cells, 3 were located in the Colliculus superior, 3 were located in Area 17, 1 was located in Area 18, and 1 was located in the dLGN. The proportions of these cells are shown on the pie-graph in **Figure 16**. These cells constitute, in our judgement, the basis for specific color processing circuitry, given their capacity to map a specific domain of chromatic stimulation into a range of distinct activity patterns unequivocally and in a way adequate for color discrimination.

Besides narrow-band group, a significant number of cells in diverse locations displayed a strong bias to blue, meaning that there is a powerful input from the short-wavelength cones (SWC) although, as has been mentioned in the introduction, this is but a slight minority of the total cone photoreceptor population. Although the blue-biased cells are not generally Narrow-band, their sensitivity to blue is remarkable. All such cells have been labeled blue in our listing in **Appendix I**.

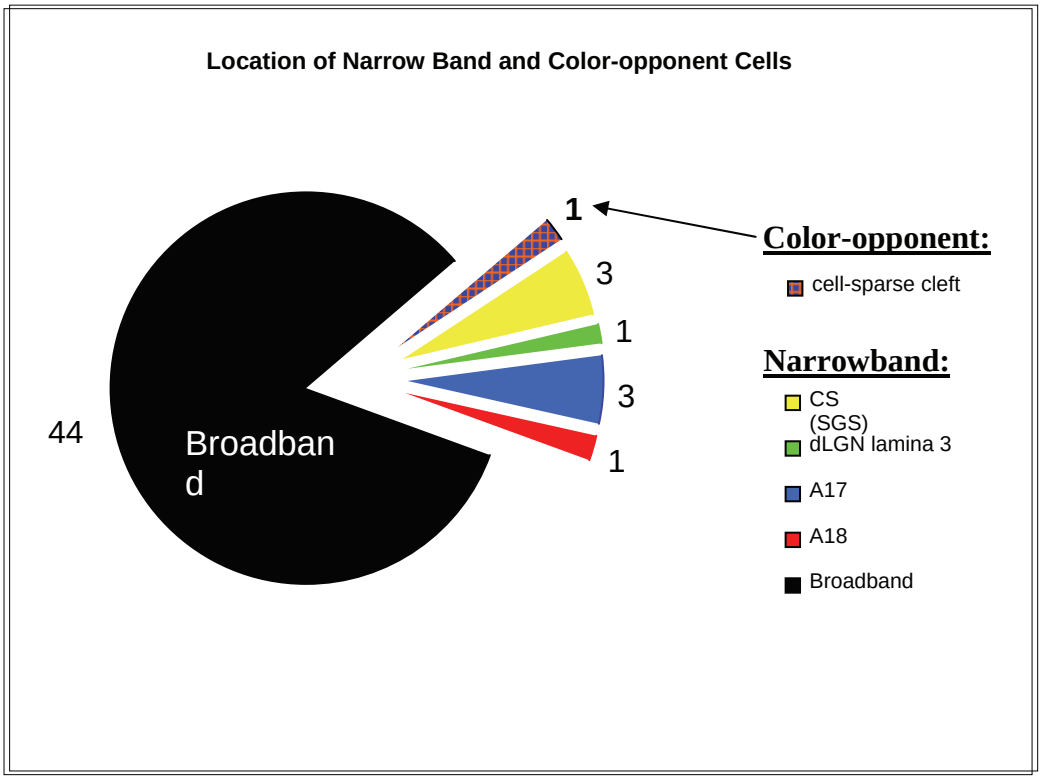

Fig. 16 – Pie graph illustrating the localization of narrow-band cells in our study.

3.2. Narrow-band cells

3.2.1. Extragenicular system

3.2.1.1 Narrow-band Cell A

Let us now examine these cells in further detail. The first of the narrow-band cells is **cell 2** (number refers to list in **Appendix I**). This cell was recorded during experiment T.AD. 170.

It was found in the Stratum griseum superficiale (SGS) of the Colliculus superior (at a depth of 4620 microns measured from the pial surface of the cortex). It responded to contralateral stimuli, both stationary and moving and gave an ON-OFF response. This cell responds well to long-wavelength stimuli (red and green filters), however with short-wavelength stimuli (blue filter) even at maximum intensity there is a slight inhibition.

This narrow-band activity is limited to the ON-channel. In the OFF-channel, broad-band characteristics can be observed, although blue gives only a phasic response. The other wavelengths elicit both a phasic and a tonic component.

In **Figure 17** on the following page, we give a series of histograms showing the activity of the cell for different stimuli. In the second column we see the responses to blue. It can be observed that in the interval here used (from 400 to 700 ms – stimulus ON), no response is given to blue.

As in all subsequent histograms, *the dotted vertical bar-line on the histograms*, here located at 2000 ms, *refers to the start of the reference window for measurement of spontaneous activity* which goes up to 4000 ms (see Methods section).

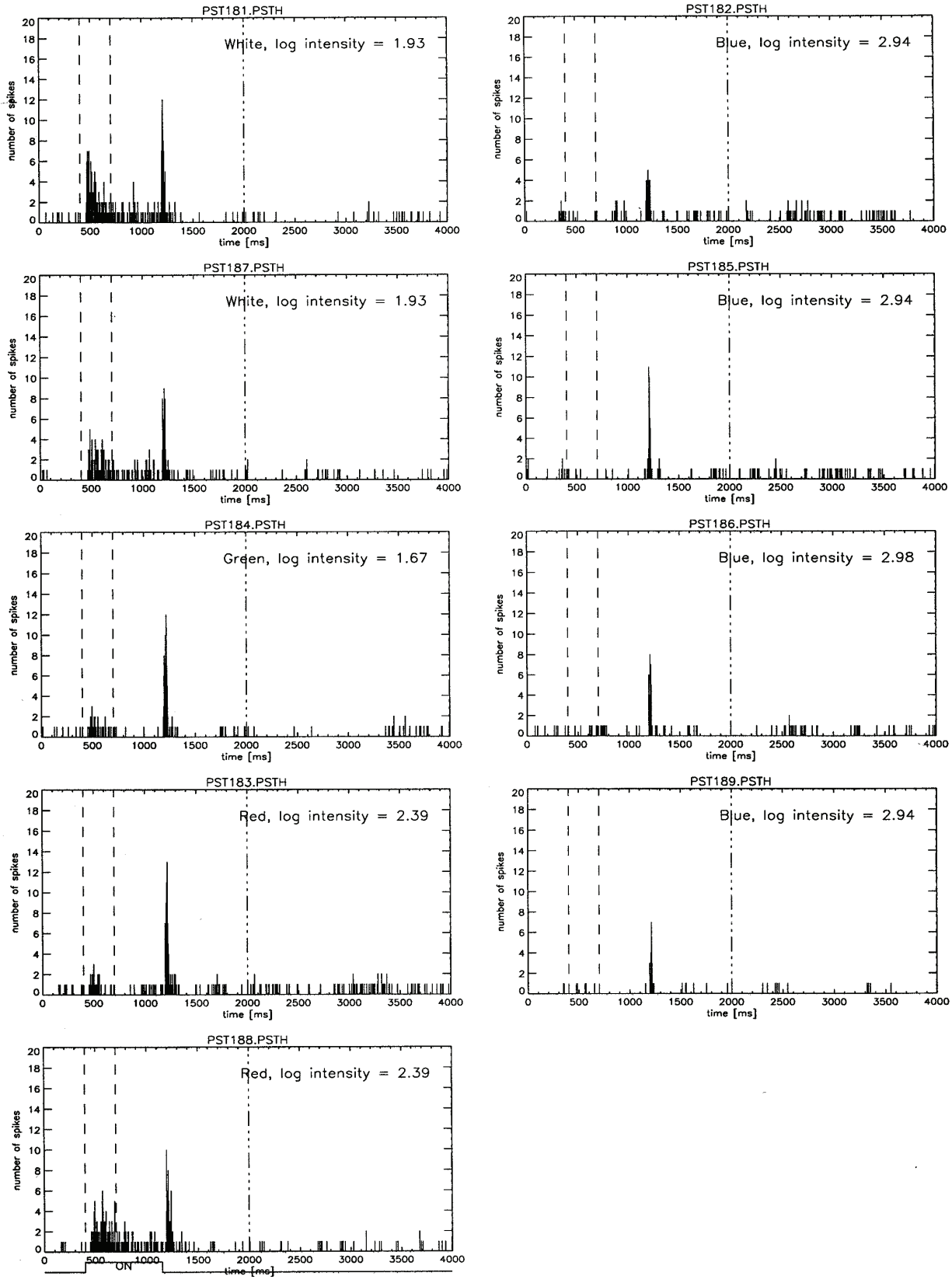

Fig.17 – Peristimulus histograms of **cell 2.** The narrow-band activity is limited to the ON-channel, maximum intensity for blue gives no response. In the OFF-channel, broad-band characteristics can be observed, although blue gives only a phasic response. The other wavelengths elicit both a phasic and a tonic component.

3.2.1.2 Narrow-band Cell B

The second of our narrow-band cells is also located in the Colliculus superior in the Stratum griseum superficiale (4330 microns depth). This cell was recorded in T.AD. 185 and corresponds to **cell 16** in our listing. It gave an ON response to moving stimuli. As in all cells responding to moving stimuli, we tested for optimal direction tuning, and measured response in both directions: approaching the receptive-field center from one side and from the other, as shown in **Figure 11** of the Methods section.

From the R/I curves shown in **Figures 18** and **19**, one can see that white, green, and red give very strong responses. Blue, however, which was tested with the maximum intensity (log intensity = 2.94 mW/m^2), gave only a negative response (a slight suppression of spontaneous activity).

In **Figure 18**, we see the response of the cell to a light bar going in one direction and in **Figure 19,** the response with the light bar returning in the opposite direction.

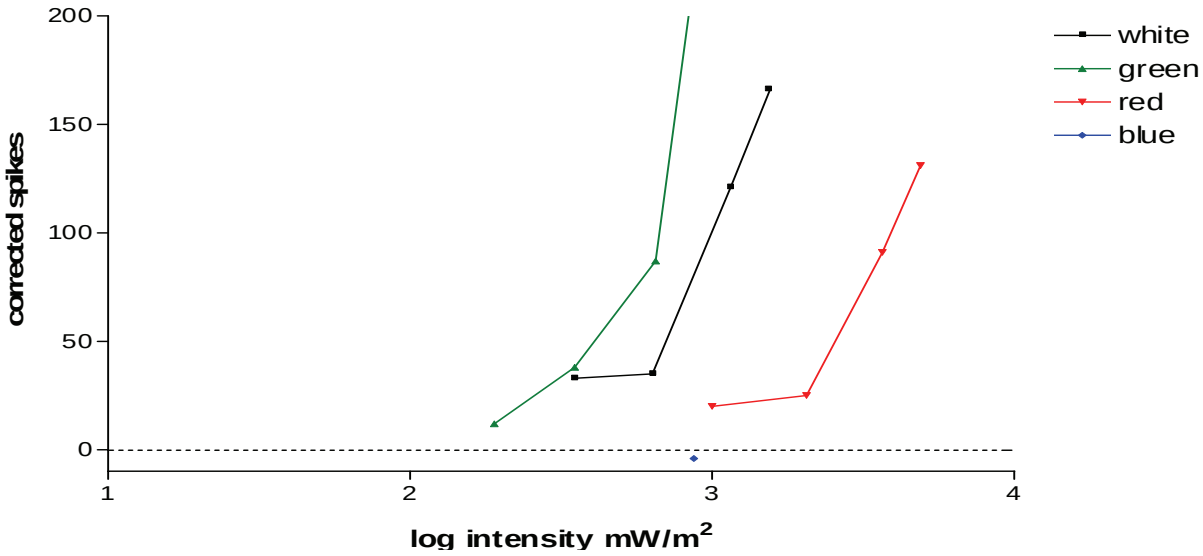

Fig. 18 – Narrow-band cell B. R/I curves showing that long wavelengths give a positive response and gain, whereas short wavelengths give a negative response. The dotted line is put in to emphasize the fact that blue gives negative values.

In **Figure 19,** the cell's response to a stimulus returning to the receptive field center (i.e. movement at a 180-degree angle to the previous one) is shown. It can be seen that there are slight differences in response for the two movement directions.

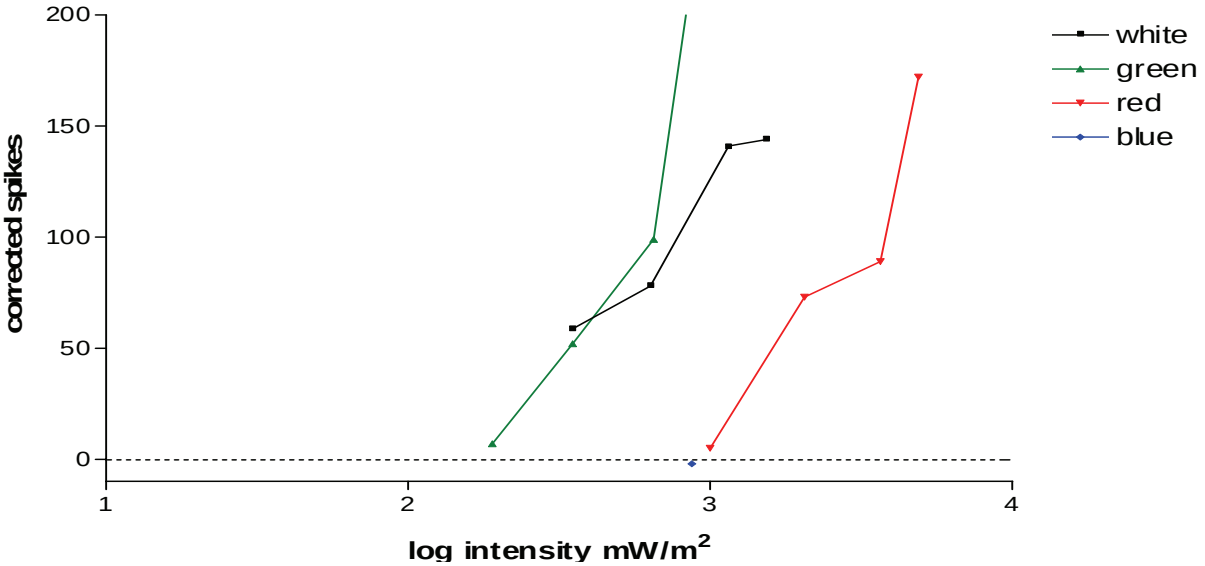

Fig. 19 – Response narrow-band cell B in the opposite direction. Notice that, again, blue gives a negative response.

This Colliculus superior cell has definite specificity for long-wavelength light, whereas short-wavelength cone input is inhibitory. It is noteworthy that this cell is both color-specific and sensitive to movement. Indeed, the cell responds *only* to moving stimuli. In **Figure 20** and **Figure 21** we show the histograms corresponding to **Figure 18** and **Figure 19,** respectively.

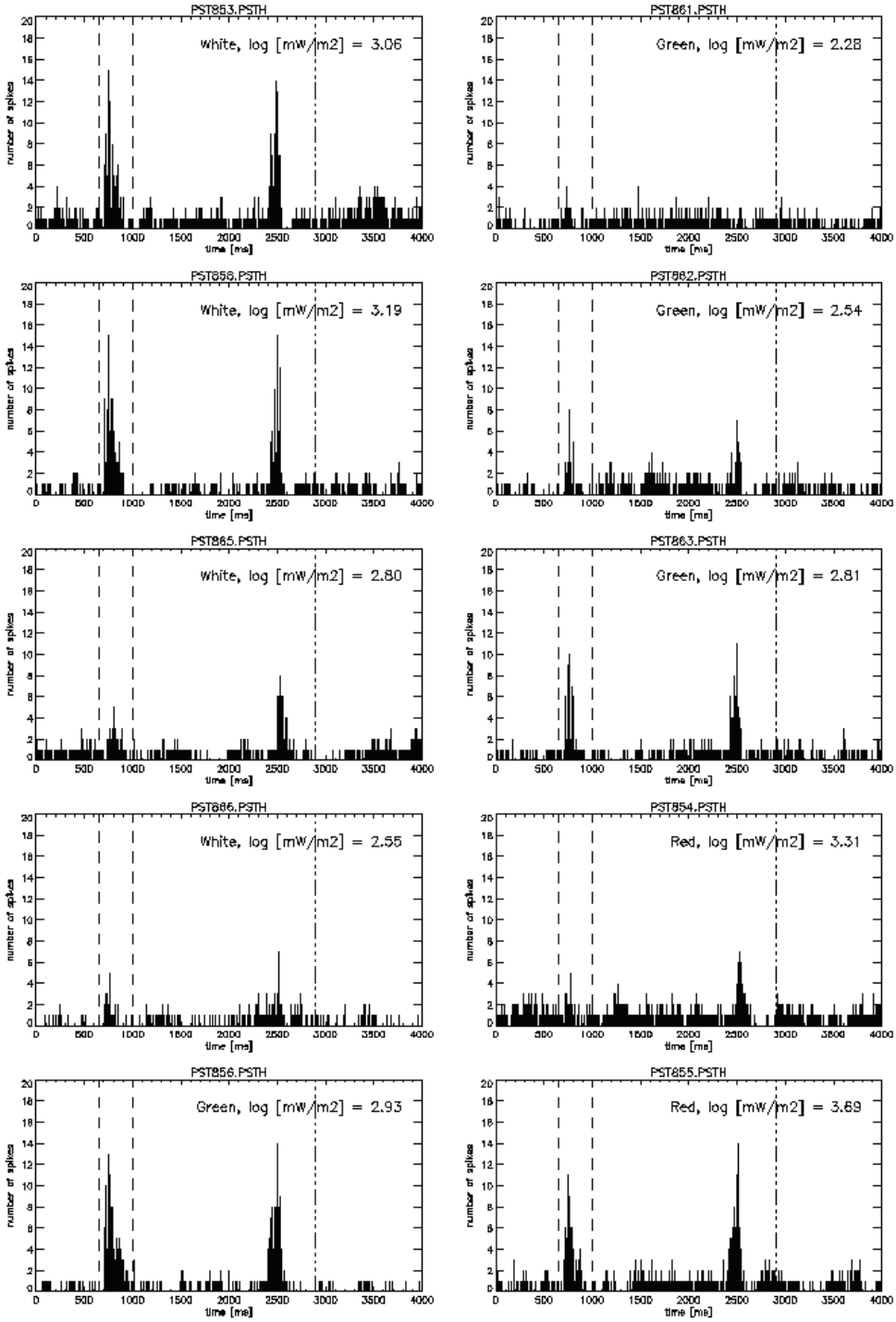
PST853.PSTH
White, log [mW/m2] = 3.06
PST861.PSTH
Green, log [mW/m2] = 2.28
PST858.PSTH
White, log [mW/m2] = 3.19
PST862.PSTH
Green, log [mW/m2] = 2.54
PST865.PSTH
White, log [mW/m2] = 2.80
PST863.PSTH
Green, log [mW/m2] = 2.81
PST866.PSTH
White, log [mW/m2] = 2.55
PST854.PSTH
Red, log [mW/m2] = 3.31
PST856.PSTH
Green, log [mW/m2] = 2.93
PST855.PSTH
Red, log [mW/m2] = 3.69
number of spikes
time [ms]

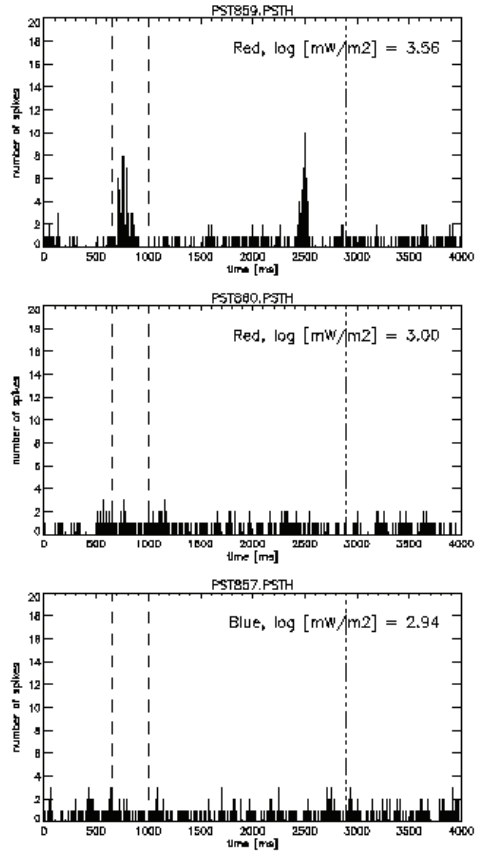

Fig. 20 – Histograms corresponding to R/I curves in **Figure 18** (Narrow-band B – cell No. 16).

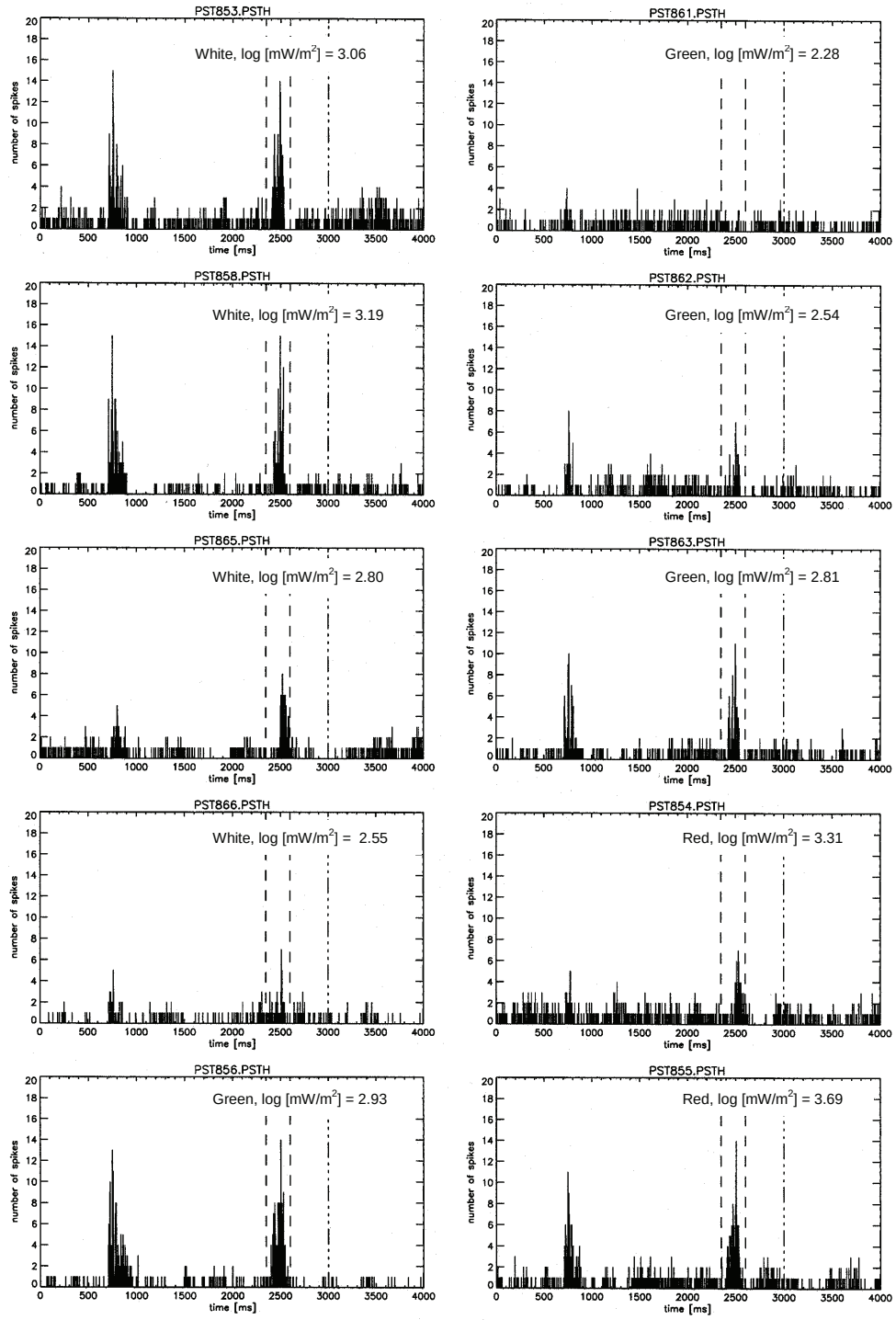
PST853.PSTH
White, log [mW/m2] = 3.06
PST861.PSTH
Green, log [mW/m2] = 2.28
PST858.PSTH
White, log [mW/m2] = 3.19
PST862.PSTH
Green, log [mW/m2] = 2.54
PST865.PSTH
White, log [mW/m2] = 2.80
PST863.PSTH
Green, log [mW/m2] = 2.81
PST866.PSTH
White, log [mW/m2] = 2.55
PST854.PSTH
Red, log [mW/m2] = 3.31
PST856.PSTH
Green, log [mW/m2] = 2.93
PST855.PSTH
Red, log [mW/m2] = 3.69
number of spikes
time [ms]

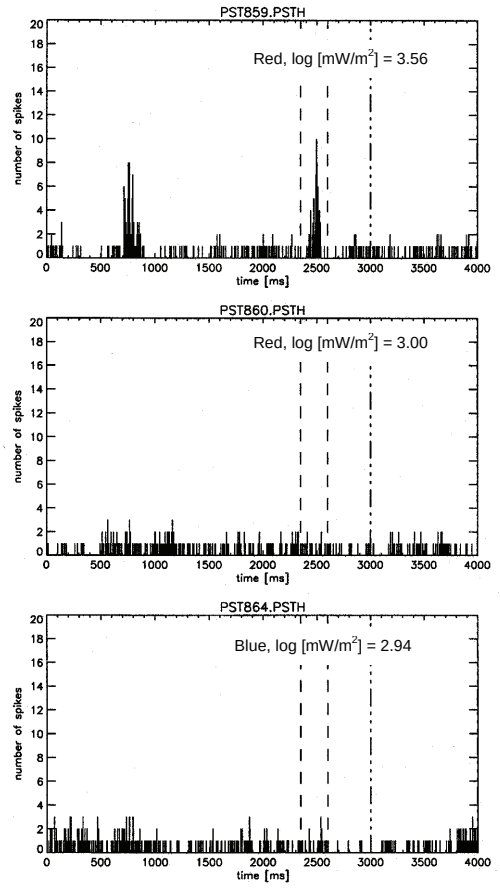

Fig 21 – Histograms corresponding to Figure 19. (Narrow-band B – cell No. 16).

3.2.1.3 Narrow-band Cell C

The third of our narrow-band cells was also found in the Stratum griseum superficiale of the Colliculus superior, at a depth of 3820 microns This narrow-band unit is cell **number 20**, which was recorded during experiment T.AD. 189. The cell is driven by the contralateral eye, and responds to stationary stimulation. Both ON and OFF responses were given initially, although subsequently, the latter died out.

This cell's response to blue is exclusively phasic, whereas the other wavelengths evoke responses with both phasic and tonic components.

In **Figure 22**, we present the R/I curves showing phasic ON response of the cell. The stimulus begins at 400 ms and lasts 750 ms. The window used to measure phasic activity goes from bin 100 to 125 i.e. from 400 ms to 500 ms as shown in the histograms in **Figure 23**.

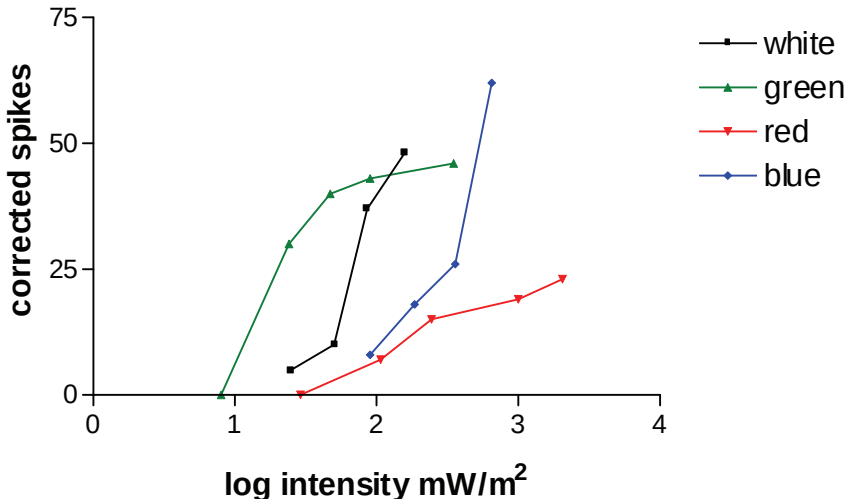

Fig. 22 – R/I curves showing ON-phasic response of cell No. 20. Notice all wavelengths give a vigorous response. This constitutes a broad-band response.

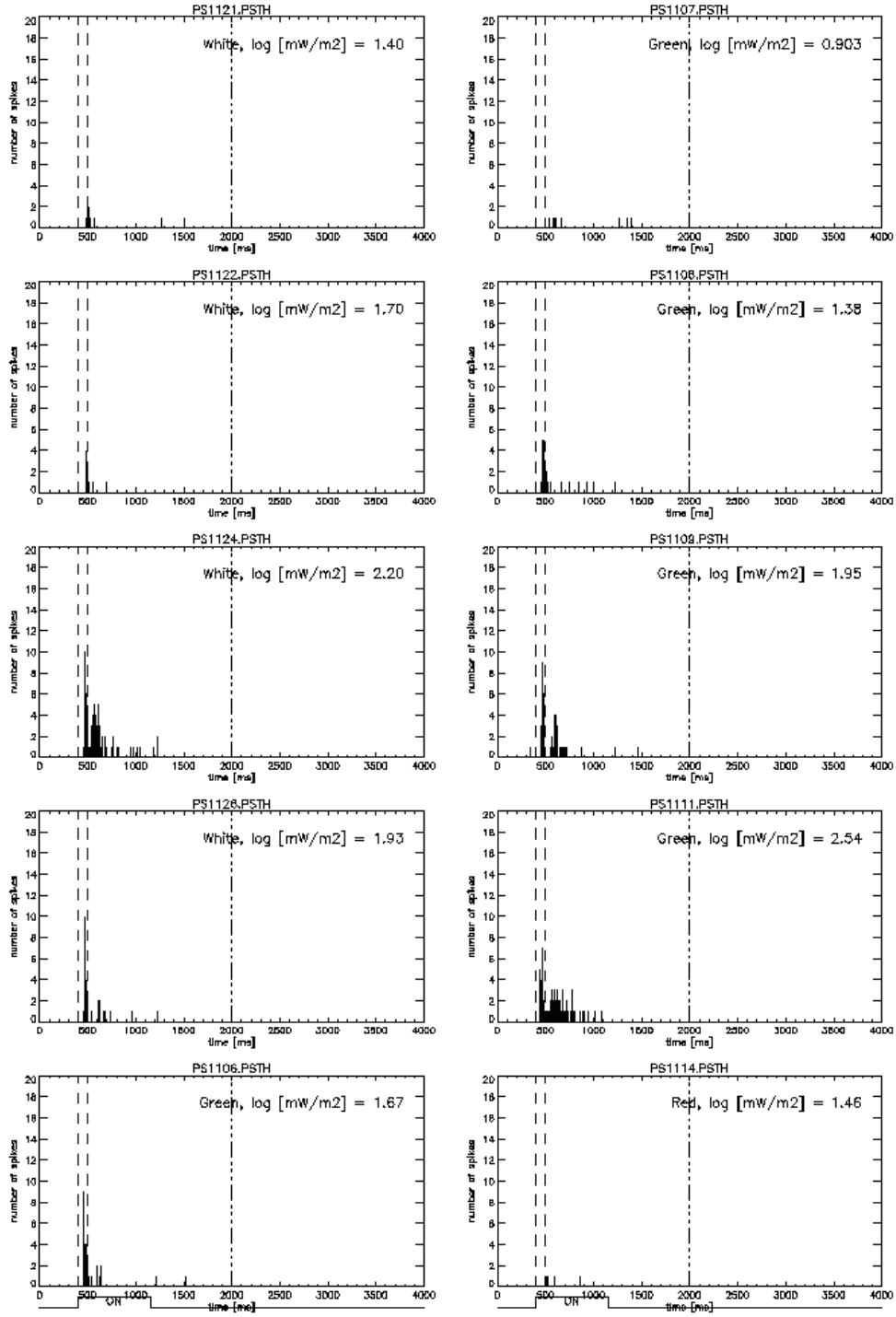
PS1121.PSTH
White, log [mW/m2] = 1.40
PS1107.PSTH
Green, log [mW/m2] = 0.903
PS1122.PSTH
White, log [mW/m2] = 1.70
PS1108.PSTH
Green, log [mW/m2] = 1.38
PS1124.PSTH
White, log [mW/m2] = 2.20
PS1109.PSTH
Green, log [mW/m2] = 1.95
PS1126.PSTH
White, log [mW/m2] = 1.93
PS1111.PSTH
Green, log [mW/m2] = 2.54
PS1106.PSTH
Green, log [mW/m2] = 1.67
PS1114.PSTH
Red, log [mW/m2] = 1.46
number of spikes
time [ms]
ON

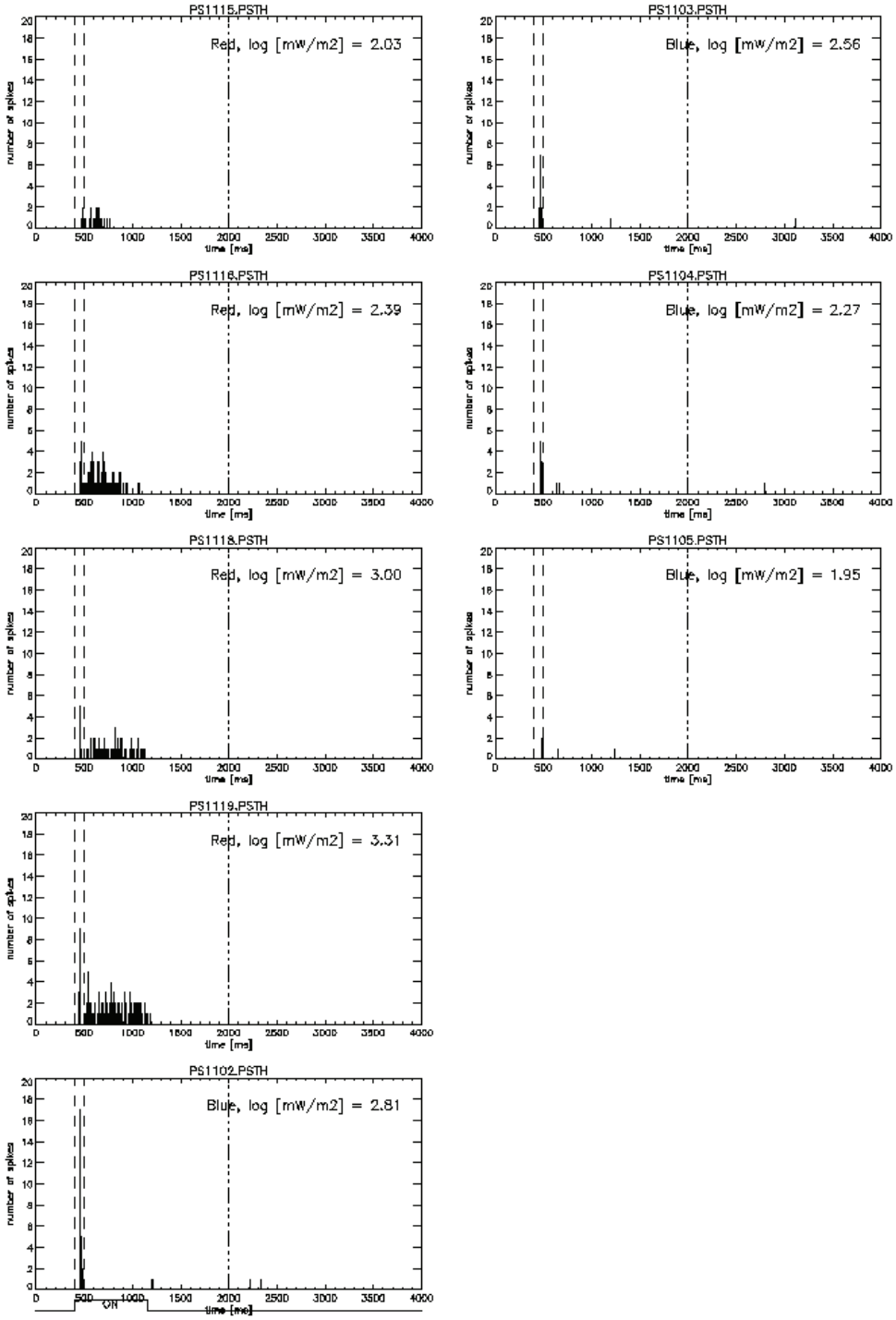

Fig. 23 – Histograms corresponding to **Figure 22**. Notice that blue elicits only a phasic response.

Thus, in the phasic part, the response is that of a broad band cell. If we examine, however, the tonic response as shown in the R/I curves in **Figure 24,** we notice that blue gives a response close to zero or even a slight suppression.

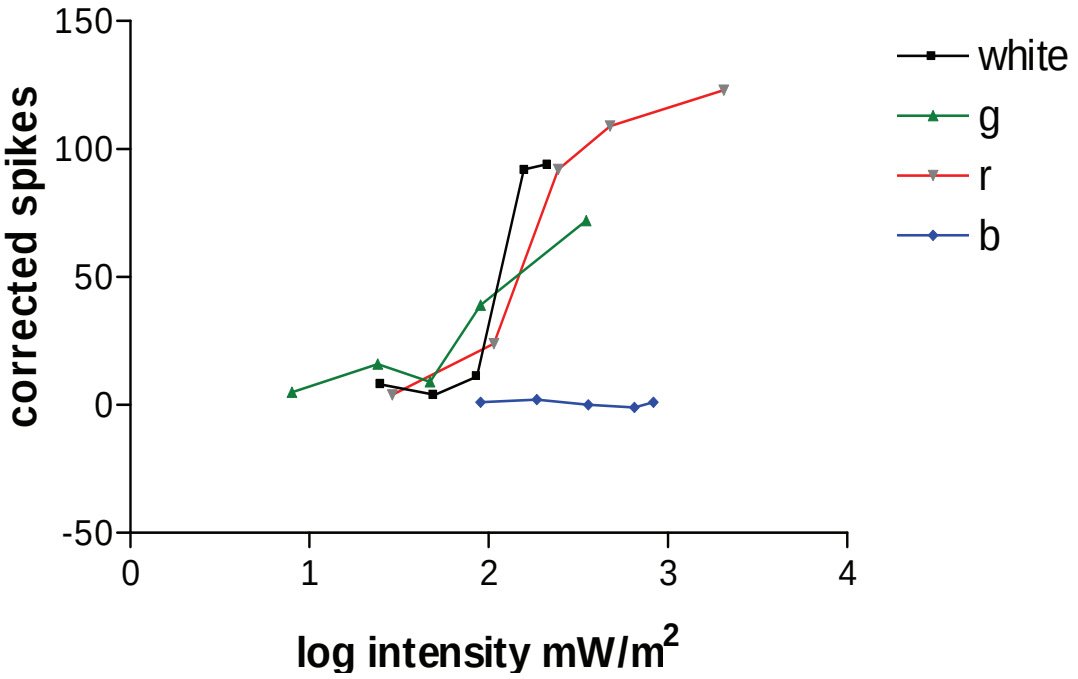

Fig. 24 - R/I curves showing ON-tonic response of cell No. 20. Notice that long wavelengths give a vigorous response. However blue (short wavelength) gives no response whatsoever.

The histograms shown in **Figure 25**, correspond to the R/I curves in **Figure 24**. It can be seen without ambiguity that blue consistently fails to evoke a tonic response. At very low intensities the tonic component evoked by the other wavelengths can be minimal as well.

With blue, the difference is that no tonic response is given at ***any*** intensity, although the phasic response is obvious. This response pattern suggests the convergence of two very different types of inputs: a broadband rapidly adapting cell, on the one hand and a slowly adapting long-wavelength specific cell, on the other hand.

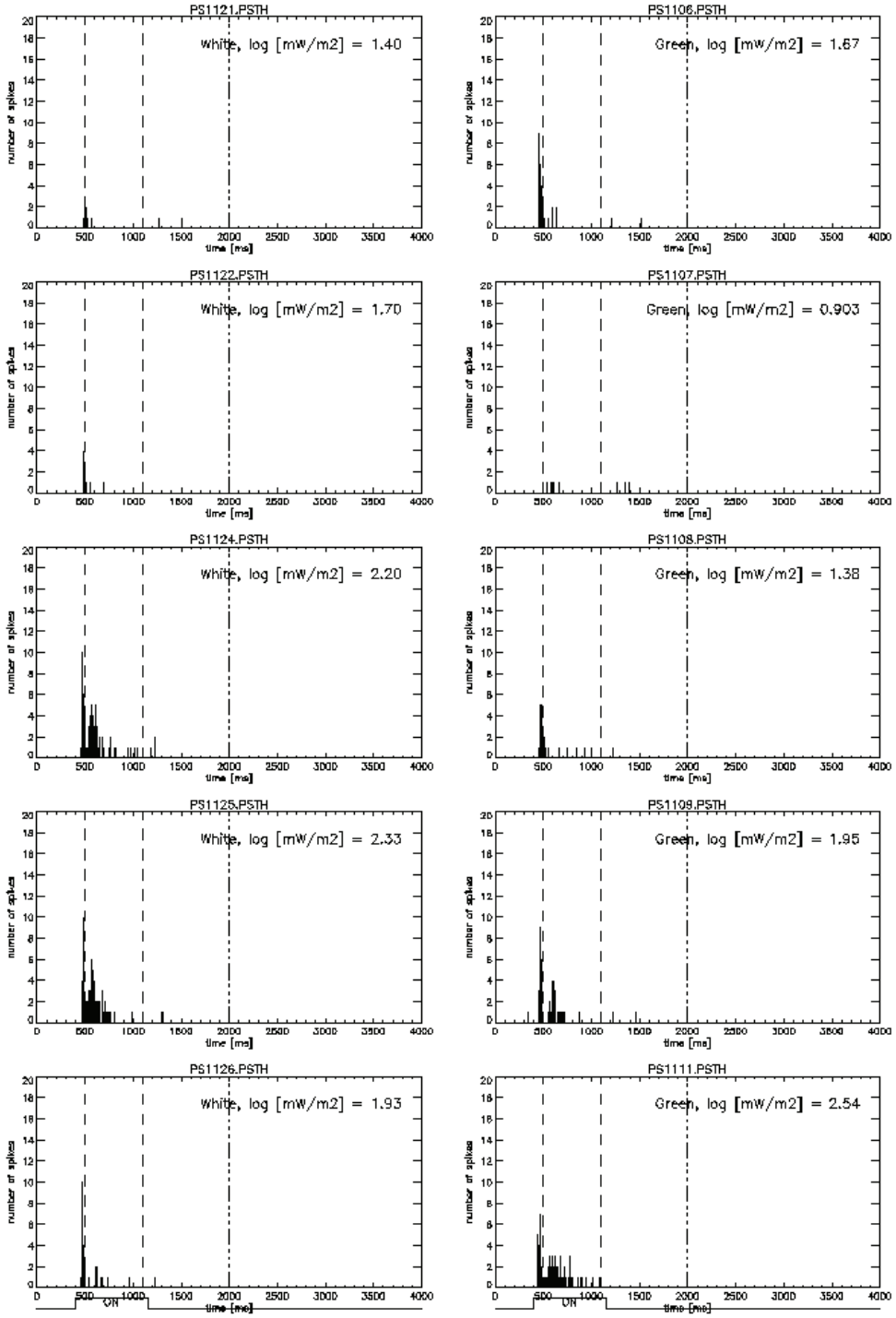
PS1121.PSTH
White, log [mW/m2] = 1.40
PS1106.PSTH
Green, log [mW/m2] = 1.67
PS1122.PSTH
White, log [mW/m2] = 1.70
PS1107.PSTH
Green, log [mW/m2] = 0.903
PS1124.PSTH
White, log [mW/m2] = 2.20
PS1108.PSTH
Green, log [mW/m2] = 1.38
PS1125.PSTH
White, log [mW/m2] = 2.33
PS1109.PSTH
Green, log [mW/m2] = 1.95
PS1126.PSTH
White, log [mW/m2] = 1.93
PS1111.PSTH
Green, log [mW/m2] = 2.54
number of spikes
time [ms]
ON

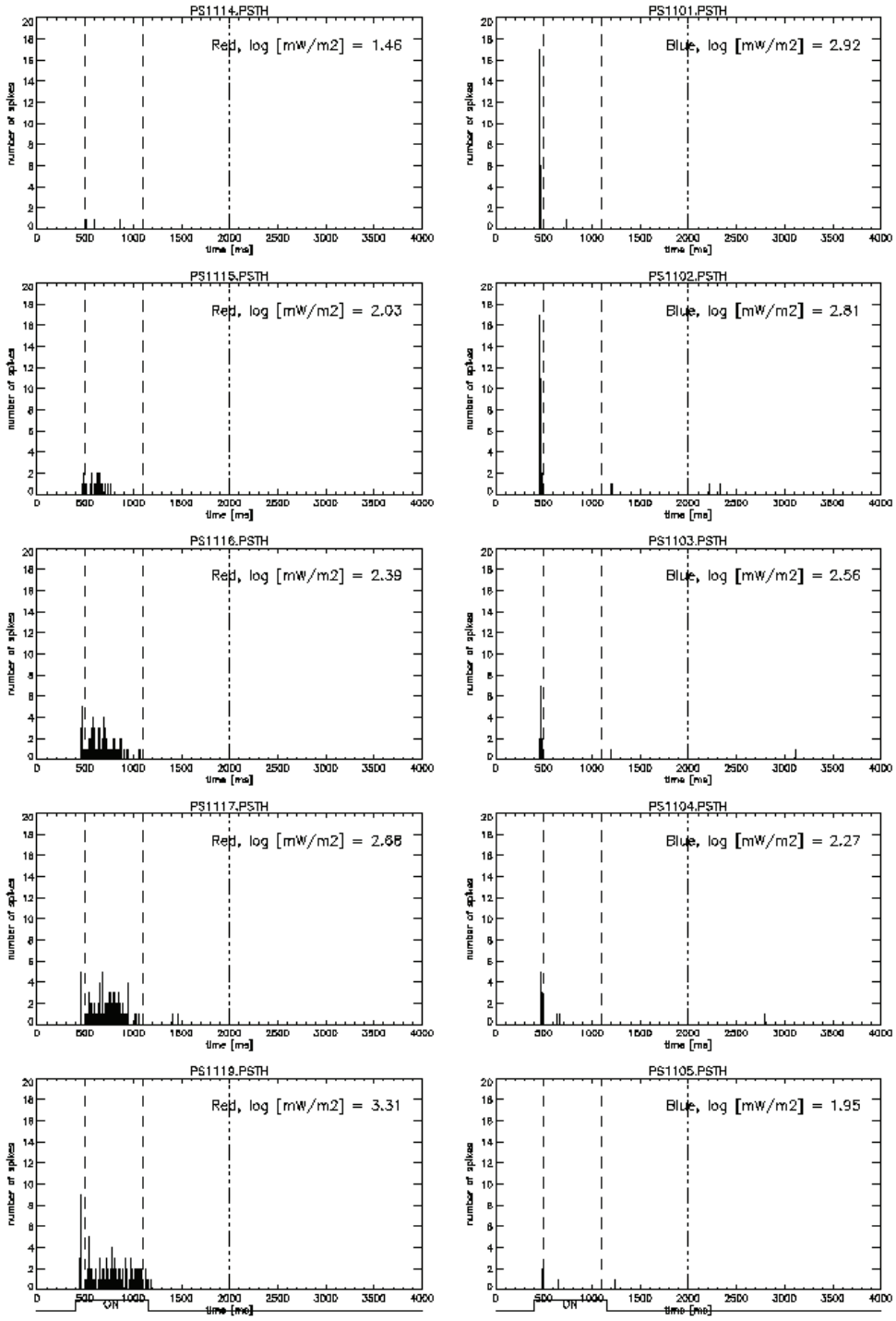

Fig. 25 – These histograms correspond to the R/I curves in **Figure 24** (cell No. 20). Notice the absolute absence of a tonic response with blue stimulation. Although the cell is broadband in its phasic component, the tonic component is clearly narrow-band with preference for long wavelength stimulation.

3.2.2. Geniculo-cortical system

3.2.2.1 Narrow-band Cell D (A17 - supragranular)

This cell (**cell 3**) was recorded during experiment T.AD. 172. It was found in Area 17, layer III between sublayers a and b at a depth of 580 microns. The cell is binocularly driven and responds to both stationary and moving stimuli (the latter show a certain directional preference). The histograms in **Figure 26** show the cell's response to contralateral stationary stimulation. The response is ON.

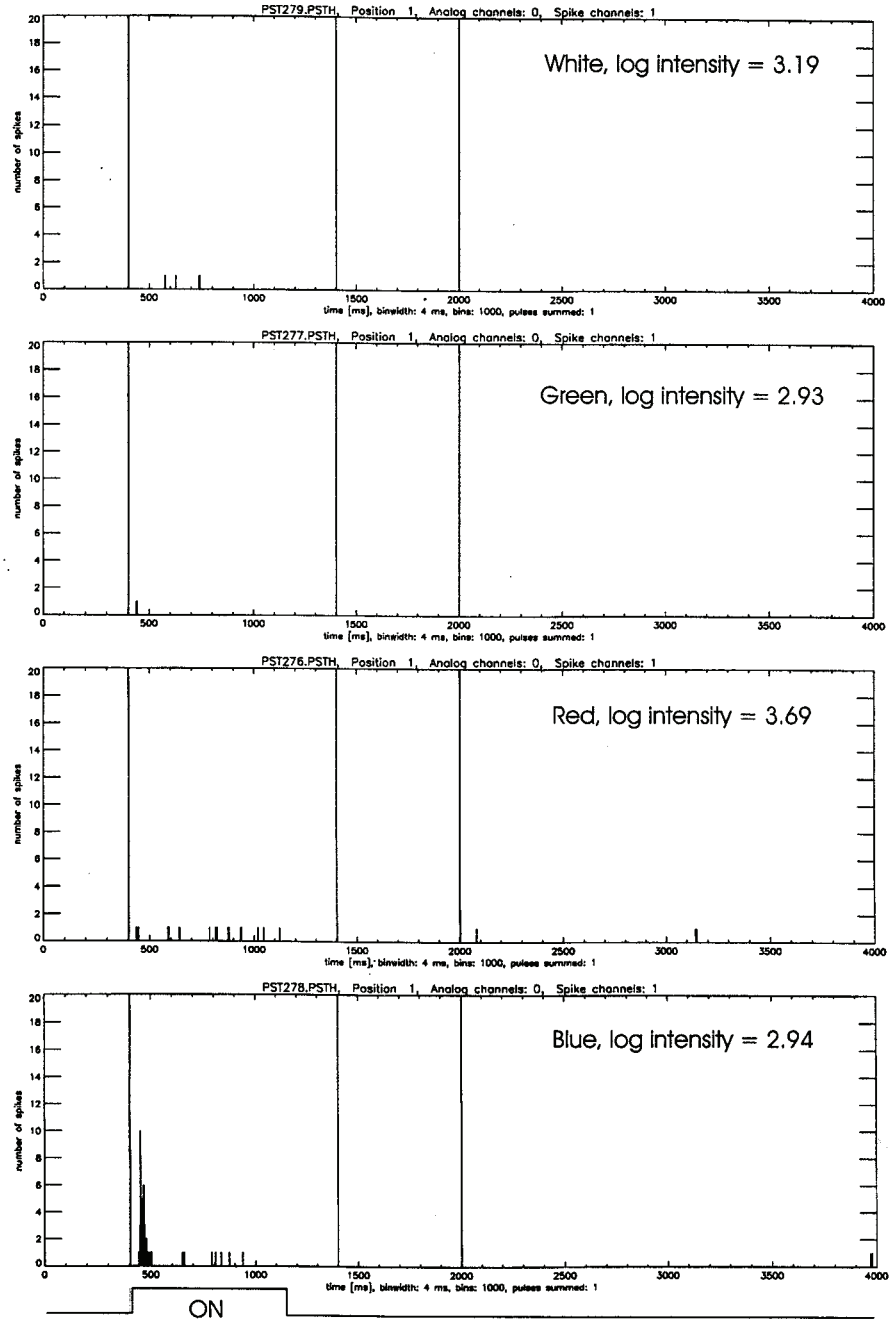

Fig. 26 – Histograms indicating response of narrow-band cell D (cell No. 3) to contralateral stationary stimulation. Notice that only blue elicits a response.

As can be seen from the preceding histograms, only blue light is capable of activating the cell (even though its intensity is lower than for long-wavelength stimulation). It is not clear, however, why the cell does not respond to white light, which also has a short-wavelength component. Presumably, this is due to inhibition by the long-wavelength component. In conformity with this hypothesis, we observed that red stimulation immediately preceding blue, will completely inhibit the response to blue (see **Figure 27)**. Blue had exactly the same intensity as in the previous figure, where a strong response had been observed.

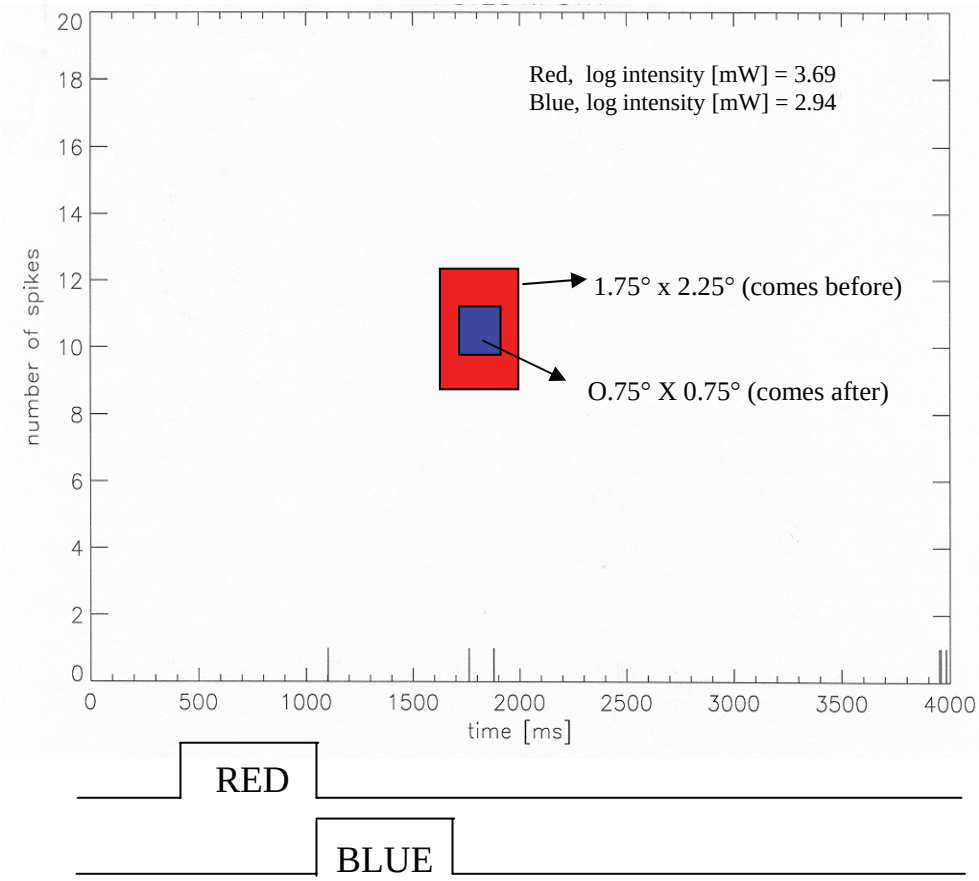

Fig. 27 – This histogram illustrates how red preceding blue can inhibit the cell's response to blue. Notice that blue had the same intensity, which had previously elicited a strong response (cf. **Figure 26**).

The two previous histograms illustrated the cell's response to stimulation from the contralateral eye. When the stimulation comes from the ipsilateral eye, a wholly different response is elicited as shown in **Figure 28.**

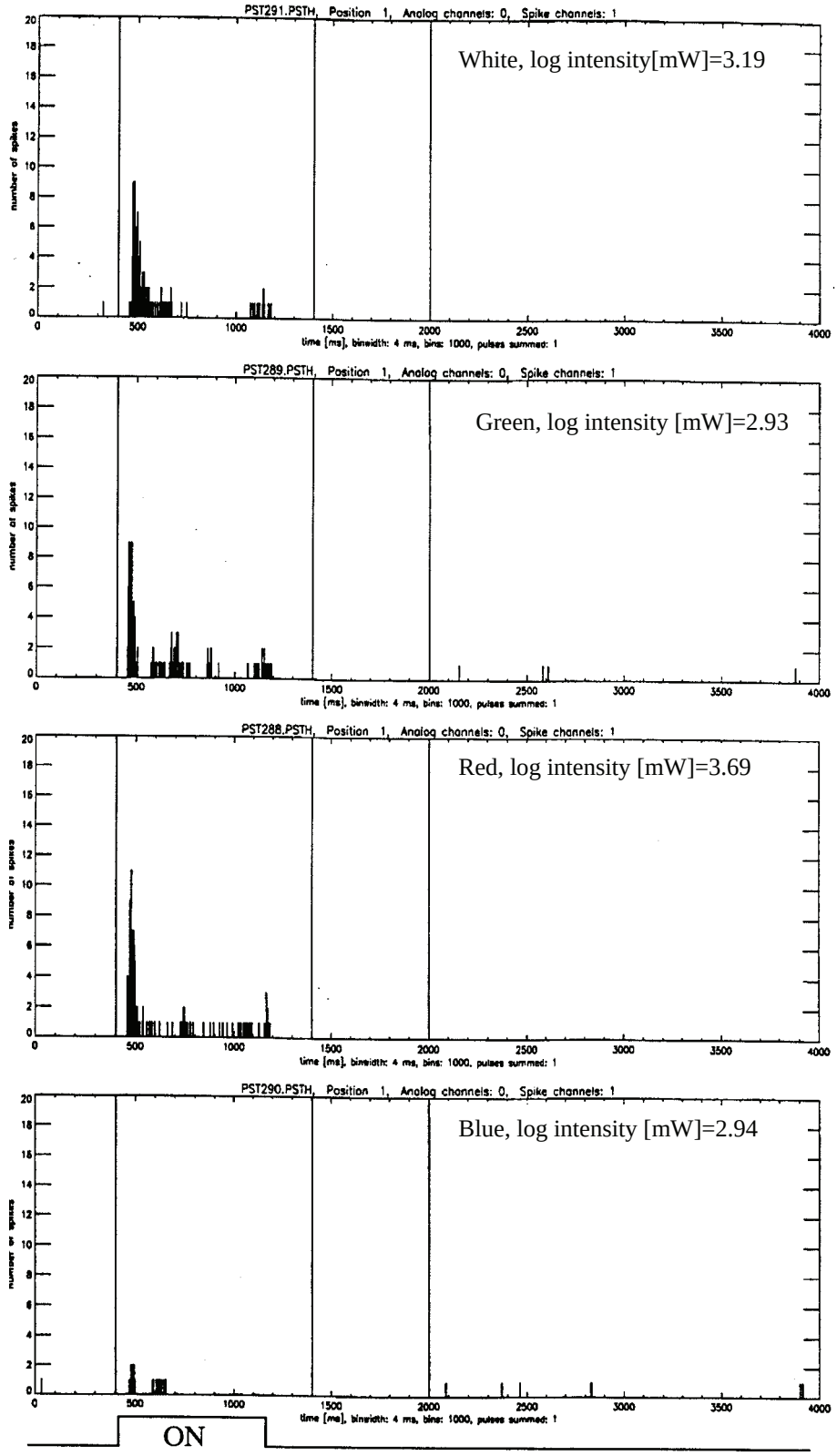

Fig. 28 – Response of narrow-band cell D to ipsilateral stationary stimulation. Notice the stronger response to long-wavelength stimulation. (Cf. **Figure 26**).

One can see that during ipsilateral stimulation, blue gives rise to the weakest response. In summary, this cell is narrow-band for one eye (contra) and broadband for the other (ipsi), but with a strong bias towards long wavelengths.

3.2.2.2 Narrow-band cell E (A17 - supragranular)

This cell corresponds to **number 6** in our listing and was found in animal T.AD. 175. It is localized in sublayer IIIb of area 17 at a depth of 850 microns. The cell is driven by stationary stimuli through both the contra- and the ipsilateral eye giving a phasic ON-OFF response. Although only two intensities could be tested for each wavelength, we noticed that in the R/I curves of the **contralateral** eye, only blue gave a response showing a positive slope as illustrated in **Figure 29** and **Figure 30**; corresponding histograms are shown in **Figures 31** and **32**, respectively.

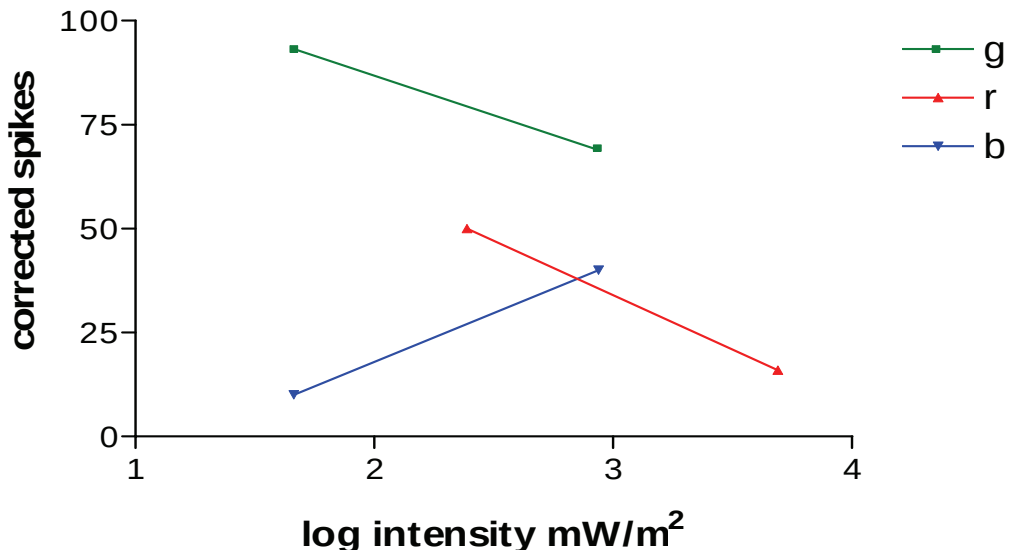

Fig. 29 - Narrow-band cell E. ON-response to different wavelengths. Notice that only blue gives positive slope in response to contralateral stimulation. Compare this also to previous cell (Narrow-band cell D).

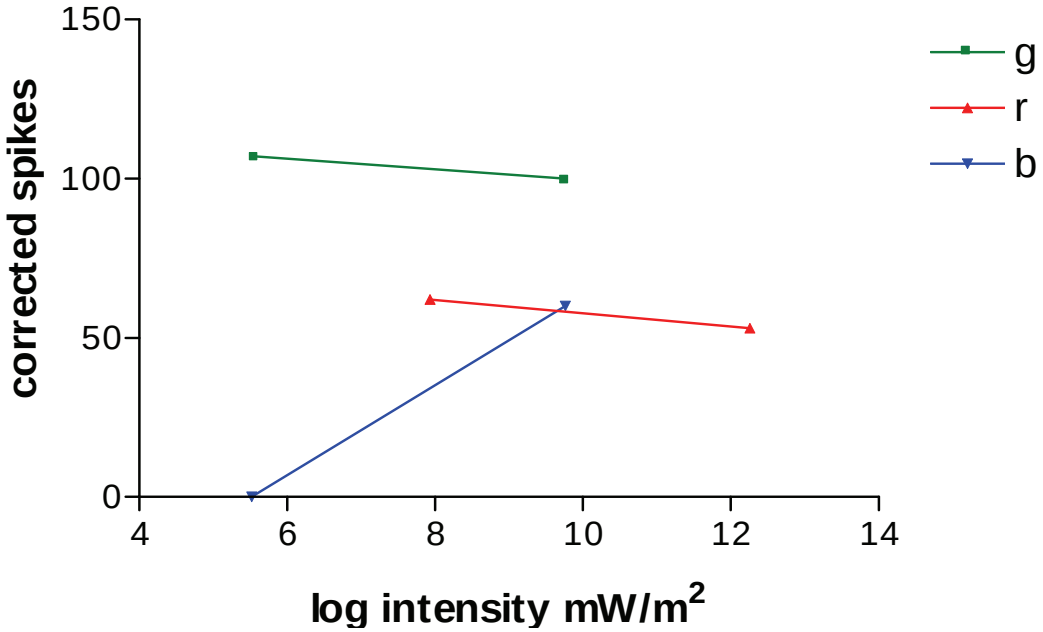

Fig. 30 – Narrow-band cell E. OFF-response to different wavelengths. Notice that only blue gives positive slope.

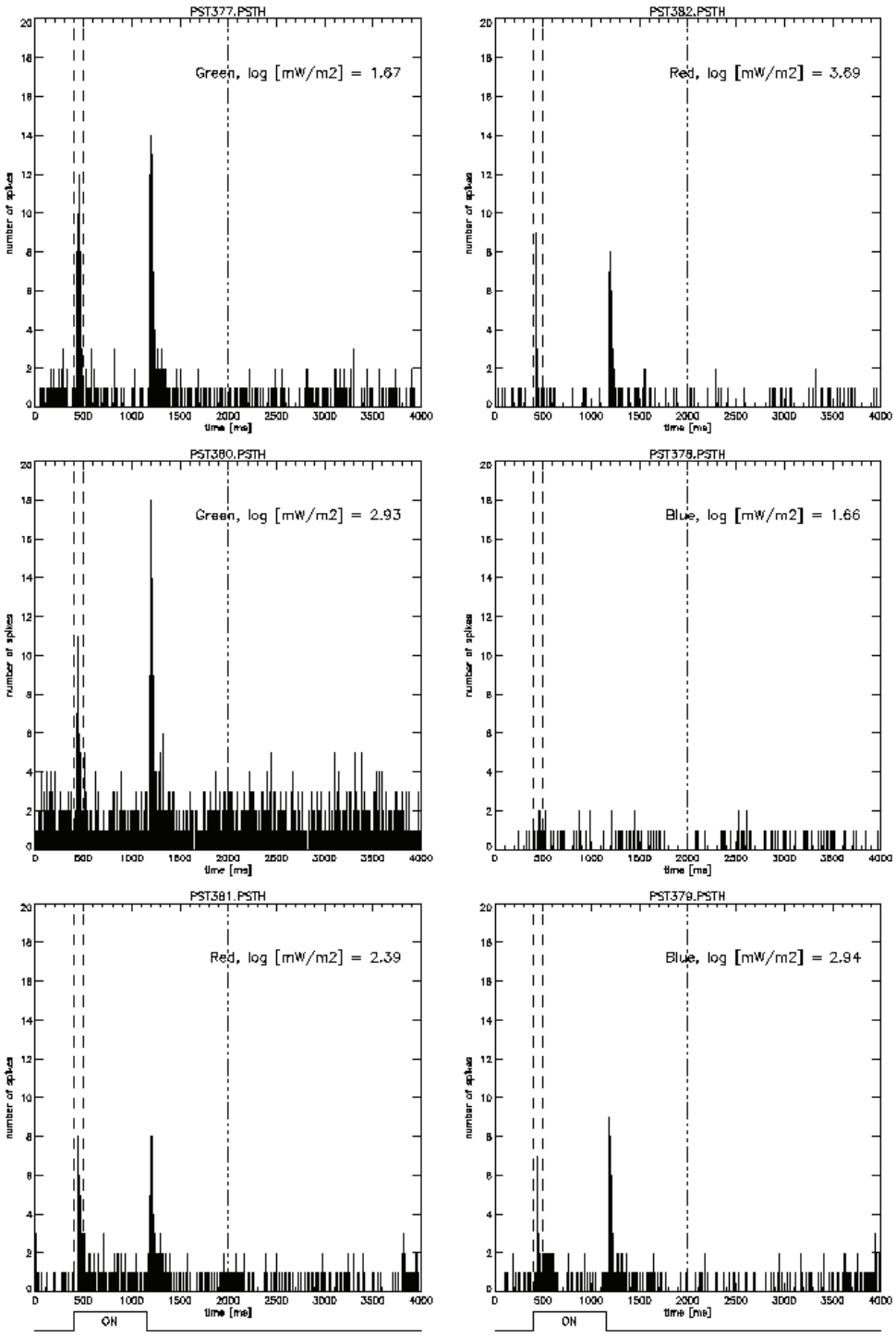

Fig. 31 – Histograms corresponding to **Figure 29**. ON – response.

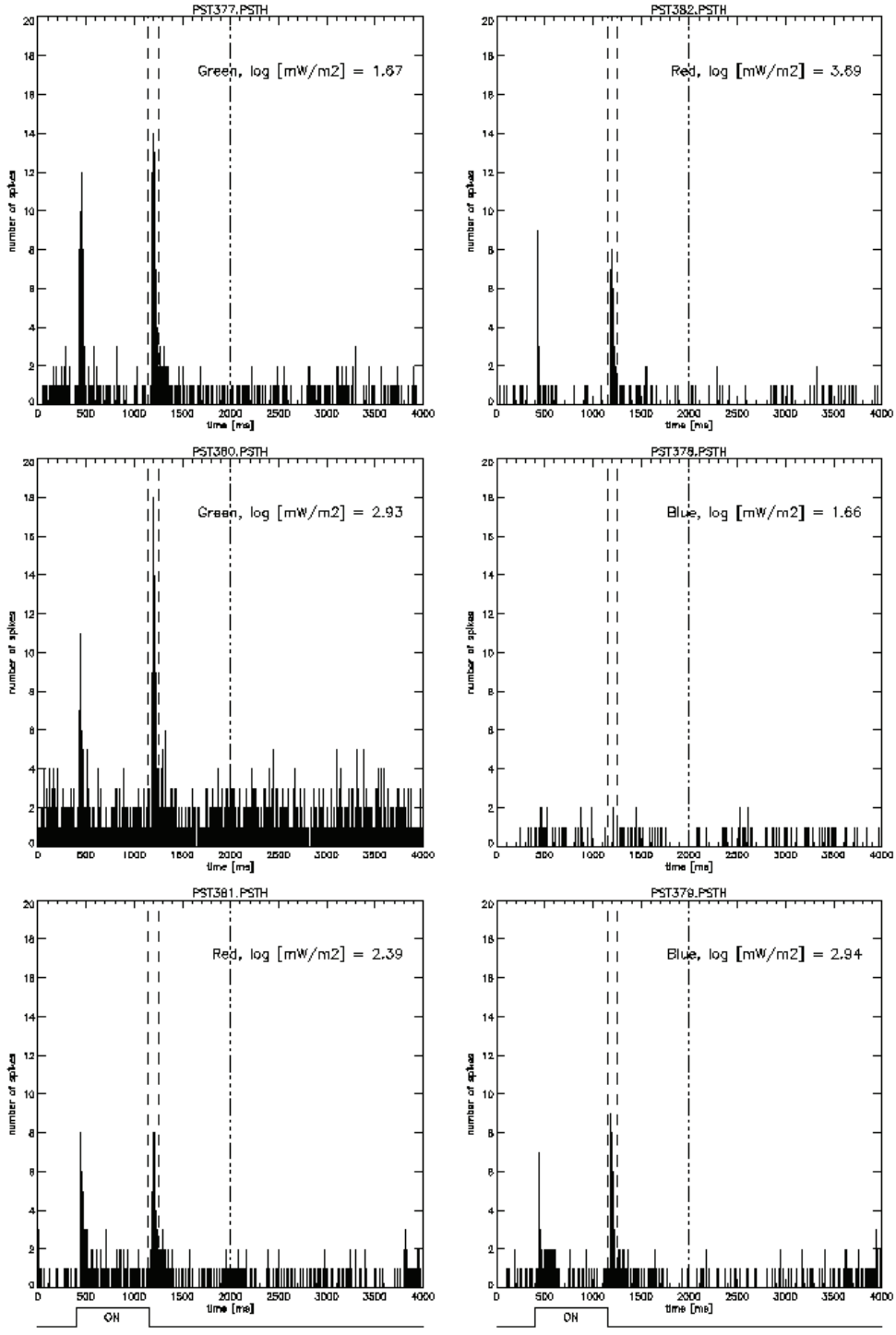

Fig. 32 - Histograms corresponding to **Figure 30**. OFF – response.

It is remarkable that for the other eye (ipsilateral), exactly the opposite phenomenon can be observed: only the short-wavelength stimulation gives a negative slope as seen in **Figure 33** (the corresponding histograms are shown in **Figure 34**). It appears that this cell like the previous one (narrow-band cell D) manifests ocularity-dependent color-bias inversion eye.

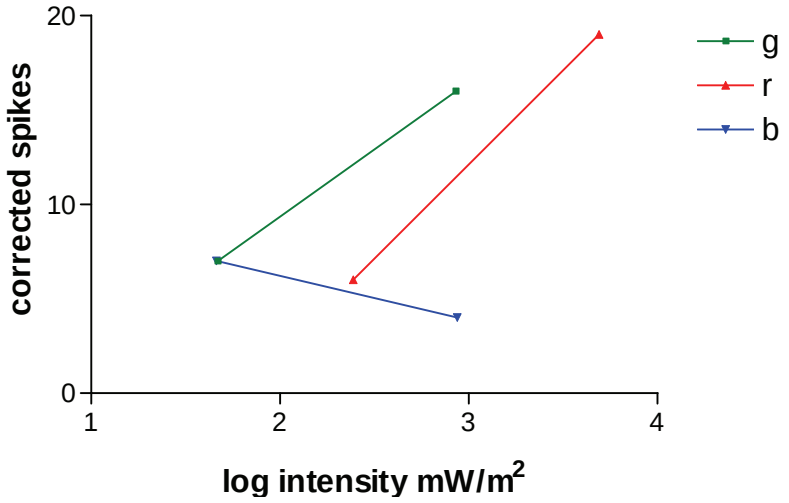

Fig. 33 – Narrow-band cell E. ON-response to different wavelengths. Ipsilateral stimulation. Notice that only blue gives negative slope. This is the opposite effect as with contralateral stimulation.

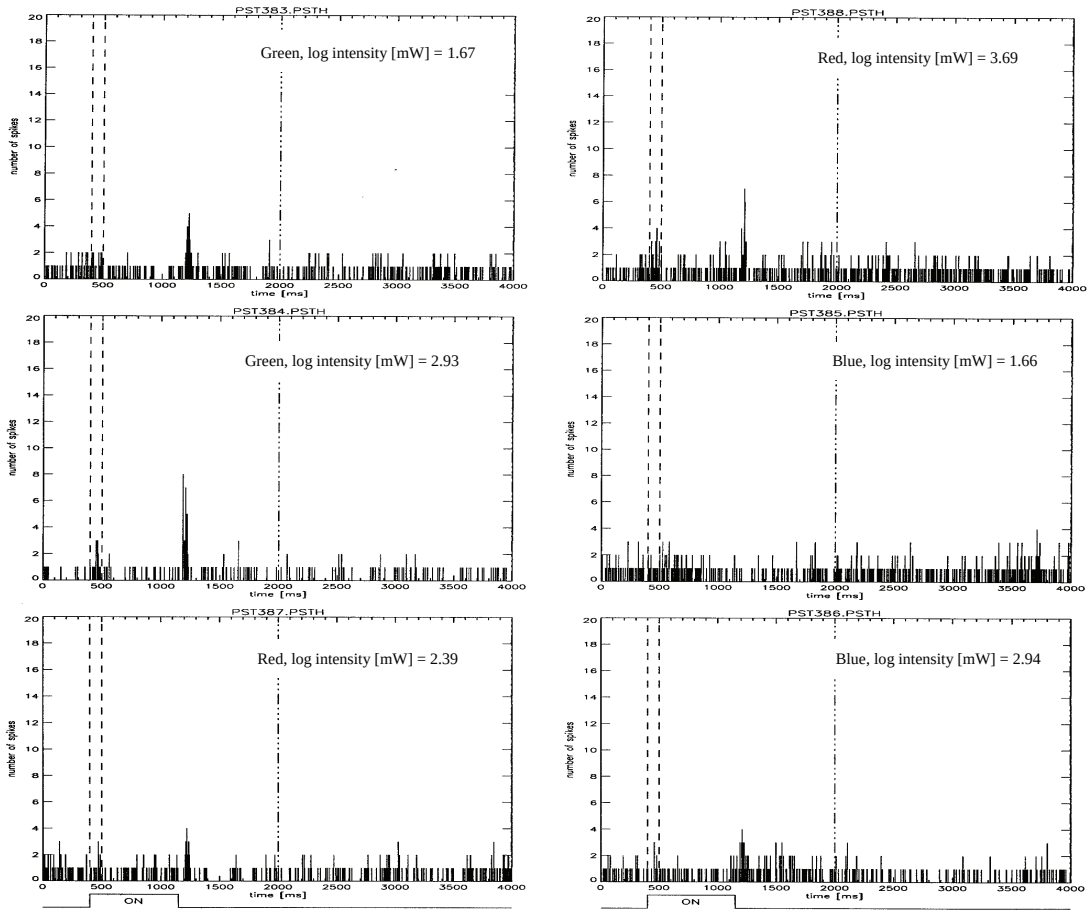

Fig. 34 – Histograms corresponding to **Figure 33**. Ipsilateral stimulation.

3.2.2.3 Narrow-band Cell F (A17 - granular)

This cell was recorded during the experiment carried out on animal T.AD. 180, and corresponds to cell **number 9** in our listing. It is localized in Area 17 - sublayer IVb, at a depth of 1210 microns, and gives an OFF response (as is mostly the case in this sublayer) to stationary stimuli. The cell is color-opponent in the restricted sense that its gain, as can be observed from R/I curves, is positive for one set of wavelengths, namely white and blue, and negative for red and green. This is not classical color-opponency, for that, presumably would require not only negative gain, but also a progressive suppression of activity in one domain of wavelengths, and the opposite effect in the other.

Expressed in different terms, this means that all wavelengths evoke a response, however, as intensity increases, the short wavelengths increase response, and the long wavelengths decrease response, as can be seen in the following R/I curves in **Figure 35.**

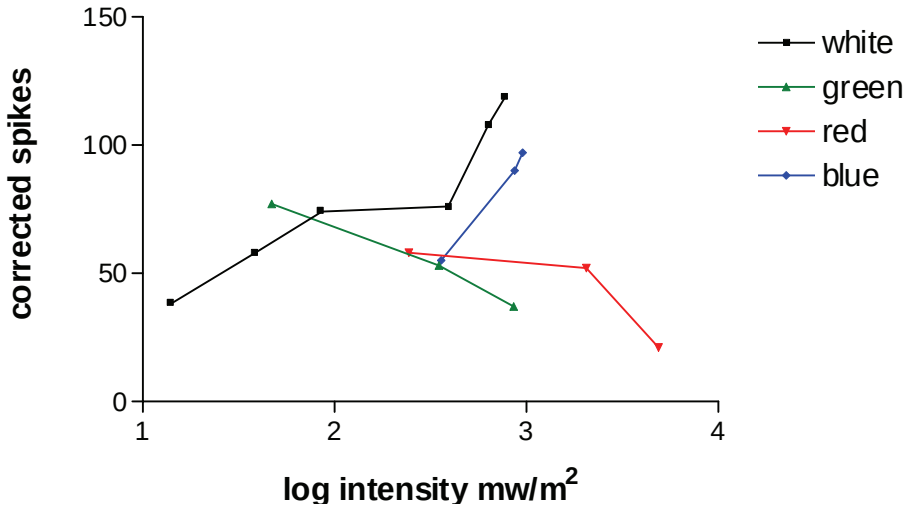

Fig. 35 – R/I curves of narrow-band cell F (cell No. 9). Observe the negative slopes for green and red, whereas blue has a positive slope, similarly to white.

3.2.2.4 Narrow-band Cell G (A18)

This corresponds to cell **number 8**, which was found in animal T.AD. 180 in Area 18. This was short lived and no histograms could be generated. Nonetheless, during the brief span of stimulation, the cell responded exclusively to short wavelength light and demonstrated peculiar characteristics, such as sensitivity to rotation. (However we must be circumspect of findings from cells for which we lack hard data).

3.2.2.5 Narrow-band Cell H (dLGN)

This narrow-band cell corresponds to **number 26** in our listing and was found during experiment T.AD. 191. It is localized in lamina 3 of the dLGN at a depth of 5420 microns from the pial surface of the cortex. The cell is driven by the contralateral eye, and responds to stationary stimulation. The response is ON-OFF and comprises both a phasic and a tonic component. The R/I curves for this cell are shown in **Figure 36**, the corresponding histograms are shown in **Figure 37**.

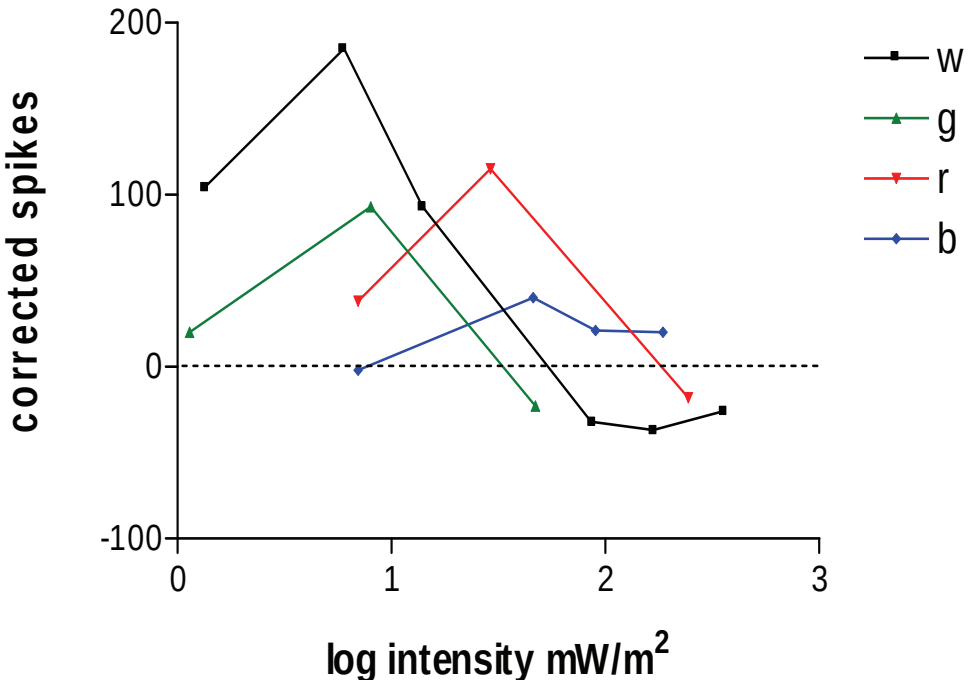

Fig. 36 – R/I curves showing response of cell No. 26 (lamina 3 dLGN – OFF response). Observe that in the saturation range, activity sinks to below zero for all but blue. Notice also that throughout the dynamic range of the blue curve, the green and white curves have a negative slope.

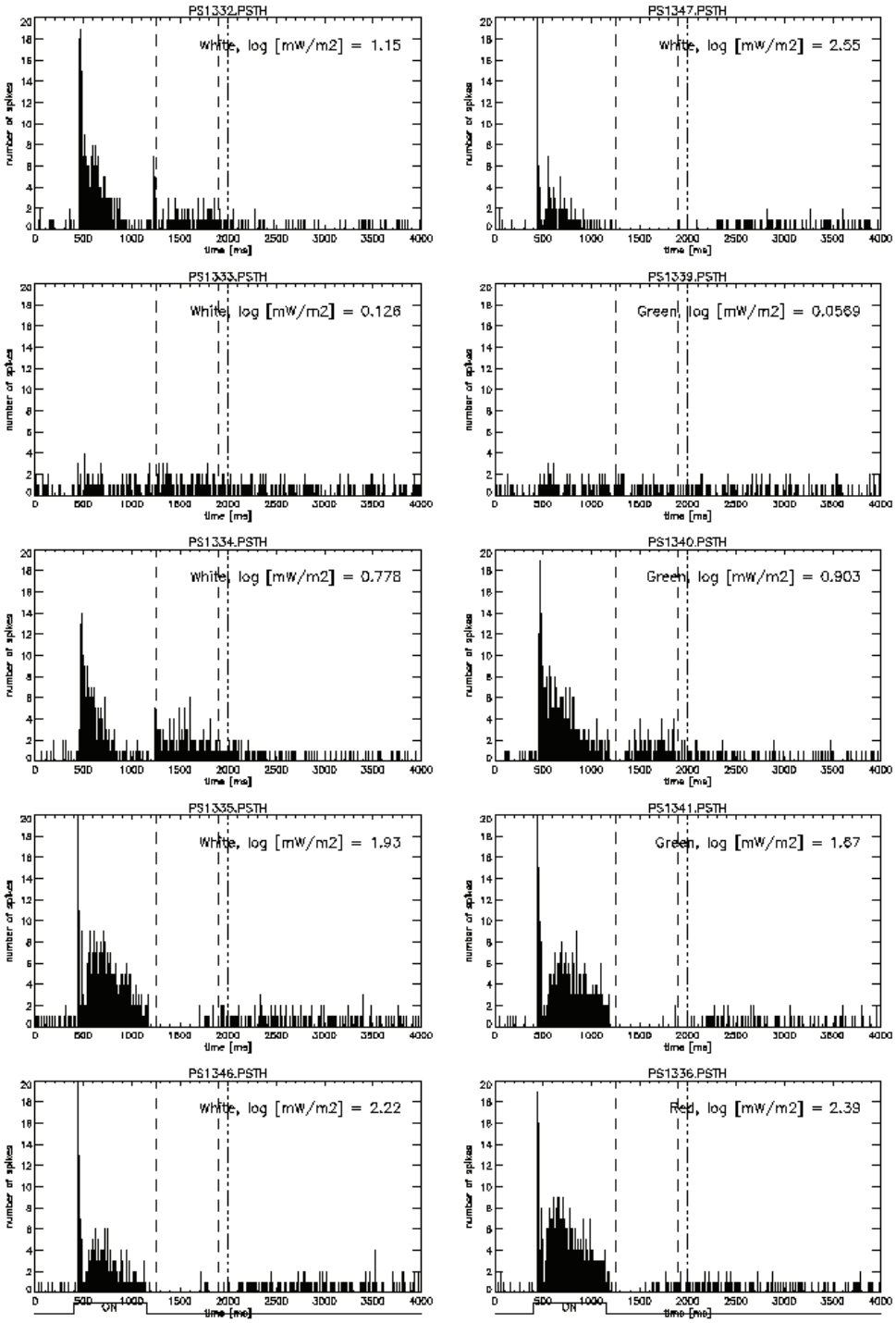
PS1332.PSTH
White, log [mW/m2] = 1.15
PS1347.PSTH
White, log [mW/m2] = 2.55
PS1333.PSTH
White, log [mW/m2] = 0.126
PS1339.PSTH
Green, log [mW/m2] = 0.0589
PS1334.PSTH
White, log [mW/m2] = 0.778
PS1340.PSTH
Green, log [mW/m2] = 0.903
PS1335.PSTH
White, log [mW/m2] = 1.93
PS1341.PSTH
Green, log [mW/m2] = 1.87
PS1346.PSTH
White, log [mW/m2] = 2.22
PS1336.PSTH
Red, log [mW/m2] = 2.39
number of spikes
time [ms]
ON

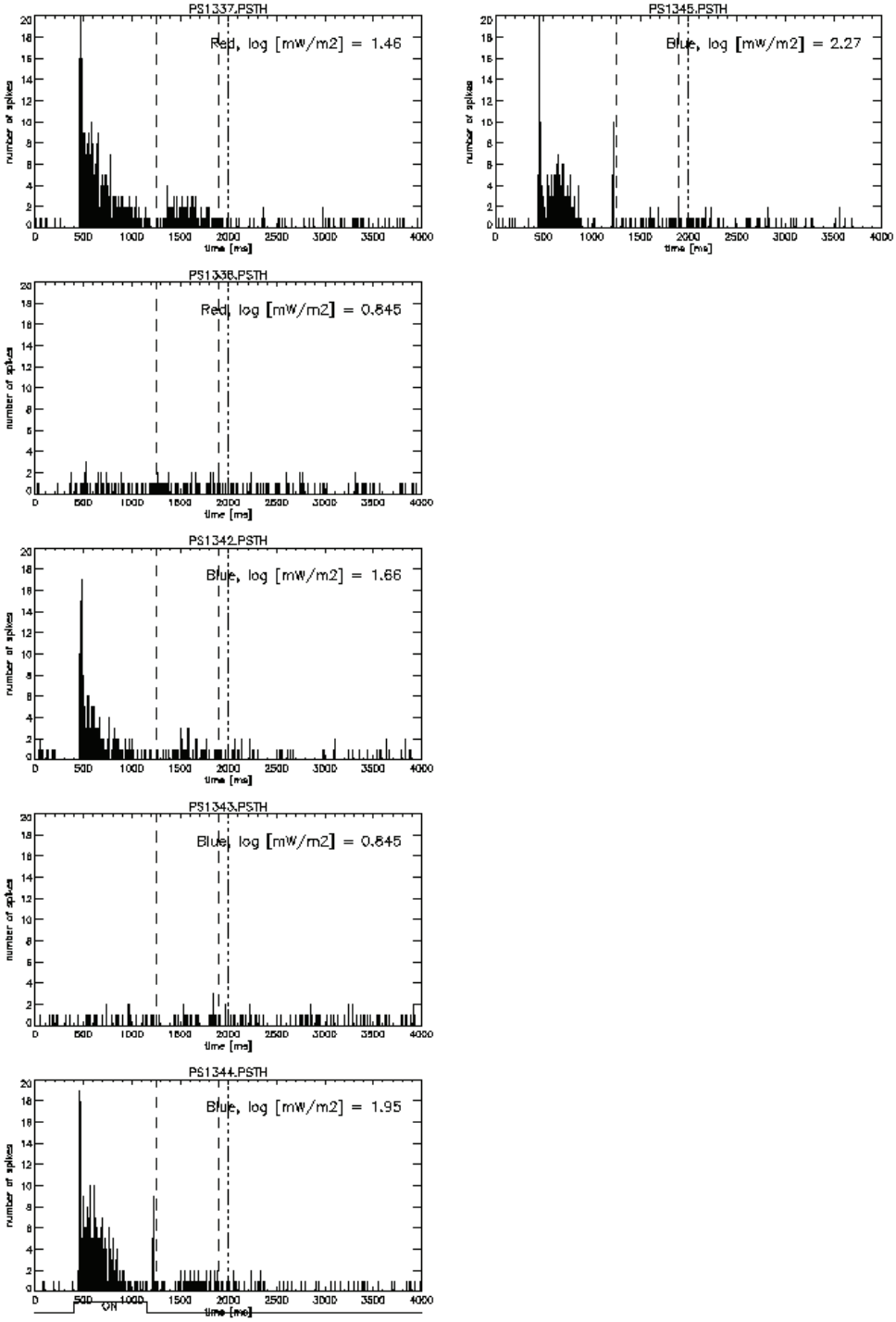

Fig. 37 – Histograms from cell No. 26 (dLGN – lamina 3).

In this R/I curve, it is noticeable that practically throughout the dynamic range of the blue curve, the green curve has a negative slope. This suggests that, at least at this domain of intensity and with this wavelength mixture, the cell may function as a color-opponent cell with the short-wavelength channel acting as an excitatory input, and the long-wavelength channel (in this case green) inducing a progressive inhibition. Observe also that in the saturation range, corrected spike activity sinks to below zero for all but blue.

3.3 Broadband blue-biased cells – Criteria for definition

While, the response of the majority of cells to short-wavelengths stimulation in this study is either negligible or a fraction of what is to other wavelengths, the blue-biased cells show stronger than usual responses to short wavelengths. Blue-biased cells respond both to long and short wavelengths, and are, in this sense, broadband. Unlike narrow-band cells, they do not show, inverted slopes of gain functions, ocularity dependant inversion of color-bias, or selective restriction of responses to one wavelength in the phasic or tonic modality. Their peculiarity lies in their strong absolute response in short-wavelength domain and/or an unusually strong gain (steep R/I curves). In total, six such cells were found (11.11 %) in different locations: Only one in the extragenicular system (CS) and all the others in the geniculo-cortical system.

3.3.1 Extragenicular system

3.3.1.1 Blue-biased cell A (Colliculus superior – Stratum opticum)

This cell corresponds to **number 13** in our listing. It was found in animal T.AD. 185. The cell is localized in the Colliculus superior (Stratum opticum) and is driven by stationary stimuli in both the contra- and the ipsilateral eye giving a phasic ON and OFF response. Although, the absolute response is only slightly higher in blue than in green, as shown in **Figure 38**, this represents extraordinary sensitivity to blue considering most cell's response to this wavelength.

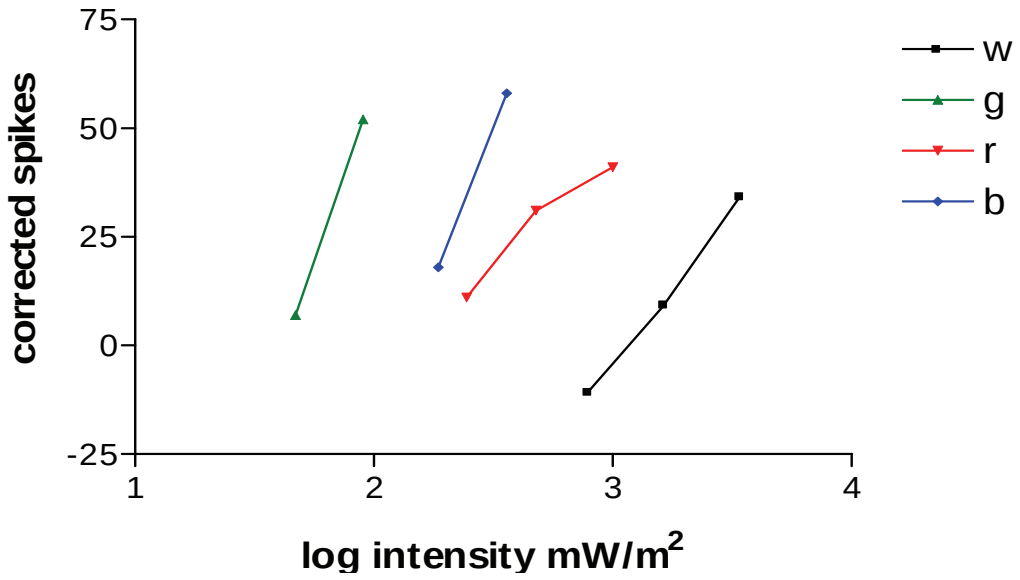

Fig. 38 – Blue-biased cell A (cell No. 13). Notice blue gives the highest response.

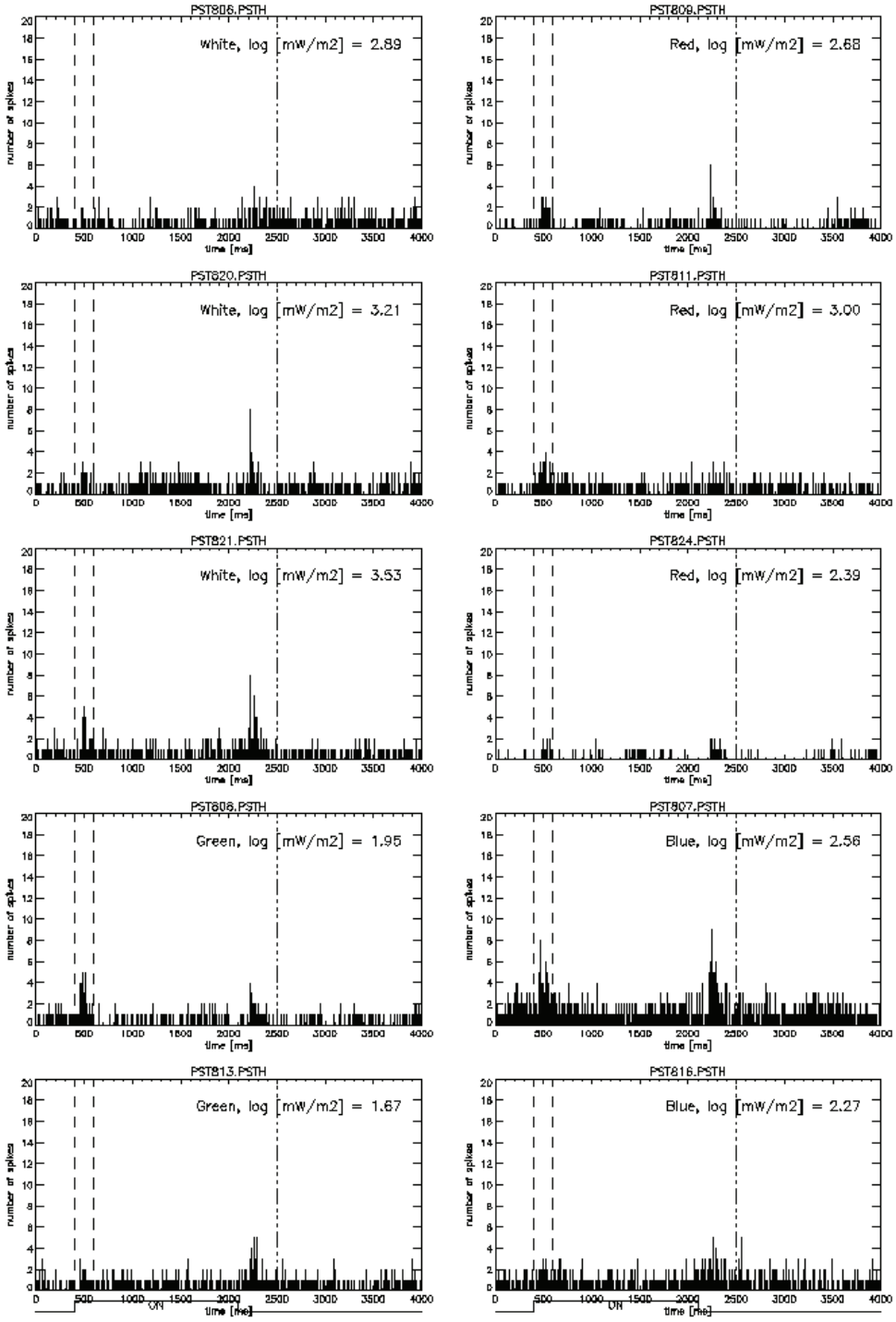

Fig. 39 – Histograms corresponding to R/I-curves in **Figure 38**.

3.3.2 Geniculo-cortical system

3.3.2.1 Blue-biased cell B (dLGN – lamina 2)

This cell corresponds to **number 27** in our listing and was found in animal T.AD. 191. It is localized in dLGN lamina 2. The cell is driven by contralateral stimulation with stationary stimuli giving an ON-response with both phasic and tonic components. A complete R/I curve is available only for white, since cell-survival time was limited.

In the phasic component (up to 68 msec after stimulus onset), blue gives a response comparable to green, albeit at a different intensity. Nonetheless, if one considers the phasic *and* tonic components, in this case, from 68 to 1800 msec after stimulus onset, one notices that blue gives the highest absolute response at an intensity of 90 mW, corresponding to 1.95 in log units. Indeed, this cell had an unusually strong tonic component, lasting throughout and even slightly beyond the interval during which the stimulus was on (1750 msec). The strong response to blue is shown in **Figure 40** and the corresponding histograms in **Figure 41**.

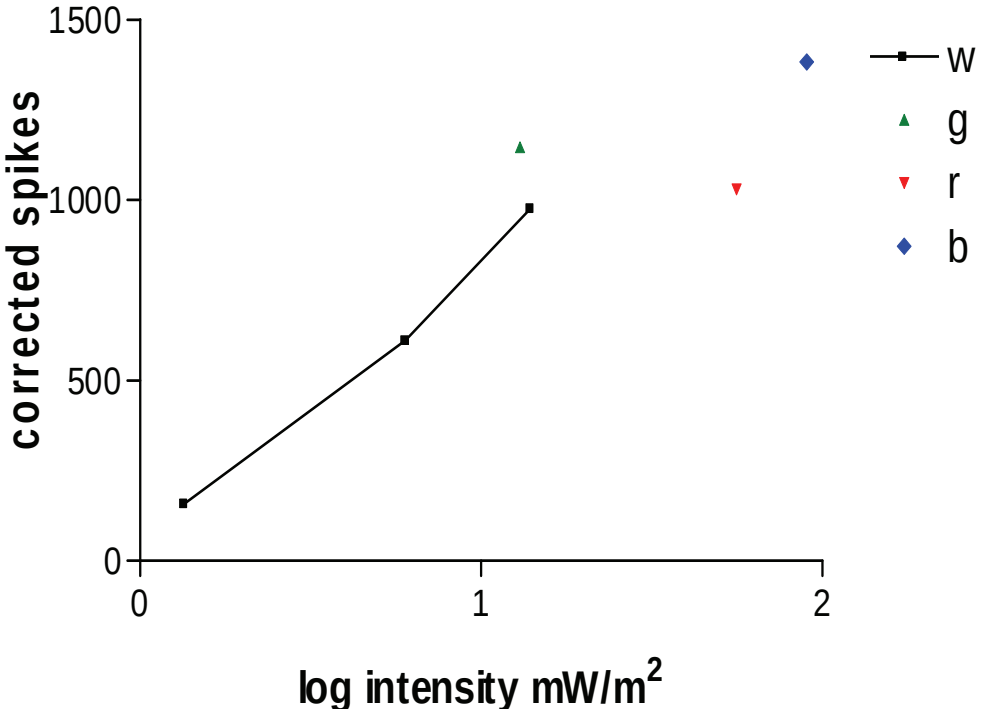

Fig. 40 – Cell No. 27. Notice the strong response given by blue.

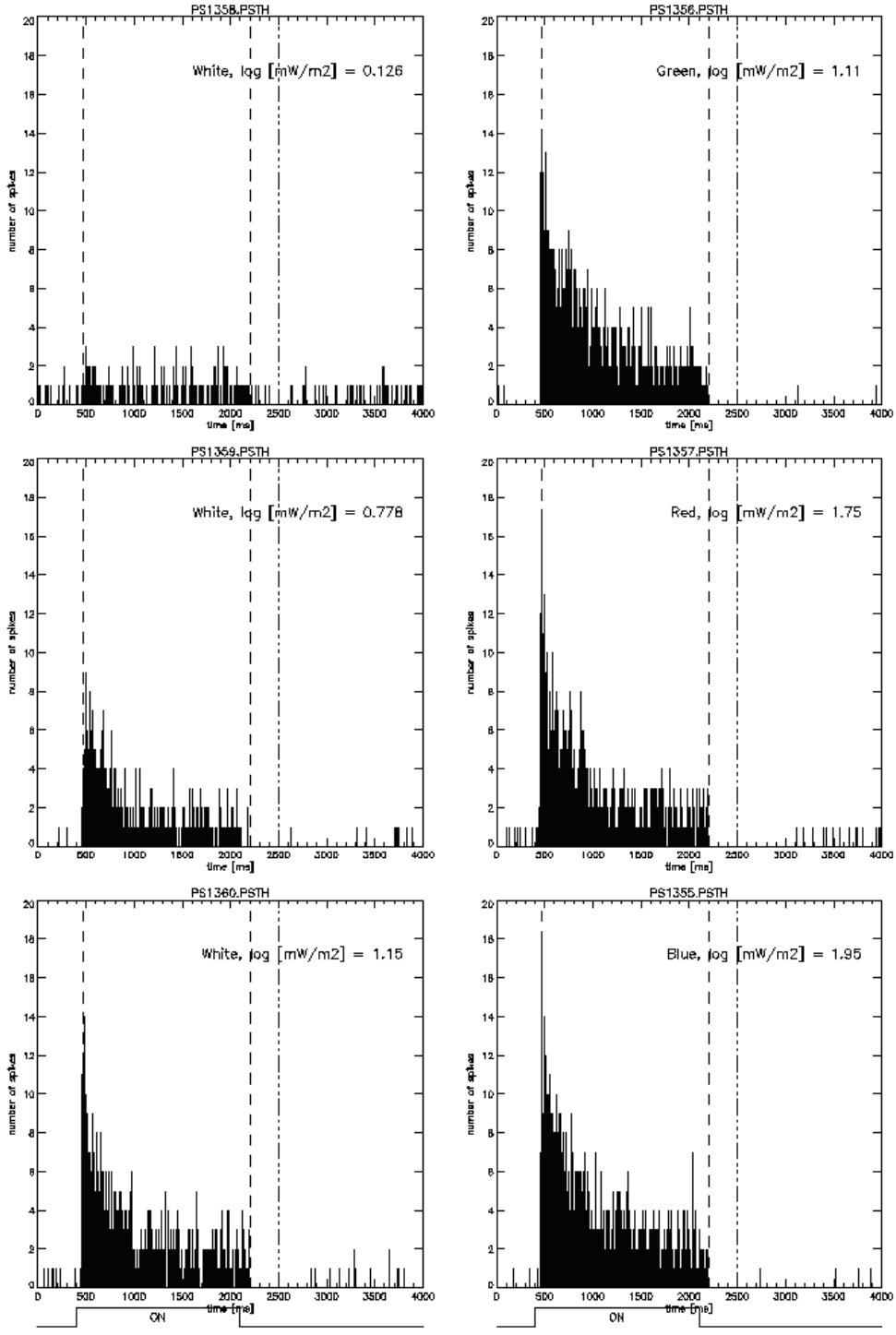

Fig. 41 – Histograms from cell No. 27, corresponding to data on **Figure 40**. Notice the strong response in blue (even though the only stimulus that could be tested was of relatively low intensity).

3.3.2.2 Blue-biased cell C (dLGN – lamina 6)

This cell corresponds to **number 21** in our listing. It was found in animal T.AD. 191. The cell is localized in lamina 6 of the dLGN at a depth of 4420 microns. The cell is driven by contralateral stimulation with stationary stimuli giving an OFF-response with both phasic and tonic components. The R/I curves in **Figure 42** illustrate this. The histograms in **Figure 43** correspond to these.

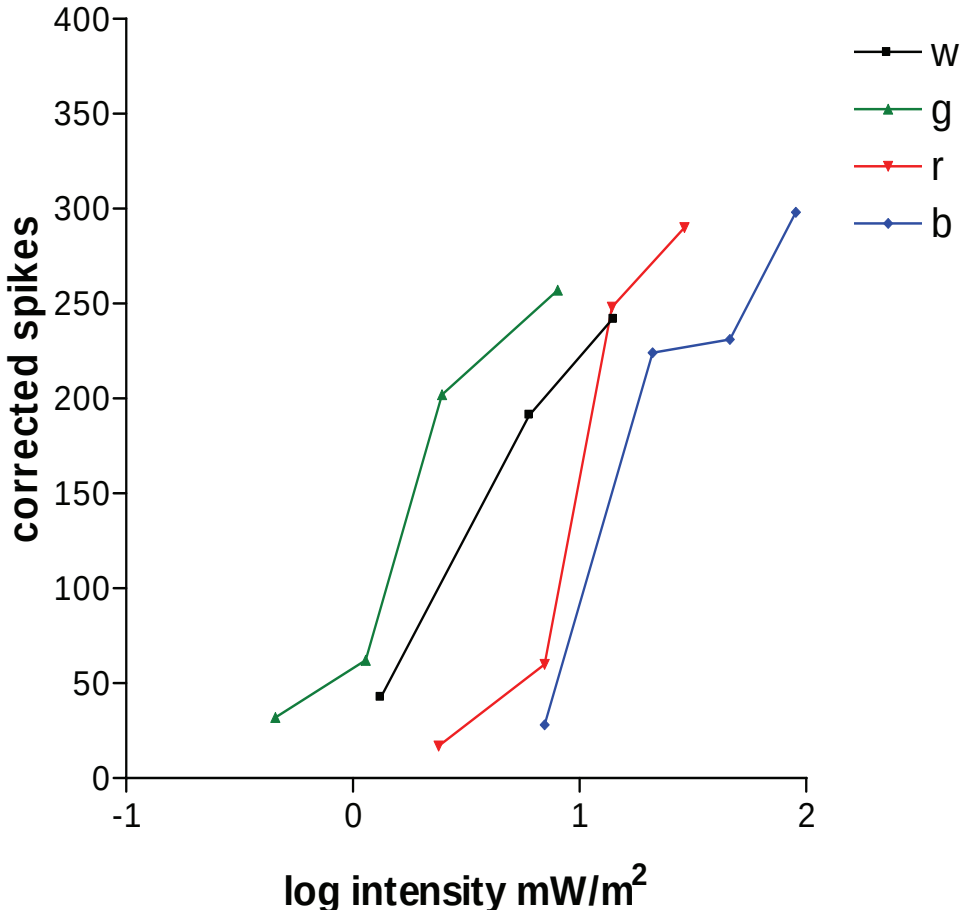

Fig. 42 – R/I curves for cell No. 21. Notice that blue gives the highest response at maximum intensity (slightly higher than red). Usually the maximum peeks for blue are considerably lower.

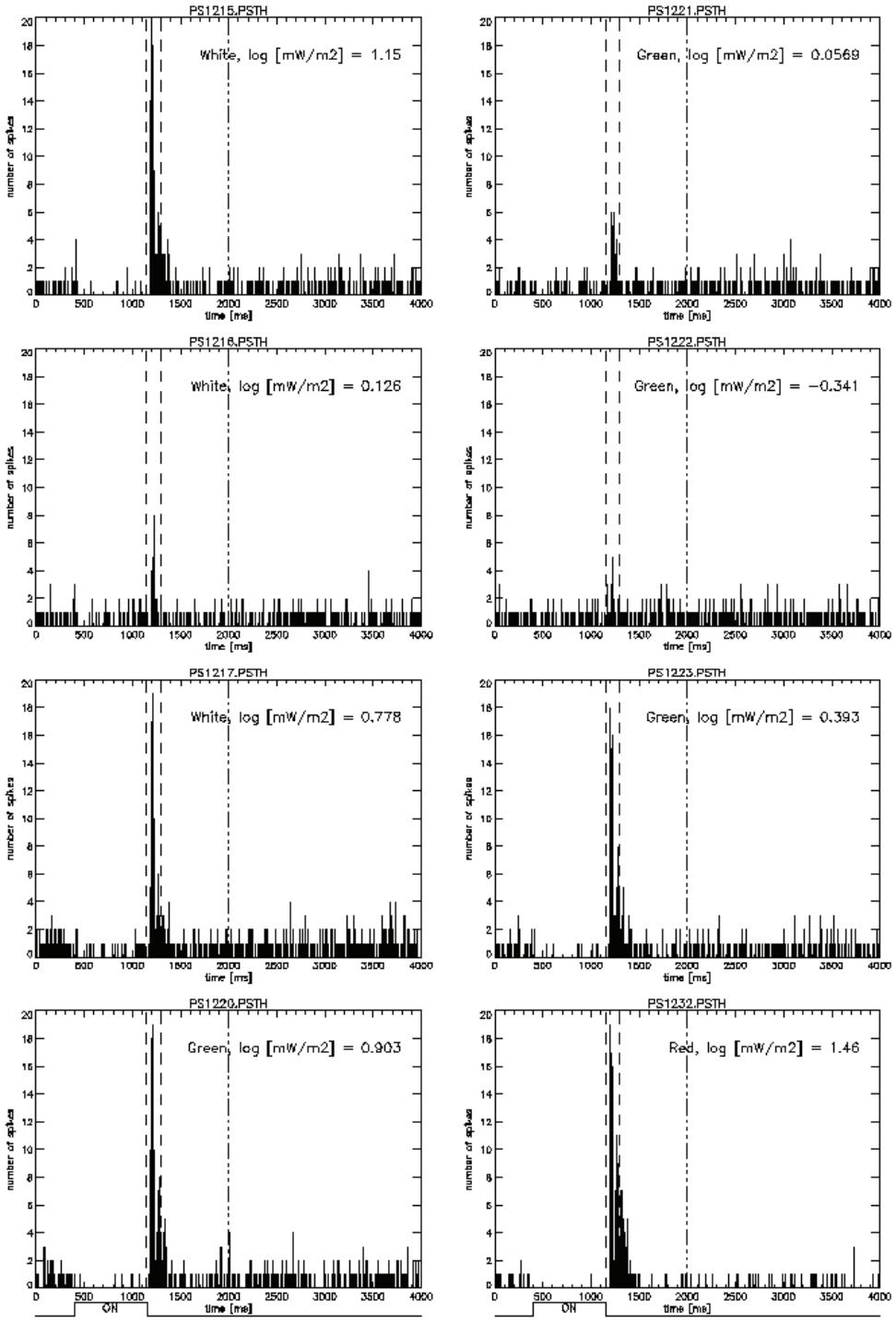
PS1215.PSTH
White, log [mW/m2] = 1.15
PS1221.PSTH
Green, log [mW/m2] = 0.0569
PS1216.PSTH
White, log [mW/m2] = 0.126
PS1222.PSTH
Green, log [mW/m2] = −0.341
PS1217.PSTH
White, log [mW/m2] = 0.778
PS1223.PSTH
Green, log [mW/m2] = 0.393
PS1220.PSTH
Green, log [mW/m2] = 0.903
PS1232.PSTH
Red, log [mW/m2] = 1.46
number of spikes
time [ms]
ON

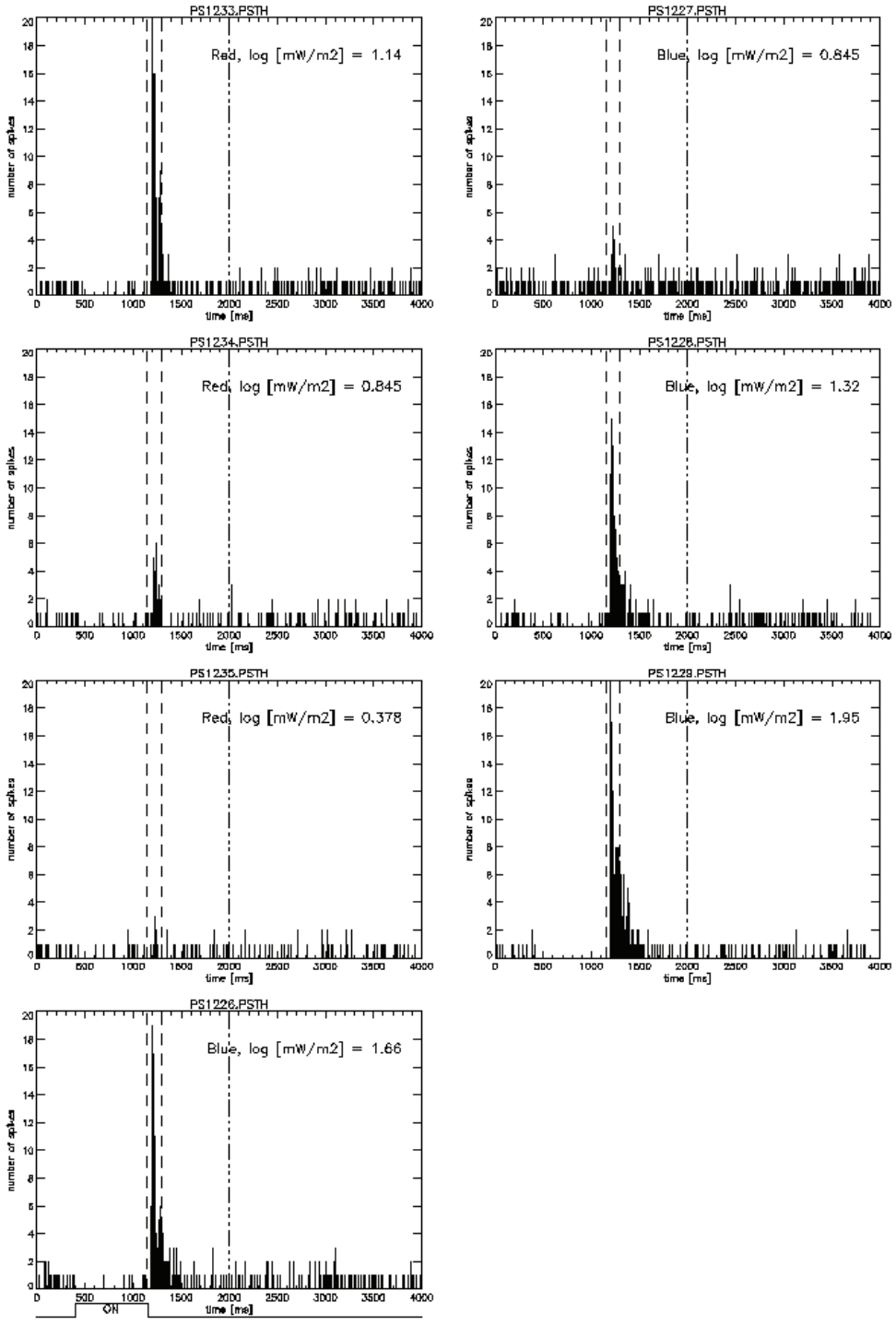

Fig. 43 – Histograms corresponding to R/I curves in **Figure 42**.

3.3.2.3 Blue-biased cell D (A17 – supragranular)

This cell corresponds to **number 43** in our listing. It was found in animal T.AD. 210, and is localized between sublayers IIIc and IVa of Area 17 at a depth of 1065 microns. The cell is driven by moving contralateral stimuli. The response is phasic. It was impossible to determine whether the response was ON or OFF since in order to fire, the cell required very rapidly moving stimuli and one could not tell whether the cell fired when the stimulus entered or exited the receptive field. The R/I curves in **Figure 44** show that white gives the highest response, probably a sum of the short- and long-wavelength components. This suggests that there is a convergence of excitatory inputs from the short-wavelength cones and the long-wavelength cones. The response is stronger to blue than red. Moreover, a part of the dynamic range in blue is rather steep (strong gain).

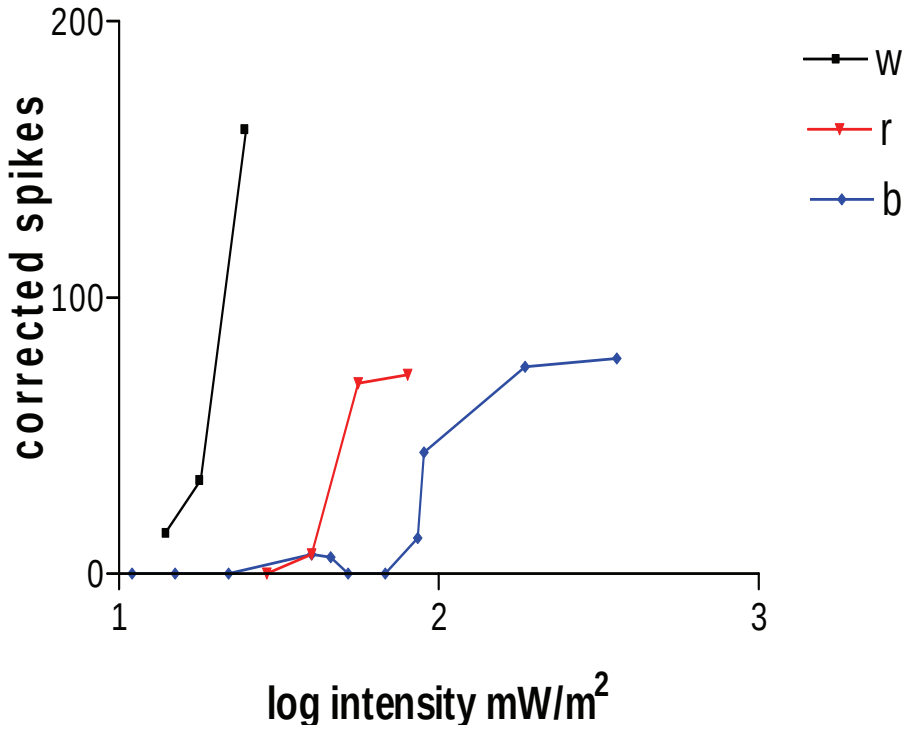

Fig. 44 – R/I curves for cell No. 43. Notice the strong gain and maximum response with blue stimulation.

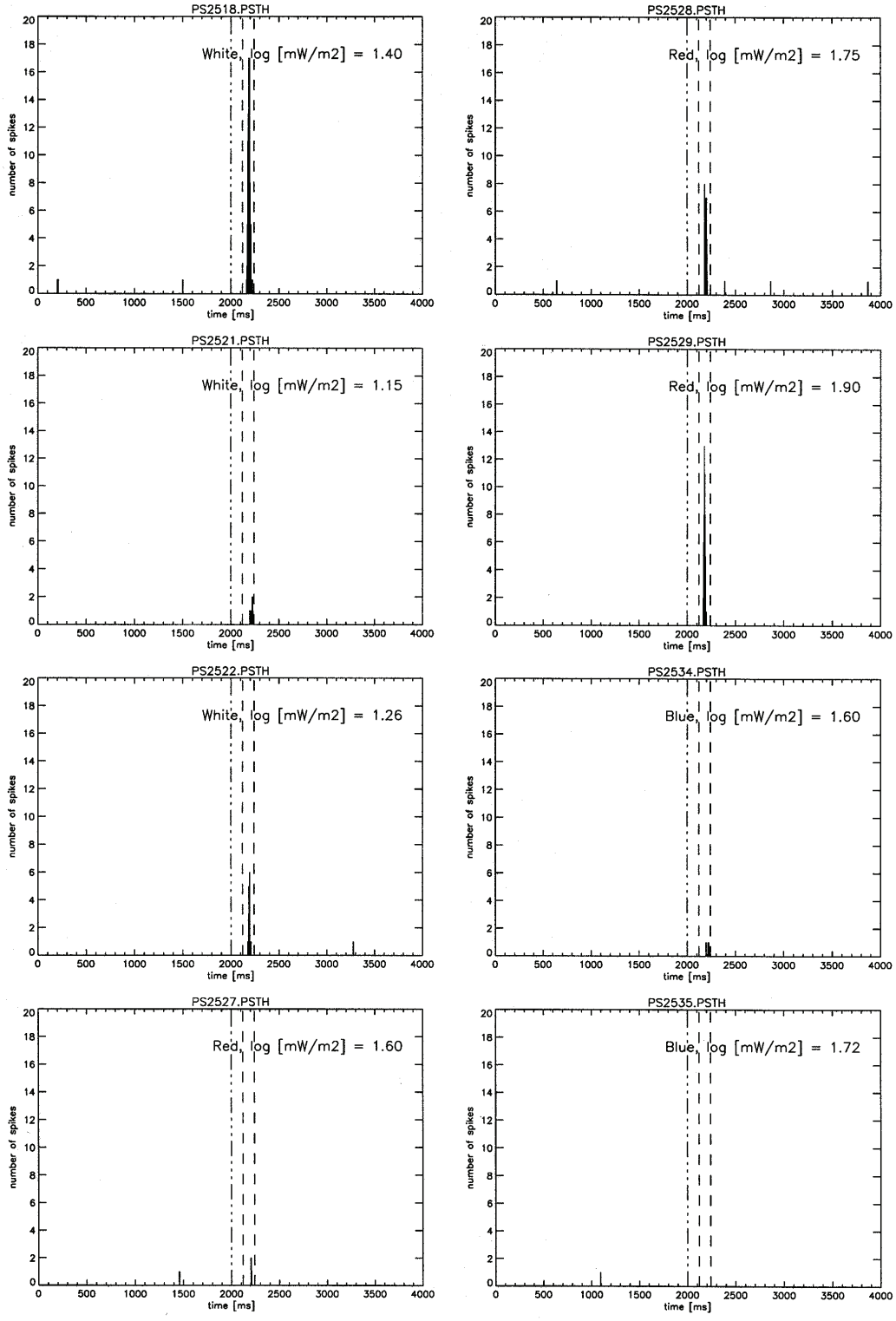
PS2518.PSTH
White, log [mW/m2] = 1.40
PS2528.PSTH
Red, log [mW/m2] = 1.75
PS2521.PSTH
White, log [mW/m2] = 1.15
PS2529.PSTH
Red, log [mW/m2] = 1.90
PS2522.PSTH
White, log [mW/m2] = 1.26
PS2534.PSTH
Blue, log [mW/m2] = 1.60
PS2527.PSTH
Red, log [mW/m2] = 1.60
PS2535.PSTH
Blue, log [mW/m2] = 1.72
number of spikes
time [ms]

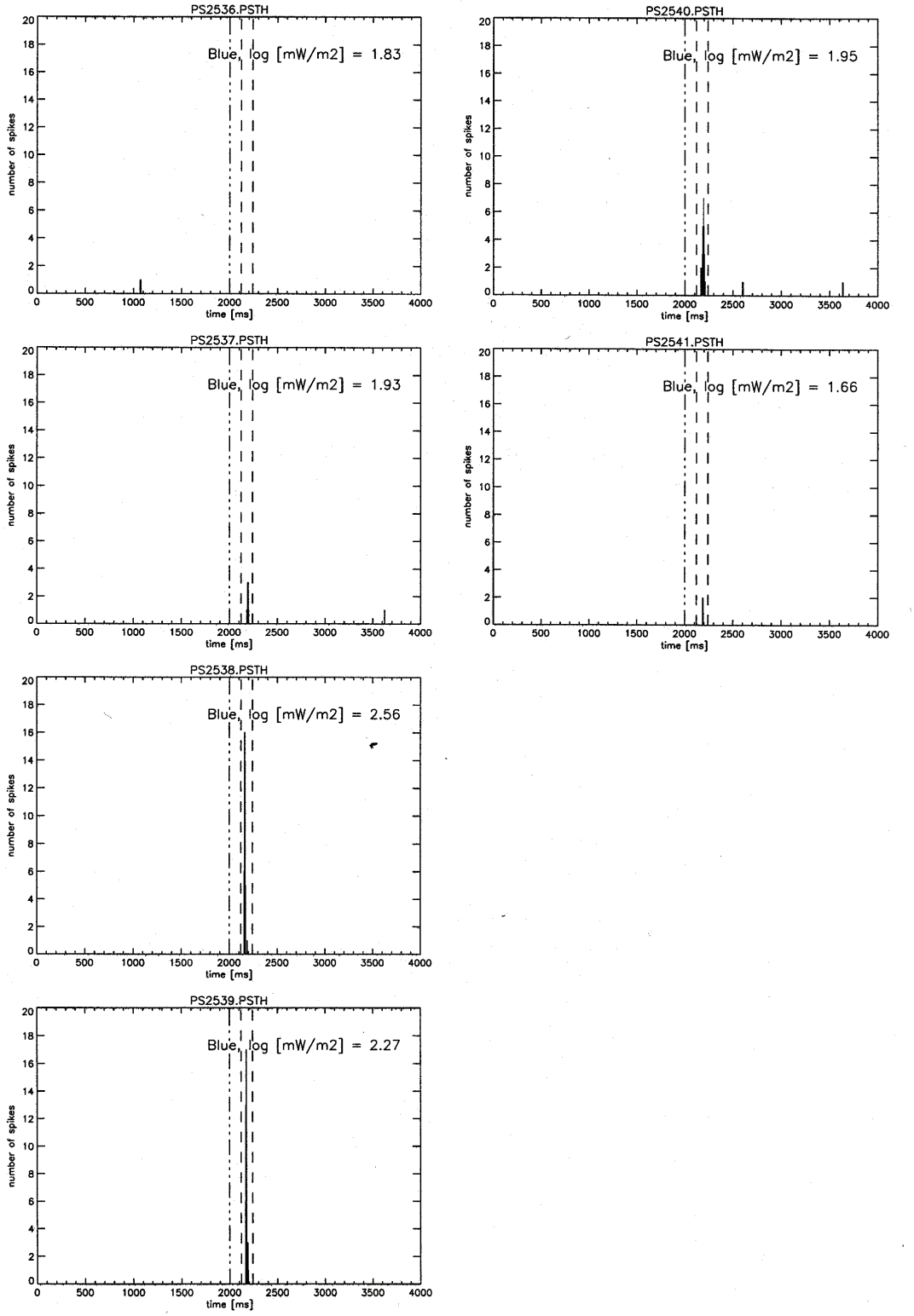

Fig. 45 – Histograms for **Figure 44**. Notice the sharp, sudden increase in response to blue stimulation between 1.93 and 2.56 log intensity units.

3.3.2.4 Blue-biased cell E (A17 – granular)

This cell corresponds to **number 42** in our listing and was found in animal T.AD. 210. It is localized in sublayer IVa of Area 17, at a depth of 1208 microns. It is driven by contralateral stationary stimuli and gives an ON response with both phasic and tonic components. The cell gave a response to a wide range of stimulus sizes, hence the response to stimuli of nearly equal intensity (86-90 mW) and different sizes was tested. Blue stimulation gives stronger responses than red (although lower than white), as shown in **Figure 46.** The matching histograms are in **Figure 47**.

Corrected Spikes

stimulus size (deg^2)	red	blue	white
0.5	227	263	171
1	461	292	626
1.5	494	777	1060
2	625	874	1483
2.5	725	953	1578
3	541	982	1605
3.5	435	960	1587
4	772	1017	1601
4.5	853	930	1505
5	630	863	1555
6	561	821	1408

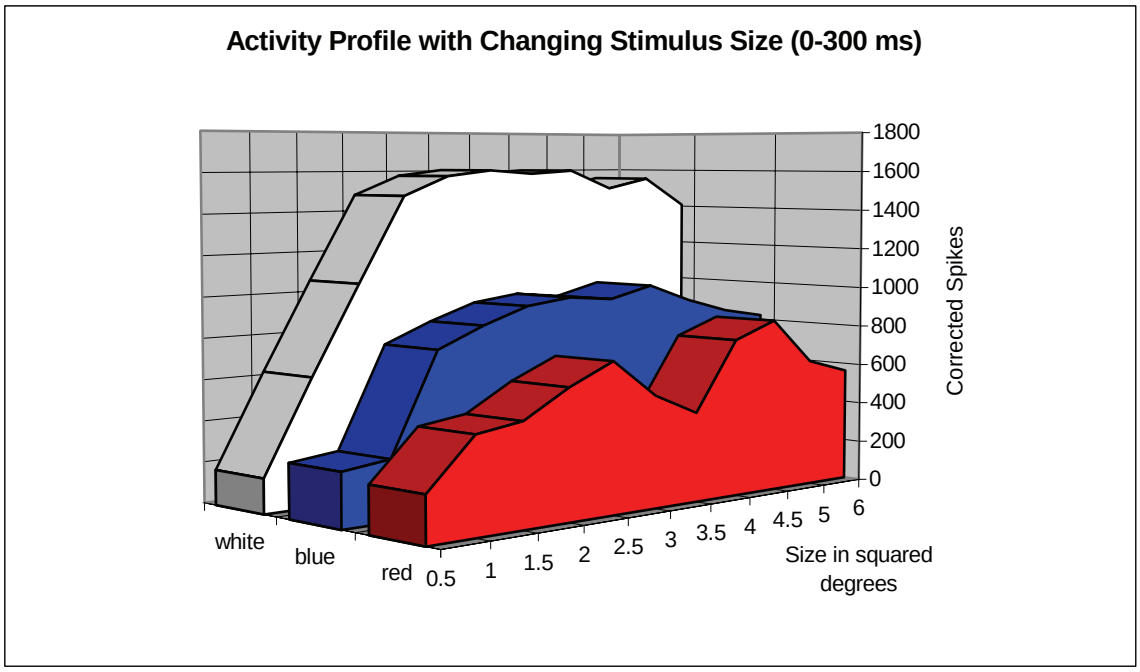

Fig. 46 – Activity profile of cell No. 42 to different stimulus sizes and wavelengths. Observe that blue generally gave higher responses than red.

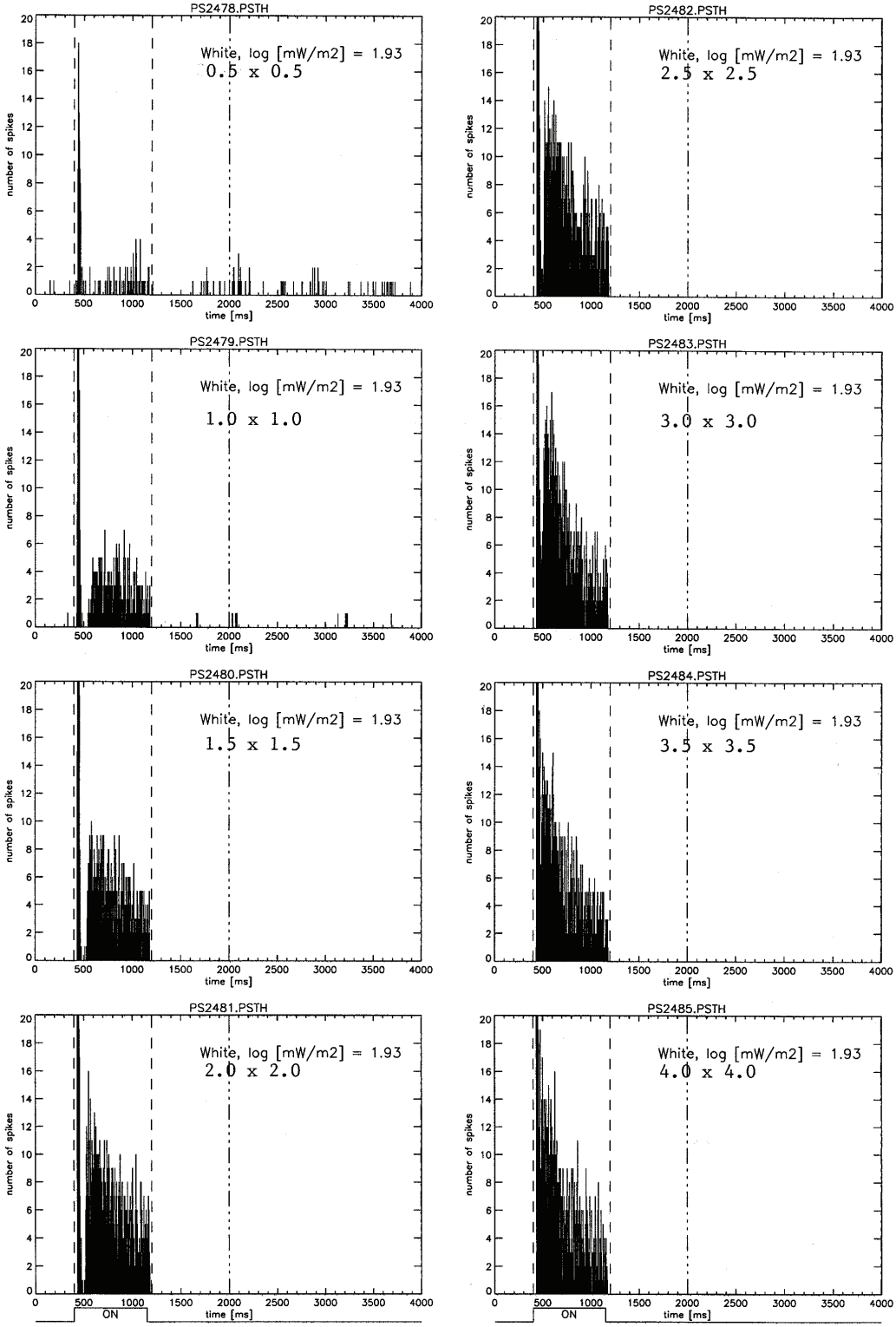
PS2478.PSTH
White, log [mW/m2] = 1.93
0.5 x 0.5
PS2482.PSTH
White, log [mW/m2] = 1.93
2.5 x 2.5
PS2479.PSTH
White, log [mW/m2] = 1.93
1.0 x 1.0
PS2483.PSTH
White, log [mW/m2] = 1.93
3.0 x 3.0
PS2480.PSTH
White, log [mW/m2] = 1.93
1.5 x 1.5
PS2484.PSTH
White, log [mW/m2] = 1.93
3.5 x 3.5
PS2481.PSTH
White, log [mW/m2] = 1.93
2.0 x 2.0
PS2485.PSTH
White, log [mW/m2] = 1.93
4.0 x 4.0
number of spikes
time [ms]
ON

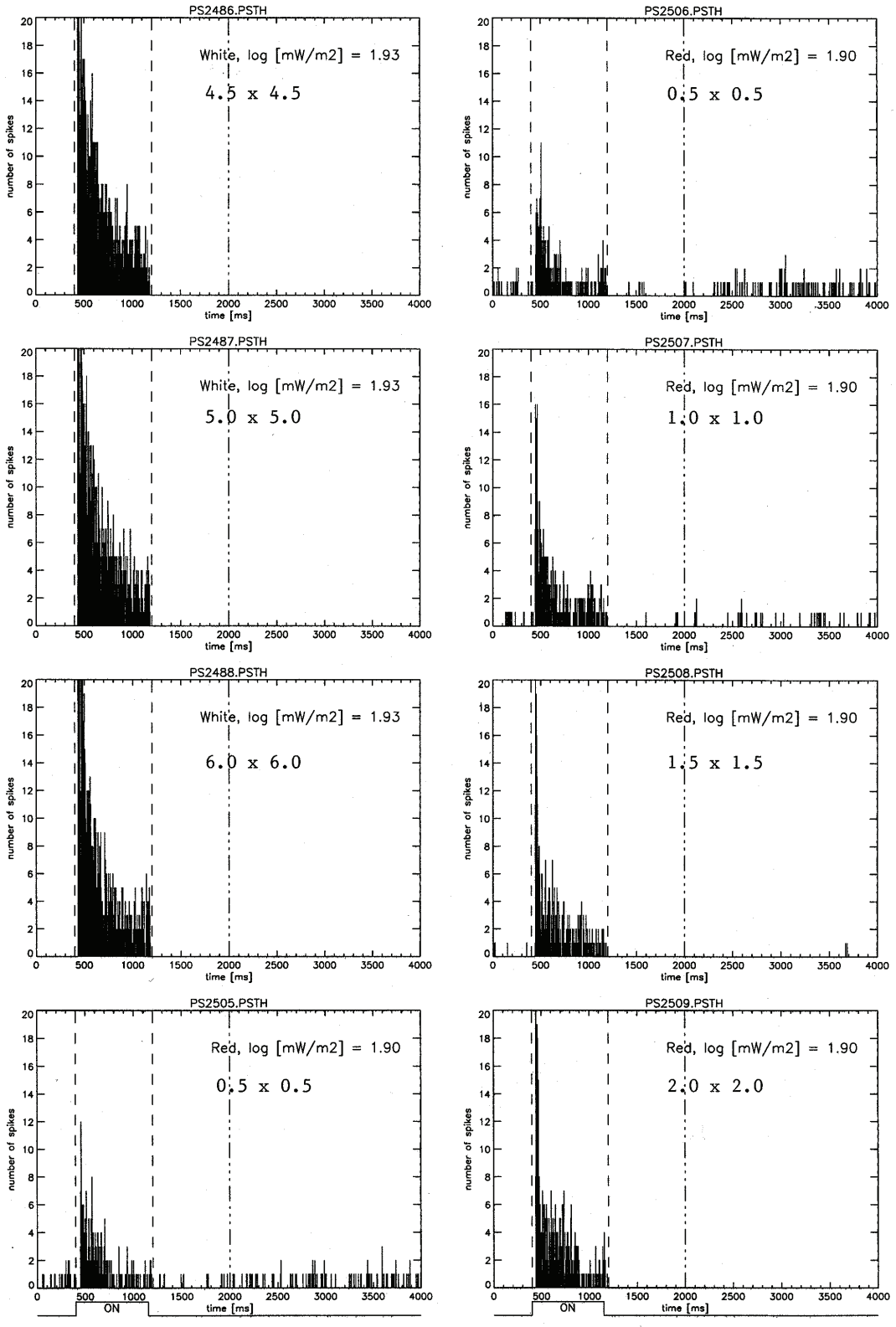
PS2486.PSTH
White, log [mW/m2] = 1.93
4.5 x 4.5
PS2506.PSTH
Red, log [mW/m2] = 1.90
0.5 x 0.5
PS2487.PSTH
White, log [mW/m2] = 1.93
5.0 x 5.0
PS2507.PSTH
Red, log [mW/m2] = 1.90
1.0 x 1.0
PS2488.PSTH
White, log [mW/m2] = 1.93
6.0 x 6.0
PS2508.PSTH
Red, log [mW/m2] = 1.90
1.5 x 1.5
PS2505.PSTH
Red, log [mW/m2] = 1.90
0.5 x 0.5
PS2509.PSTH
Red, log [mW/m2] = 1.90
2.0 x 2.0
number of spikes
time [ms]
ON

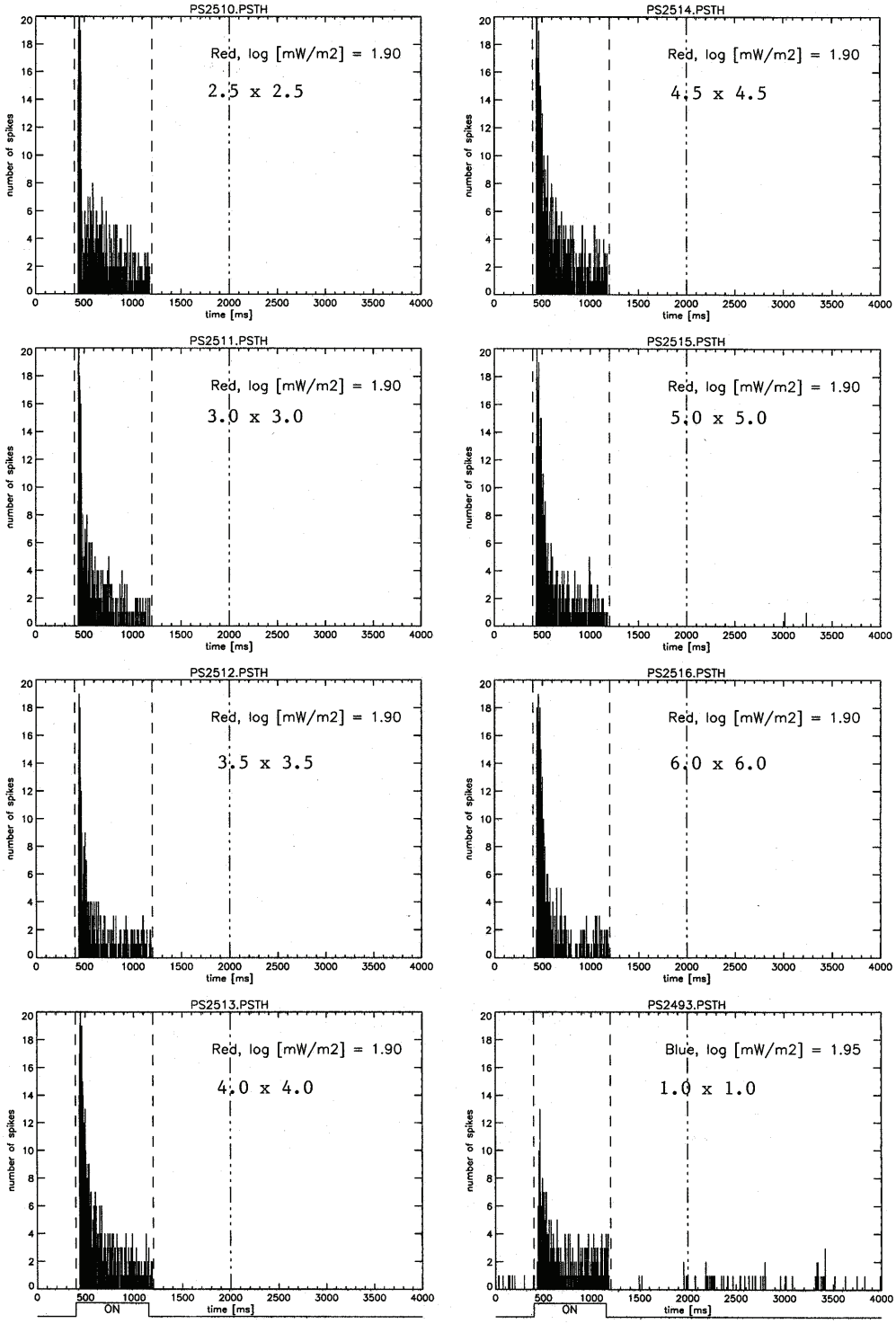
PS2510.PSTH
Red, log [mW/m2] = 1.90
2.5 x 2.5
PS2514.PSTH
Red, log [mW/m2] = 1.90
4.5 x 4.5
PS2511.PSTH
Red, log [mW/m2] = 1.90
3.0 x 3.0
PS2515.PSTH
Red, log [mW/m2] = 1.90
5.0 x 5.0
PS2512.PSTH
Red, log [mW/m2] = 1.90
3.5 x 3.5
PS2516.PSTH
Red, log [mW/m2] = 1.90
6.0 x 6.0
PS2513.PSTH
Red, log [mW/m2] = 1.90
4.0 x 4.0
PS2493.PSTH
Blue, log [mW/m2] = 1.95
1.0 x 1.0
number of spikes
time [ms]
ON

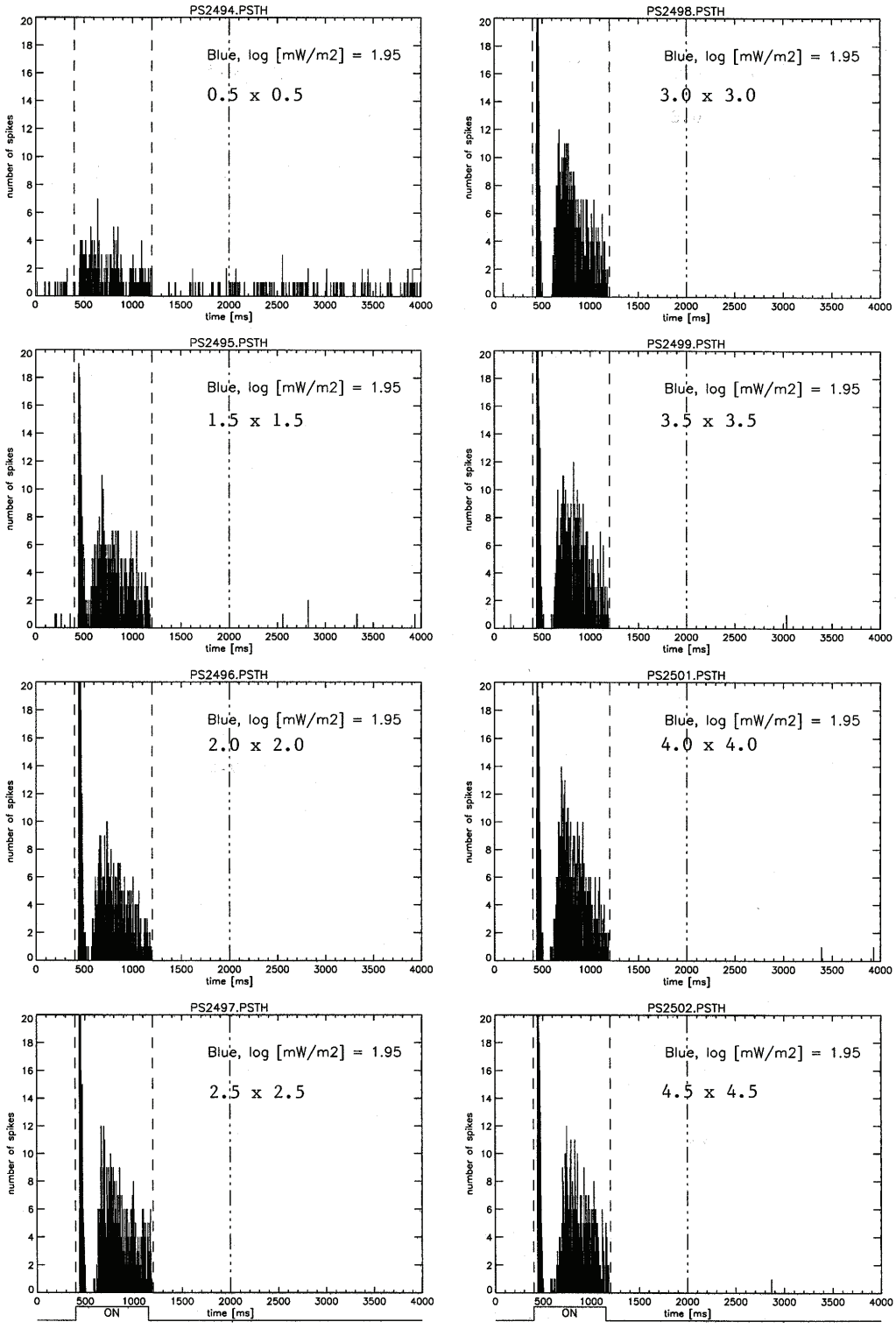
PS2494.PSTH
Blue, log [mW/m2] = 1.95
0.5 x 0.5
PS2498.PSTH
Blue, log [mW/m2] = 1.95
3.0 x 3.0
PS2495.PSTH
Blue, log [mW/m2] = 1.95
1.5 x 1.5
PS2499.PSTH
Blue, log [mW/m2] = 1.95
3.5 x 3.5
PS2496.PSTH
Blue, log [mW/m2] = 1.95
2.0 x 2.0
PS2501.PSTH
Blue, log [mW/m2] = 1.95
4.0 x 4.0
PS2497.PSTH
Blue, log [mW/m2] = 1.95
2.5 x 2.5
PS2502.PSTH
Blue, log [mW/m2] = 1.95
4.5 x 4.5
number of spikes
time [ms]
ON

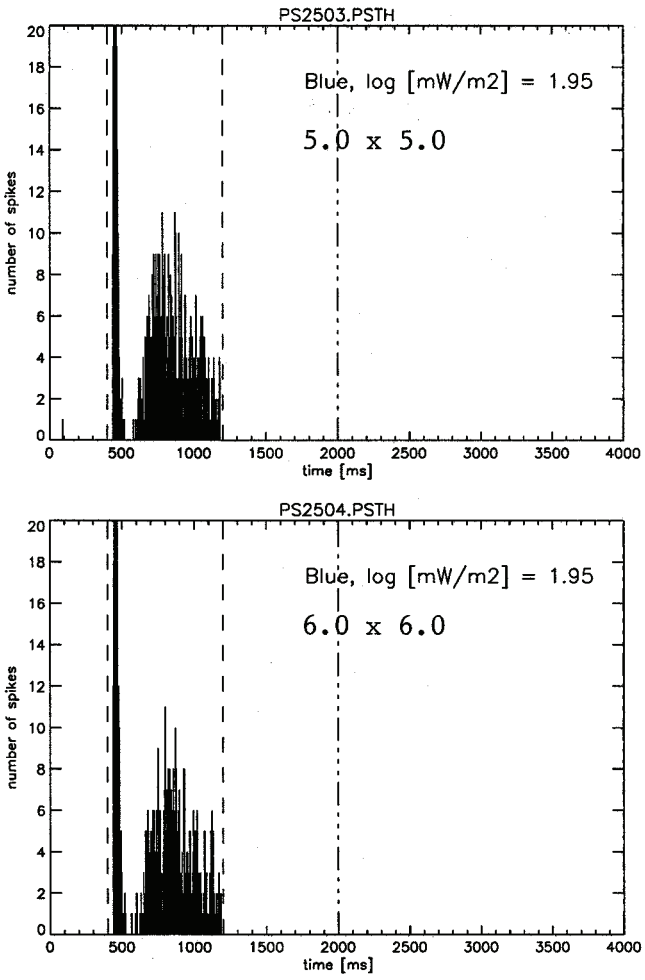

Fig. 47 – Histograms corresponding to graph in **Figure 46**. Numbers underneath color and intensity indicate the size (in degrees) of the stimulus.

3.3.2.5 Blue-biased cell F (infragranular)

This cell corresponds to **number 45** in our listing. It was found in animal T.AD. 210 and is localized in layer VI of Area 17 at a depth of 1880 microns. The cell was driven by both stationary and moving stimuli coming from either the contra- or the ipsilateral eye. The cells' response is ON-OFF with phasic and tonic components. The R/I curves in **Figure 48** and histograms in **Figure 49** show the response within the phasic range 0-68 msec after stimulus onset (only the ON-component is shown here), with a stationary stimulus for both eyes. Blue gives responses considerably higher than red.

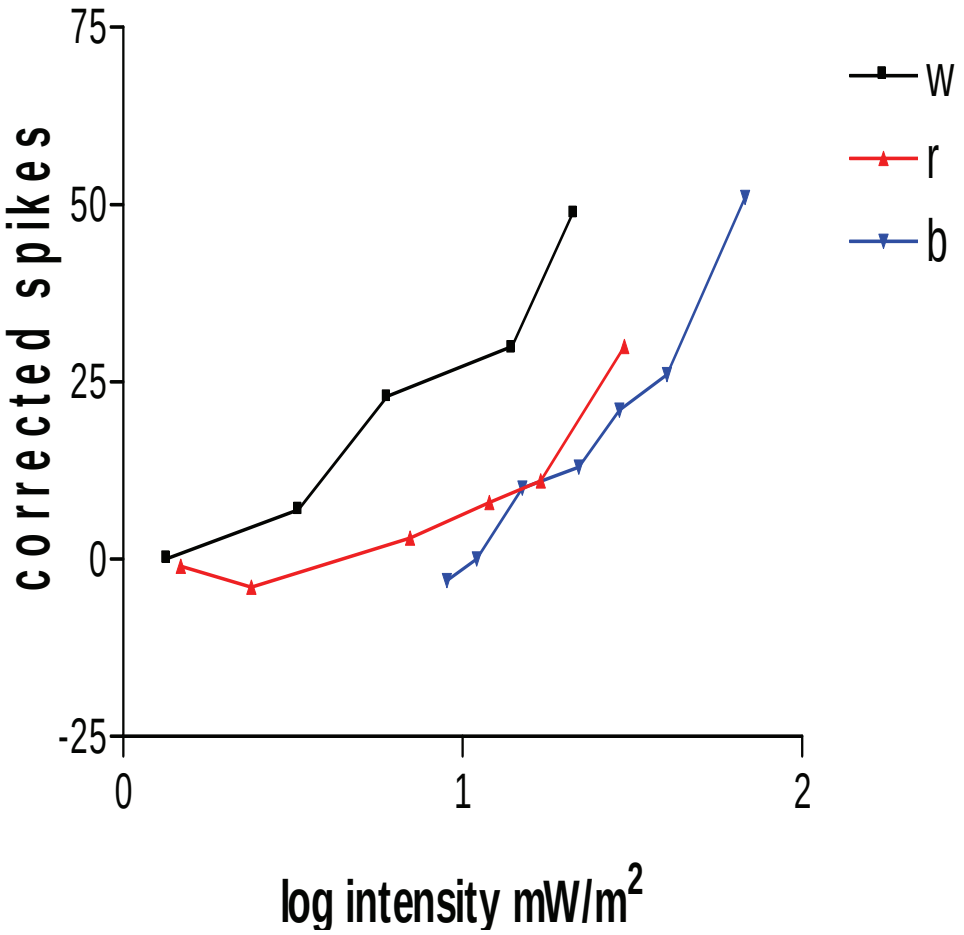

Fig. 48 – R/I curves for cell No. 45, with stationary stimulation. Notice the strong response evoked by blue.

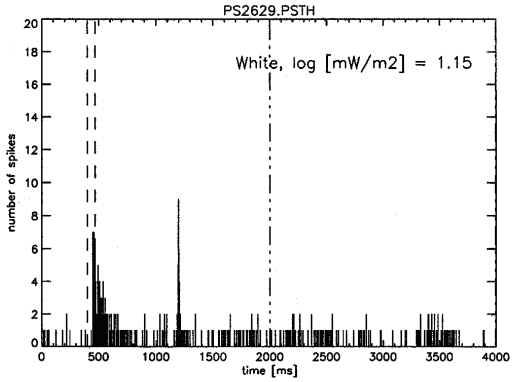
PS2629.PSTH
White, log [mW/m2] = 1.15
number of spikes
time [ms]

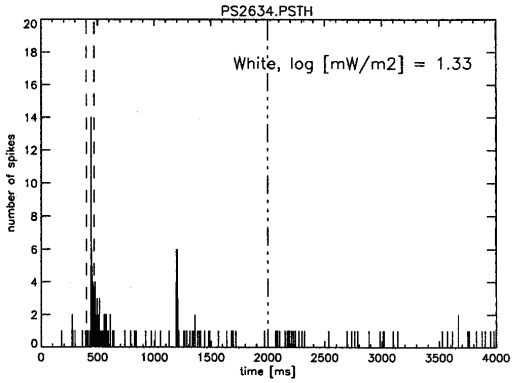
PS2634.PSTH
White, log [mW/m2] = 1.33
number of spikes
time [ms]

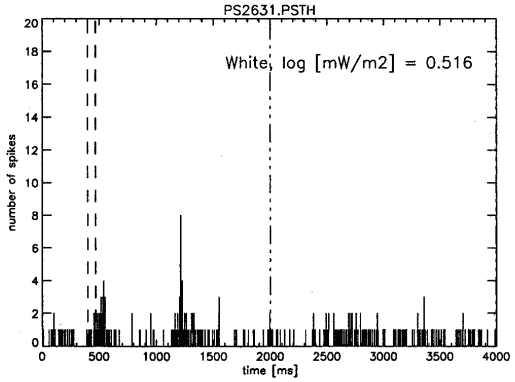
PS2631.PSTH
White, log [mW/m2] = 0.516
number of spikes
time [ms]

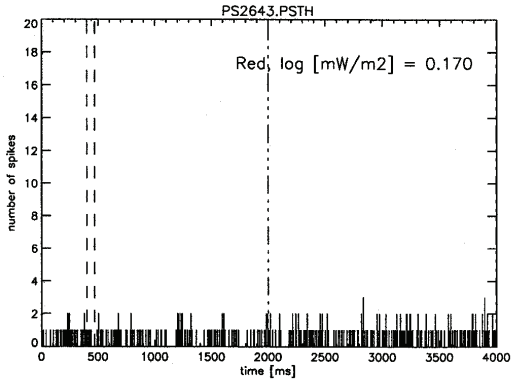
PS2643.PSTH
Red, log [mW/m2] = 0.170
number of spikes
time [ms]

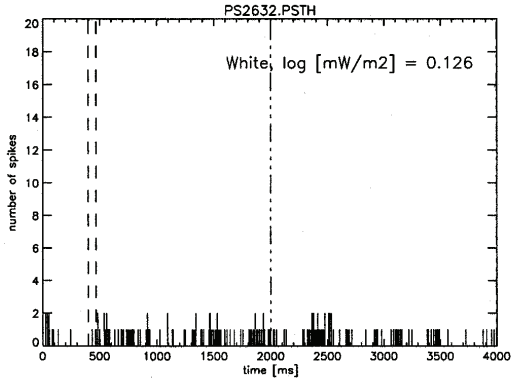
PS2632.PSTH
White, log [mW/m2] = 0.126
number of spikes
time [ms]

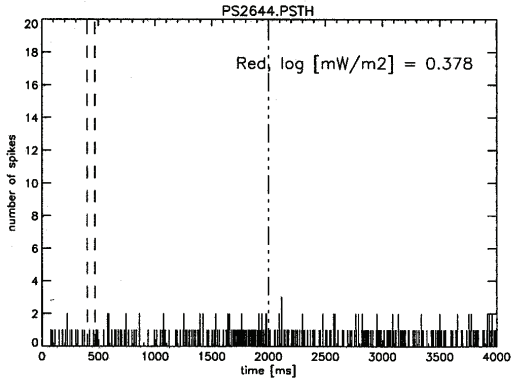
PS2644.PSTH
Red, log [mW/m2] = 0.378
number of spikes
time [ms]

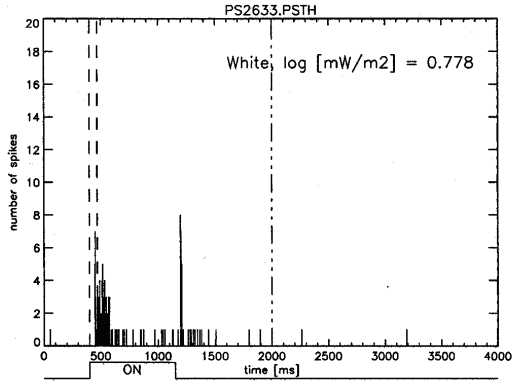
PS2633.PSTH
White, log [mW/m2] = 0.778
number of spikes
ON
time [ms]

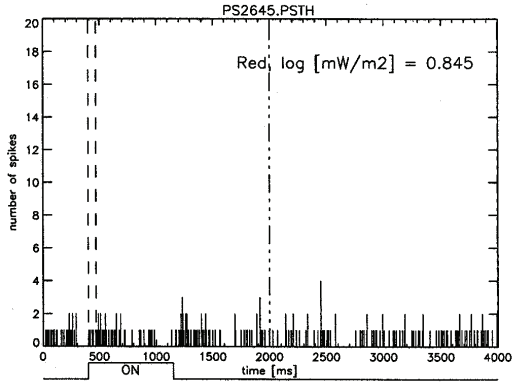
PS2645.PSTH
Red, log [mW/m2] = 0.845
number of spikes
ON
time [ms]

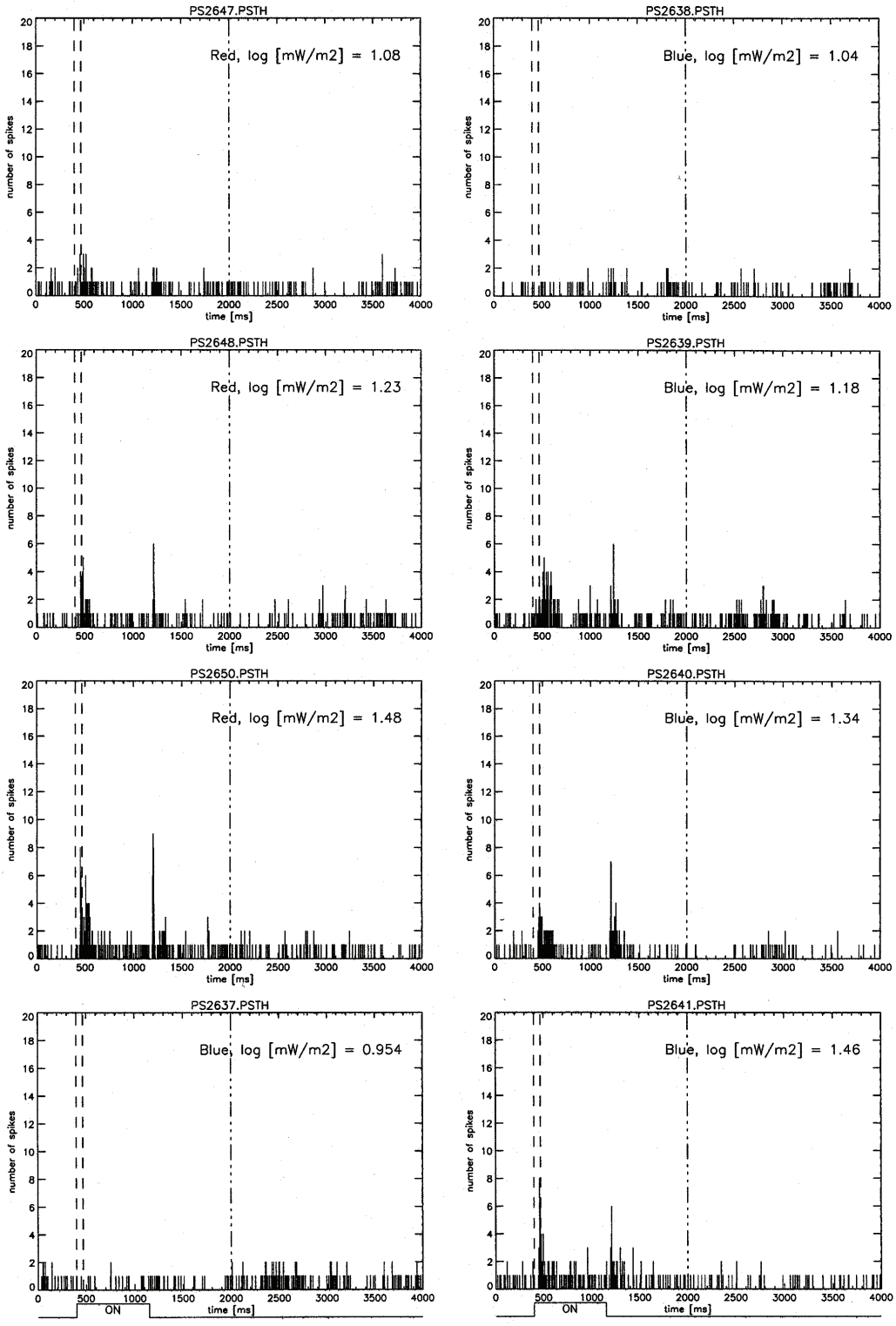
PS2647.PSTH
Red, log [mW/m2] = 1.08
PS2638.PSTH
Blue, log [mW/m2] = 1.04
PS2648.PSTH
Red, log [mW/m2] = 1.23
PS2639.PSTH
Blue, log [mW/m2] = 1.18
PS2650.PSTH
Red, log [mW/m2] = 1.48
PS2640.PSTH
Blue, log [mW/m2] = 1.34
PS2637.PSTH
Blue, log [mW/m2] = 0.954
PS2641.PSTH
Blue, log [mW/m2] = 1.46
number of spikes
time [ms]
ON

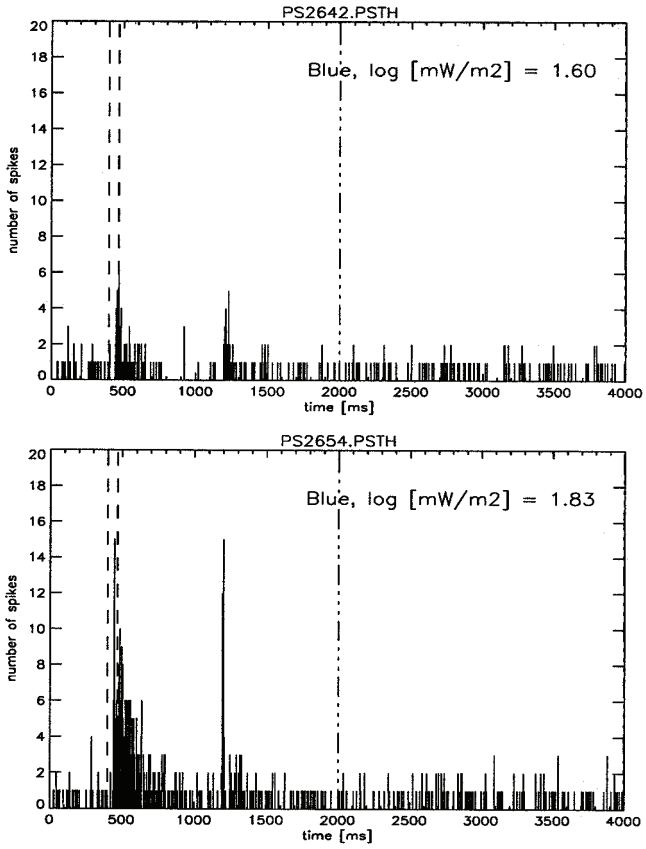

Fig. 49 – Histograms for R/I curves in **Figure 48** (cell No. 45).

The unusually strong responses of blue over red can also be seen with moving stimuli, as is shown by the R/I curves and histograms in **Figure 50 and 51**.

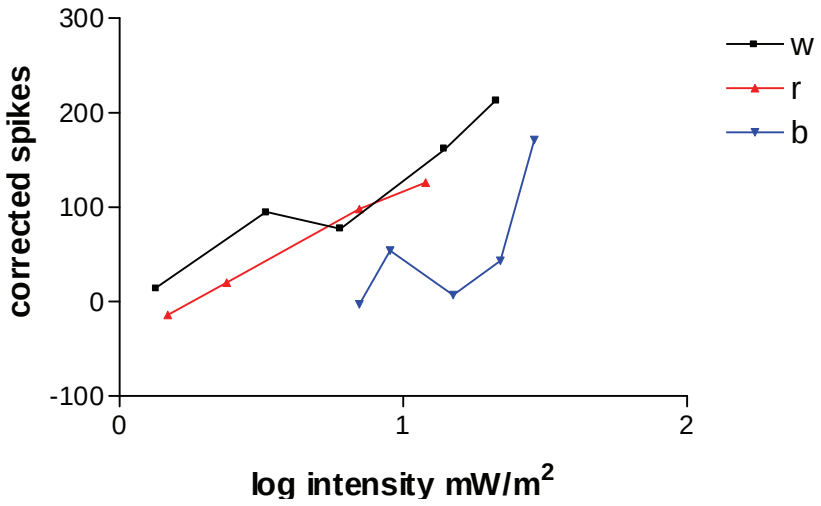

Fig. 50 – Strong responses from cell No. 45 with blue light can also be obtained with moving stimuli.

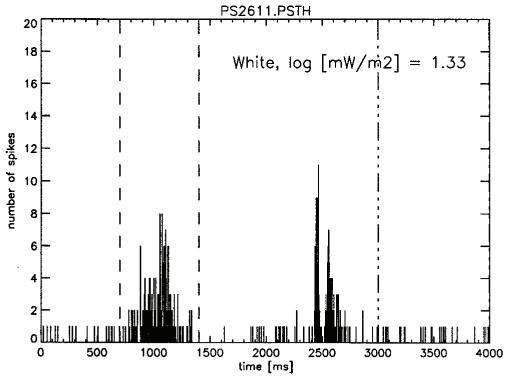
PS2611.PSTH
White, log [mW/m2] = 1.33
number of spikes
time [ms]

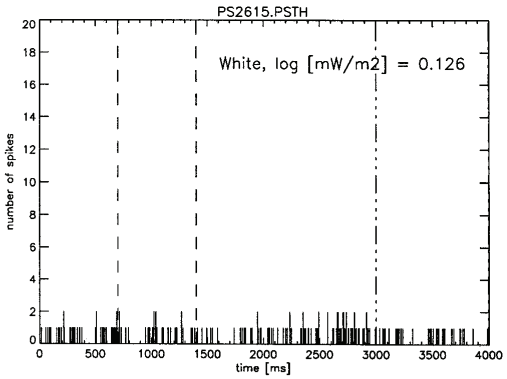
PS2615.PSTH
White, log [mW/m2] = 0.126
number of spikes
time [ms]

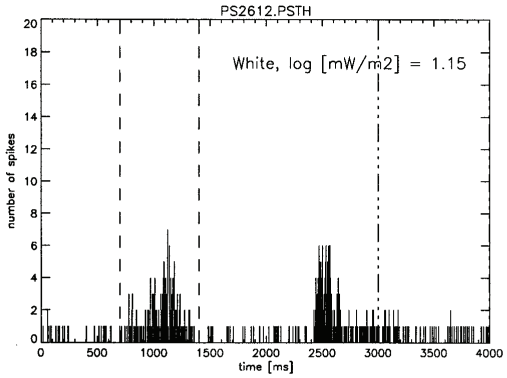
PS2612.PSTH
White, log [mW/m2] = 1.15
number of spikes
time [ms]

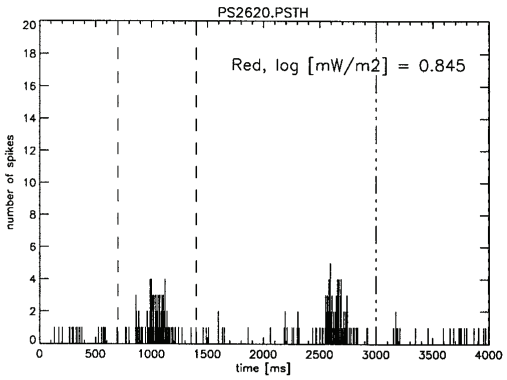
PS2620.PSTH
Red, log [mW/m2] = 0.845
number of spikes
time [ms]

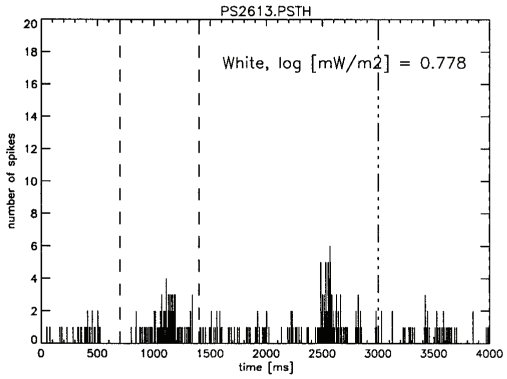
PS2613.PSTH
White, log [mW/m2] = 0.778
number of spikes
time [ms]

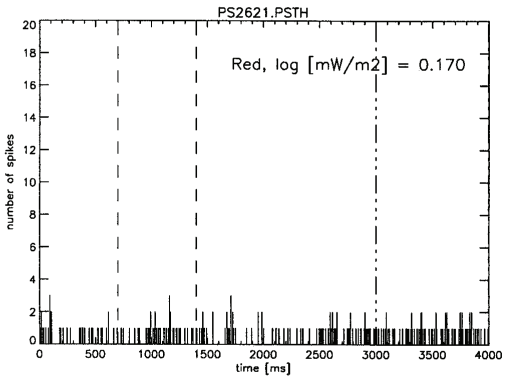
PS2621.PSTH
Red, log [mW/m2] = 0.170
number of spikes
time [ms]

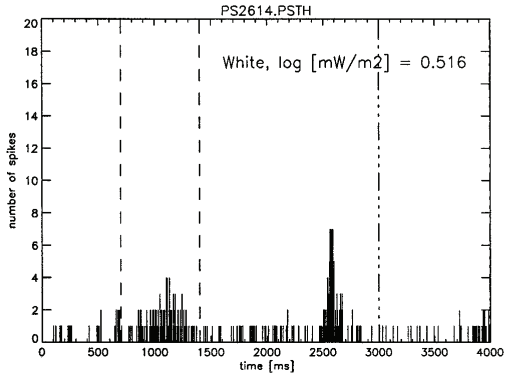
PS2614.PSTH
White, log [mW/m2] = 0.516
number of spikes
time [ms]

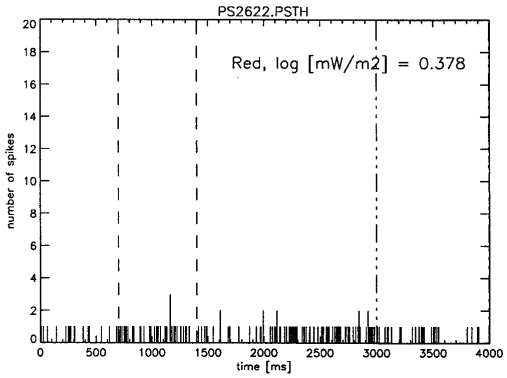
PS2622.PSTH
Red, log [mW/m2] = 0.378
number of spikes
time [ms]

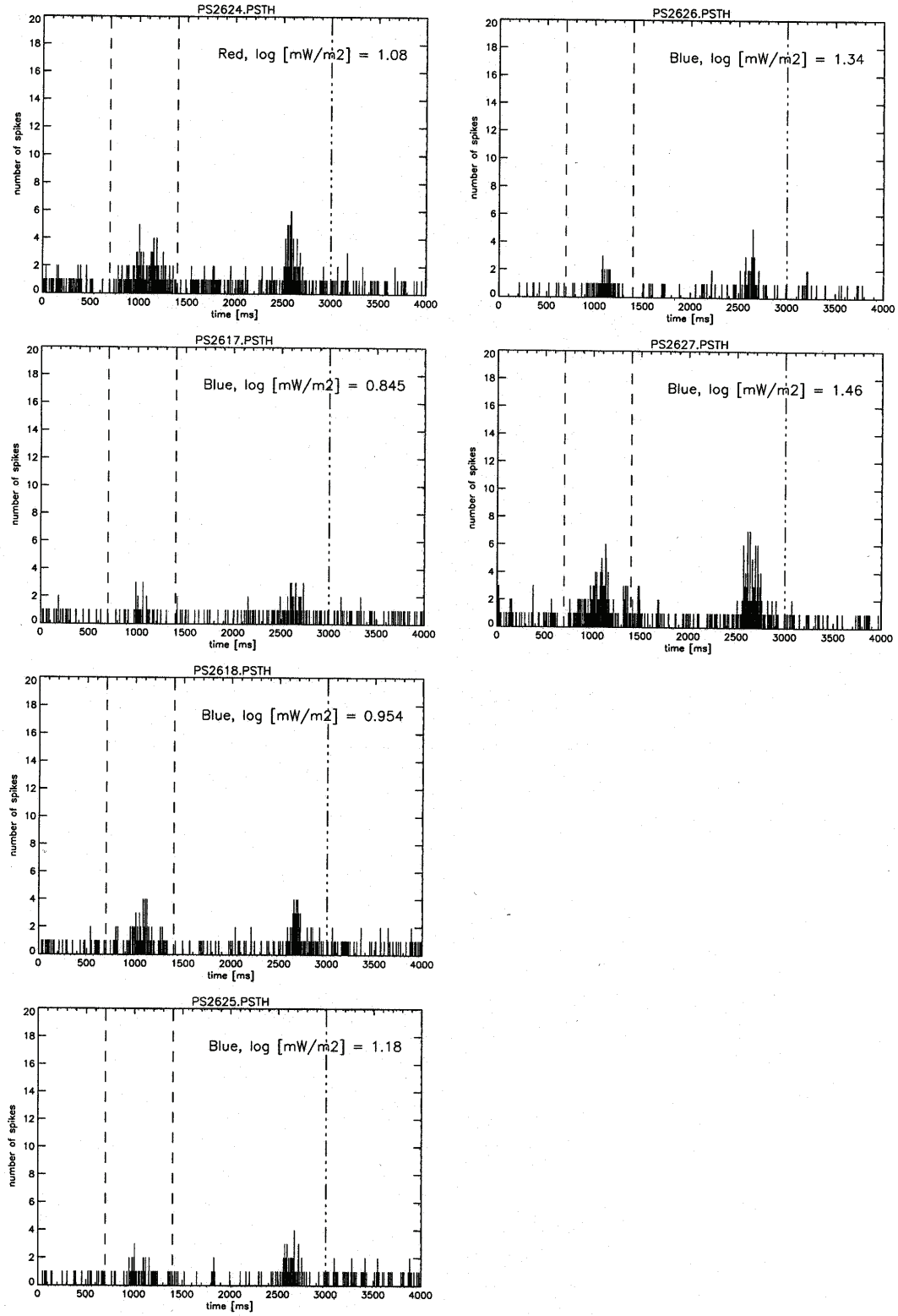

Fig. 51 – Histograms for cell No. 45 with moving stimuli.

3.3.3 Cortical and Receptive Field Positions of Blue-biased and Blue-specific cells

It is known from immunohistochemical studies that the Tupaia retina is cone dominated. Furthermore, as we have mentioned in the introduction, only two types of cones exist: namely the SWC (short-wavelength cones) and LWC (long-wavelength cone) populations, of which the latter is by far dominant. Considering that most of the SWCs are concentrated in the ventral retina (Müller and Peichl 1989, Petry, Erichsen, and Szel 1993), we expect most narrow-band cells tuned to blue, as well as blue-sensitive cells to be located predominantly in regions representing this part of the retina (i.e. the upper visual field). However, sampling bias is not excluded, since most of our recordings were done in the part of cortex representing the visual field close to the horizontal meridian (HM ± 10 deg. , see Appendix II).

In **Table 5**, we can see the receptive field elevations of these cells. Mooser calculated trigonometrically the elevation of the optic disc (Doctoral dissertation 1998, p. 56) and comparing it with the height of the eyes he determined the average optic disc elevation to differ by 4.2 ± 0.1 deg., mean ± S.D., n=18). In our study we used the same stereotaxic apparatus. We therefore subtracted 4.2 from the eye level to obtain the following values:

		Strong responses for blue in the Geniculo-cortical system		
Cell	Layer or Lamina	Depth in μm	RF size in degrees	RF elevation in degrees
3	A17 - III a/b	580	0.75 x 0.75	2.55
6	A17 - IIIb	850	1 x 1	2.8
8	A18	825	NA	5.8
9	A17 - IVb	1210	1 x 1	2.2
13	Collic. sup. (SO)	4155	4 x 4	8.3
21	dLGN lamina 6	4420,4470	1 x 2.5	-2.2
26	dLGN lamina 3	5420	0.75 x 1.25	-10.7
27	dLGN lamina 2	5600	0.75 x 1.5	-13.2
36 *	A17 - IIIb	1010	1.5x1.5 , 4.75x4.75	2.8
42	A17 - IVa	1208	different sizes	5.8
43	A17 - IIIc/IVa	1065	.3 x 4, 4 x 6	3.8
45	A17 - VI	1880	0.5 x 7.5	-0.45

* This cell has very high gain for blue, however no recordings for green and red are available for comparison, and hence was not included in the blue-biased group earlier.

3.4 The influence of contrast on cell response

In all experiments hitherto described, the variations in stimulus intensity refer solely to stimulus centers. The changes in intensity produced a change in the center surround contrast. In the following section, we describe a few particular tests in which stimulus center and surround intensities were incremented simultaneously by the same factor. In this way, the respective intensities of center and surround are maintained at the same ratio. By thus maintaining constant contrast we were able to examine the role it played in cell response.

3.4.1 Constant contrast cell A (A17 - supragranular)

This cell corresponds to **number 36** in our listing. It was found in animal T.AD. 200 and is localized in Area 17, sublayer IIIb at a depth of 1010 microns. It is driven by the contralateral eye and stationary stimulation and gives a phasic ON-response. Differential response to contrast variant and invariant stimuli was tested only in white. In **Figure 52**, we see the cell's response. The suppression of contrast flattens out the response curve. We conclude that the cell is contrast-driven. Accompanying histograms are found in **Figure 53** (variable contrast) and **Figure 54** (constant contrast).

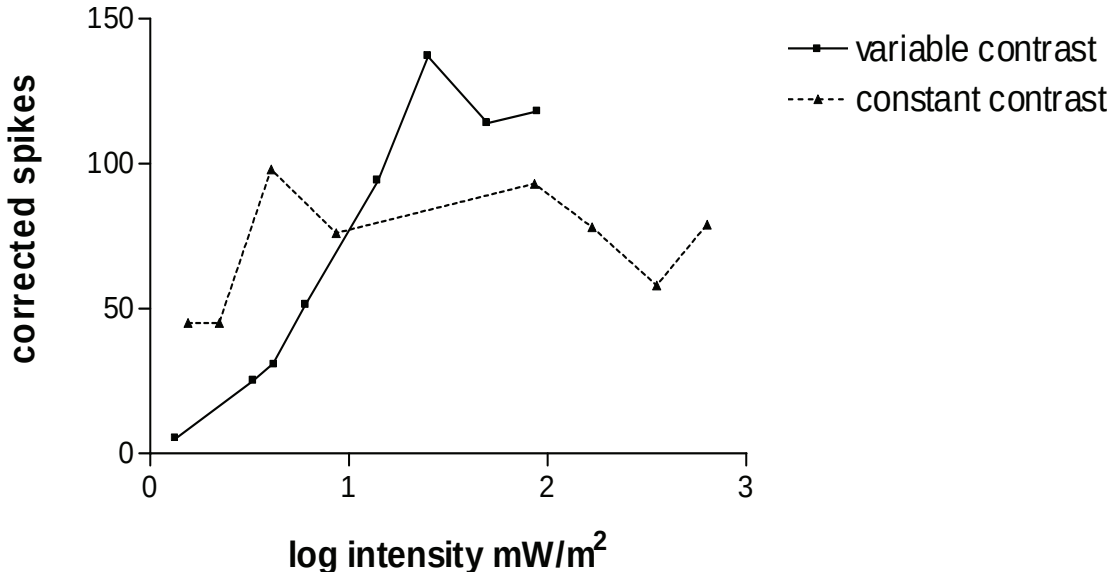

Fig. 52 - R/I curves from cell No. 36. Solid line indicates response to variable contrast. Dotted line indicates response to constant contrast. Stimulus center and surround had an intensity ratio of 10:1 white on white. Notice that the lack of variation in contrast flattens out the response curve.

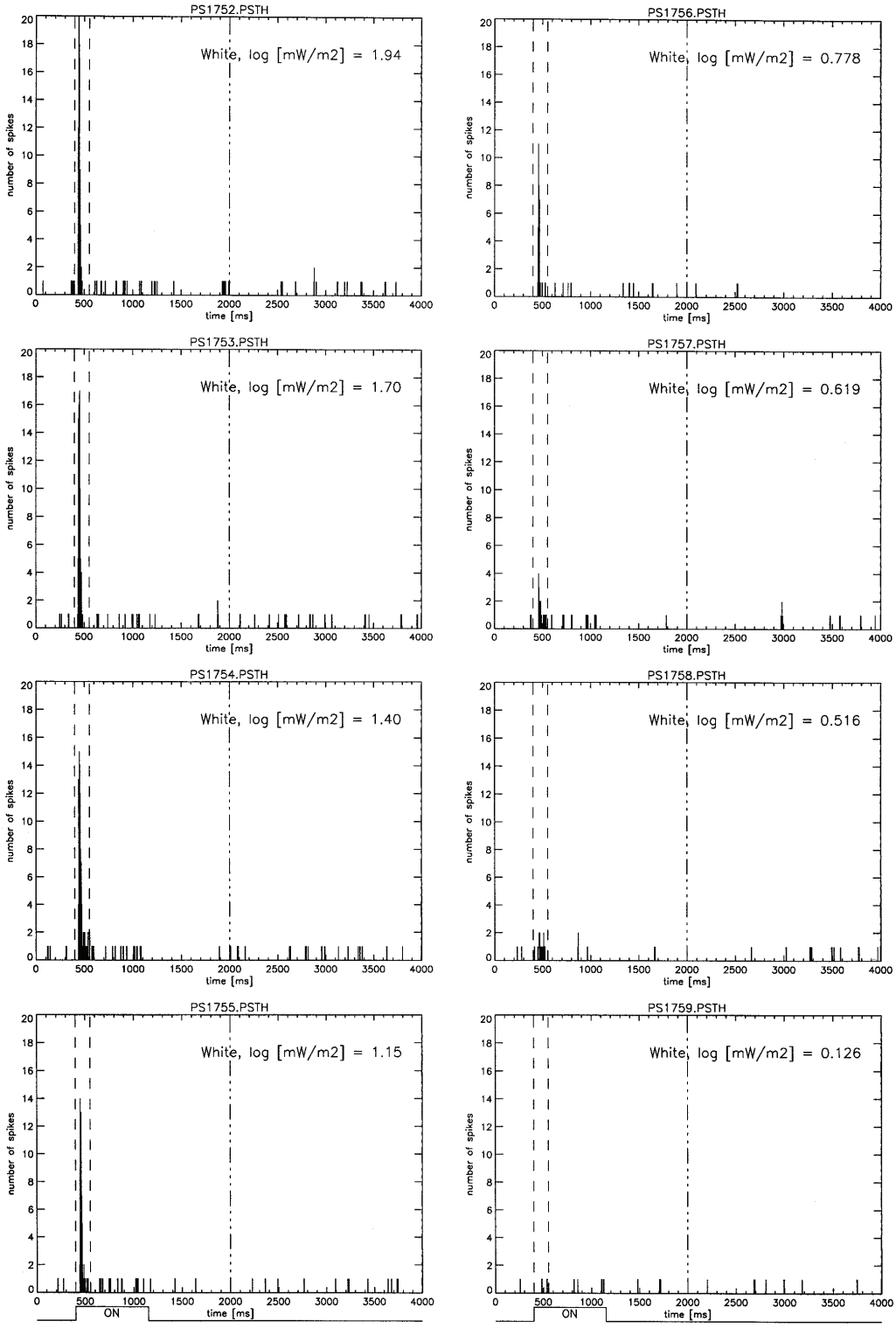

Fig. 53 – Histograms from cell No. 36. These correspond to the solid line (variable contrast) in **Figure 52.**

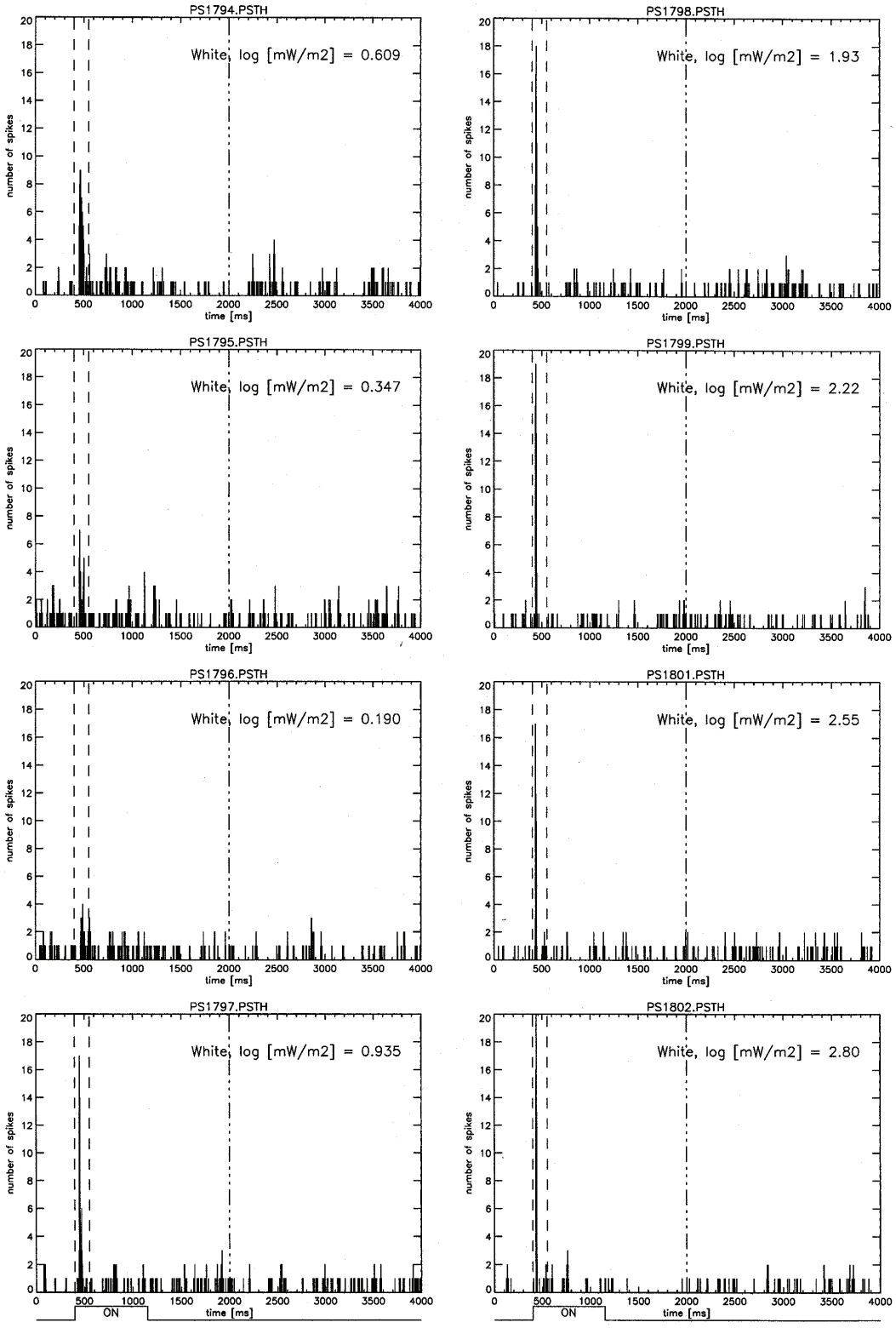

Fig. 54 – Histograms for cell No. 36. These correspond to the dotted line in **Figure 52** (constant contrast).

3.4.2 Contrast cell B (A17 – granular)

This cell corresponds to **number 47** in our listing and was found in animal T.AD. 212. It is localized in Area 17 in the cell-sparse cleft of layer IV at a depth of 1240 microns. The cell is binocularly driven but with preference to the contralateral eye. The response to stationary stimuli is phasic ON-OFF, but optimal responses are with moving stimuli. In **Figure 55**, the response to moving stimuli for different wavelengths is shown, with variant and invariant contrast. The corresponding histograms are found in **Figure 56** (constant) and **Figure 57** (variable). It can be observed that stimulation with contrast-invariant stimuli elicits a higher response in all wavelengths, although the difference is less conspicuous in blue.

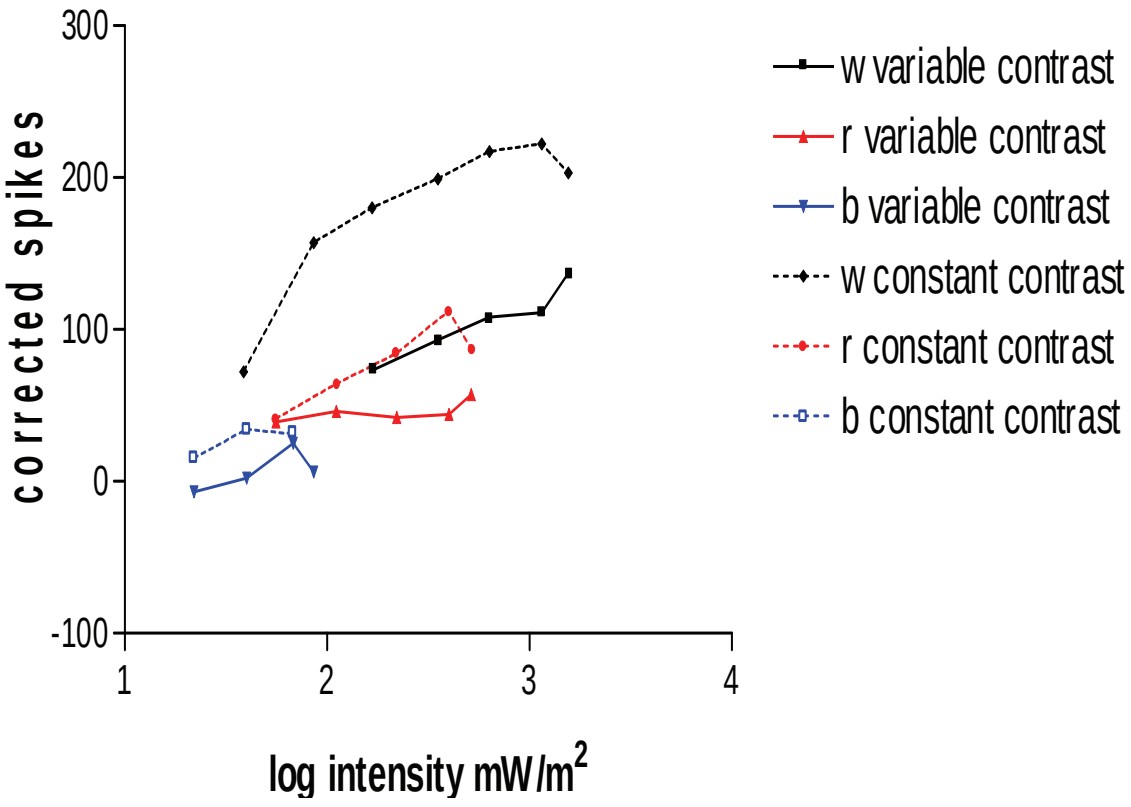

Fig. 55 - Response of cell No. 47 to stimulation with different wavelengths. Solid lines indicate response to variable contrast. Dotted lines indicate response to constant contrast. Notice that with variable contrast the response is weaker.

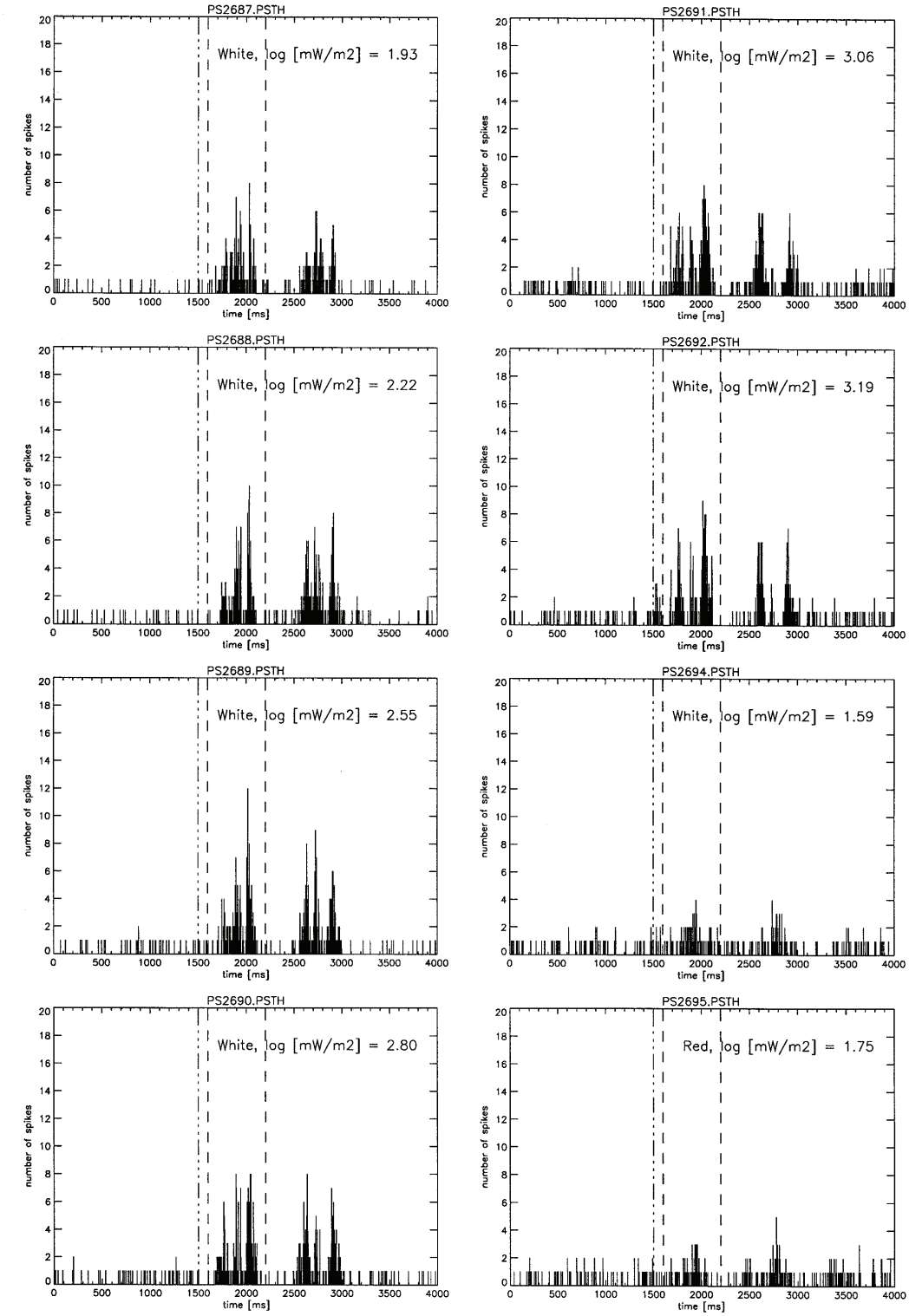
PS2687.PSTH
White, log [mW/m2] = 1.93
PS2691.PSTH
White, log [mW/m2] = 3.06
PS2688.PSTH
White, log [mW/m2] = 2.22
PS2692.PSTH
White, log [mW/m2] = 3.19
PS2689.PSTH
White, log [mW/m2] = 2.55
PS2694.PSTH
White, log [mW/m2] = 1.59
PS2690.PSTH
White, log [mW/m2] = 2.80
PS2695.PSTH
Red, log [mW/m2] = 1.75
number of spikes
time [ms]

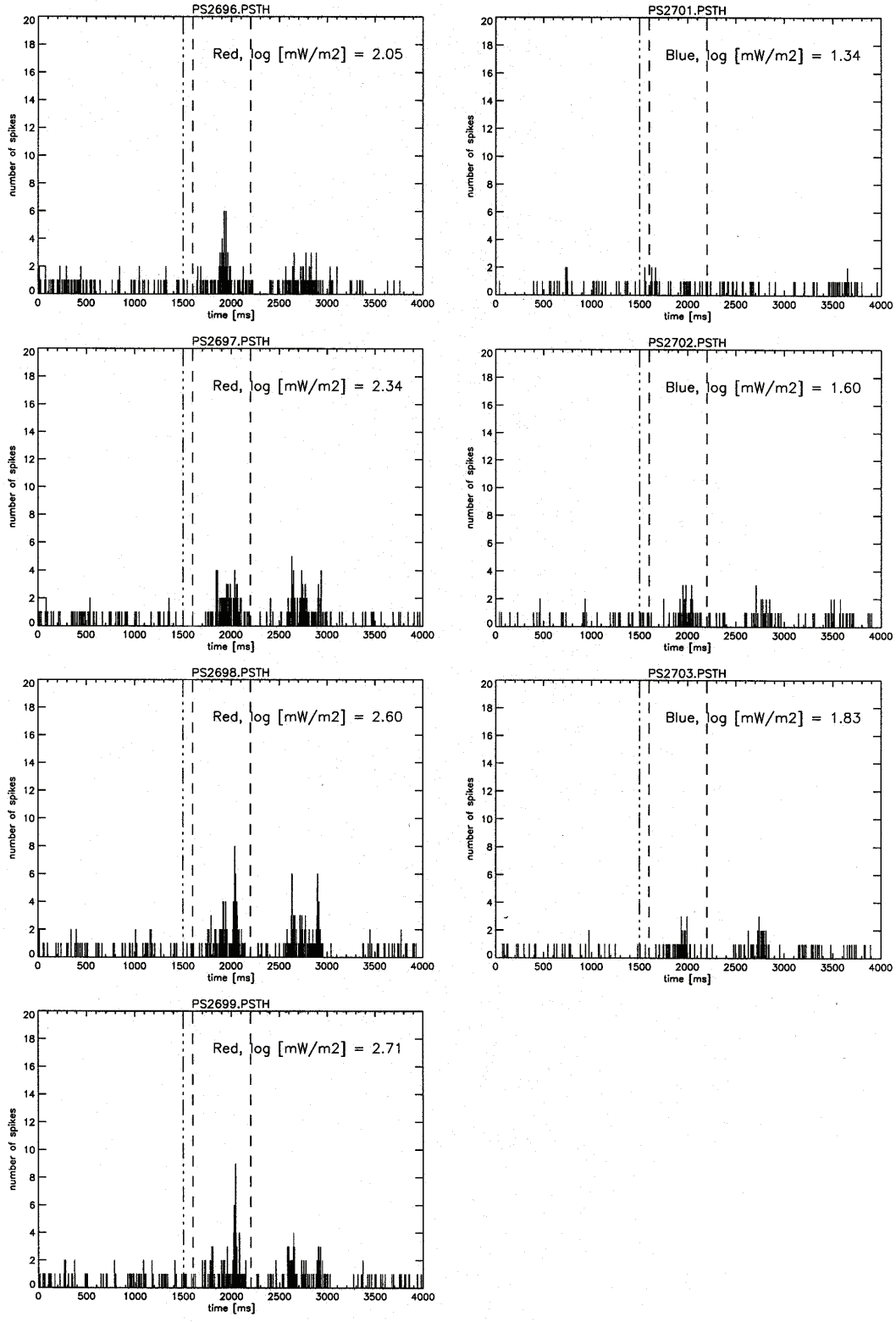

Fig. 56 - Response of cell No. 47 to stimulation with different wavelengths. These histograms and the ones on the previous page, correspond to the dashed lines in **Figure 55** (i.e. stimuli with constant contrast).

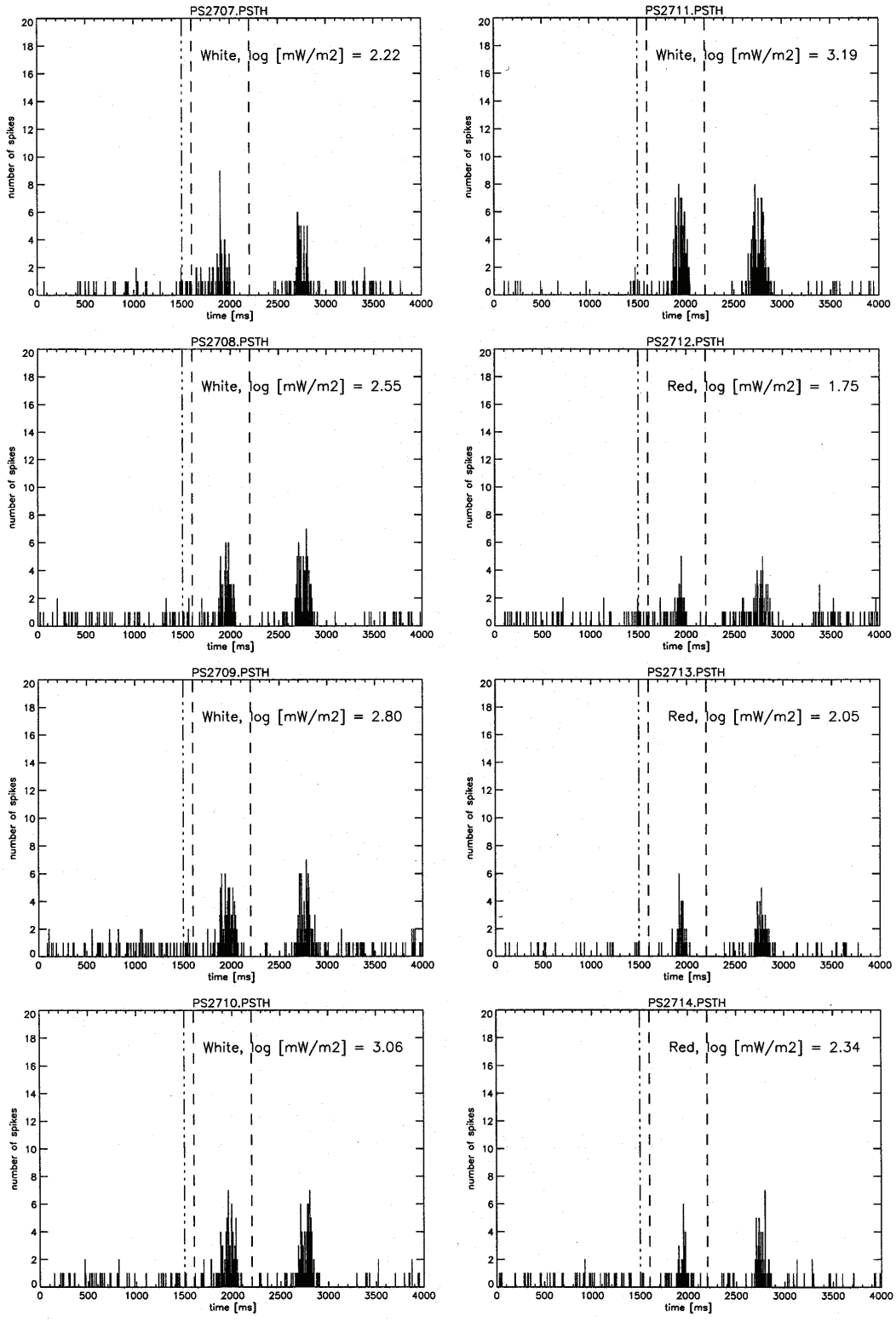
PS2707.PSTH
White, log [mW/m2] = 2.22
PS2711.PSTH
White, log [mW/m2] = 3.19
PS2708.PSTH
White, log [mW/m2] = 2.55
PS2712.PSTH
Red, log [mW/m2] = 1.75
PS2709.PSTH
White, log [mW/m2] = 2.80
PS2713.PSTH
Red, log [mW/m2] = 2.05
PS2710.PSTH
White, log [mW/m2] = 3.06
PS2714.PSTH
Red, log [mW/m2] = 2.34
number of spikes
time [ms]

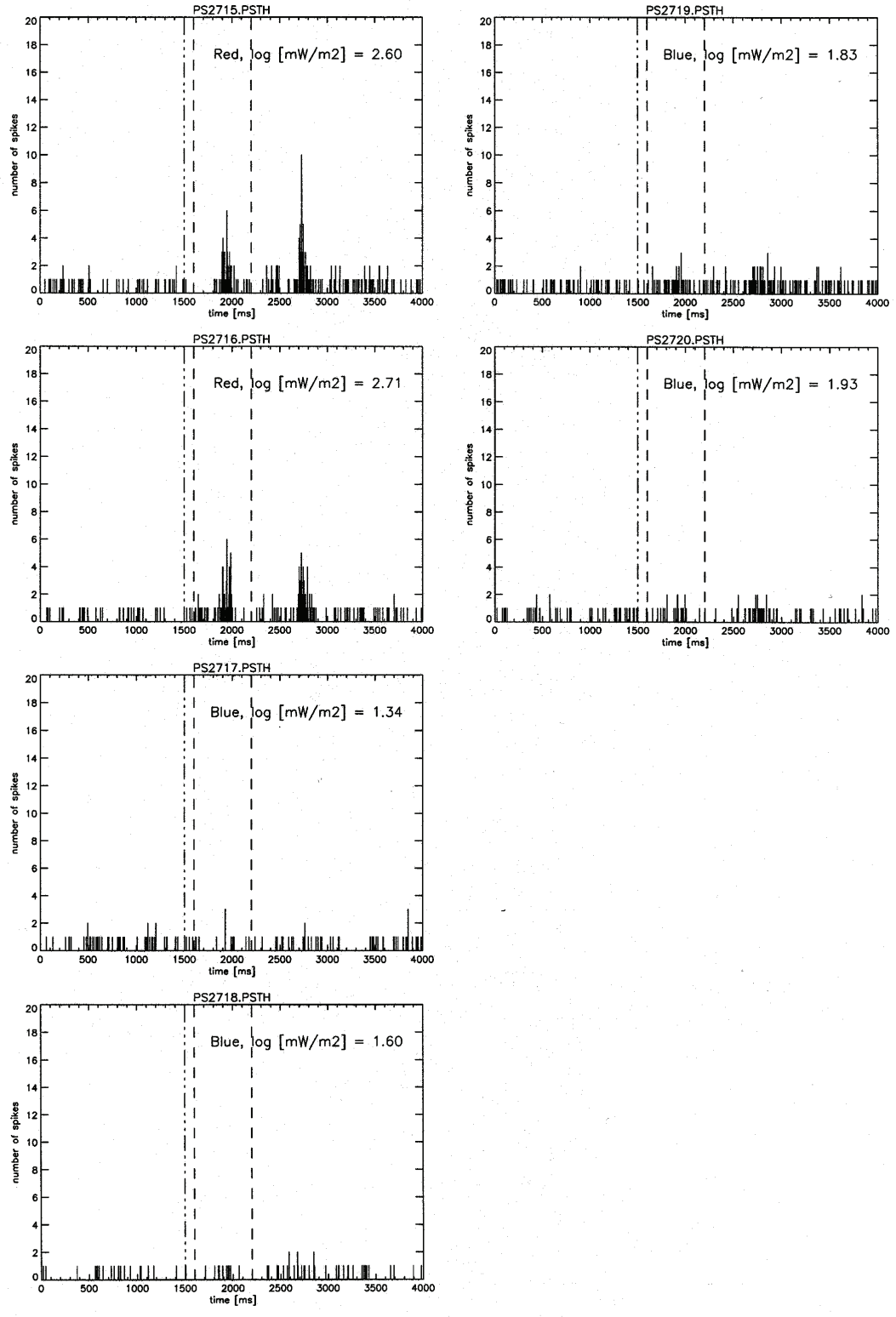

Fig. 57 - Response of cell No. 47 to stimulation with different wavelengths. These histograms and the ones on the previous page, correspond to the solid lines in **Figure 55** (i.e. stimuli with variable contrast).

3.4.3 Contrast cell C (A17 – infragranular)

This cell corresponds to **number 49** in our listing. It was found in animal T.AD. 213 and is situated in layer V of Area 17, at a depth of 1342 microns. The cell is binocularly driven and responds to moving stimuli. The response has both phasic and tonic components. The response to different wavelengths and intensities is shown in **Figure 58**. Contrast-variant (histograms in **Figure 59**) and contrast-invariant stimuli (histograms in **Figure 60**) were tested. It gave higher responses to contrast-invariant stimulation in all colors. The stimulus surround (background) was always white for the contrast invariant stimuli.

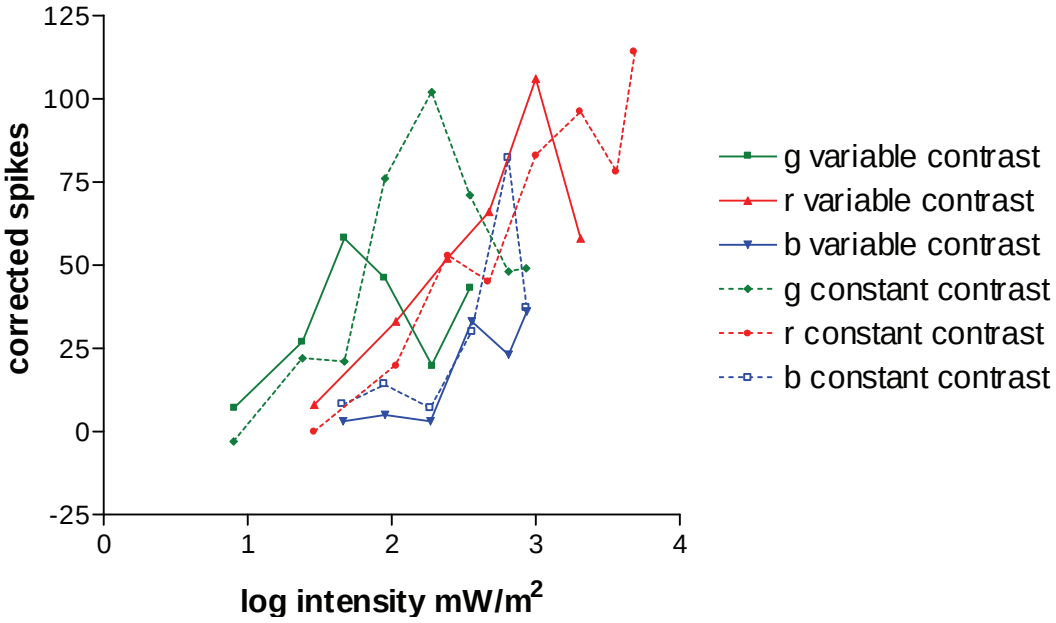

Fig. 58 - R/I curves for cell No. 49. Only the intensity of the stimulus center is used for plotting along the x-axis. Solid lines indicate response to variable contrast. Dotted lines indicate response to constant contrast (white background). Constant contrast evoked higher peeks in all three wavelengths.

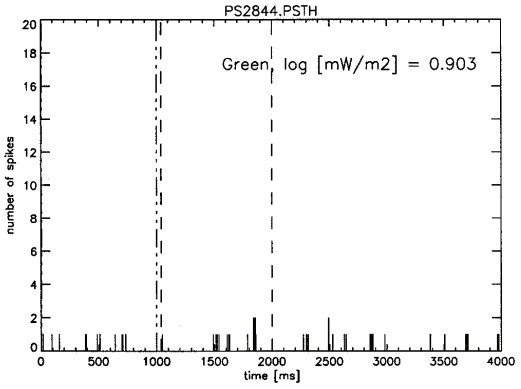
PS2844.PSTH
Green, log [mW/m2] = 0.903
number of spikes
time [ms]

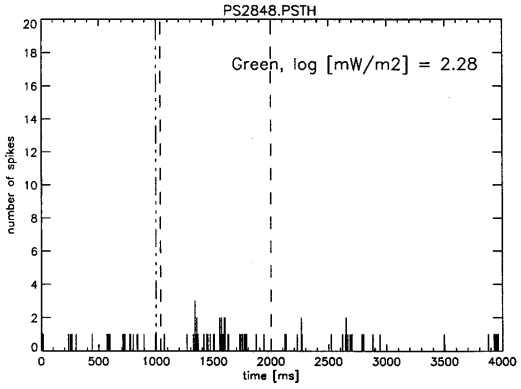
PS2848.PSTH
Green, log [mW/m2] = 2.28
number of spikes
time [ms]

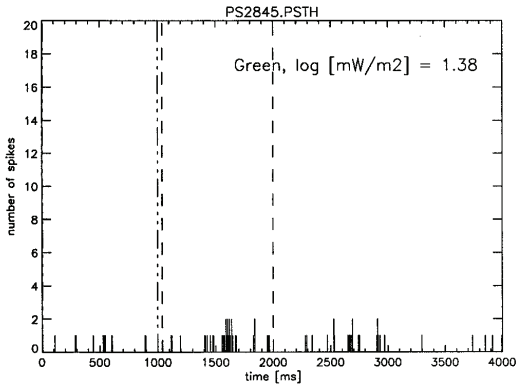
PS2845.PSTH
Green, log [mW/m2] = 1.38
number of spikes
time [ms]

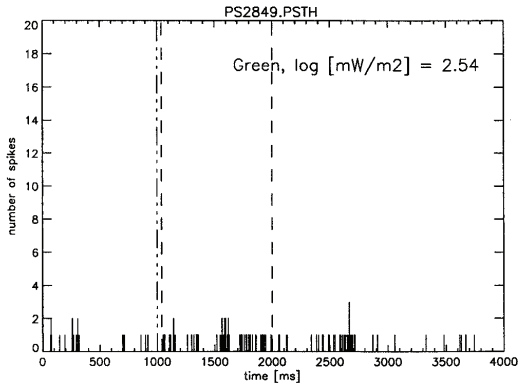
PS2849.PSTH
Green, log [mW/m2] = 2.54
number of spikes
time [ms]

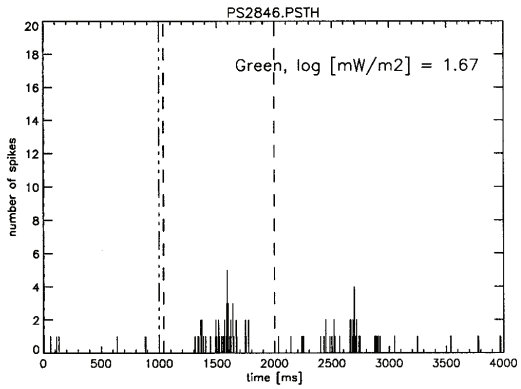
PS2846.PSTH
Green, log [mW/m2] = 1.67
number of spikes
time [ms]

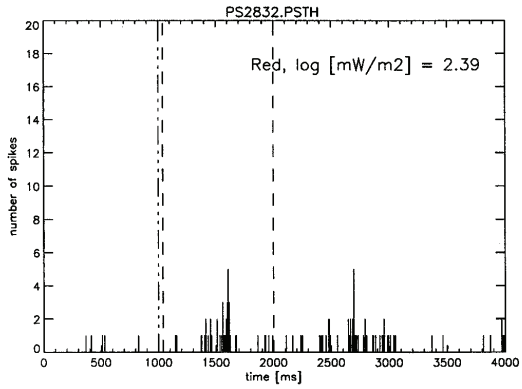
PS2832.PSTH
Red, log [mW/m2] = 2.39
number of spikes
time [ms]

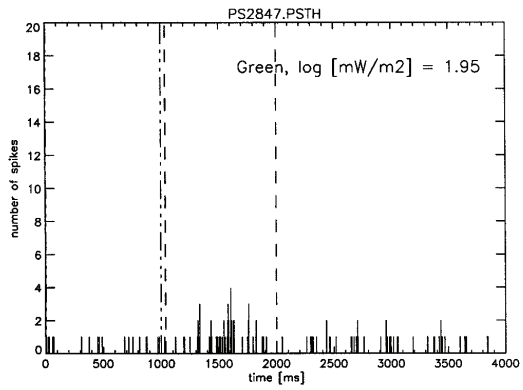
PS2847.PSTH
Green, log [mW/m2] = 1.95
number of spikes
time [ms]

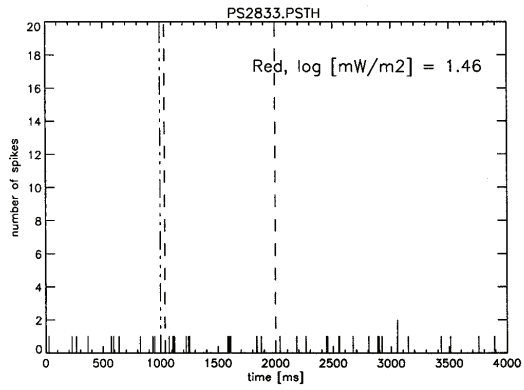
PS2833.PSTH
Red, log [mW/m2] = 1.46
number of spikes
time [ms]

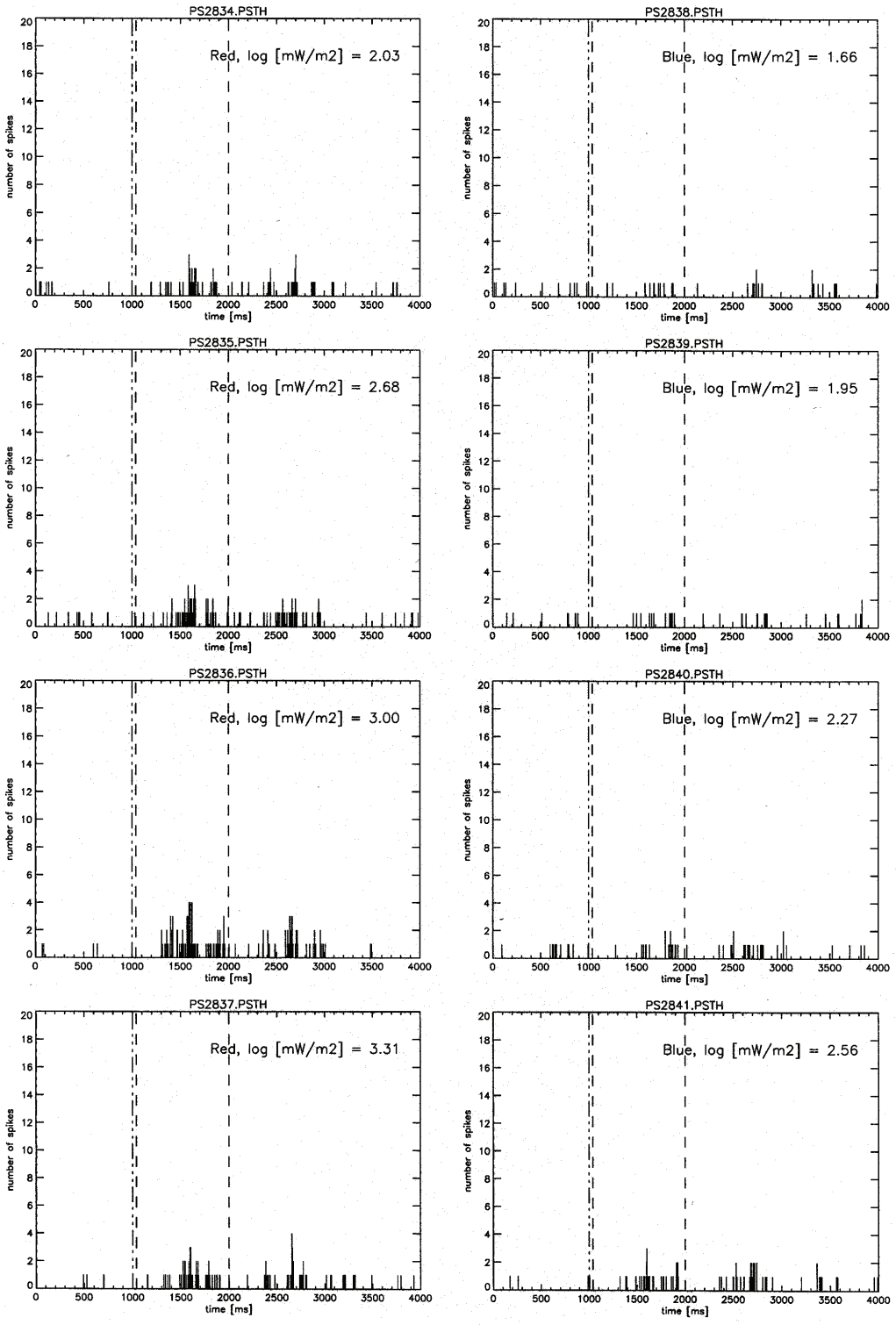
PS2834.PSTH
Red, log [mW/m2] = 2.03
PS2838.PSTH
Blue, log [mW/m2] = 1.66
PS2835.PSTH
Red, log [mW/m2] = 2.68
PS2839.PSTH
Blue, log [mW/m2] = 1.95
PS2836.PSTH
Red, log [mW/m2] = 3.00
PS2840.PSTH
Blue, log [mW/m2] = 2.27
PS2837.PSTH
Red, log [mW/m2] = 3.31
PS2841.PSTH
Blue, log [mW/m2] = 2.56
number of spikes
time [ms]

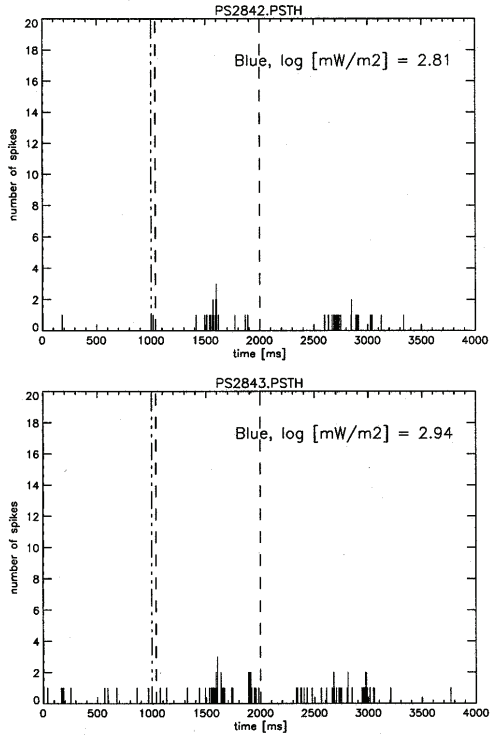

Fig. 59 – Histograms for cell No. 49 corresponding to solid lines in **Figure 58** (variable contrast). Spike window is from 1040 to 2000 msec; reference window is from 0 to 1000 msec.

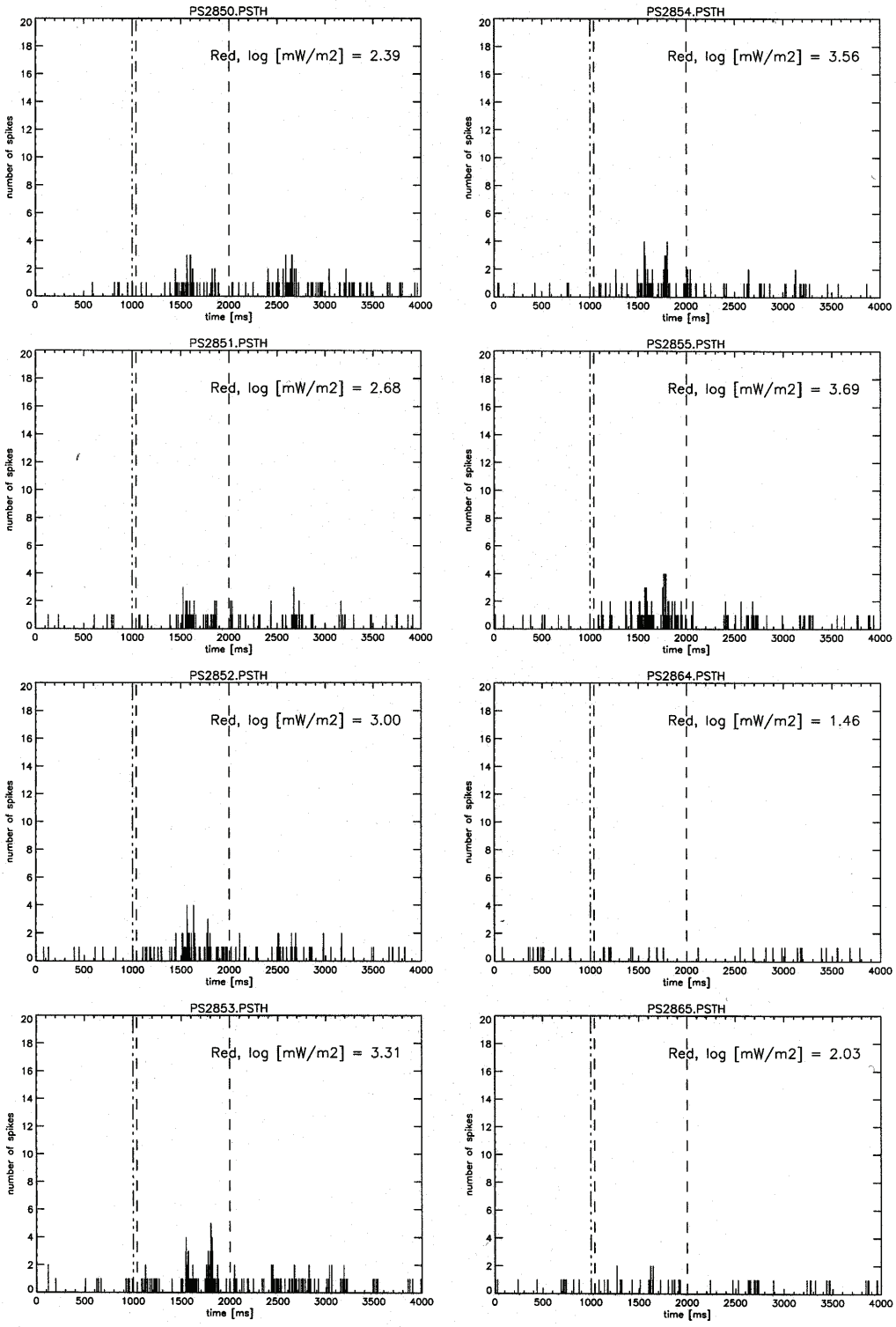
PS2850.PSTH
Red, log [mW/m2] = 2.39
PS2854.PSTH
Red, log [mW/m2] = 3.56
PS2851.PSTH
Red, log [mW/m2] = 2.68
PS2855.PSTH
Red, log [mW/m2] = 3.69
PS2852.PSTH
Red, log [mW/m2] = 3.00
PS2864.PSTH
Red, log [mW/m2] = 1.46
PS2853.PSTH
Red, log [mW/m2] = 3.31
PS2865.PSTH
Red, log [mW/m2] = 2.03
number of spikes
time [ms]

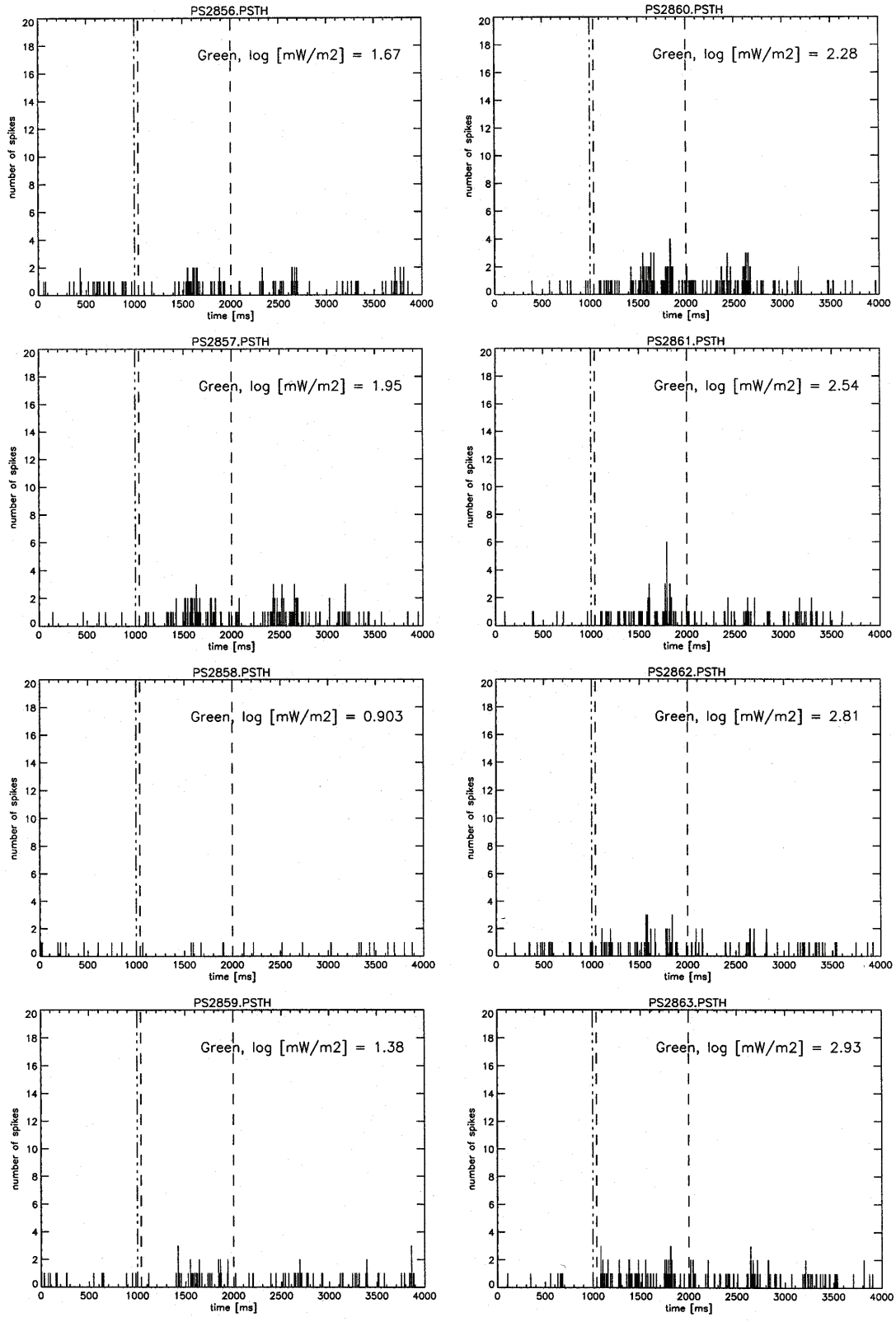
PS2856.PSTH
Green, log [mW/m2] = 1.67
PS2860.PSTH
Green, log [mW/m2] = 2.28
PS2857.PSTH
Green, log [mW/m2] = 1.95
PS2861.PSTH
Green, log [mW/m2] = 2.54
PS2858.PSTH
Green, log [mW/m2] = 0.903
PS2862.PSTH
Green, log [mW/m2] = 2.81
PS2859.PSTH
Green, log [mW/m2] = 1.38
PS2863.PSTH
Green, log [mW/m2] = 2.93
number of spikes
time [ms]

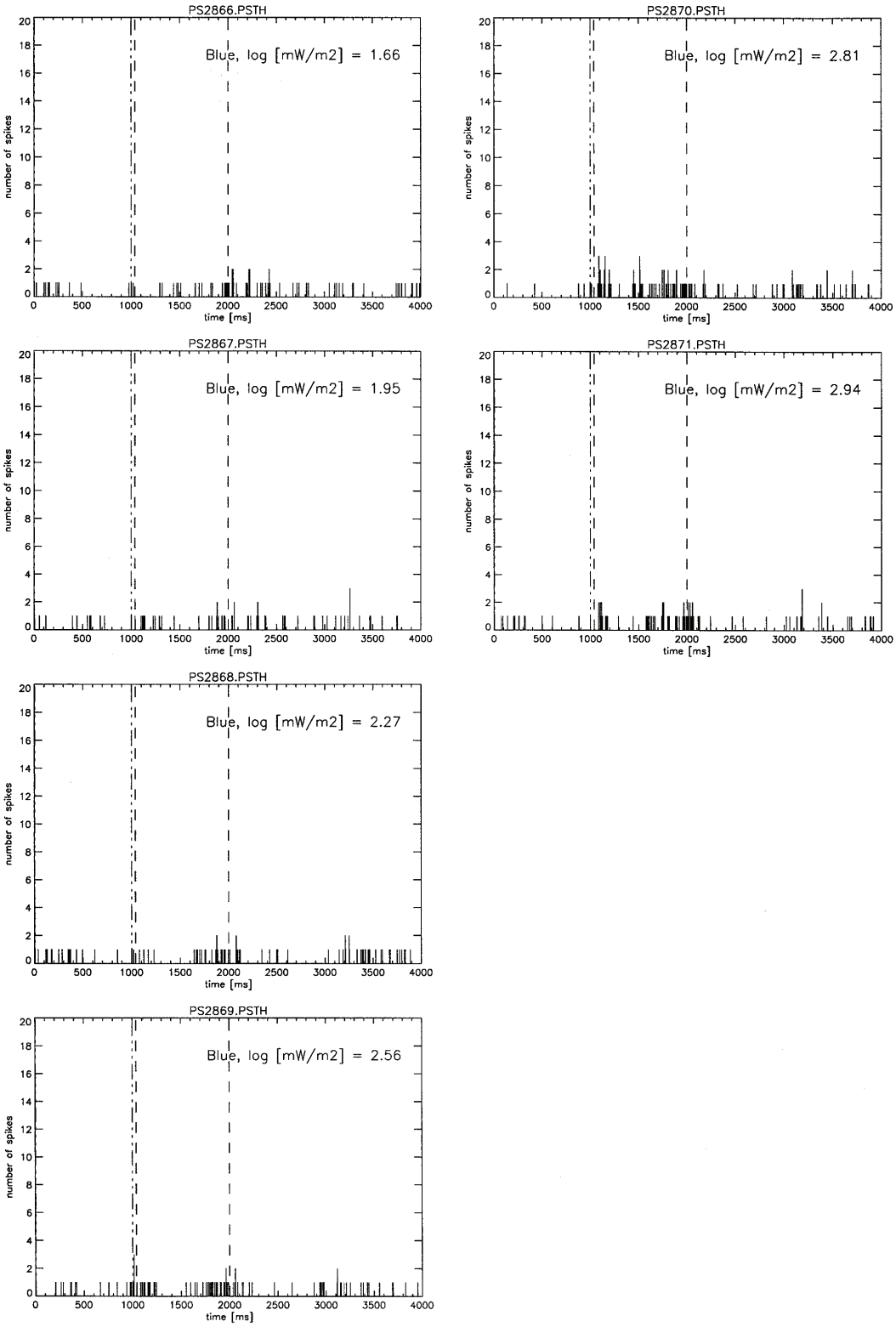

Fig. 60 – Histograms for cell No. 49 corresponding to dotted lines in **Figure 58** (constant contrast). Only the intensity of the stimulus center is indicated. Spike window is from 1040 to 2000 msec; reference window is from 0 to 1000 msec.

3.4.4 Contrast cell D (A18)

This cell corresponds to **number 35** in our listing and was found in animal T.AD. 200. It is localized in Area 18 at a depth of 1215 microns. The cell is driven by contralateral stationary stimuli and gives a phasic OFF response. In **Figure 61**, we see the response of the cell to white light with and without constant contrast. The corresponding histograms are in **Figure 62** (variable contrast) and **Figure 63** (constant contrast). We can observe that the absence of contrast variation flattens and reduces the response of the cell. The cell is "driven" by contrast. In the absence of it, response diminishes.

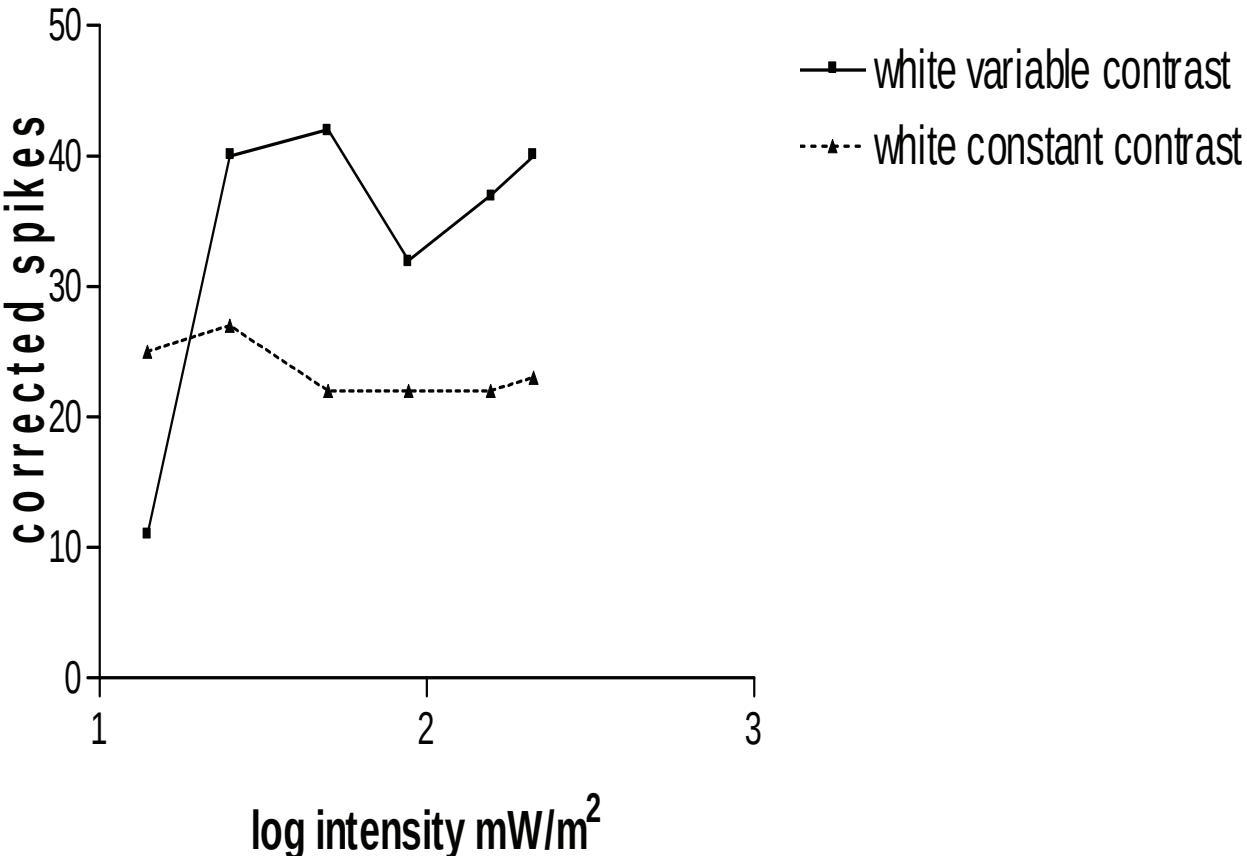

Fig. 61 - R/I curves of cell No. 35. The solid line response to variable contrast and the dotted line response to stimuli with constant intensity ratio between stimulus center and background. For plotting, only the intensity of the stimulus center is used. Notice that the curve is much flatter in the absence of variable contrast.

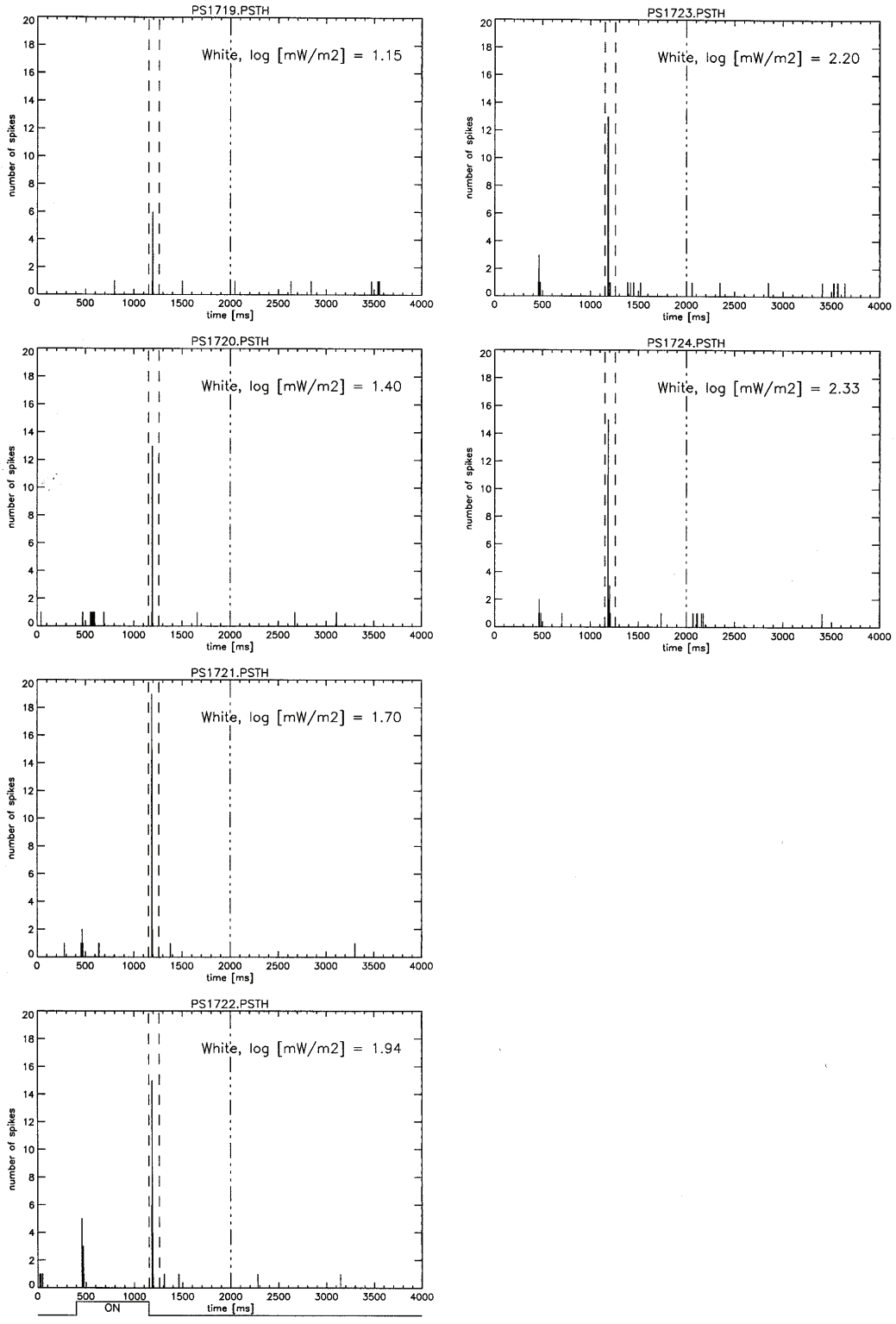

Fig. 62 - Histograms of cell No. 35. These correspond to the solid line (variable contrast) in **Figure 61** above.

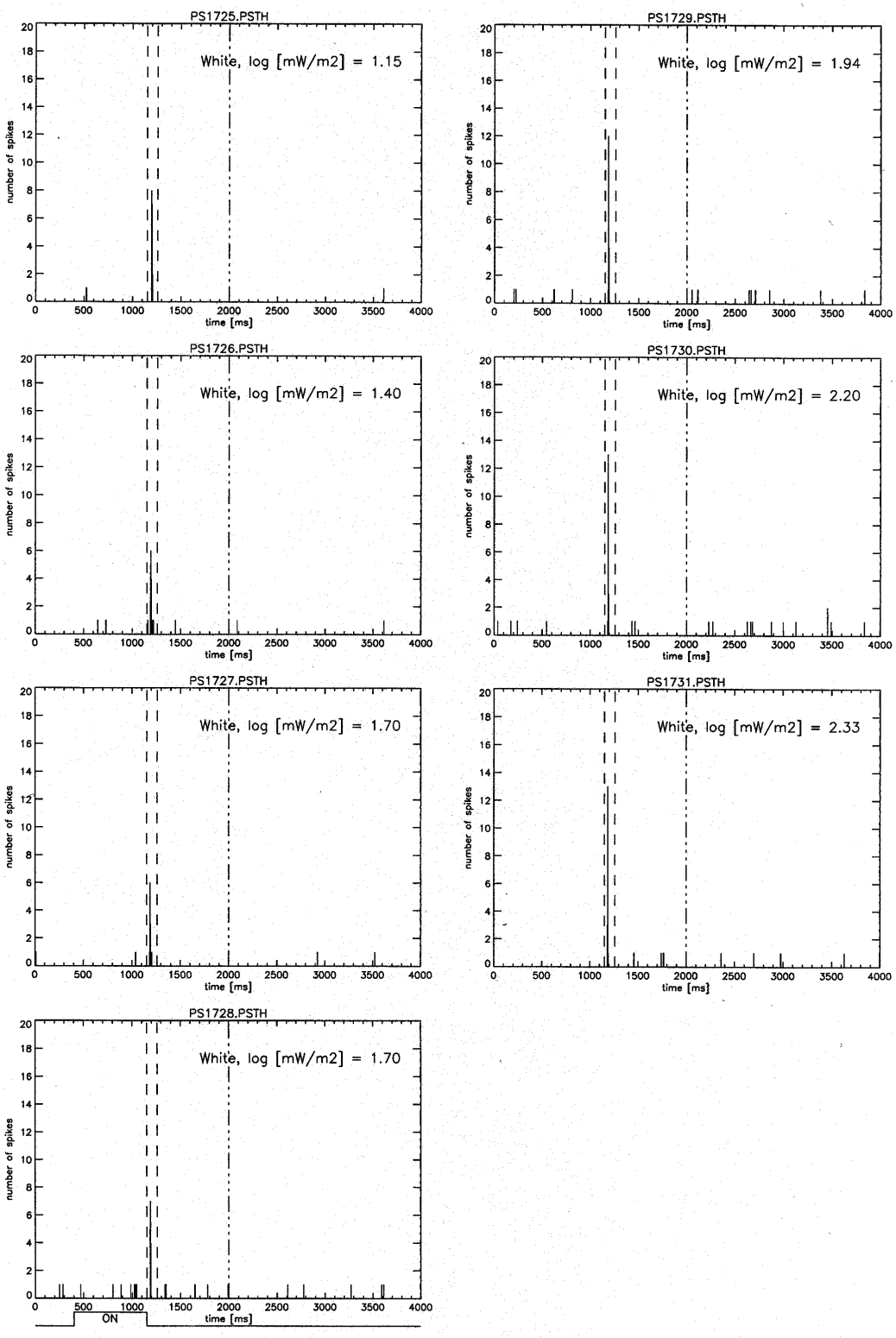

Fig. 63 – Histogram of cell No. 35. These correspond to the dotted line (constant contrast) in **Figure 61**.

3.5 Possible influence of movement on response

In contrast with previous findings postulating strictly separate processing pathways for color and motion (Livingstone and Hubel 1988, Schiller and Logothetis 1990) we find a number of narrow band units responding well to movement, or indeed, responding exclusively to moving stimuli. Of the eight narrow band cells we have examined above, four respond to movement. Of these, two respond exclusively to moving stimuli. Thus our data is in agreement with recent studies refuting the movement/color pathway dichotomy (Gegenfurtner 1996). In **Table 6** we show a listing of narrow band units' response to moving and stationary stimuli.

Narrow band cell	**Inventory number**	**Location**	**Stationary**	**Moving**
A	2	CS (SGS)	x	x
B	16	CS (SGS)		x
C	20	CS (SGS)	x	
D	3	A17 – III a/b	x	x
E	6	A17 - IIIb	x	
F	9	A17 - IVb	x	
G	8	A18		x
H	26	dLGN - 3	x	x

Table 6 – Narrow band cells' preference for stationary or moving stimuli.

The speed of movement can actually influence the cell's chromatic tuning as we can see in the following example.

3.5.1 A cell with motion-induced variation in spectral response

This cell corresponds to **number 50** in our listing and was found in animal T.AD. 213. It is located in A17, layer V (depth of 1435 microns). Both contra- and ipsilateral eyes drive the cell. The response is both phasic and tonic (only to moving stimuli). In **Figure 64** (histograms in **Figure 65**) we see a graph showing the cells' response to long-wavelength and short-wavelength stimulation. Response is usually stronger for the former than for latter type of stimulation. This is not the case with rapidly moving stimuli.

This influence of movement on spectral response suggests the possibility that the two cone populations may have different sensitivities in terms of latency and optimal stimulation speed. This could have a morphological basis, such as a preferred range of axon diameters for one subset of the population. It was not, within the scope of this study to test this systematically.

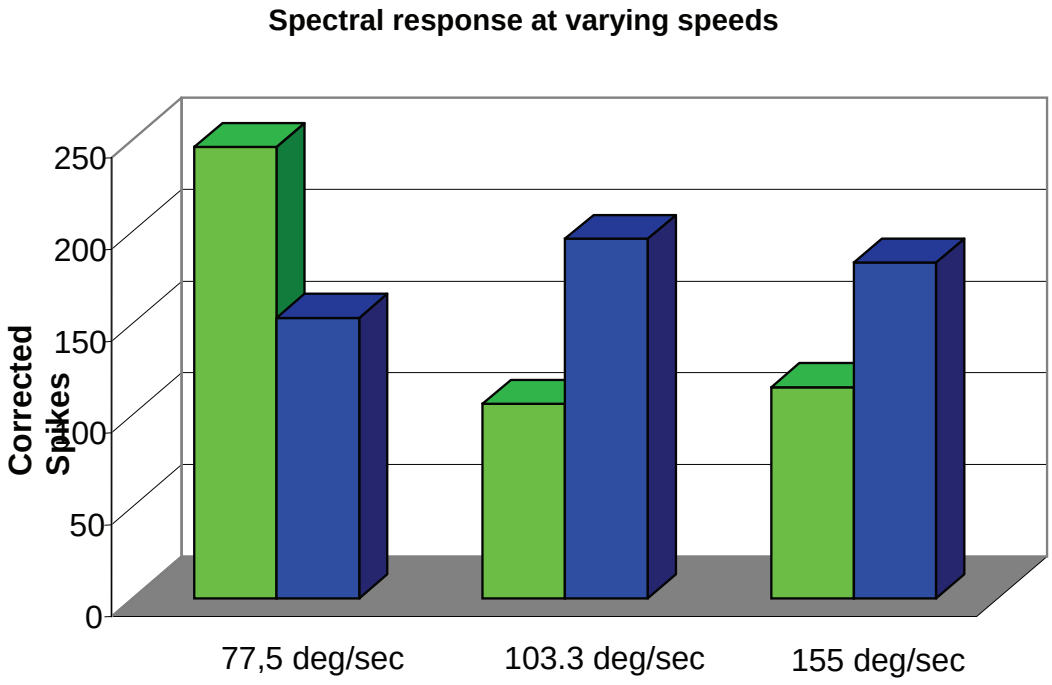

Fig. 64 - Spectral response at different speeds. Notice that the short-wavelength response tends to increase at higher speeds, whereas the long-wavelength response decreases.

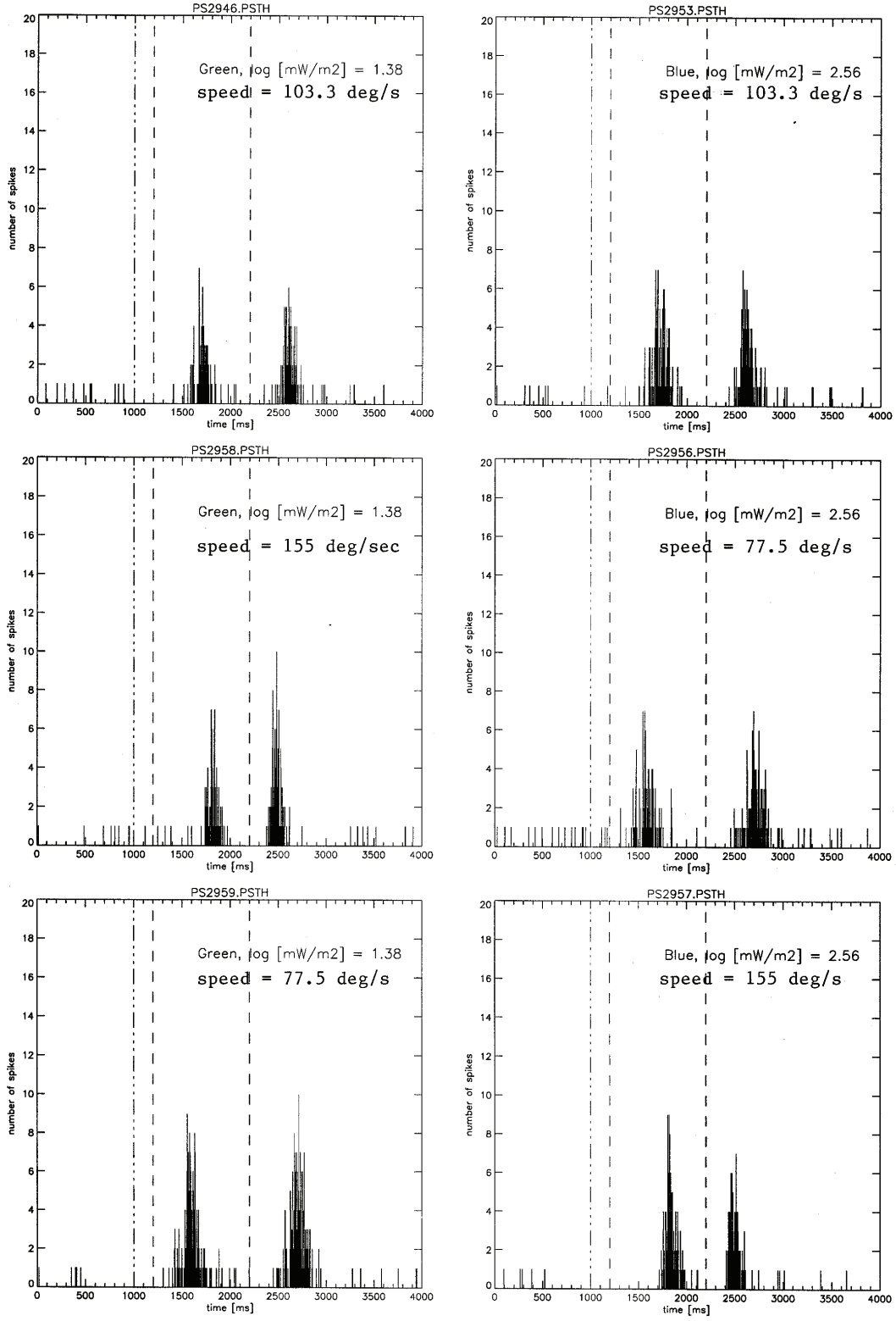

Fig. 65 Spectral response at different speeds. These histograms correspond to cell No. 50 (see previous figure).

3.6 Luminance – Cone weights

Luminance is the term used to define the relative luminous efficiency of light having a given wavelength in stimulating the visual system (see Gegenfurtner and Hawken, 1996). Typically, the visual systems' response to two different wavelengths will be compared, and the relative intensities adjusted until the responses are the same. This is generally done in psychophysical experiment requiring subjects to match stimulus intensities.

In one of the cells which we have discussed elsewhere (contrast cell D, No. 35) we noticed an extraordinary similarity in the shape of the curves elicited by the different wavelengths as can be seen in **Figure 66**. The cell is localized in A18. The intensity of the stimulus center and surround were varied in such a way as to keep their ratio constant (i.e. constant contrast). By shifting these curves slightly, we can get the peeks and valleys to match almost perfectly. This means that by simply multiplying the intensities by a scalar factor, we can align these curves. The factor thus obtained for each wavelength represents its efficacy relative to another wavelength. From it we can deduce the relative cone weights.

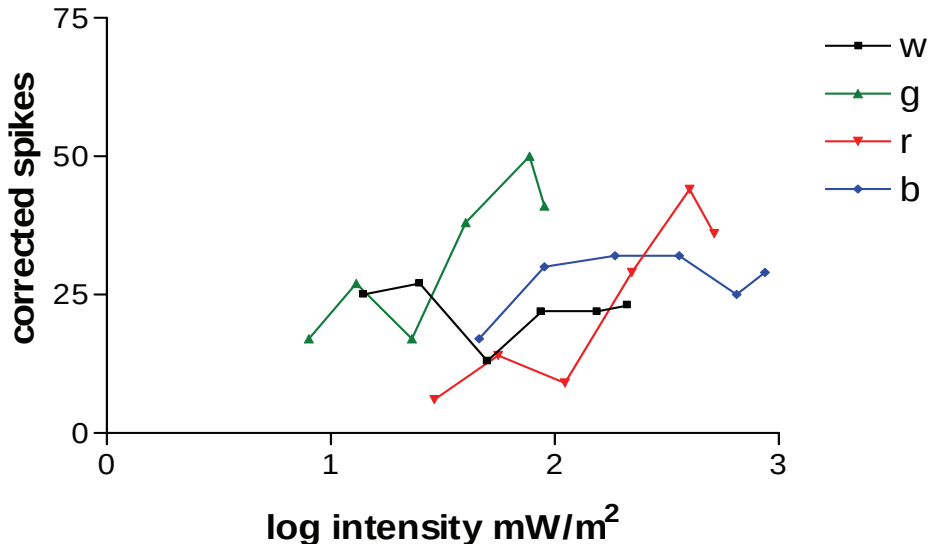

Fig. 66 – These are the R/I curves taken from cell No. 35. Notice that the general pattern of peeks and valleys is rather similar. Constant contrast between center and surround were used.

In **Figure 67**, we can see the result of this displacement along the intensity axis. Green was used as the basis for the comparison, since it gave the best response at the lowest intensity. Notice that with blue, the highest intensities are required to get a response, if any.

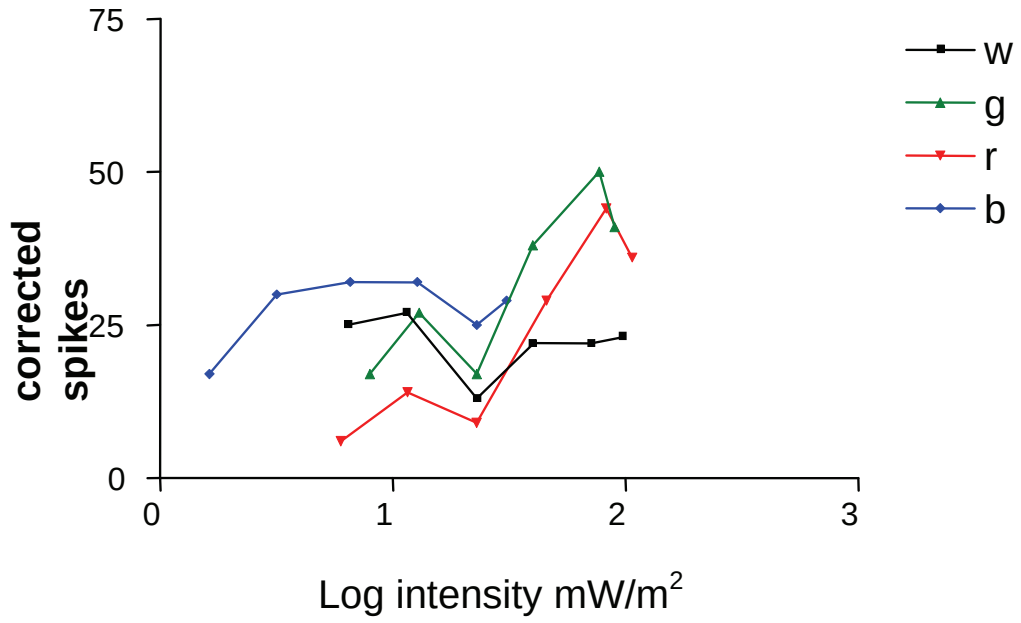

Fig. 67 – R/I curves of cell No. 35 with intensity values multiplied by a factor in order to align them. Contrast between stimulus center and background was kept constant.

The intensity values are taken from the first valley in the curve. The intensity ratios calculated are shown in **Table 7**. The histograms for the above curves are shown in **Figure 68**.

Wavelength	Intensity of Wavelength /Intensity in Green (mW)	Factor
green	23/23	1
white	50/23	2,17
red	111/23	4,83
blue	650/23	28,26

Table 7 –Factors used to align response curves in previous figure.

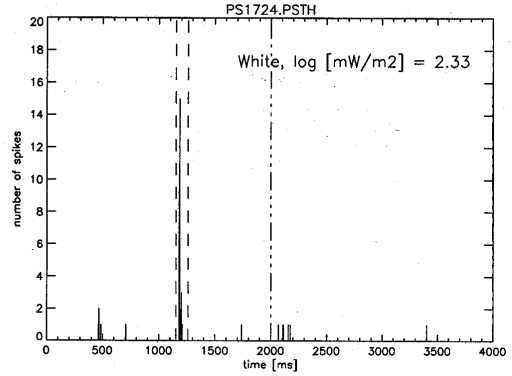
PS1724.PSTH
White, log [mW/m2] = 2.33
number of spikes
time [ms]

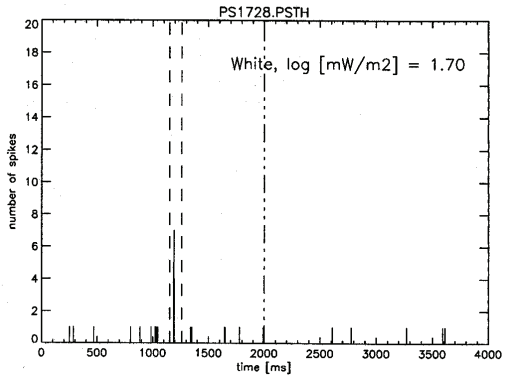
PS1728.PSTH
White, log [mW/m2] = 1.70
number of spikes
time [ms]

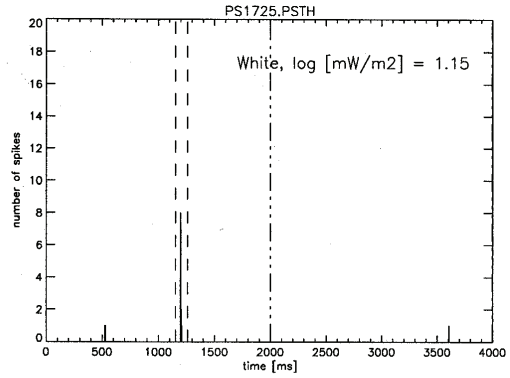
PS1725.PSTH
White, log [mW/m2] = 1.15
number of spikes
time [ms]

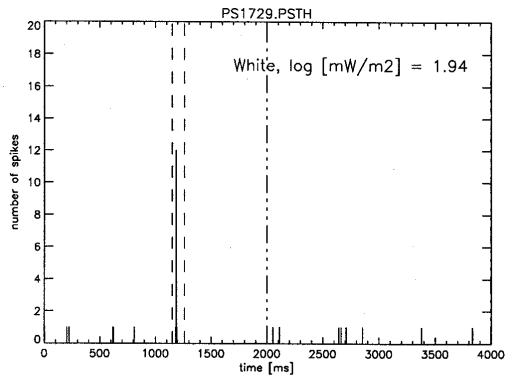
PS1729.PSTH
White, log [mW/m2] = 1.94
number of spikes
time [ms]

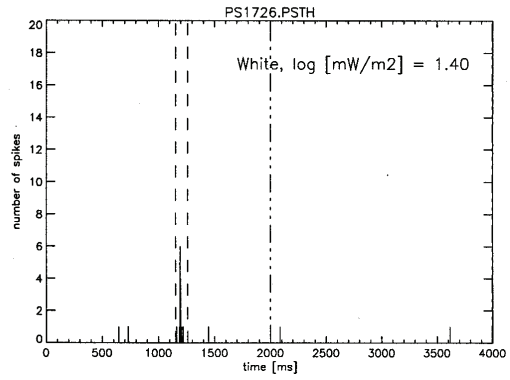
PS1726.PSTH
White, log [mW/m2] = 1.40
number of spikes
time [ms]

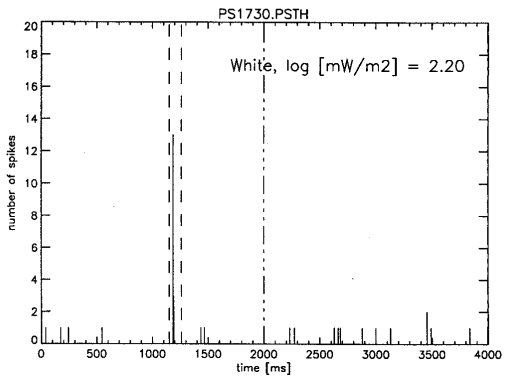
PS1730.PSTH
White, log [mW/m2] = 2.20
number of spikes
time [ms]

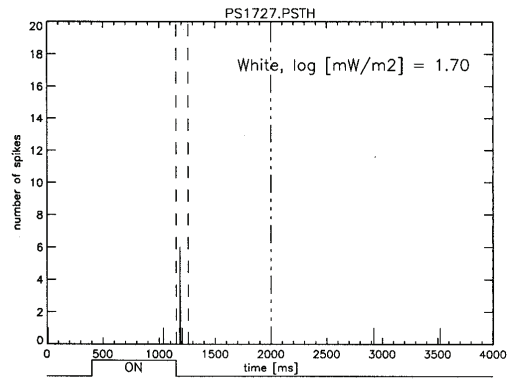
PS1727.PSTH
White, log [mW/m2] = 1.70
number of spikes
ON
time [ms]

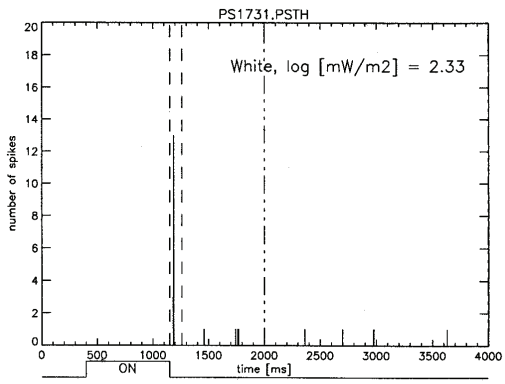
PS1731.PSTH
White, log [mW/m2] = 2.33
number of spikes
ON
time [ms]

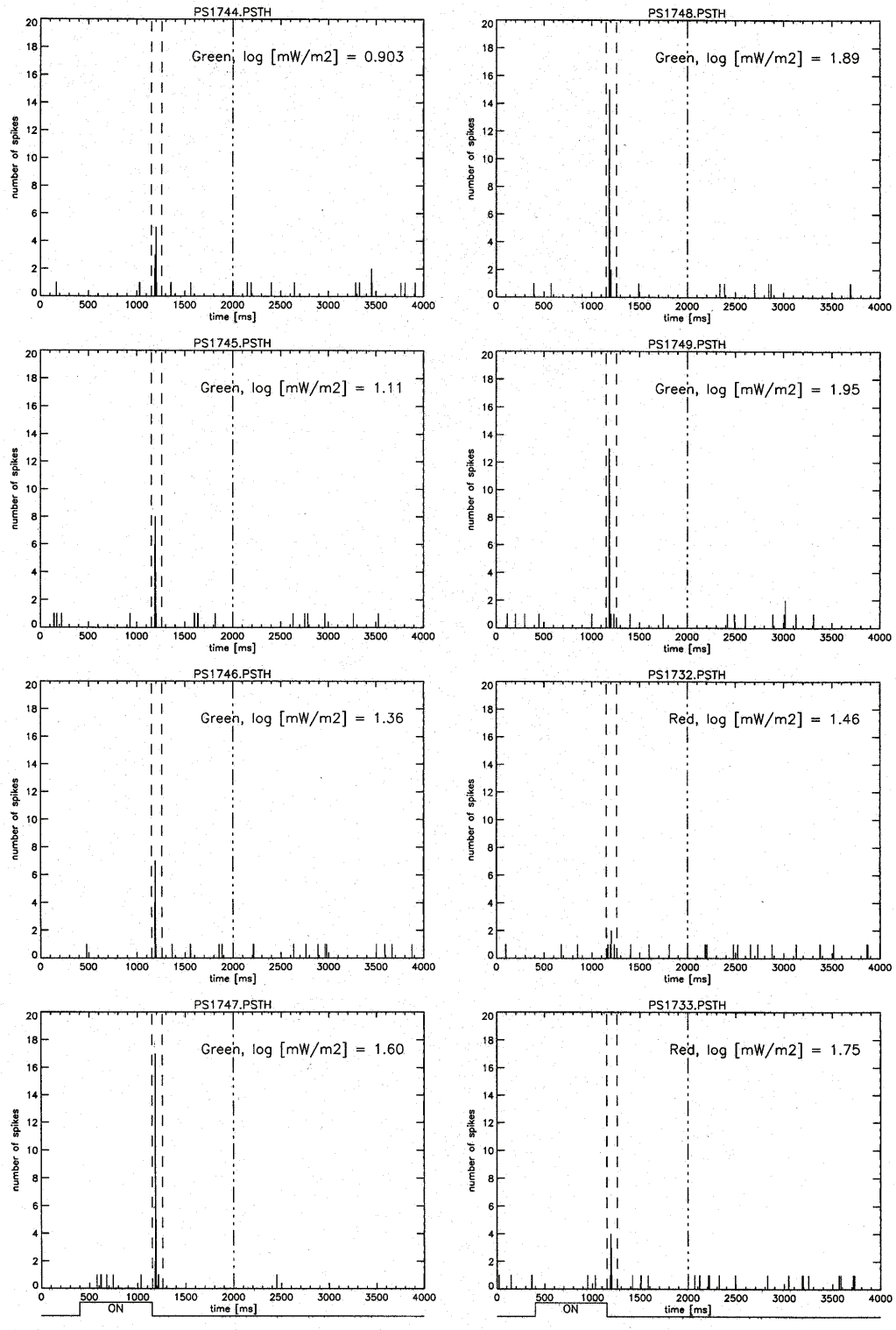
PS1744.PSTH
Green, log [mW/m2] = 0.903
PS1748.PSTH
Green, log [mW/m2] = 1.89
PS1745.PSTH
Green, log [mW/m2] = 1.11
PS1749.PSTH
Green, log [mW/m2] = 1.95
PS1746.PSTH
Green, log [mW/m2] = 1.36
PS1732.PSTH
Red, log [mW/m2] = 1.46
PS1747.PSTH
Green, log [mW/m2] = 1.60
PS1733.PSTH
Red, log [mW/m2] = 1.75
number of spikes
time [ms]
ON

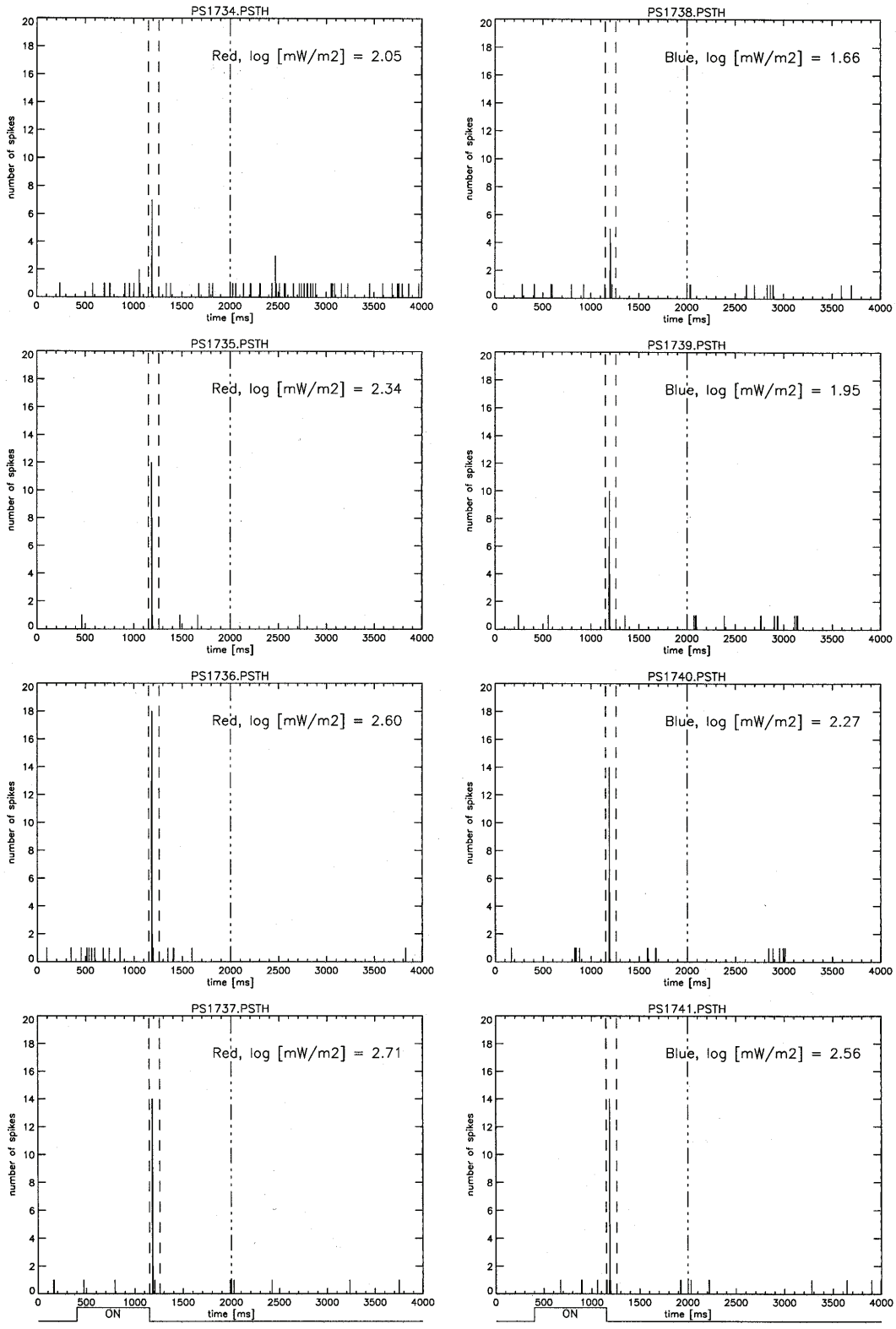
PS1734.PSTH
Red, log [mW/m2] = 2.05
PS1738.PSTH
Blue, log [mW/m2] = 1.66
PS1735.PSTH
Red, log [mW/m2] = 2.34
PS1739.PSTH
Blue, log [mW/m2] = 1.95
PS1736.PSTH
Red, log [mW/m2] = 2.60
PS1740.PSTH
Blue, log [mW/m2] = 2.27
PS1737.PSTH
Red, log [mW/m2] = 2.71
PS1741.PSTH
Blue, log [mW/m2] = 2.56
number of spikes
time [ms]
ON

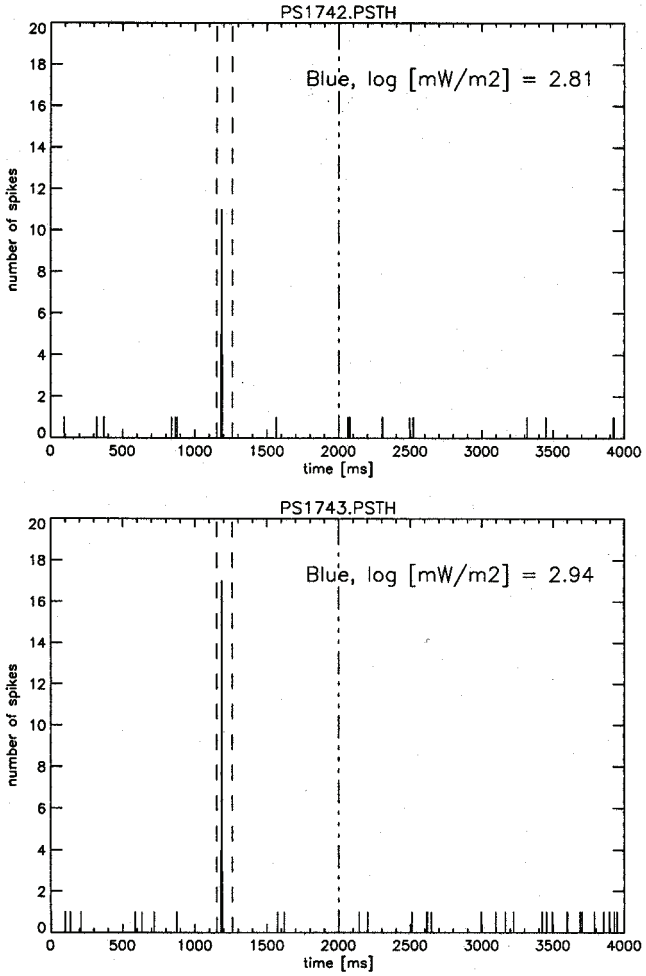

Fig. 68 – Histograms corresponding to cell No. 35, using constant contrast stimuli. R/I curves can be seen in **Figures 66 and 67**.

3.7 A cell with center surround color-opponency (cell-sparse cleft)

A single cell in our study showed center surround color-opponency. This cell corresponds to **number 47** in our listing. which was found in the cell-sparse cleft (A17) of animal T.AD. 212 at a depth of 1240 microns. The cell responds to stimulation from both the contra- and ipsilateral eyes, and to both stationary and moving stimuli. The response is both phasic and tonic, except with stationary stimuli, where it is almost only phasic. We have already encountered this cell under the heading of "Contrast cell B", where we observed that this cell is not contrast driven and hence responds better to contrast-invariant stimuli. In **Figure 69**, we can see its peculiar center-surround interactions.

stimulus	*colors*	*corrected spikes*
A	blue center and surround	11
B	red center only	95
C	A + B	79
D	red center and surround	127
E	blue center only	24
F	E + D	107

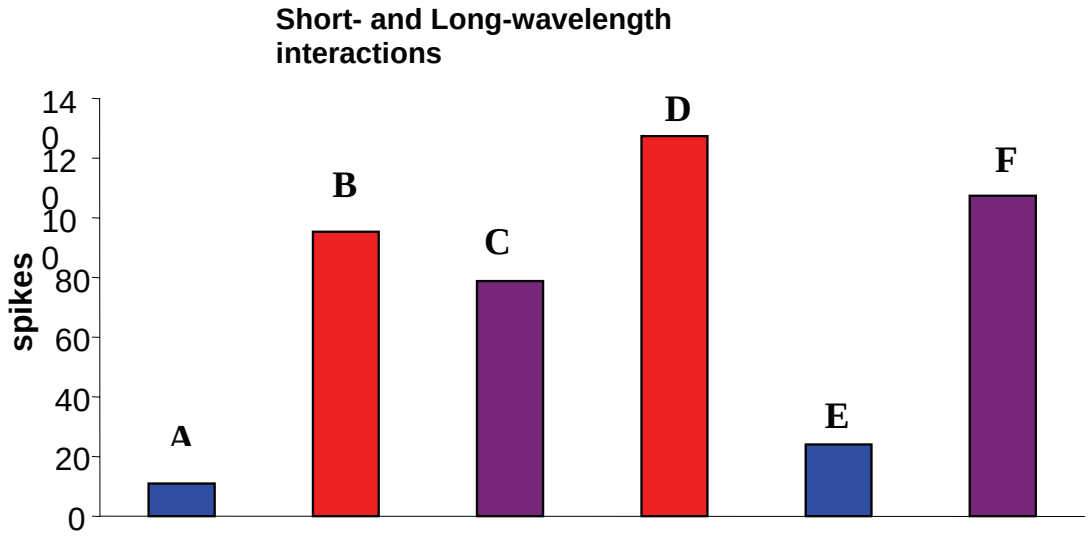

Fig. 69 Center and surround interactions with short and long wavelengths. Center and surround are first shown independently and then paired.

At first glance, this data does not seem to indicate a chromatic center-surround color opponency, especially since all of the spots of any given size or wavelength give the same kind of response (a positive one with respect to baseline). Closer examination, however, reveals that the spectral sensitivities of the center and surround are not the same. If a red center (B) is paired with a red surround, the result D (red center plus surround), gives a stronger response. This suggests an RF such as the one in **Fig. 70a**. If, on the other hand, the red center (B) is paired with A (blue-center surround), the activity is diminished. The blue surround antagonizes the red center, as in **Fig. 70b**. Conversely, if we start with blue center only (E) and add a surround, the result obtained (A) gives a weaker response **Fig. 70c**. If, however, the blue center (E) is paired with D (red center and surround), the result (F) is stronger than E as seen in **Fig. 70d**.

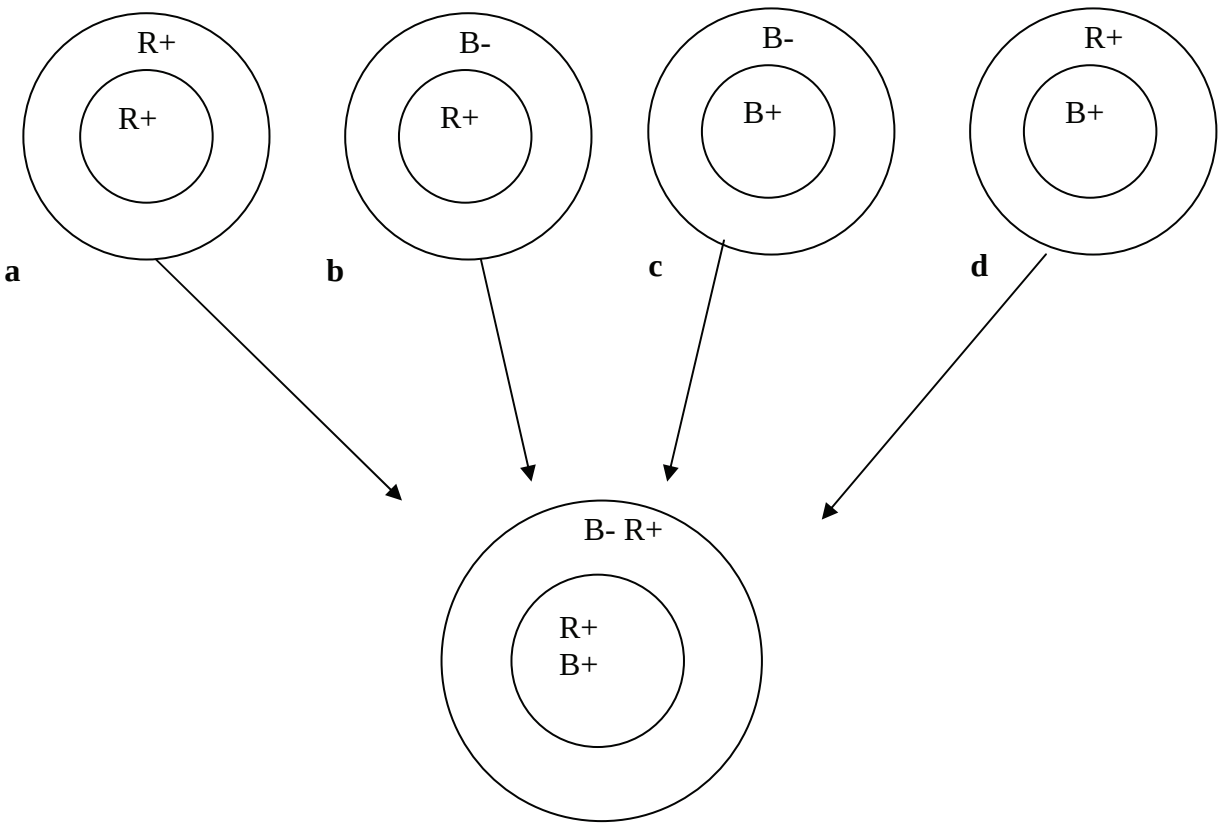

Fig. 70 – Different types of center surround interactions and antagonisms as explained in text. The emerging picture is one of a color-opponent cell similar to the Type I described by Livingstone and Hubel (1984).

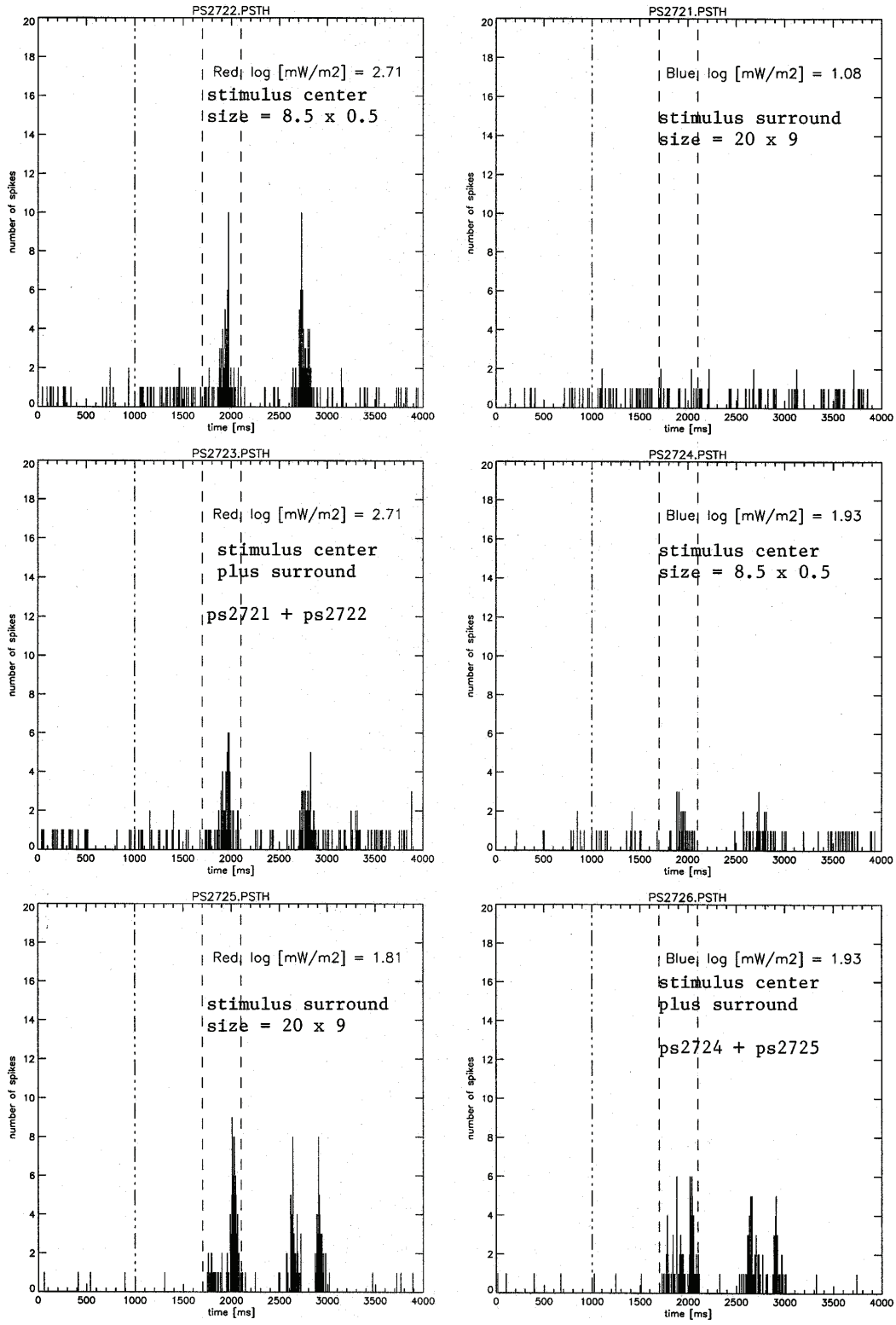

Fig. 64 – Histograms showing center surround interactions (see text) with different wavelengths in cell No. 47.

In **Figure 71**, we can see the response at different speeds (histograms in **Figure 72**). The different stimulus angular speeds were all tested with the same wavelength (white light) and intensity of 167 mW/cm^2. Stimulus vs. background contrast remained the same.

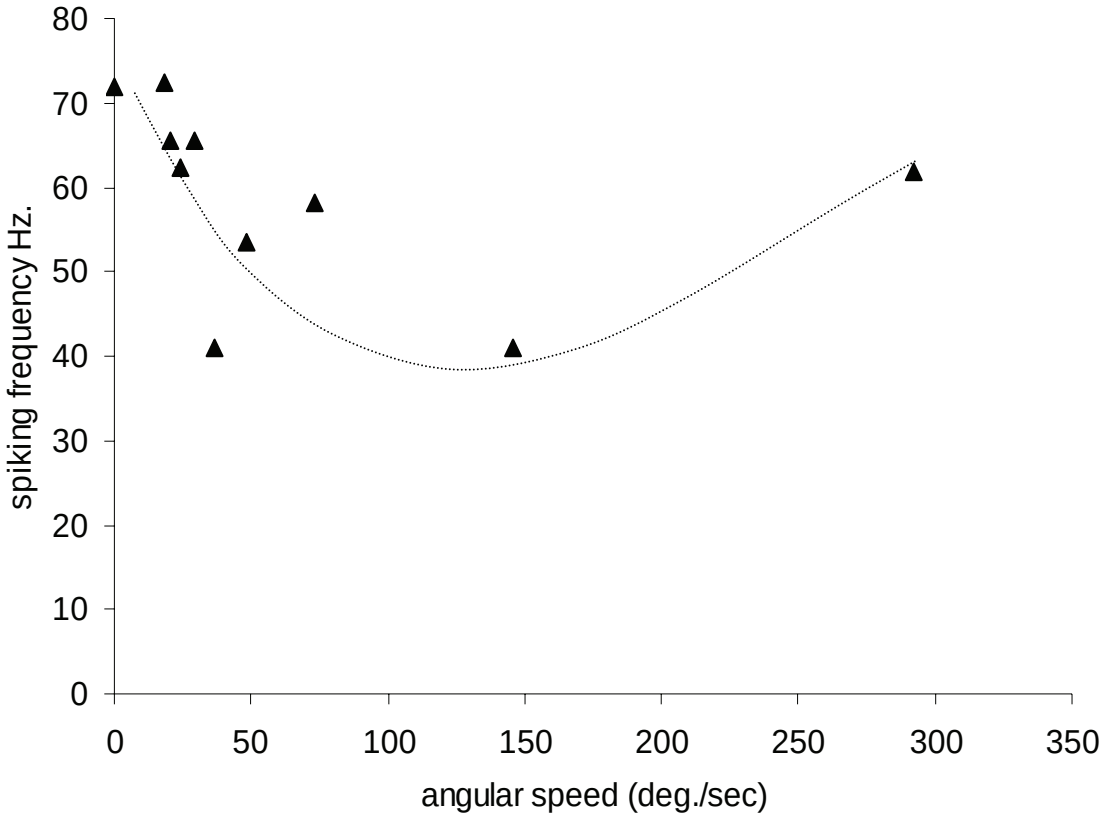

Fig. 71 Response with different stimulus speeds. Only white was tested. Notice there is no veridical coding of speed. All stimuli had an intensity of 167 mW/cm^2.

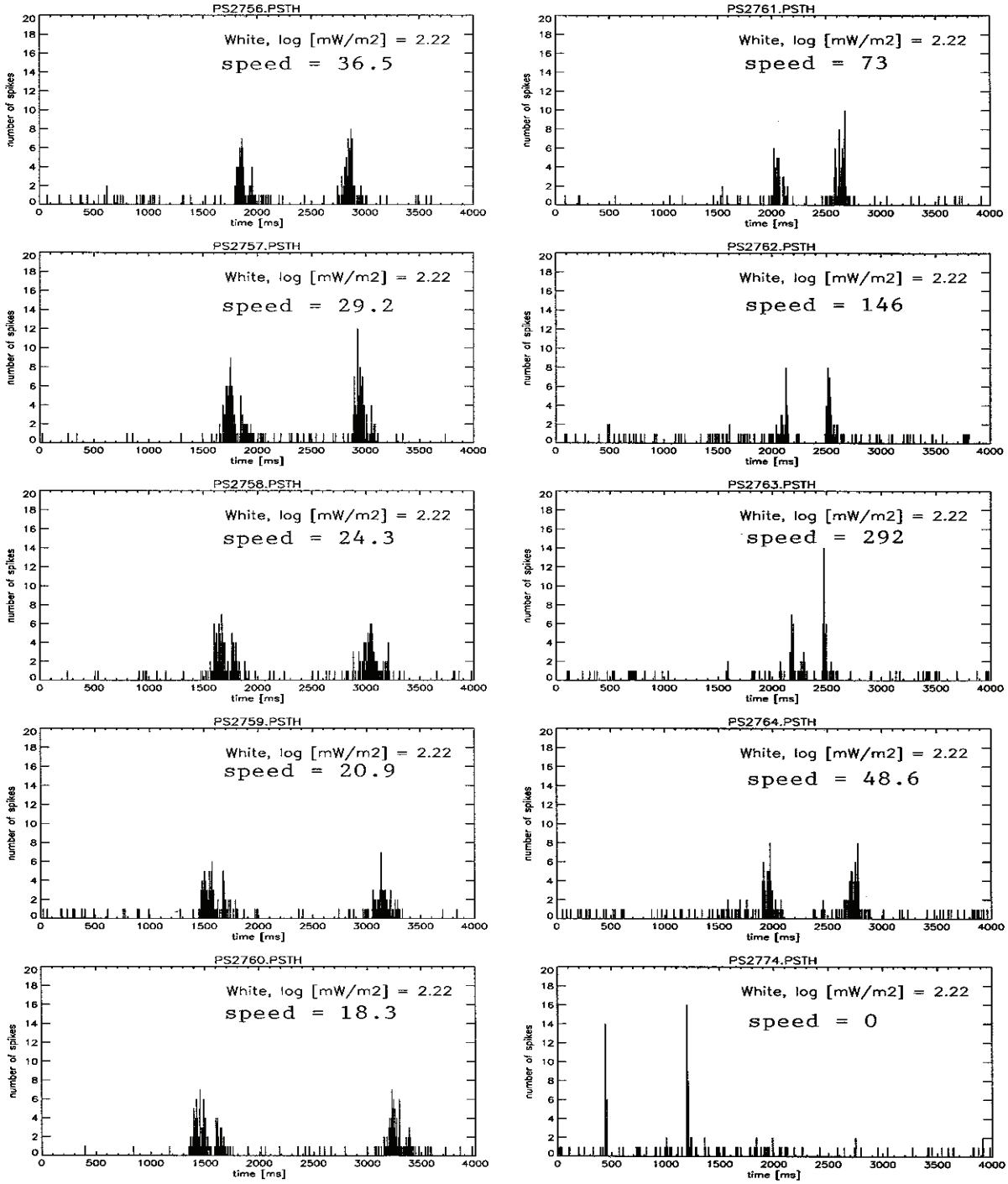

Fig. 72 – Histograms corresponding to graph in **Figure 71**. The two set of peeks represent the two moments when the light bar goes over the RF, moving forward and backward.

The cell was also tested for response fluctuations in time. This is shown in **Figure 73**.

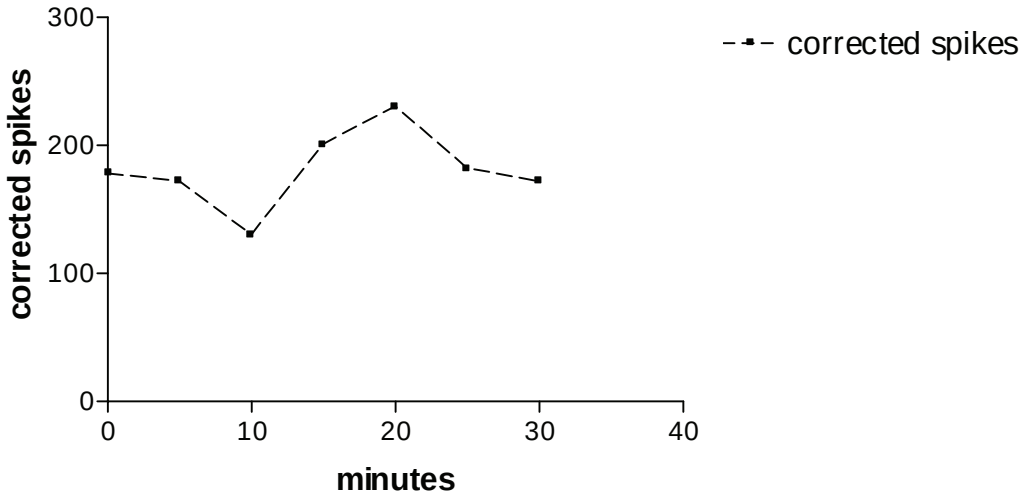

Fig. 73 – This graph shows the fluctuations in cell response and baseline activity with time.

Discussion

4. Discussion

4.1 Methodology

Color vision is the capacity to discriminate different wavelengths or mixtures of wavelengths independently of their intensity. The visual systems' capacity to discriminate color is determined primarily by the number of photoreceptors in the system. In the tree shrew, with its cone-dominated retina, two cone types are available: the SWCs (short-wavelength cones) and the LWCs (long-wavelength cones) with λ_{max} at approx. 428-444 nm and 550-556 nm (Polson 1968, Jacobs and Neitz 1986, Petry and Harosi 1990). Being a dichromat, the tree shrew has a neutral point at ca. 505 nm (Polson 1968, Jacobs & Neitz 1986).

The cells that have been examined in this study have been analyzed so as to generate Reaction/Intensity curves (R/I curves). These curves show the variations in firing rates as intensity changes. Broad-band filters with maximal transmission in the blue, green, and red regions were used to stimulate the visual system of the tree shrew, during single-cell recordings. The transmission curves of these filters are given in **Appendix III**.

These R/I curves show a typical non-monotonic shape similar to a logistic function (Kretz 1973, 1977), and three different parts can be observed. Initially, there is a threshold region, below which the stimulus is too weak to produce a reaction. Above threshold, one finds the dynamic region, where the stimulus produces an increase in cell firing rates. This increase is approximately proportional to the logarithm of the stimulus intensity. Finally there is a saturation region, where the cell has reached its maximum firing rate, and further increase in the stimulus intensity does not significantly increase the firing rate and often produces some inhibition, as expected from non-monotonic functions. The slopes of the R/I curves within the dynamic domain are nearly linear, when they are plotted on a logarithmic scale for abcissas (log intensity), which is in sound agreement with the Weber-Fechner law.

4.2 Psychophysics – Preliminary Considerations

4.2.1 The Weber-Fechner law

The Weber-Fechner law, perhaps the best known result from nineteenth-century psychophysics, claims that for the various perceptual modalities, the intensity of the percept is a logarithmic function (alternatively, a power function) of the intensity of the stimulus. In the case of vision, for example, this law relates differences in the apparent brightness (luminance) of a stimulus. The relationship between luminance and its actual physical brightness is not linear, but logarithmic. In accordance with this law, the apparent (subjective) intensity of a stimulus can be calculated using the following formula:

$$S = K(\log I),$$

where S is the perceived magnitude of a stimulus, K is a constant and I is the physical intensity of the stimulus. This logarithmic relation implies that the nervous system *compresses* the intensity range of physical stimuli.

4.2.2 The Principle of Univariance

We should be aware that the concept of univariance is critical to any analysis of color discrimination (Naka & Rushton 1966). “The output of a photocell depends upon the intensity of the incident light and also upon its wavelength. But since the output is only of one kind (univariant) it cannot give simultaneously separate information as to both intensity and wavelength.”

Hence, the visual system cannot determine the wavelength of a stimulus simply from the response of a single photoreceptor. Let us suppose that the photoreceptor has a λ_{max} at 444 nm, and that we stimulate it with light of this wavelength. We also test the response at 505 nm (the tree shrews neutral point). We could get the cell to respond identically if we adjusted the intensities either of the stimulating lights (i.e., increase the intensity of the 505 nm light or

reduce the intensity of the 444 nm light). Thus a color-vision system cannot obtain information about hue from a single receptor. Therefore, in a single photoreceptor system, color discrimination is *not* possible; objects are only seen as more or less bright. For this reason, scotopic vision, which involves a single photoreceptor type (rods) is achromatic, yet objects can have different apparent brightness.

4.2.3 Young-Helmholz theory of color vision

As a result of the principle of univariance, no chromatic information can be gained from a single photoreceptor. The implication is therefore that chromatic information can be obtained only by comparing the responses of photoreceptors with different absorption spectra. According to this theory, color is perceived through a comparison of the relative response rates of different types of photoreceptors. In the case of trichromats, this means short-wavelength cones for the blue region, medium-wavelength cones for the green region, and long-wavelength cones for the red region.

Although the Young-Helmholz theory was conceived originally to explain color vision in humans (i.e. thrichromats), taking into account the principle of univariance we can conclude that color vision requires at least two sets of photoreceptors (as is the case in the tree shrew) with overlapping absorption curves. With two sets of photoreceptors there are two responses for any given wavelength impinging on the retina. Based on these relative responses, the visual system can determine the actual frequency of the stimulating light, however there will necessarily be a neutral point as we have explained in the section devoted to Polson's thesis.

4.2.4 Hering's opponent process theory of color

Ewald Hering in the 1860's proposed the opponent process theory of color. This theory suggests that certain colors are mutually inhibitory (i.e., red/green, yellow/blue, & black/white). That colors antagonize each other *within* the object of vision is clear from colored after-images. As physiological support of Hering's theory, one should consider that many retinal ganglion cells and dLGN cells show wavelength opponency. For example, some cells are excited by long-wavelength stimuli and inhibited by short-wavelength stimuli (or vice versa).

4.3 Electrophysiological data

Having outlined the latter psychophysical considerations, which are helpful for putting our data into perspective, let us now turn to a discussion of our data. The results here presented represent an original contribution to the study of color-processing mechanisms in the tree shrew. Studies hitherto carried out examined psychophysical or developmental/anatomical aspects of color vision in this species. Our work corroborates and completes previous research with electrophysiological data. We wish to summarize our findings and consider them in the light of previous works. A summary of our results is:

a) We have found narrow-band cells in the visual system of the tree shrew and characterized their response properties. We assume that these cells, or some interconnected set thereof, must be the neural basis for the processing of chromatic information.

b) We have demonstrated that these narrow-band cells are not strictly insensitive to movement, thus challenging postulates of segregated processing (Zeki 1978, Schiller and Logothetis 1990) and in agreement with more recent observations (Gegenfurtner 1994).

c) A number of narrow-band cells were localized in the Colliculus superior, which gives electrophysiological confirmation of previous studies, showing that tree shrews are capable of performing color discrimination tasks after removal of visual cortex.

d) The majority of units showing strong response to short-wavelength stimulation have receptive fields in the upper visual field (ventral retina) in agreement with histological studies of retina, which show that the majority of short-wavelength cones are localized there.

e) Center surround opponency was found in one cell (cell no. 48) located in the cell-sparse cleft, confirming Petry's proposal that this is the locus of color processing in this species.

Having outlined these points, let us turn to a more detailed discussion of our data.

4.3.1 Summary of Narrow-band cell responses

4.3.1.1 Extragenicular system

We begin by summarizing the results from the narrow-band cells in the extragenicular system. The first of the narrow-band cells is **cell 2**. It was found in the Stratum griseum superficiale (**SGS**) of the Colliculus and responds to both stationary and moving stimuli. This cell responds well to long-wavelength stimuli (red and green filters), however with short-wavelength stimuli (blue filter) even at maximum intensity there is a slight inhibition. This narrow-band activity is limited to the ON-channel. In the OFF-channel, broad-band characteristics can be observed, although blue gives a stronger response than the other wavelengths.

The second of our narrow-band cells is **cell 16**. It is also located in the Colliculus superior in the Stratum Griseum Superficiale (**SGS**) and responds to moving stimuli. While the cell responds well to long-wavelength stimuli (red and green filters), with short-wavelength stimuli (blue filter), even at maximum intensity, there is a slight inhibition.

The third narrow-band cell is **cell 20**. It was also found in the Stratum griseum superficiale (**SGS**). The cell is driven by stationary stimuli. This cell's response to blue is exclusively phasic, whereas the other wavelengths evoke responses with both phasic and tonic components.

4.3.1.1.1 Common features of narrow-band cells in the extragenicular system

These three cells (**cells 2, 16,** and **20**) are the extragenicular narrow-band cells. What do they have in common? They are all located in the SGS and they all have a color-bias that is inclined towards the long-wavelength part of the spectrum. Cells 2 and 16 are slightly inhibited by blue, whereas cell 20 gives a response to blue but only in the phasic "modality".

4.3.1.2 Geniculocortical system

4.3.1.2.1 dLGN

Let us now summarize the narrow-band responses in the geniculocortical system. The only narrow-band cell in the dLGN was **cell 26**, in lamina 3. It responds to stationary stimulation from the contralateral eye and gives an OFF-response. In the R/I curve, throughout the dynamic range of the blue curve, the blue curve has a positive slope while the green curve has a negative slope. In the saturation range, activity sinks to below zero for all wavelengths except blue.

4.3.1.2.2 Striate Cortex

We begin with two cells in the supragranular layers. The first cell is **cell 3**, located in layer III. It responds to stationary and moving stimuli. The response to stimulation from the ipsilateral eye is broad band (blue is weakest). Response to the contralateral eye is narrow-band i.e. only blue gives a response, except when it is preceded by red (temporal inhibition of blue by red).

The second cell is **cell 6**, located also in layer III (sublayer IIIb). It responds only to stationary stimuli. When the contralateral eye is stimulated, only blue gives a response with a positive slope. When the ipsilateral eye is stimulated, only blue gives a negative slope.

Let us now see the responses in the granular layer. The cell is **cell 9**, located in sublayer IVb and responding to stationary stimuli in the contralateral eye only. Blue gives responses with positive gain, whereas red and green give negative slopes.

4.3.1.2.3 Extrastriate cortex (A18)

The only narrow-band cell in extrastriate cortex is **cell 8**. This cell proved very fragile; hence no histograms could be generated. Nonetheless, during the brief span of stimulation, the cell responded exclusively to short wavelength light and demonstrated peculiar characteristics, such as sensitivity to rotation.

4.3.1.2.4 Common features of narrow-band cells in Geniculocortical system

In contrast to the narrow-band cells in the extragenicular system, which all seem to exhibit a color bias towards the long-wavelength part of the spectrum, the cells in the geniculocortical system all seem to show a bias in favor of the short-wavelength part of the spectrum. In striate cortex, both of the narrow-band cells recorded in the supragranular layers, in both cases in layer III, showed a very peculiar phenomenon: an ocularity-dependent color-bias inversion.

4.3.2 Lennie's observations on Neural Coding

In his study of neural coding in primate visual cortex, Lennie (1999) has shown that the spectral tuning of cortical cells is nowhere near as clear cut as that found in cells in the retina or dLGN. According to him, physiologists working on peripheral mechanisms have the advantage that the cells respond reliably to chromatic stimuli, and cells of a particular class behave in the same way. On the other hand, the physiologist who studies the cortex has "much less firmly stated expectations of what to find, sees relatively few cells that look as though they are interested in color, finds great heterogeneity in the properties of cells, and encounters marked nonlinearities that often make it difficult to characterize cells." (Lennie, 1999).

Lennie suggests that cells in the cortex perform simultaneous analysis on different stimulus dimensions: orientation, spatial frequency, and color. It is misleading to seek exclusive monodimensional tuning. Instead one should look for cells tuned along several dimension and occupying a particular position in multidimensional stimulus-space. Hence, one should avoid looking for cortical mechanisms responding specifically and exclusively for color, for this would encourage a study of color as an abstraction. Rather than looking for pathways designed expressly for carrying information about color, one should think about the chromatic attributes of mechanisms that are solving problems in image analysis.

The reader may be surprised that there is such a small proportion of color opponent cells in our study, however according to van Dongen data (1976) based on recordings in the optic nerves, less than 1% of the cells are color-opponent.

4.3.3 Summary of narrow-band cells, observations on the variety of neural coding for color

We have 8 narrow-band cells. Of these, three were found in the Colliculus superior, all of them in the SGS, three in A17, two in supragranular layer III, and one in granular sublayer IVb as well as one cell in extrastriate A18, and one in the dorsal lateral geniculate nucleus. The nature of the narrow-band response is indicated in **Table 6**.

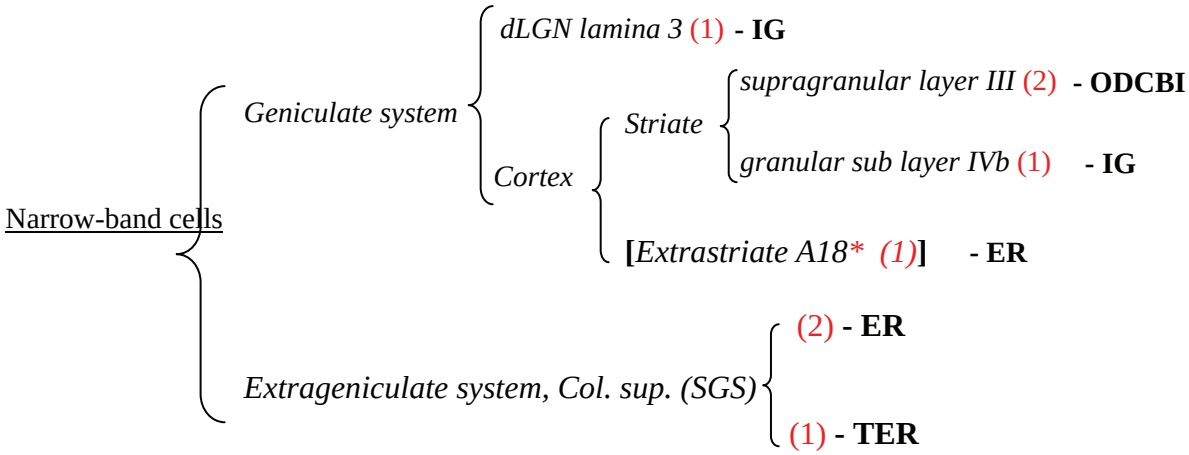

ER - **exclusive response**, fires to one wavelength, not to the other - inhibition.

TER - **temporally exclusive response**, for one wavelength, response is only phasic, for the other it is both phasic and tonic (exclusiveness depends on time interval).

IG - **inverted gain functions**, the R/I-curves have slopes of the opposite sign

ODCB - **ocularity-dependent color-bias inversion**, different color-preferences in contra- and ipsi-lateral eyes.

Numbers in parentheses indicate the number of cells found.

[ ]* - We have arbitrarily included A18 in the geniculocortical system. However, it also receives afferences from the superficial layers of the Colliculus superior via the Pulvinar. See **Figure 74**

Table 6 - Different kinds of response seen in the narrow-band cells.

The firing pattern of the narrow-band cells we have characterized is such, that specific wavelengths evoke a specific firing pattern and different hues are “mapped” into different activity patterns so that one can assume that these cells are playing a role in color coding within this visual system.

One of the shortcomings of any study of the physiology of the visual system, is that the most one can often do is simply identify isomorphisms between stimulus and activation patterns in determined regions of the brain. The cells, which we report as narrow-band, have a certain *color bias*, yet this does not resolve the question of whether their functional role in the visual system is to serve as *color selective units*. It is also relevant that the sensitivity for a given wavelength or set of wavelengths does not always manifest itself in exactly the same firing pattern in every narrow-band cell.

The narrow -band cells in primary visual cortex showed a definite chromatic preference. Their wavelength tuning, however, was not as crisp as that evidenced in some dLGN cells (Kretz, 1989). This is in agreement with findings in *Macaca fascicularis* (Lennie et al. 1990). Double opponent cells were not found.

4.3.4 The interaction of color and movement pathways

The hitherto dominant paradigm in visual system processing in primates postulates the existence of two separate pathways: the movement pathway (originating in the magnocellular layers of the dLGN) responds strongly to moving stimuli, shows strong directional tuning and has high contrast sensitivity. The color pathway (originating in the parvocellular layers of the dLGN) is supposedly unresponsive to movement, has little or no orientation tuning and shows low-luminance contrast sensitivity, but responds well to color (Livingstone and Hubel 1988, Zeki 1978, Schiller and Logothetis 1990). It was believed that these two pathways were diametrically opposed in their preferred stimuli, so that cells along one pathway leading to MT were technically ”color-blind” and those on the pathway leading to V4 ”motion-blind”.

Gegenfurtner et al. (1994) have examined the ways in which MT combines input from different cone types in the macaque. They have determined whether the chromatically induced responses in this area can account for the sensitivity evidenced in psychophysical experiments with moving stimuli. A cell can generate its response by either adding or subtracting (i.e. comparing) the input from cones responding to different wavelengths. In one case, the inputs from cones of different wavelengths are both excitatory, in the other case, one of the inputs is excitatory and the other is inhibitory (or vice-versa). In the first case, the chromatic component of the stimulus will not affect the cell's response, which will be greater whenever there is an increase in the intensity of the inputs, regardless of wavelength. These cells respond to changes in luminance. And thus no change in response will be evoked when one channel is increased by the same amount as the other channel is reduced. This situation is called isoluminance.

On the other hand, the "subtractive" or opponent cells will behave differently. Changes in luminance will not affect the response, provided the relative strength of both short- and long-wavelength sensitive cones remain the same. However, depending on the preferred chromatic tuning of the cell, a shift in the stimuli's wavelength composition towards one end of the spectrum, will make the difference between the inputs greater and thus increase the firing rate.

In their study, when luminance modulation was removed and only chromatic stimulation was used (isoluminant stimuli) the responses of all MT neurons were weakened. Nonetheless, for about a third of the neurons tested, there was no color composition of the isoluminant stimuli, which completely abolished the response. Hence, although MT neurons responded to isolumant stimuli inconsistently and with poor contrast sensitivity, the cells in this part of the "motion" pathway were proven not to be "color-blind". Hence although cells in MT receive input principally from magnocellular neurons, based on the residual responses to isoluminant stimuli, it is likely that many cells in MT receive input from *both* magno- and parvocellular LGN neurons.

This is in good agreement with the finding of Maunsell et al. (1990) that a small portion of MT multiunit responses remains even after a block of the magnocellular LGN. In these experiments, measurement of change in activity in MT following selective pharmacological deactivation of LGN magno- and parvocellular subpopulations show that MT is principally driven by the magnocellular laminae of the LGN, whereas the parvocellular component is

relatively scarce. According to Maunsell, ”although the P channel input to the MT was relatively minor, an unequivocal contribution could be demonstrated for some sites. […] Tasks that rely on several types of visual information may depend on direct communication between the motion and color and form pathways”. In instance of the latter, may be stimuli whose movement can only be discerned if color or texture clues are first detected.

Thus the studies showing that MT has residual processing of chromatic stimuli (as shown by non-null responses to isoluminant stimulation), have questioned the validity of the strictly segregated processing claim (Gegenfurtner et al. 1994). In agreement with the notion that the color pathway is not motion-blind, our data shows a certain number of narrow-band cells responding well to moving stimuli. Indeed, some of these cells respond only to moving stimuli.

4.4 Mesencephalic color coding circuitry and the problem of encephalization

The importance in Tupaia of the extragenicular system has been underlined in the Introduction. The extragenicular system is the target of the majority of retinal afferences. In this pathway, the retinal ganglion cells project to the superficial layers of the CS, whose cells in turn project to the pulvinar (Snyder and Diamond, 1968). The system is drawn schematically in **Figure 74**.

As mentioned in the Introduction, Snyder et al. (1969) have shown that Tupaias carry out color discrimination tasks with near perfect performance levels after severe lesions in both hemispheres going well beyond A17 and including extrastriate cortex up to the auditory areas. One is therefore led to suppose that the tree shrew’s Colliculus superior can mediate color in the absence of all of the visual cortical areas. Until now, no electrophysiological data was available to make this supposition conclusive. Thanks to our study, we can now confirm that important proportions of the narrow-band cells are likely to be located in the Colliculus superior. This constitutes the first electrophysiological confirmation of the existence of mesencephalic color coding circuitry and is of considerable importance for supporting Snyder et al.’s theory of brain evolution (which is still cited in textbooks among the major theories – see Buttler, Hodos 1996).

Whereas in lower vertebrates, the optic tectum is the target of the optic nerves and the locus of color coding circuits, primates cannot perform color discrimination tasks after ablation of visual cortex (Kluver, 1941). Thus, the tectal mechanisms for color in Tupaia are homologous with those present in reptiles and birds. Considering that as the telencephalon evolved in mammals, there were transition stages in which either the forebrain or the midbrain played the leading part, tree shrew represent an intermediate stage of evolution, with both mesencephalic and cortical color circuitry.

The sheer size of the superior colliculus relative to other species corroborates its importance as a locus of visual processing. The SGS of the tree shrews has a volume approximating one half of the striate cortex and six times that of the dLGN. In monkeys, the SGS has one-fifth the volume of the dLGN (Norton 1982). Its position as the first relay of retinal ganglion cells is analogous to that of the dLGN in the geniculostriate system. We have seen that chromatic tuning of dLGN is quite sharp, in comparison to the cortex. This also seems to hold true of the Colliculus superior cells recorded. The relatively small size of the receptive field is compatible with the classical view that color selective units have small receptive field sizes.

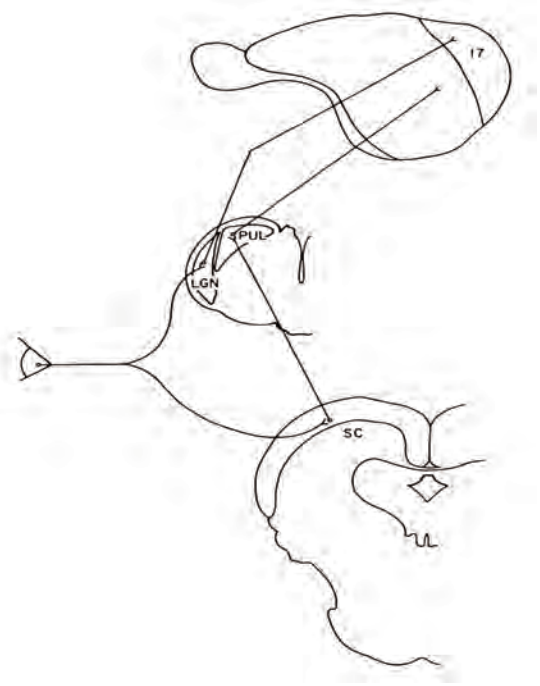

Fig. 74 – Schematic diagram of the genicular and extragenicular visual systems. In the former, the retina projects to the cortex via the dLGN. In the latter retinal ganglion cells project to the SC, the superficial layers of which then project to extra striate cortex via the pulvinar. After ablation of striate and extrastriate cortex, tree shrews preserve an uncanny color discrimination ability, suggesting, as our study confirms, that color vision is mediated not only by cortical, but also by mesencephalic structures.
(Figure taken from T.T. Norton 1982)

Accordingly, the CS of monkeys and cats, the receptive field properties are quite different from those of the cells in the dLGN. In these species, the receptive fields are much larger and many cells respond exclusively to moving stimuli. In the tree shrew, however, the dominant cell class in the CS is the S-R (stationary-responsive) cell, which is characterized by responses that make it similar to cells in the dLGN, especially in terms of their small receptive field size. As Norton points out, “it is clear that S-R cells in the tree shrew SGS are generally quite similar in a number of their receptive-field properties to the X and Y cells in the tree shrew dorsal dLGN. Low convergence (i.e. small RF size) and good response to stationary stimuli characterize the CS cells of tree shrew brain. Norton suggests, “it is possible that the expansion of the SGS and the increase in the number of neurons with narrow, vertically oriented dendritic fields may have produced the small receptive field center of the S-R cells by providing a huge population of neurons onto which the retinal inputs can synapse without a great deal of convergence”. Furthermore, in contrast to these species, tree shrews have only very few binocularly driven cells, as most colliculus cells are driven solely by inputs through the contralateral eye.

4.4.1 Differences in color coding in geniculate and extrageniculate systems

Assuming a diversity of ways in which chromatic information can be encoded in the different paths of the visual system (see **Table 6**) and the interconnections existing among these different anatomical regions (see **Figure 74**), we can make the following observations. Certain narrow-band cells in the dLGN tend to show inverted gain function for different wavelengths i.e. R/I curves with slopes of different signs. Since these cells project first of all to the granular layer in the cortex, it is not surprising to find here the same type of response.

We know that, unlike cats and monkeys, tree shrews do not posses ocular dominance columns; ocularity is organized tangentially in this species. The convergence of inputs from both eyes takes place in the supragranular layers of area 17 (Kretz 1986, Rager 1991). It is therefore not inconsistent to find here the phenomena of ocularity-dependant color-bias inversion (ODCBI), which is probably the result integration of broad-band signals from one eye and narrow-band signals from the other.

In the extragenicular system, we have witnessed in our study a pronounced phenomenon of exclusive response (**ER**) to one set of wavelengths, to the exclusion of others. Both stationary and moving stimuli are effective, but there is a preference for the latter. In view of this it comes to no surprise that in the single cell recorded in the extrastriate cortex (a projection target of the colliculus superior via the pulvinar) we find an ER type response to moving stimuli.

4.5 Predominance of blue-sensitive cells in the upper visual field

The majority of cells showing unusually high responses to short-wavelength light had receptive fields in the upper visual field. This was the case for 10 out of 12 cells. This finding is coherent with what we know about the distribution of the two existing cone types in the tree shrew retina.

Indeed it is known that the highest percentage of SWCs (short-wavelength cones) is localized in the ventral retina. (Müller and Peichl 1989, Petry et al. 1993, Petry and Murphy 1995). **Figure 75** illustrates the distribution of SWCs over the entire cone population for two retinae.

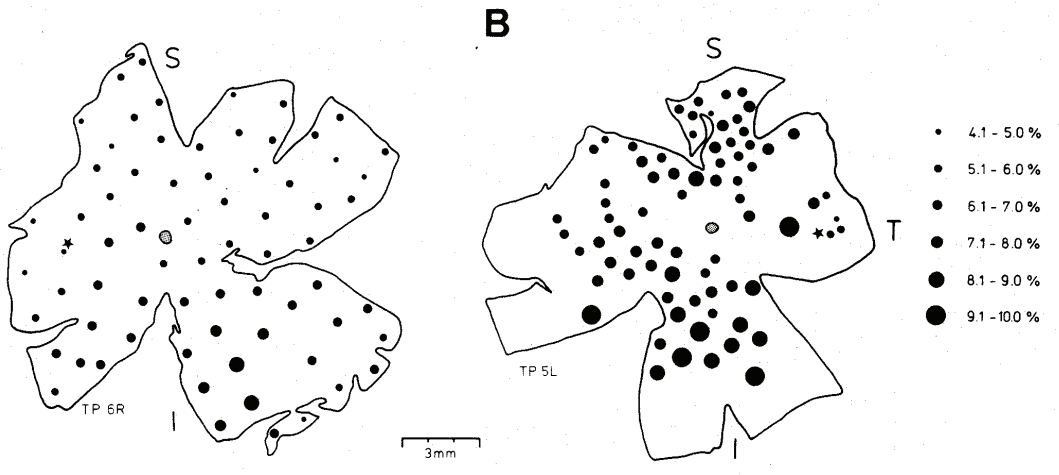

Fig. 75 Proportion of blue-sensitive cones in the entire cone population of two retinae. Each dot represents a sample field. Size represents the local blue cone percentage. Notice ventral retina contains the highest SWC densities. (From Müller and Peichl 1989).

The blue-sensitive cones or SWCs represent 4 to 10 % of all cones. According to Müller and Peichl (1989), in the dorsal retina this subpopulation makes out 4 to 6.5%, whereas in ventral retina the value exceeds 7 % with maxima of 10% in inferior and inferonasal midperiphery. These maps are based on the darker toluidine-blue staining of the blue-sensitive cones and were confirmed with immunohistochemistry using the S-antigen antibody. For many mammalian species, cone-specific monoclonal antibodies have been developed. OS-2 is a specific monoclonal marker for blue-sensitive cones. Using the OS-2 monoclonal antibody, Petry et al. (1993) confirmed Müller and Peichl's findings. More recently, Petry and Murphy (1995) have reported the use of NADPH diaphorase histochemistry as a means for investigating the architecture of tree shrew retina. Neuronal NADPH diaphorase has been shown to be a nitric oxide synthase. NO plays a role in photoreceptor function and NADPH can be used reliably as a marker of nitric oxide synthase activity. Their findings reveal that, while all cones show intense labeling of inner segment ellipsoids, short-wavelength-sensitive cones and rods displayed intense staining of the myoid inner segment subcompartments as well. Only SWCs and rods had surface labeling of their nuclei, suggesting biochemical differences within cone subpopulations.

Petry postulates that some of the unusual functional properties reported in the short-wavelength sensitive cone system may arise form differences in photoreceptor biochemistry. The short-wavelength sensitive cones are reported to posses the following specific characteristics: a) poorer spatial acuity, b) low temporal resolution, c) response saturation at low light levels, d) longer response latencies, e) lack of an OFF-response (for review see Zrenner 1983).

Tree shrews are comparable with ground squirrels (Citellus), which also have a cone-dominated retina and a negligibly small rod population (5-10 %). Under dark-adapted conditions during ERG (electroretinogram), two thirds of the ground squirrels showed Purkinje shift and a spectral sensitivity function resembling that predicted by the rhodopsin nomogram. In the tree shrew, however, no ERG or behavioral evidence for rod-mediated scotopic vision has been found (Tigges et al. 1967, Schäfer 1969). Müller and Peichl (1989) suggest that the sparse rod population of about 5 % in the tree shrew retina is probably below the limits detectable by these methods. They also suggest that the photoreceptor concentration in the inferior retina is an indicator of the functional importance of the upper visual field in the behavior of the tree shrew.

4.6 Peculiarities of the blue channel in tree shrews

One of the cells in our study (**cell 50**) showed higher responses to short-wavelengths only when faster moving stimuli were used, challenging the notion that the blue-channel has lower temporal resolution (see heading 3.5.1). Another cell (**cell 2**), showed OFF responses with blue, challenging the idea that the short-wavelength system is lacking in an OFF-response (Zrenner 1983, pp. 26, 82).

4.7 Presence of color-opponent cells (cell number 48) in the cell-sparse cleft of A17

Petry (1993) views the cell-sparse cleft as the locus of color processing circuitry in this species, based on his observation of development outcomes in animals reared in red light. Silencing of the color-opponent channels produces an atrophy of the cleft observed in cytochrome oxidase stains. Neighboring sublayers IVa and IVb encroach on deprived IVm analogously to the expansion of ocular dominance columns corresponding to one eye after enucleation of the other eye (Petry 1993). In our study, a single cell thoroughly characterized in the cell-sparse cleft (**cell no. 47**). The cell has poor luminance contrast sensitivity (**Figure 55**). Tests with different chromatic stimuli show center surround opponency (**Figure 76**).

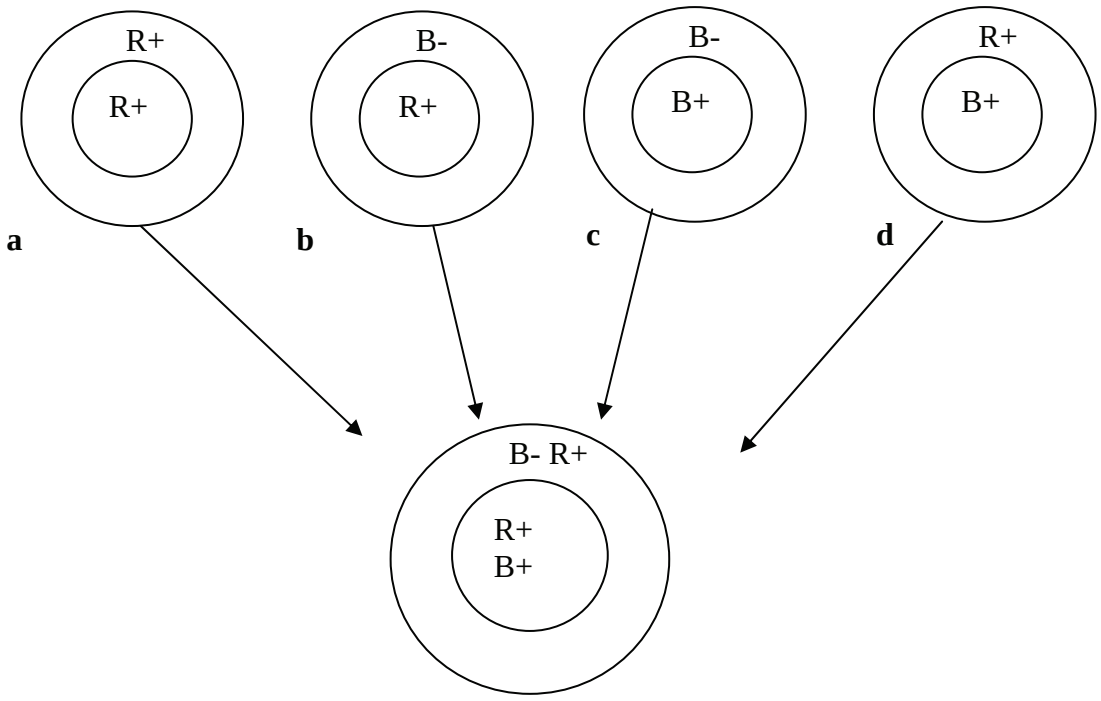

Fig. 76 – Center-surround chromatic opponency of cell 47 in the cell-sparse cleft.

The cell exhibits non-veridical (non-linear) coding for movement speed (**Fig. 71**), and poor orientation tuning (**Fig. 77**). These are typical characteristics of color cells.

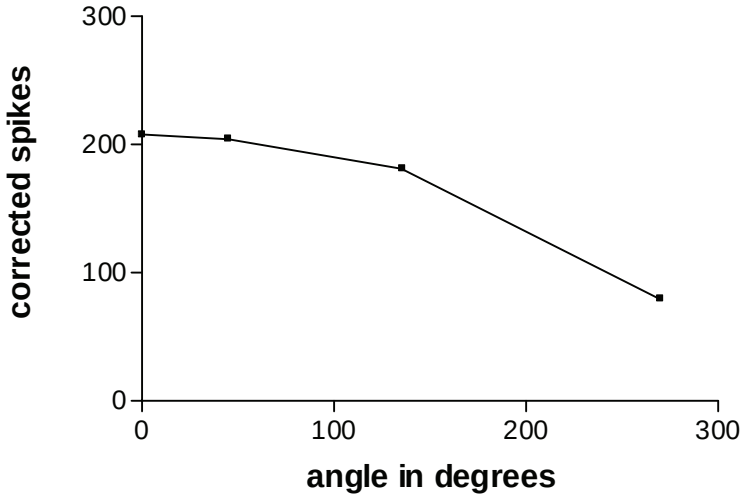

Fig. 77 – Orientation tuning curve for cell No. 47 located in the cell-sparse cleft. Clearly no sharp tuning is observable.

Conclusions

5 Conclusions and directions for future research

We have sought to examine the nature of spectral interaction in the visual system of the tree shrew. Having characterized the respective contributions of the two cone types electrophysiologicaly, we have found a surprisingly low proportion of color opponent cells. The fact that color opponent units are most likely found sublaminarly segregated in the cell sparse cleft, as originally proposed by Petry (1993), together with other aspects of tree shrew cortical architecture (e.g. ON, OFF segregation, ocularity), underscores tangential segregation as a principle of tree shrew cortical architecture. This is a fascinating idiosyncracy of Tupaia considering that columnar modules are the accepted paradigm of cortical functional architecture in other species.

Of hardly less importance is the presence of color processing circuitry in the mesencephalus of Tupaia, electrophysiological proof of which is for the first time provided in the present work. The redundancy of color sensitive modules in the cortex and Colliculus sup. together with the observation that in this species, color vision is preserved after decortication is thought provoking, as it suggests that in the process of progressive encephalization and specialization of function, this animal would occupy and intermediate stage with information of the same type being treated in both cortical and subcortical regions (Snyder et al. 1969).

Thus the study of functional circuits in this species gives results which are also of relevance to theories of development. In this respect, it would be interesting to pursue further study of animals under monochromatic light rearing (short-wave light rearing is also a possibility).

The possible role of GABA-ergic inhibition in tuning color-selective blob cells of monkey primary visual cortex has been explored by others (Sato, et al. 1994). In the auditory thalamus of the cat, differences in tonal selectivity could be associated with the use of different anesthetics (Zurita et al. 1994). Based on these observations, it would be interesting to explore possible pharmacological influences on color-tuning in the tree shrew.

Another line of research is to examine the fine chromatic tuning of visual cortex cells, using isoluminant stimuli as is now frequently done in primates. This could also help us determine the interaction between movement and color in activating the visual cortex of this species.

Bibliography

Bibliography

Albano, J.E., Humphrey, A.L., Norton, T.T. (1978) Laminar organization of receptive field properties in the tree shrew superior colliculus. J.Neurophysiol. **41**, 1140-1164

Baylor, D.A., Nunn, B.J., Schnapf, J.L. (1987) Spectral sensitivity of cones of the monkey *Macaca fascicularis*. Journal of Physiology (London) **390**: 145-160

Butler, A.B., Hodos, W. (1996) Comparative Vertebrate Neuroanatomy – Evolution and Adaptation. New York, Wiley-Liss

Butler, P.M. (1972) The problem of insectivore classification. In K.A. Joysey and T.S. Kemp (eds.): Studies in Vertebrate Evolution. Edinburgh: Olivier and Boyd, pp. 253-265

Carandini, M., Ferster, D. (1997) A tonic hyperpolarization underlying contrast adaptation in cat visual cortex. Science **276**: 949-952

Casagrande, V.A., Diamond, I.T. (1974) Ablation study of the superior colliculus in the tree shrew (Tupaia glis). J. Comp. Neurol.. **156**, 207-237

Casagrande, V.A. (1974) The laminar organization and connections of the lateral geniculate nucleus in the tree shrew (Tupaia glis), Anat. Rec. **178:**323

Charles, E.R., Logothetis, N.K. (1989) The responses of middle-temporal (MT) neurons to isoluminant stimuli. *Investigative Ophthalmology and Visual Science* (Suppl.) **30**: 427

Churchland, P.M. (1989) A Neurocomputational Perspective. Massachusetts Institute of Technology Press, Cambridge, Mass.

Conley, M., Fitzpatrick, D., Diamond, I. (1984) The laminar organization of the lateral geniculate body and the striate cortex in the tree shrew (Tupaia glis). Journal of Neuroscience **4**:171-197

Conway, J.L., Schiller, P.H. (1983) Laminar organization of tree shrew dorsal lateral geniculate nucleus. Journal of Neurophysiology **50**:1330-1342

Critchley, M. (1965) Acquired anomalies of colour perception of central origin. Brain **88**: 711-724

Dacey, D.M., Lee, B.B. (1994) The 'blue-on' opponent pathway in primate retina originates from a distinct bistratified ganglion cell type. Nature **367**: 731-734

Damasio, A.T., Yamada, H., Corbett, J., McKee, J. (1980) Central achromatopsia: behavioral, anatomic, and physiologic aspects. Neurology **30**:1064-1071

Derrington, A.M., Krauskopf, J., Lennie, P. (1984) Chromatic mechanisms in lateral geniculate nucleus of macaque. Journal of Physiology **357**: 241-265

Diamond, I.T., Hall, W.C. (1969) Evolution of neocortex. Science **164**: 251-261

DeBruyn, E.J. (1983) The organization and central terminations of retinal ganglion cells in the tree shrew (Tupaia glis). Doctoral dissertation, Vanderbilt University, Nashville

Dowling, J.E. (1979) Information processing by local circuits: The vertebrate retina as a model system. In: Schmitt F.O. and F.G. Worden, The Neurosciences Fourth Study Program. MIT Press, Cambridge, Mass., and London, pp. 163-181

Engel, A.K., König, P. (1993) Paradigm Shifts in Neurobiology - Towards a New Theory of Perception. In Casati, R., and G. White (eds.), Philosophy and the Cognitive Sciences, pp. 131-138, Proceedings of the Austrian Ludwig Wittgenstein Society

Finlay, B.L., Derrington, R.B., (1995) Linked regularities in the development and evolution of mammalian brains. Science **268**: 1578-1584

Fitzpatrick, D. (1996) The functional organization of local circuits in visual cortex: insights from the study of tree shrew striate cortex. Cerebral Cortex **6**:329-341

Gegenfurtner, K.R., Kiper, D.C., Beusmans, J.M.H, Carandini, M., Qasim, Z., Movshon, J.A. (1994) Chromatic properties of neurons in macaque MT. Visual Neuroscience **11**: 455-466

Gegenfurtner, K.R., Sharpe, L.T. (eds.) Color Vision - From Genes to Perception. Cambridge University Press, 1999.

Green, D., Dowling, J.E. (1975) Electrophysiological evidence for rod-like receptors in the gray squirrel, and ground squirrel and prairie dog retinas. J. Comp. Neurol., **159**:461-472

Helmholz, H. von (1911) Handbuch der Physiologischen Optik. Voss, Hamburg.

Hering, E. (1878) Zur Lehre vom Lichtsinne. Translated by K. Butler. In: R.C. Teevan and R.C. Birney (eds.) Color Vision, Selected Readings, Van Nostrand Reinhold, New York, pp.28-31

Holdefer, R.N., Norton, T.T. (1995) Laminar organization of receptive-field properties in the dorsal lateral geniculate nucleus of the tree shrew (Tupaia belangeri). J. Comp. Neuol. **358**, 401-413

Hubel, D.H. (1975) An autoradiographic study of the retinocortical projections in the tree shrew (Tupaia glis). Brain Research 96, 41-80

Hubel, D.H., Wiesel, T.N. (1977) Functional architecture of the macaque monkey striate visual cortex (Ferrier lecture). Proc. R. Soc. London Ser. B., **198**:1-59

Hubel, D.H. (1978) Effects of deprivation on the visual cortex of cat and monkey. Harvey Lectures, pp. 1-51, Academic Press, New York

Hubel, D.H. (1982) Exploration of the primary visual cortex 1955-78. Nature **299**:515-524

Hubel, D.H., Livingstone, M.S. (1987) Segregation of form, color, and stereopsis in primate Area 18. Journal of Neuroscience **7(11)**:3378-3415

Humphrey, A.A., Norton, T.T. (1980a) Topographic organization of the orientation column system in the striate cortex of the tree shrew (Tupaia glis). I. Microelectrode Recording. Journal of Comparative Neurololgy **192**:531-547

Humphrey, A.A., Norton, T.T. (1980b) Topographic organization of the orientation column system in the striate cortex of the tree shrew (Tupaia glis). II. Deoxyglucose mapping. Journal of Comparative Neurology **192**: 549-566

Jacobs, G.H., Neitz, J. (1986) Spectral mechanisms and color vision in the tree shrew (Tupaia Belangeri). Vision Research **26**, No.2: 291-298

Kaas, J.H., Killackey, H., Diamond, I.T. (1972) Visual cortex of the tree shrew (Tupaia glis): architectonic subdivisions and representation of the visual field. Brain Research **42**:491-496

Kaas, J.H. (1980) A comparative survey of visual cortex organization in mammals. In: S.O.E. Ebbesson ed., Comparative Neurology of the Telencephalon, Plenum Press, New York, pp. 483-502

Kaufmann, P.G., G.G. Somjen (1979a) Receptive fields of neurons in Areas 17 and 18 of tree shrews. Brain Research Bulletin **4**(3):319-325

Kaufmann, P.G., G.G. Somjen (1979b) Influence of striate lesions on visually evoked activity in tree shrew temporal cortex. Brain Research Bulletin **4**(3):327-332.

Kiper, D.C., Fenstemaker, S.B., Gegenfurtner, K. (1997) Chromatic properties of neurons in macaque area V2,. Visual Neuroscience **14**:1061-1072

Kluver, H. (1941) Visual functions after removal of the occipital lobe. Journal of Psychology **11**: 23-45

Kretz, R. (1973) Verhaltensphysiologische Bestimmung der spektralen Empfindlichkeit bei Cataglyphis bicolor FABR. (Formicidae, Hymenoptera). Diplomarbeit, Universität Zürich

Kretz, R (1977) Verhaltensphysiologische Analyse des Farbensehens der Ameise Cataglyphis bicolor (Formicidae, Hymenoptera). Doctoral Dissertation, Institute of Zoology, University of Zürich 1977

Kretz, R., Rager, G., Norton, T.T. (1986) Laminar organization of ON and OFF regions and ocular dominance in the striate cortex of the tree shrew (Tupaia belangeri). Journal of Comparative Neurology **251**: 135-145

Kretz, R., Saini, K., Rager, G. (1989) Visual system of the tree shrew: spectral interactions. In: Elsner, N. and W. Singer (eds.) , Dynamics and Plasticity. Proceedings of the 17th Göttingen Neurobiology Conference. Georg Thieme Verlag, Stuttgart, New York

Kretz, R., Rager, G. (1990) Histochemial localization of cytochrome oxidase activity in the visual cortex of Tupaia belangeri: selective inactivation of the ON and OFF retinal inputs. In: Brain - Perception - Cognition, Elsner, N., and G.Roth (eds.). Thieme Verlag Stuttgart, New York

Land, E.H. (1979) The retinex theory of colour vision. Proceeding of the Royal Institute of Great Britain **47**:23-58

Land E.H., Hubel, D.H., Livingstone, M.S., Perry, S.H., Burns, M.M. (1983) Colour-generating interactions across the corpus callosum. Nature **303:**616-618

Land, E.H. (1983) Recent advances in Retinex theory and some implications for cortical computation. Proceedings of the National Academy of Sciences U.S.A. **80**:5163-5169

Le Gros Clark, W.E. (1960) The Antecedents of Man. An Introduction To The Evolution of The Primates. Quadrangle Books, Chicago

Lennie, P., Krauskopf, J., Sclar, G. (1990) Chromatic Mechanisms in Striate Cortex of Macaque. Journal of Neuroscience **10(2)**: 649-669

Lennie, P. (1999) Color coding in the cortex. In K. R. Gegenfurtner, L.T. Sharpe (eds.), Color Vision - From Genes to Perception. Cambridge University Press, 1999

Liu, S., Wong-Riley, M.T.T. (1990) Quantitative light- and electron-microscopic analysis of cytochrome oxidase distributions in neurons of the lateral geniculate nucleus of the adult monkey. Visual Neuroscience **4**:269-288.

Livingstone, M., Hubel D.H (1984) Anatomy and physiology of a color system in the primate visual cortex. Journal of Neuroscience **4**:309-356

Livingstone, M.S., Hubel, D.H. (1987a) Connections between layer 4B of area 17 and the thick cytochrome oxidase stripes of area 18 in the squirrel monkey. Journal of Neuroscience **7(11)**:3371-3377

Livingstone, M.S., Hubel, D.H. (1987b) Psychophysical evidence for separate channels for the perception of form, color, movement, and depth. Journal of Neuroscience **7**:3416-3468

Livingstone, M., Hubel, D. (1988) Segregation of form, color, movement, and depth: anatomy, physiology, and perception. Science **240(4853)**:740-749

Long, K.O., Fisher, S.K. (1983) The distributions of phtoreceptors and ganglion cells in the California ground squirrel. J. Comp. Neurol., **221**: 329-340

Lucket W.P. (1980) Comparative Biology and Evolutionary Relationships of Tree Shrews. Plenum Press, New York

Lund, J.S., Fitzpatrick, D.F., Humphrey, A.L. (1985) The striate visual cortex of the tree shrew. In: Cerebral Cortex, Vol 3 - Visual Cortex, Peters, A., E.G. Jones (eds.) Plenum Press, New York and London

Martin, R.D. (1990) Are tree-shrews primates ? In R.D. Martin (ed.) Primate Origins and Evolution. A Phylogenetic Reconstruction. Chapman and Hall, London, pp. 191-213

Maunsell, J.H.R., Nealey, T.A., DePriest, D.D. (1990) Magnocellular and parvocellular contributions to responses in the middle temporal visual area (MT) of the macaque monkey. Journal of Neuroscience **10**: 3323-3334

Merill, E.G.,Ainsworth, A. (1972) Glass-coated platinum-plated tungsten microelectrodes. Medical Biology and Engineering **10**: 495-504

Mooser, F. (1998) Functional Aspects of Visual Callosal Connections in the Tree Shrew. Doctoral Dissertation, Université de Fribourg

Müller, B., Peichl L. (1989) Topography of cones and rods in the tree shrew retina. Journal of Comparative Neurology. **282**: 581-594

Muly, E., Fitzpatrick, D., Raczkowsi, D. (1989) Efferent projection of layer 4 in tree shrew striate cortex: evidence of parallel pathways to the superficial layers. Society of Neuroscience Abstracts, Vol. **15**, pp. 1398

Muly E.C., Fitzpatrick D. (1992) The morphological basis for binocular and ON/OFF convergence in tree shrew striate cortex. Journal of Neuroscience **12**:1319-1334

Naka, K.I, Rushton, W.A.H. (1966) An attempt to analyse colour reception by electrophysiology. Journal of Physiology, **185**: 556-586

Nay, P.L. (1994) Die Topographische Organisation der Retinogeniculären Projektion des Spitzhörnchens (Tupaia belangeri). Doctoral Dissertation, Faculty of Medicine. University of Basel.

Nicholls, J.G., Martin A.R., Wallace B.G. (1992) From Neuron to Brain. A Cellular and Molecular Approach to the Function of the Nervous System. Third Edition, Sinauer Associates, Inc., Sunderland, MA.

Northcutt, R., Kaas, J. (1995) Evolution and development of neocortex. Trends in Neuroscience **18:** 373-379

Norton, T.T. (1982) Geniculate and Extrageniculate Visual Systems. In Changing Concepts of the Nervous System, Proceedings of the First Institute of Neurological Sciences Symposium in Neurobiology, Academic Press, New York

Norton, T.T., Rager, G., Kretz, R. (1985) ON and OFF regions in layer IV of striate cortex. Brain Res. **327**, 319-323

Novikoff, A.B., Goldfischer, S. (1969) Visualization of peroxisomes (microbodies) and mitochondria with diaminobenzidine. Journal Histochemichal Cytochemistry **17**:675-680

Palm, G., Aersten, A. (eds.) (1986a) Brain Theory. Proceedings of the First Trieste Meeting on Brain Theory, Springer-Verlag, Berlin, Heidelberg, New York

Palm, G. (1986b) Warren McCulloch and Walter Pitts A logical calculus of the ideas immanent in nervous activity. In: Palm, G., & Ad Aersten, Brain Theory, Proceedings of the first Trieste Meeting on Brain Theory, Springler, pp.229-230.

Pearlman, A., Birch, J., Meadows, J.C. (1979) Cerebral color blindness: an acquired defect in hue discrimination. Annals of Neurology **5**:253-261

Peters, A., Jones, E.G. (1991) Cerebral Cortex, vol. 3 - Visual Cortex. Plenum Press, New York and London

Petry, H.M., Harosi, F.I. (1987) Tree shrew visual pigments by microspectrophotometry. Annals of the New York Academy of Sciences **494**: 250-252

Petry, H.M., Harosi, F.I. (1990) Visual pigments of the tree shrew (Tupaia belangeri) and greater galago (Galago crassicaudatus). A microspectrophotometric investigation. Vision Res. vol. 30, no. 6: 839-851

Petry, H.M., Erichsen, J.T., Szél, A. (1993) Immunocytochemical identification of photoreceptor populations in the tree shrew retina. Brain Research **616**:344-350

Petry, H.M. (1993) Long-term changes in visual mechanisms following differential stimulation of color and luminance channels during development. Progress in Brain Research **95**:235-250

Petry, H.M**.,** Murphy, H.A. (1995) Differentiation of short-wavelength-sensitive cones by NADPH-diaphorase histochemistry. Proceedings of the National Academy of Sciences U.S.A. **92**: 5121-5123

Polson, M.C. (1968) Spectral sensitivity and color vision in Tupaia glis. Doctoral dissertation, Indiana University, Bloomington, Indiana

Pöppel, E. (1986) Long-range colour-generating interactions across the retina. Nature **20**: 523-525

Raczkowski, D., Fitzpatrick, D. (1990) Terminal arbors of individual, physiologically identified geniculocortical axons in the tree shrew's striate cortex. Journal of Comparative Neurology **302**: 500-514

Rager, G. (1983) Vertical and tangential organization in the neocortex. In: Basar, E., H. Flohr, H. Haken, A.J. Mandell (eds.): Synergetics of the brain. Proceedings of the International Symposium on Synergetics at Schloss Elmau, pp. 28-41

Rager, G., Nowakowski, R.S. (1983) Development of afferents to the striate cortex of the tree shrew (Tupaia belangeri). Experientia 39:671

Rager, G. (1991) Der visuelle Cortex von Tupaia: ein alternatives Modell ? Hirnforschung **32(5)**: 537-540

Rakic, P. (1979) Genetic and epigenetic determinants of local neuronal circuits in the mammalian central nervous system. In: Schmitt, F.O. and F.G. Worden (eds.): The Neurosciences Fourth Study Program, MIT Press, Cambridge, Mass., and London, pp. 109-127

Sato, H, Narumi, K., Katsuyama, N., Tamura, H., Hata, Y., Tsumoto, T. (1994) Broad Tuned Chromatic Inputs to Color-Selective Neurons in the Monkey Visual Cortex, J. of Neurophysiology, Vol. 72 No. 1, pp.163-168.

Sato, H., Tanaka, K., Isono, H., Yasuda, M., Mikami, A., (1989) Directionally selective response of cells in the middle temporal area (MT) of the macaque monkey to movement of equiluminous opponent color stimuli. Experimental Brain Research **75**: 1-14

Schäfer, D. (1969) Untersuchungen zur Sehphysiologie des Spitzhörnchens *Tupaia glis* (Diard 1820). Zeitschrift für Vergleichende Physiologie, 63:204-226

Schiller, P.H., Malpeli, J.G. (1978) Functional specificity of lateral geniculate laminae of the rhesus monkey. Journal of Neurophysiology **41**: 788-797

Schiller, P.H., Logothetis, N.K. (1990) The color-opponent and broad-band channels of the primate visual system. Trends in Neuroscience **13**:392-398

Schmitt, F.O. and Worden, F.G. (eds.) (1979) The Neurosciences Fourth Study Program. MIT Press, Cambridge, Mass., and London

Seligman A.H., Karnovsky, M.J., Wasserkrug, H.L., Hanker, J.S. (1968) Nondroplet ultrastructural demonstration of cytochrome oxidase activity with a polymerizing osmiophilic reagent, diaminobenzidine (DAB). Journal of Cell Biology **38**:1-14

Sherman, S.M., Norton, T.T., Casagrande, V.A. (1975) X- and Y-cells in the dorsal lateral geniculate nuclus of the tree shrew (Tupaia glis). Brain Res. **93**, 152-157

Shriver, J.E., Noback, C.R. (1967) Color vision in the tree shrew (Tupaia glis). Folia primatologica **6**:161-169

Snyder, M., Diamond, I.T. (1968) The organization and fuction of the visual cortex in the tree shrew. Brain Behavior and Evolution 1:244-288

Snyder, M.,Killackey, H., Diamond, I.T. (1969) Color vision in the tree shrew after removal of posterior neocortex. Journal of Neurophysiology **32**:554-563

Schwaier, A. (1975) The Breeding stock of Tupaias at the Battelle-Institut. In Laboratory Animal Handbooks **6**:141-149

ter Laak, H.J., Thijseen, J.M. (1978) Receptive field properties of optic tract fibres from on-center sustained and transient cells in a tree shrew (Tupaia chinensis). Vision Res. **18**, 1097-1109

Thijssen, J.M., Ter Laak, H.J., van Well, P.M.A. (1978) Masking, DeLange curves and integration times as revealed by ERG of a tree shrew (Tupaia chinensis). Pflügers Archiv **373**: 199-204

Tigges, J. (1963) Untersuchungen über den Farbensinn von Tupaia glis. Zeitschrift für Anthropologische Morphologie **53**: 109-123

Tigges, J. (1964) On visual learning capacity, retention, and memory in Tupaia glis. Folia primatologica **2**:232-245

Tigges, J. (1966) Ein experimenteller Beitrag zum subkortikalischen optischen System von Tupaia glis. Folia primatologica **4**:103-123

Tigges, J., Brooks, B.A., Klee, M.R. (1967) ERG recordings of primate pure cone retina (Tupaia glis). Vision Research **7**: 553-563

Tigges, J., Shantha, T.R., (1969) A Stereotaxic Brain Atlas of the Tree Shrew (Tupaia glis). Williams & Wilkins Company, Baltimore

Ts'o, D.Y., Gilbert, C.D. (1988) The Organization of Chromatic and Spatial Interactions in the Primate Striate Cortex. Journal of Neuroscience **8(5)**: 1712-1727

Ts'o, D.Y. (1989) The functional organization and connectivity of color processing. In Neural Mechanisms of visual perception. Gulf Publishing, Eds. Lam and Gilbert, Houston

van Dongen, P.A.M., ter Laak, H.J., Thijssen, J.M., Vendrik, A.J.H. (1976) Functional classification of cells in the optic tract of a tree shrew. Exp. Brain Res. **24**, 441-446

Wallace, M.T., McHaffie, J.G., Stein, B.E. (1998) Visual response properties and visuotopic representation in the newborn monkey superior colliculus. Journal of Neurophysiology,**78**:2732-2741

Ward, J.P., Masterton, R.B. (1970) Encephalization and visual cortex in the tree shrew (Tupaia glis). Brain, Behav. Evol. **3**, 421-469

Ware, C.B., Casagrande, V.A., Diamond, I.T. (1972) Does the acuity of the tree shrew suffer from removal of striate cortex? Brain, Behav. Evol. **5**, 18-29

Wiesel, T.N.(1982) Postnatal-development of the visual cortex and the influence of environment. Nature **299**: 583-591

Wong-Riley M.T.T., Merzenich, M.M., Leake, P.A. (1978) Changes in endogenous enzymatic reactivity to DAB induced by neuronal inactivity. Brain Research **141**: 185-192

Wong-Riley M.T.T., Norton, T.T. (1988) Histochemical localization of cytochrome oxidase activity in the visual system of the tree shrew: Normal patterns and the effect of retinal impulse blockage, Journal of Comparative Neurology **272**: 562-578

Wong-Riley, M.T.T. (1989) Cytochrome oxidase: An endogenous metabolic marker for neuronal Activity. Trends in Neurosciences, **12(3)**: 94-101

Zeki, S. (1973) Colour coding in rhesus monkey prestriate cortex. Brain Research **53**: 422-427

Zeki, S. (1978) Uniformity and diversity of structure and function in rhesus monkey prestriate visual cortex. Journal of Physiology **277**:273-290.

Zeki, S. (1980) The representation of colours in the cerebral cortex. Nature **284**: 412-417

Zeki, S. (1993) A Vision of the Brain. Blackwell Scientific Publications, Oxford, London

Zrenner, E. (1983) Neurophysiological Aspects of Color Vision in Primates. Springer Verlag, Berlin

Zurita, P., Villa, A.E.P., de Ribaupierre, Y., de Ribaupierre, F., Rouiller, E.M. (1994) Changes of single unit activity in the cat's auditory thalamus and cortex associated to different anesthetic conditions. Neuroscience Research 19 (1994) 303-316.

Appendix I

Cell Inventory

Cell No.	Experiment	Localization	Depth	RF size	ipsi/contra	Stat.	Mov.	ON	OFF	Phas	Ton	NB	Observations
1	T.AD. 170	A17 - IIIb	660	1 x 1	c	x	x	x		x	x	no	reacts to ipsilateral stimuli too. Also to moving stimuli.
2	T.AD. 170	Collic. Sup. (SGS)	4620	3 x 3, 6 x 6	c	x	x	x	x	x	x	yes	corrected spikes for blue are negative despite stimulus strenght.
3	T.AD. 172	A17 - III a/b	580	0.75 x 0.75	c	x		x		x		yes	cell responds exclusively to blue, previous red stimulus supresses blue response.
4	T.AD. 172	Collic. Sup. (SGS)	4970	1 x 1	c	x		x	x	x	x	no	made recordings for different sizes
5	T.AD. 172	A17 - IIIb	600	1.5 x 1.5	c	x		x	x	x		no	
6	T.AD. 175	A17 - IIIb	850	1 x 1	c + i	x		x	x	x		no	only two points for each color (no white). Only blue has postive slope.
7	T.AD. 175	A17 - V	2320	2.5 x 2.5	c + i	x		x	x	x		no	cell responds also to moving stimuli. Orientation selective
8	T.AD. 180	A18	825				x					yes	insensitive to red, complex characteristics, reacts to rotation
9	T.AD. 180	A17 - IVb	1210	1 x 1	c	x				x	x	yes	cell responds well to blue (and white), red and green give negative slopes
10	T.AD. 182	Collic. Sup. (SO)	4594	0.65 x 6.5	c		x		x	x	x	no	"go" and "return"
11	T.AD. 182	Collic. Sup. (SGS)	5450	NA	c + i		x		x	x			too few recordings for R/I curve
12	T.AD. 185	Collic. Sup. (SGS)	3444	1 x 1	c		x	x		x	x	no	responds also to stationary stimuli with ON - OFF (phasic). Direction specific.
13	T.AD. 185	Collic. Sup. (SO)	4155	circle 4 diam.	c + i	x		x	x	x		no	cell is unusually responsive to blue at low intensities. Negative slope after saturation.
14	T.AD. 185	A17 - IIIc	1344	1.1 x 2.75	c + i	x			x	x	x	no	probably multi-unit
15	T.AD. 185	Collic. Sup. (SGS)	4222	1.8 x 22.7	c		x	x		x		no	too few intensities with blue tested (2), otherwise no indication of spectral tuning
16	T.AD. 185	Collic. Sup. (SGS)	4330	1.8 x 22.7	c		x	x		x	x	yes	In blue, only one intensity was tested. Maximum int. was required, couldn't give more
17	T.AD. 187	Collic. Sup. (SGS)	3826	1.36 x 20.85	c		x			x		no	
18	T.AD. 187	Collic. Sup. (SGS)	3650	6.25 x 6.25	c	x	x	x	x	x	x	no	In this cell, color (or intensity) may influence phasic/tonic ratio.
19	T.AD. 187	Collic Sup. (SGS)	3830	3.9 x 3.9	c		x					no	"go" and "return" together
20	T.AD. 189	Collic Sup. (SGS)	3820	1.13 x 1.13, 2.56 x 3.24	c	x		x	x	x	x	yes	OFF behavior somewhat erratic. Blue phasic, strongest peaks, suppress in tonic
21	T.AD. 191	LGN Layer 6	4420,4470	1 x 2.5	c	x			x	x	x	no	blue gives strong peeks, red sorround inhibits, contrast experiments
22	T.AD. 191	LGN Layer 6	4560	NA	c	x			x	x		no	surround enhances green and red response, but inhibits blue (slightly).
23	T.AD. 191	LGN Layer 5	4770	1 x 3	i	x			x	x	x	no	good R/I curves. OFF - ipsi response corresponds to LGN layer 5
24	T.AD. 191	LGN Layer 5	4910	6.25 x 6.25	i	x			x	x	x	no	examined response wit different stimulus sizes
25	T.AD. 191	LGN Layer 4	5180	0.5 x 0.75	c	x			x	x	x	no	good R/I curves. OFF contra response corresponds to LGN layer 4
26	T.AD. 191	LGN Layer 3	5420	0.75 x 1.25	c	x		x	x	x	x	yes	only blue is phasic, green and red only tonic with suppress after saturation.
27	T.AD. 191	LGN Layer 2	5600	0.75 x 1.5	c	x		x		x	x	no	strong response to blue, caesura appears with lower intensities
28	T.AD. 199	A17 layer unknown	1774	NA	c + i		x						not enough recordings to test spectral sensitivity
29	T.AD. 199	A17 layer unknown	1632	NA	c + i		x						not enough recordings to test spectral sensitivity
30	T.AD. 199	A17 - IIIa	671	NA	c + i		x					no	blue slightly, but not significantly higher than others
31	T.AD. 199	A17 - IIIb	910	NA	c + i		x						not enough recordings to test spectral sensitivity
32	T.AD. 199	A17 - IIIc / IVa	1500	1.2 x 1.5, 2.8	c + i	x	x	x	x	x	x		not enough recordings to test spectral sensitivity
33	T.AD. 199	Collic. Sup. (SGI)	4880	3.4 x 3.4	c		x						not enough recordings to test spectral sensitivity
34	T.AD. 199	A17 - IIIc	1190	3.4 x 3.4	c		x			x	x		Movement in both directions, and color-contrast tested
35	T.AD. 200	A18	1215-270	2.25 x 2.25, 1x1	c	x			x	x			**constant stimulus/background contrast,** only white and red tested
36	T.AD. 200	A17 - IIIb	1010	1.5x1.5 , 4.75x4.75	c	x		x		x		no	**color and luminance contrast tested** sorround inhibition, **spontaneous activity variations**
37	T.AD. 200	A17 - IVb/V	1838	5.75 x 0.4	c		x			x		no	Tested "go" and "return". Difficult to say wether response is on or off. Good curves
38	T.AD. 209	A17 - IIIc	886	circle diam. 2.5	i		x		x	x	x		only white tested.
39	T.AD. 209	A17 - IIIc	920	circle diam. 2.5	i		x			x			only three points (white)
40	T.AD. 209	A17 - V	1390	circle diam 2.5	c	x		x	x	x	x		white only - cell responded ON - OFF
41	T.AD. 209	A17 - IIIb *	2682	0.79 x 8.33	c	x	x	x	x	x	x	no	good R/I curves, slight oscillations, compared stationary and moving stimul
42	T.AD. 210	A17 - IVa	1208	different sizes	c	x		x		x	x	no	activity profiles with different stimulus sizes and different colors. Higly sensitive to blue
43	T.AD. 210	A17 - IIIc/IVa	1065	.3 x 4, 4 x 6	c		x			x		no	strong gain in blue, **color contrast experiments**
44	T.AD. 210	A17/18 V	1450	1 x 12, 17 x 8.5	i + c	x	x	x	x	x	x	no	Good R/Is, "go" and "return". Tested stimulus and background with different wavelengths
45	T.AD. 210	A17 - VI	1880	0.5 x 7.5	i + c		x	x	x	x	x	no	"go", "return" response for blue increases sharply (strong gain)
46	T.AD. 211	A17 IIIc/IVa	727	0.5 x 1.5	c	x		x		x		no	good R/I curves
47	T.AD. 212	A17 - Iva/cleft	1240	8.5 x 0.5, 20 x 9	c + i		x			x	x	no	**contrast invariance, color contrast** stimulus at 5 minute intervals, different speeds
48	T.AD. 212	A17 - V	1604	3 x 0.3, 25 x 13.5	c + i		x			x	x	no	tested white with different speeds, color interactions
49	T.AD. 213	A17 - V	1342	4 x 0.5, 8 x 0.5, 15 x 13, 16 x 18	c + i		x			x	x	no	**contrast variance & invariance,** different orientations, red on blue, blue on red
50	T.AD. 213	A17 - V	1435	0.5 x 4	c + i		x			x	x	no	different speeds **(response is different for SW and LW)**, different directions
51	T.AD. 214	A17 - IIIb	640	3 x 3	c	x		x	x	x	x	no	white only tested
52	T.AD. 214	A17 - IIIb/c	831	circle 4	c	x				x		no	moving dark spot - gives very strange looking R/I curves "go" and "return"
53	T.AD. 214	A17 - IIIc	920	0.8 x 19	c		x			x	x	no	good R/I curves "go" and "return"

Legend

Stat - stationary Mov - moving Phas - phasic Ton - tonic NB - narrow band

- strong response to short-wave stimuli

Appendix II

Cortical Penetration Sites referring to cell numbers in Appendix I

Stereotaxic Coordinates of Recording Sites

(plotted in the dorsal view of the Tupaia brain)

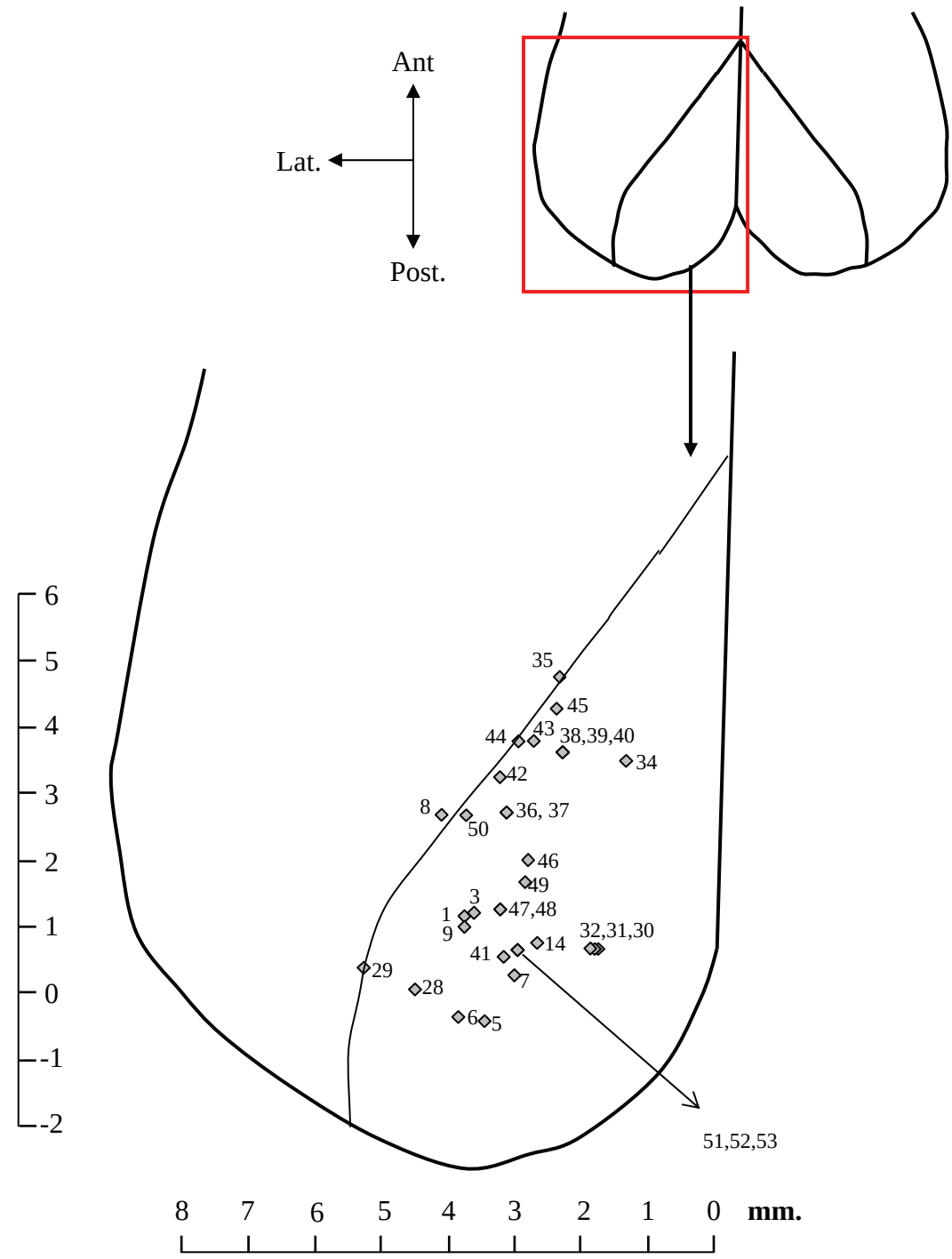

Appendix III

Filter Values and Curves

λ_{max}=430 nm λ_{max} =548 nm $\lambda_{1/2max}$ =625nm

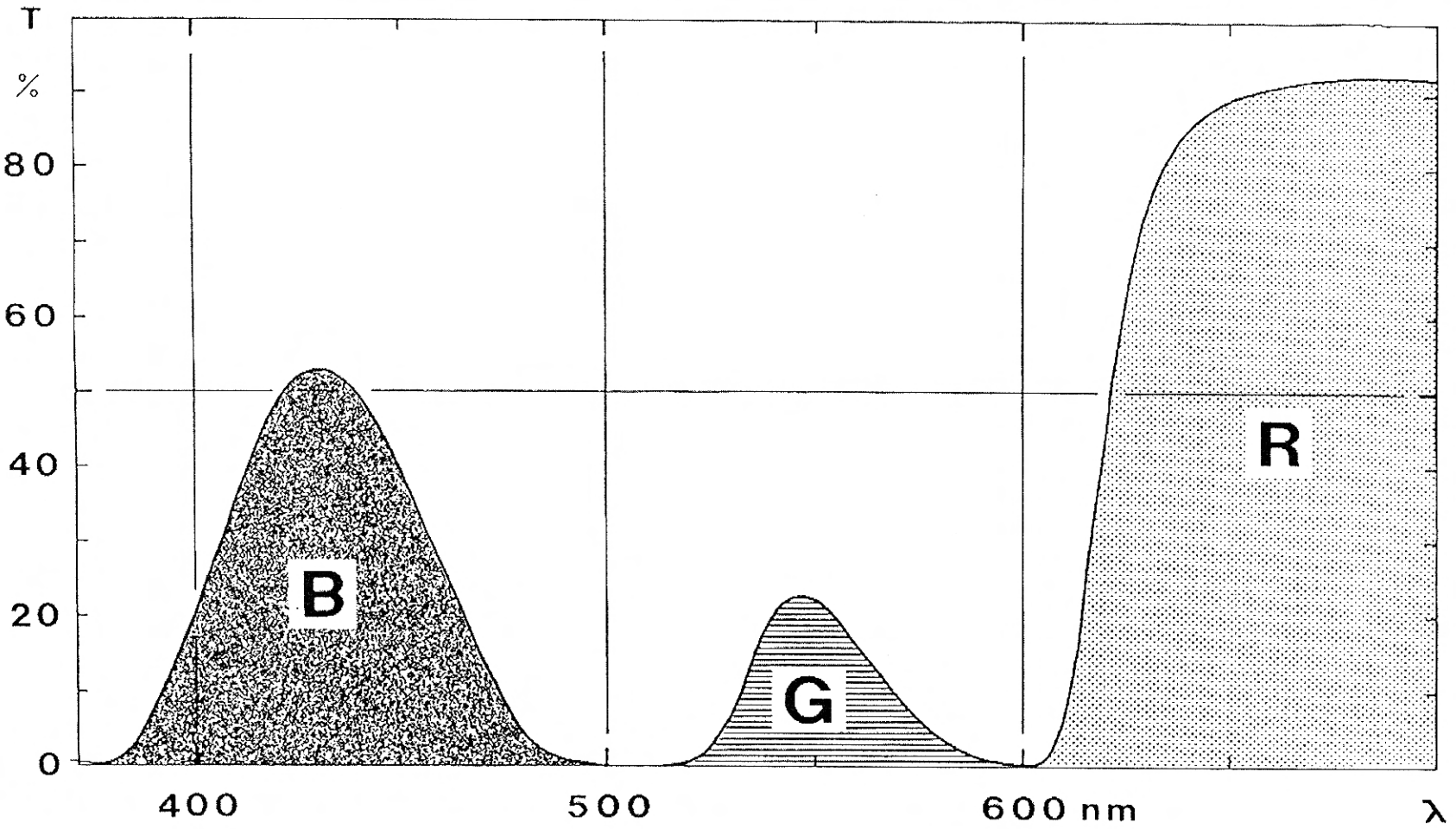

F. Mooser/ L. Murillo 7 July 1996

Table 2 .

Measures of intensities, projector „Stufe 1“, perfusion light-ON (J16, Digital Photo-meter, J6502, mW/m2, stimulus size: 2° x 2°, distance screen-animal : 114 cm)

Values proj. x filter (%)	Intensity (mW/m2)				Log (intensity)			
	White	Green	Red	Blue	White	Green	Red	Blue
22	780.00	47.00	244.00	46.00	2.89	1.67	2.39	1.66
22 x 70%	538.20	32.43	168.85	31.00	2.73	1.51	2.23	1.49
22 x 50%	392.00	24.00	107.00	21.00	2.59	1.38	2.03	1.32
22 x 25%	205.14	13.02	69.54	12.97	2.31	1.11	1.84	1.11
22 x 10%	86.00	8.00	29.00	7.00	1.93	0.90	1.46	0.85
22 x 1%	14.00	1.14	7.00	3.00	1.15	0.06	0.85	0.48
22-16	1140.00	65.00	339.00	65.00	3.06	1.81	2.53	1.81
22-16 x 70%	786.60	44.85	234.59	43.81	2.90	1.65	2.37	1.64
22-16 x 50%	517.00	32.00	149.00	28.00	2.71	1.51	2.17	1.45
22-16 x 25%	299.82	18.01	96.62	12.35	2.48	1.26	1.99	1.09
22-16 x 10%	112.00	10.00	40.00	9.00	2.05	1.00	1.60	0.95
22-16 x 1%	18.00	1.70	9.00	3.90	1.26	0.23	0.95	0.59
16	1620.00	90.00	476.00	90.00	3.21	1.95	2.68	1.95
16 x 70%	1117.80	62.10	329.39	60.66	3.05	1.79	2.52	1.78
16 x 50%	775.00	45.00	211.00	39.00	2.89	1.65	2.32	1.59
16 x 25%	426.06	24.93	135.66	25.38	2.63	1.40	2.13	1.40
16 x 10%	167.00	13.00	56.00	11.00	2.22	1.11	1.75	1.04
16 x 1%	25.00	2.00	12.00	4.30	1.40	0.30	1.08	0.63
16-11	2400.00	130.00	672.00	130.00	3.38	2.11	2.83	2.11
16-11 x 70%	1656.00	89.70	465.02	87.62	3.22	1.95	2.67	1.94
16-11 x 50%	1098.00	64.00	308.00	55.00	3.04	1.81	2.49	1.74
16-11 x 25%	631.20	36.01	191.52	36.66	2.80	1.56	2.28	1.56
16-11 x 10%	237.00	17.00	80.00	15.00	2.37	1.23	1.90	1.18
16-11 x 1%	35.00	2.00	17.00	5.00	1.54	0.30	1.23	0.70
11	3380.00	190.00	1000.00	186.00	3.53	2.28	3.00	2.27
11 x 70%	2332.20	131.10	692.00	125.36	3.37	2.12	2.84	2.10
11 x 50%	1660.00	90.00	435.00	80.00	3.22	1.95	2.64	1.90
11 x 25%	888.94	52.63	285.00	52.45	2.95	1.72	2.45	1.72
11 x 10%	353.00	23.00	111.00	22.00	2.55	1.36	2.05	1.34
11 x 1%	50.00	6.40	22.00	6.20	1.70	0.81	1.34	0.79

Values proj. x filter (%)	Intensity (mW/m2)				Log (intensity)			
	White	Green	Red	Blue	White	Green	Red	Blue
11-8	4850.00	260.00	1440.00	260.00	3.69	2.41	3.16	2.41
11-8 x 70%	3346.50	179.40	996.48	175.24	3.52	2.25	3.00	2.24
11-8 x 50%	2050.00	124.00	604.00	111.00	3.31	2.09	2.78	2.05
11-8 x 25%	1275.55	72.02	410.40	73.32	3.11	1.86	2.61	1.87
11-8 x 10%	435.00	30.00	155.00	29.00	2.64	1.48	2.19	1.46
11-8 x 1%	60.00	7.70	30.00	7.60	1.78	0.89	1.48	0.88
8	6740.00	350.00	2050.00	360.00	3.83	2.54	3.31	2.56
8 x 70%	4650.60	241.50	1418.60	242.64	3.67	2.38	3.15	2.38
8 x 50%	2970.00	166.00	865.00	154.00	3.47	2.22	2.94	2.19
8 x 25%	1772.62	96.95	584.25	101.52	3.25	1.99	2.77	2.01
8 x 10%	634.00	40.00	221.00	40.00	2.80	1.60	2.34	1.60
8 x 1%	88.00	9.20	41.00	9.50	1.94	0.96	1.61	0.98
8-5.6	8900.00	480.00	2770.00	480.00	3.95	2.68	3.44	2.68
8-5.6 x 70%	6141.00	331.20	1916.84	323.52	3.79	2.52	3.28	2.51
8-5.6 x 50%	4080.00	221.00	1165.00	202.00	3.61	2.34	3.07	2.31
8-5.6 x 25%	2340.70	132.96	789.45	135.36	3.37	2.12	2.90	2.13
8-5.6 x 10%	869.00	53.00	295.00	52.00	2.94	1.72	2.47	1.72
8-5.6 x 1%	119.00	11.40	54.00	12.00	2.08	1.06	1.73	1.08
5.6	11850.00	650.00	3660.00	650.00	4.07	2.81	3.56	2.81
5.6 x 70%	8176.50	448.50	2532.72	438.10	3.91	2.65	3.40	2.64
5.6 x 50%	5250.00	298.00	1580.00	270.00	3.72	2.47	3.20	2.43
5.6 x 25%	3116.55	180.05	1043.10	183.30	3.49	2.26	3.02	2.26
5.6 x 10%	1151.00	77.20	400.00	68.00	3.06	1.89	2.60	1.83
5.6 x 1%	157.00	14.70	73.00	15.00	2.20	1.17	1.86	1.18
5.6-4.5	14900.00	820.00	4700.00	830.00	4.17	2.91	3.67	2.92
5.6-4.5 x 70%	10281.00	565.80	3252.40	559.42	4.01	2.75	3.51	2.75
5.6-4.5 x 50%	7190.00	370.00	1975.00	345.00	3.86	2.57	3.30	2.54
5.6-4.5 x 25%	3918.70	227.14	1339.50	234.06	3.59	2.36	3.13	2.37
5.6-4.5 x 10%	1527.00	86.00	502.00	86.00	3.18	1.93	2.70	1.93
5.6-4.5 x 1%	210.00	17.00	92.00	18.00	2.32	1.23	1.96	1.26
4.5	15360.00	860.00	4890.00	870.00	4.19	2.93	3.69	2.94
4.5 x 70%	10598.40	593.40	3383.88	586.38	4.03	2.77	3.53	2.77
4.5 x 50%	7230.00	383.00	2060.00	347.00	3.86	2.58	3.31	2.54
4.5 x 25%	4039.68	238.22	1393.65	245.34	3.61	2.38	3.14	2.39
4.5 x 10%	1555.00	90.00	516.00	86.00	3.19	1.95	2.71	1.93
4.5 x 1%	212.00	18.20	96.00	18.00	2.33	1.26	1.98	1.26

University of Fribourg 12.9.96 - Tektronix J16 Digital Photometer, with probe 6503 - mW/m2

Values proj. x filter (%)	Intensity **(mW/m2)**				Logarithmic Value of Intensities			
	White	Green	Red	Blue	White	Green	Red	Blue
4.5	875	831	5500	835	2.94	2.92	3.74	2.92
4.5 x 70%	607	590	3800	573	2.78	2.77	3.58	2.76
4.5 x 50%	413	393	2550	388	2.62	2.59	3.41	2.59
4.5 x 25%	226	225	1580	225	2.35	2.35	3.20	2.35
4.5 x 10%	92	92.4	675	93.5	1.96	1.97	2.83	1.97
4.5 x 1%	14.3	17	116	17.3	1.16	1.23	2.06	1.24

Diaph=2

Values calculated from Fribourg measurements in mW/m2

Filter value	***White***	***Green 548nm***	***Red 620nm***	***Blue 430nm***
70%	69.37	71.00	69.09	68.62
50%	47.20	47.29	46.36	46.47
25%	25.83	27.08	28.73	26.95
10%	10.51	11.12	12.27	11.20
1%	1.63	2.05	2.11	2.07

Curriculum Vitae

LUIS FERNANDO MURILLO-OTHON

Born: 21 December 1968 Nationality : Mexican

ACADEMIC PROFILE

2000- **Schiller International University** Leysin
Adjunct Professor of Psychology and Sociology

1999-present **Ecole Normale Supérieure, Ecole Polytechnique** Paris, Lyon
Guest researcher

- Study of Kant, Husserl, Heidegger, Sartre (Philosophy of Subjectivity)
- History and Philosophy of Psychology

1998-1999 **Nobel Institute of Physiology** Stockholm
Guest rearcher Unit for Brain Development

- Helped to create a new research lab
- Establishing of total quality management in graduate programme.

1997–1998 **Institut de Biologie Cellulaire et Morphologie** Lausanne
Assistant

- Research into visual system topology
- Intense teaching : Neuroanatomy & Human Anatomy (dissection)

1993-1997 **Institut für Anatomie und Spezielle Embryologie** Freiburg in Ue.
Assistant

- Study of Cognitive and Visual Neurophysiology
- Taught Human Anatomy, Neuroanatomy

1991-1993 **Faculté de Lettres, Université de Fribourg** Freiburg in Ue.

- M.A. (bilingual) in Philosophy (Summa cum laude)
- English and Spanish Teacher (Inlingua, Tetrapak, Swisscom)

1987-1991 **Trinity College, University of Toronto** Toronto

- Double Honours B.A. in Classics (Greek, Latin), Philosophy, Minor: Germanic languages
- Student representative in the University of Toronto Senate

DIPLOMAS AND OTHER COURSES OF STUDY

2000 Université de Fribourg	**Dr. rer. nat**
1997 EPFL	postgraduate course Bioinspired Systems
1993 Université de Fribourg	**M.A.**, bilingual, *Summa cum laude* in Philosophy
1991 University of Toronto	**B.A. (Hons.)** Classics, Philosophy, German

COMPUTER SKILLS

Systems, languages:	Unix, MSOffice, MacOs, Basic, Assemly Language

LANGUAGES

Thoroughly Fluent:	English, Spanish, French, German, Italian
Reading Knowledge :	Dutch, Swedish, Classical Greek, Latin
At least one semester study :	Hebrew, Russian, Proto-indogermanic (Sanskrit)

HOBBIES

Piano:	**Royal Conservatory of Music,** Grade IX
Cinema:	History & Aesthetics of Cinema, Prof. Freddy Buache

PROFESSIONAL SOCIETY MEMBERSHIP

European Society of Philosophy and Psychology
American Academy of Political Science
Hegel Gesellschaft
Freunde der Antiken Kunst (Basel)

SOCIAL WORK AND CLUB FOUNDATION

Work in poor neigborhoods in Mexico City, hospitals in Montreal
Counselling of youngster in Metropolitan Toronto
Helped in founding a private school in the outskirts of Toronto
Founded Mantinean Club (philosophy) at Trinity College